Synthesis of new conjugated meso porphyrin dendrimers and oligomers and study of their optical properties

Dandan Yao

Résumé

Au cours de cette thèse, nous avons synthétisé et caractérisé de nouveaux composés en utilisant le macrocycle porphyrine en tant que brique moléculaire. L'objectif, après la synthèse, était d'étudier les propriétés photophysiques de ces nouvelles molécules.

Plus précisément, nous avons considérés trois groupes de dendrimères fluorènyles-porphyrines et deux oligomères avec des structures conjuguées. Les corrélations structures et propriétés optiques ont été discutées en détail, ainsi que le transfert d'énergie du dendron conjugué donneur.

Dans le premier chapitre, nous avons décrit la chimie des porphyrines en considérant surtout trois aspects: (i) structure, (ii) propriétés optiques et (iii) méthode synthétique. Nous avons également reporté les porphyrines préalablement étudiées dans notre groupe de recherche et proposé de nouveaux modèles lors de cette thèse.

Dans le deuxième chapitre, nous avons étudié l'influence de la position de substitution du phényle sur le cœur central qui est la porphyrine TPP. Deux groupes de nouveaux dendrimères ont été synthétisés avec différentes positions de substitution du phényle de la TPP: série para-substituée TPP1, TPP2 et TPP3, et série méta-substituée TPP4, TPP5 et TPP6. Ces dendrimères ont tous des dendrons conjugués avec des ponts phényl-alcynes et des groupements fluorènyles terminaux.

Dans le troisième chapitre, pour étudier l'influence des antennes périphériques, une série de dendrimères de porphyrine à base de TFP avec différentes positions de fluorènyles dans les dendrons conjugués (fluorényle central, fluorényle pontant et fluorényle terminal): TFP1, TFP2 et TFP3 a été synthétisée. Le fluorényle central influence principalement l'émission et le rendement quantique, alors que le fluorényle ponté et le fluorényle terminal ont un plutôt un effet sur l'absorption et l'émission du dendron en raison du transfert d'énergie prenant effet. Pour le plus gros dendrimère TFP3, lors de l'excitation du dendron, une émission résiduelle lors du processus de transfert est observée due à une trop grande distance entre ce chromophore et le cœur de la porphyrine.

Dans le quatrième chapitre, afin d'étudier l'influence des connexions dans le dendron, deux nouveaux dendrimères de porphyrine incorporant des ponts vinyles et alcynyles, TPP-D et TFP-D, ont été synthétisés et comparés aux analogues avec des ponts alcynes TPP-T et TFP-T. Ces ponts avec des doubles liaisons influencent dans une certaine mesure les propriétés optiques des dendrimères de porphyrine en fonction des positions occupées.

Dans le dernier chapitre, deux oligomères (un dimère linéaire et en un trimère en étoile), ont été synthétisés à partir du même monomère de porphyrine avec TFP comme groupement terminaux.

Abstract

During this thesis, we have worked on the synthesis and characterization of new compounds using the porphyrin macrocycle as a starting material. The aim, after synthesis, was to study the photophysical properties of these new molecules.

More precisely, we have synthesized and characterized three groups of fluorenyl-porphyrin dendrimers and two oligomers in conjugated structures. Their correlation on optical property-structure have been discussed in detail, as well as the energy transfer processes from the conjugated dendron donor to porphyrin acceptor.

In the first chapter, we introduce the general background of the porphyrin chemistry based on three aspects: (i) structure, (ii) optical properties and (iii) synthetic methods. We further review prior porphyrin studies done in our group and propose new molecular designs based on these results.

In the second chapter, we study the influence of substitution position and nature of the antennae on the central core. Two groups of new TPP-cored porphyrin dendrimers were synthesized according to different substituted positions on the peripheral phenyl rings: para-substituted series TPP1, TPP2 and TPP3, and meta-substituted ones TPP4, TPP5 and TPP6. All have conjugated dendrons with bridged phenyl-alkynyl and are terminated by fluorenyl groups.

In the third chapter, we study the influence of positions of light absorbers. To this aim, a series of TFP-cored porphyrin dendrimers presenting fluorenyls in conjugated dendrons on different positions is reported (core fluorenyl, bridging fluorenyl and terminal fluorenyl): TFP1, TFP2 and TFP3. The core fluorenyl mainly influences emission peaks and quantum yield, while the bridging fluorenyl and terminal fluorenyl have a large effect on the dendron absorption and on the energy transfer efficiency. Thus, for the largest dendrimer TFP3, dendron emission is not totally quenched by long distance energy transfer process when exciting the peripheral dendrons.

In the fourth chapter, we study the influence of linkages in the Dendron. Thus, two new porphyrin dendrimers with bridged vinyl, TPP-D and TFP-D, were synthesized and compared to analogues with alkynyl bridged TPP-T and TFP-T. Vinyl and alkynyl bridges are shown to influence the optical properties of the porphyrin dendrimers to a certain extent depending on the substituted positions.

Finally, in the last chapter, two oligomers with n-butyl substituted TFP as terminal group, a linear dimer and a star – shaped trimer, were synthesized from the same porphyrin monomer.

N° d'ordre : 15ISAR11 / D15 - 11

Institut National des Sciences Appliquées de Rennes

20, Avenue des Buttes de Coësmes • CS 70839 • F-35708 Rennes Cedex 7

Tel : 02 23 23 82 00 - Fax : 02 23 23 83 96

Thèse

2015

Dandan YAO

THESE INSA Rennes

sous le sceau de l'Université européenne de Bretagne

pour obtenir le titre de

DOCTEUR DE L'INSA DE RENNES

Spécialité : Chimie

présentée par

Dandan YAO

ECOLE DOCTORALE : *SDLM*

LABORATOIRE : *UMR6226/OMC/ISCR-INSA de Rennes*

Synthesis of New Conjugated meso Porphyrin Dendrimers and Oligomers And Study of their Optical Properties

Thèse soutenue le 16.03.2015

devant le jury composé de :

Dominique MANDON
Directeur de Recherche à l'Université de Brest-UBO / Président

Philippe BLANCHARD
Directeur de recherche CNRS à l'Université d'Angers/ Rapporteur

Bernold HASENKNOPF
Professeur à l'Université P. et M. Curie, Paris/ Rapporteur

Fréderic PAUL
Directeur de Recherche à l'Université de Rennes1 / Examinateur

Olivier MONGIN
Maître de Conférences (HDR) à l'Université de Rennes1 / Examinateur

Christine PAUL-ROTH
Maître de Conférences (HDR) à l'INSA de Rennes / Directrice de thèse

Synthesis of New Conjugated *meso*-Porphyrin Dendrimers and Oligomers And Study of their Optical Properties

Dandan YAO

En partenariat avec

Acknowledgement

Three years and half in France, I spent a colorful experience here. Rennes is a peaceful city, and it has a very mild weather and beautiful view. During my PhD period, I tried my best efforts on subject and now I am going to finish my thesis and prepare my defense. I appreciate everybody who gave me helps in studies and live.

I should thank to China Scholarship Council (CSC) for finance. It provides me the opportunity to get PhD degree and more than three years' life support.

I would like to thank Mr. Philippe BLANCHARD, Directeur de Recherche CNRS à l'Université d'Angers, and Mr. Bernold HASENKNOPF, Professeur à l'Université P. et M. Curie, Paris for reviewing this manuscript.

I deeply thank my supervisor Dr. Christine PAUL-ROTH, who provides me the PhD position on Organic Chemistry in laboratory ISCR-OMC-INSA of UMR-6226 in Rennes. Thanks for her patient guide and professional advises in my work, as well as warmhearted help in my live. Meanwhile, I sincerely thank Dr. Frederic PAUL and Dr. Olivier MONGIN who gave me many helps in experiments and measurements, and I have a wonderful experience in this excellent research team.

I also need to thank other scientists and colleagues: Prof. Marek SAMOK (NLO Z-scan) and Dr. Mireille BLANCHARD-DESCE (NLO TPA) for the cooperated measurements; Mr. Philippe JÉHAN for mass measurements and Mr. Clément ORIONE for ^{13}C NMR measurements; Mr. Gwénael COLOMBEL for equipment help.

I enjoyed my time with the PhD students in lab: Katy, Alison, Ayam, Nicolas, Amédée, Suzan, Xu and Wenyan. They are dynamic, friendly and always helpful when I was in trouble. I am very grateful for the friendship of them. My gratitude to my friends in INSA de Rennes: Bai Cong, Zhang Jinlin, Peng Linning, Wang Hongquan, Ji Hui, Yi Xiaohui, Zhao Yu, Zhang Shunying and Fu Hua.

Give my special appreciation to my family: my parents and my brother encouraged me to continue my study; my husband Xiao supported me both in experiments and live; I also thank my little baby Yuncong, his coming is my best gift!

Contents

Chapter 4 The influence of linkages in dendron: porphyrin dendrimers with bridged vinyl and alkynyl

Chapter 5 Porphyrin oligomers: linear Dimer and star Trimer

Chapter 1

Introduction on porphyrin chemistry And photophysical properties

1.1 Background for porphyrin chemistry

Porphyrins are well known as functional fragment appearing in many fundamental biological representatives. Heme proteins with iron porphyrin serve as follow: O_2 storage and transport (myoglobin and hemoglobin), electron transport (cytochromes b and c), and O_2 activation and utilization (cytochrome P450 and cytochrome oxidase). Chlorophylls, containing magnesium ion in chlorin center, are widely distributed in photosynthetic apparatus of plants and bacteria: use very elaborate light harvesting systems to capture dilute sunlight and funnel this energy to the reaction center through rapid and efficient transfer processes.[1] Moreover, the role of porphyrins in photosynthetic mechanisms indicates a good attitude of these molecules to mediate visible photon-electron energy transfer processes.

For these reasons, porphyrins have attracted considerable attention because of their prospective applications in mimicking enzymes,[2] catalytic reaction,[3] photodynamic therapy,[4] optic-electronic devices,[5] data storage,[6] and solar cells.[7] In particular, numerous porphyrins based artificial light-harvesting antennae,[8] and donor-acceptor dyads[9] and triads[10] have been prepared to improve our understanding of the photochemical aspect of natural photosynthesis.

1.1.1 Porphyrin dendrimer

Nowadays, amount of covalently linked porphyrin dendrimers[11] have been synthesized all over the world, many of them involve energy donor dendrons around the porphyrin core as an antenna system to optimize their optical properties. In this case, phenyl,[12] t-butyl,[13] truxene,[14] and fluorenyl[15] were usually chosen as light-harvesting antenna in energy donor dendron.

For the series of porphyrin dendrimers with fluorenyl unit or oligofluorene, there are already many publications reported. The group of Bo has synthesized some porphyrins dendrimers bearing linear oligofluorene arms as red light-emitting materials.[16] They also studied a series of hyperbranched polymers with fluorenyl

porphyrin as peripheral groups[17] or linked groups.[18] Fréchet[19] demonstrated that the antenna effect was facilitated in dendritic architectures *versus* the corresponding linear case and reported the synthesis of porphyrin systems with modified fluorenyl units as light-harvesting two-photon absorbing chromophores.[20] Porphyrin derivatives with multifluorenyl substituents were also applied in OLEDs as deep red emitters.[21] Thus, fluorenyl as one important light absorber was also occurred frequently in our synthetic porphyrin dendrimers.[22]

We further focus on porphyrin dendrimers containing π-conjugated rigid dendrons, which have a great progress these years:[23] Burn and Samuel reported different methods to synthesize porphyrin dendrimers with stilbene dendrons and studied their electro-optical and energy transfer properties.[24] In the group of Okada and Kozaki, a series of multi-porphyrin in conjugated networks was obtained as an efficient light-harvesting antenna.[8,13a,25]

1.1.2 Porphyrin oligomer

Because of the square planar 18-π macrocycle structure, more and more porphyrin oligomers were constructed in different arrays with covalent bonds,[10b,26] metal coordination bonds[27] or intermolecular interaction.[28] In construction of porphyrin oligomers, the group of Osuka did much work in synthesis, properties and application: *meso-meso* linked porphyrin arrays,[29] giant porphyrin wheel,[30] and porphyrin box.[31]

To construct porphyrin oligomer, *β* and *meso* positions of porphyrin monomer are usual linked points of large linear,[32] cyclic,[33] and cage[34] oligomers. Sometimes, some templates were needed to obtain multiporphyrin arrays with large hole diameter.[35] Porphyrin assemblies involving coordinate bond could as well construct porphyrin oligomers.[36]

Recently, we have reported some conjugated linear porphyrin dimer[37] and trimer,[38] and porphyrin assemblies[39] by linked coordination bond.

1.2 Structure

1.2.1 Porphyrin's structure

Porphyrin macrocycle, owning a highly conjugated planar structure, is formed by four tetrapyrrolic subunits linked by four methine bridges, and this aromatic system consists of 22 π-eletrons but only 18 of them are delocalized to form π-eletron ring according to the Hückel's rule of aromaticity (4n+2 delocalized π-electrons, where n=4 not 5), as shown in Figure 1.1. In porphyrin macrocycle, these carbon atoms are mainly named into three types: *α*, *β* and *meso*; in addition, *β* and *meso* positions are both active substituted points which could provide different porphyrin-cored derivatives in symmetric or asymmetric structures (Figure 1.1).

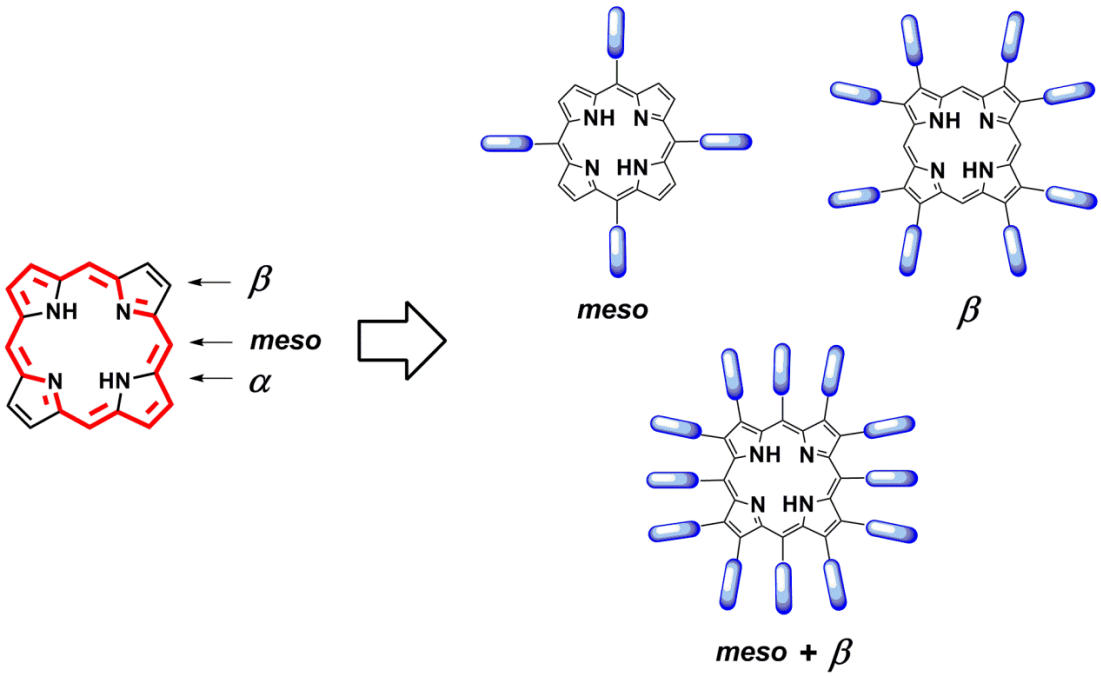

Figure 1.1 Conjugated planar structure of porphyrin and different porphyrin-cored derivatives.

1.2.2 Porphyrin dendrimer's structure

To construct a porphyrin dendrimer, porphyrin ring as a light-harvesting group could be inserted in different positions of dendritic macromolecules as see in Figure 1.2: porphyrin cored dendrimer, porphyrin bridged dendrimer and porphyrin

terminated dendrimer. For porphyrin cored dendrimer, because of two active positions, β and *meso* points, the dendron could also be linked in *meso*-, β-, or, *meso*- and β-positions. During this thesis, we mainly synthesized a series of *meso*-porphyrin cored dendrimers and studied their optical properties.

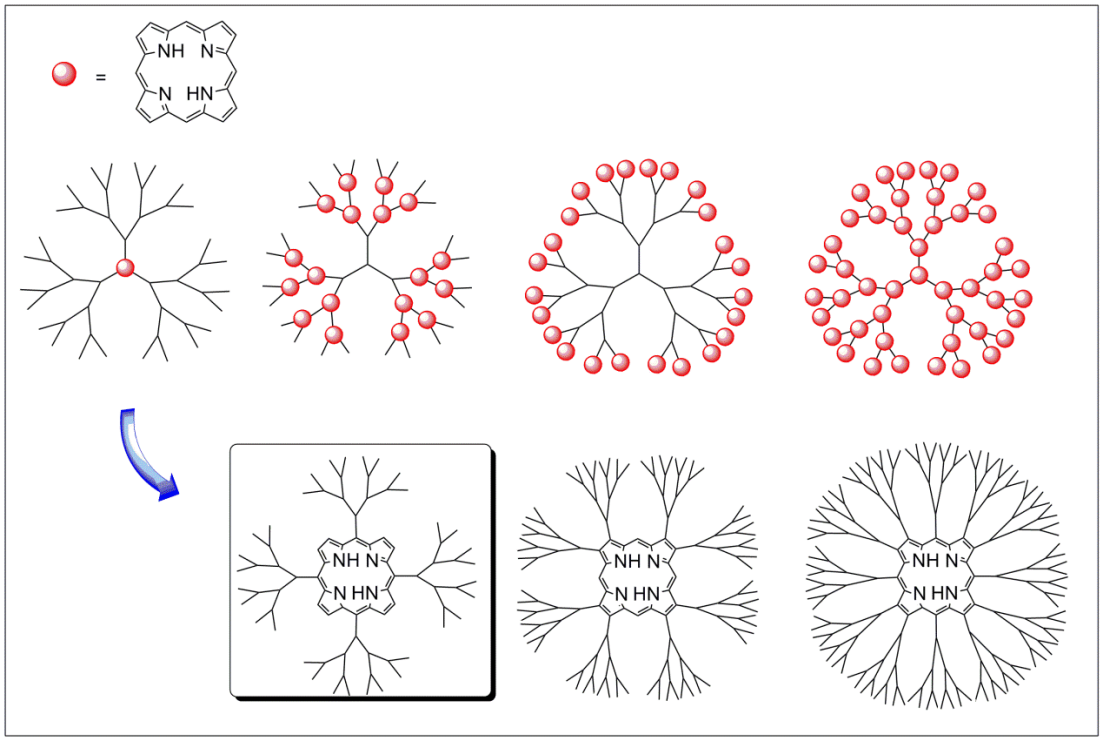

Figure 1.2 Porphyrin dendrimers with different structures.

1.3 Optical properties

Porphyrins, because of their fascinating feature on characteristic UV-visible spectra, have absorbed much interests from physicists and chemists many years on explanation of their particular spectra.[40] All the porphyrins have two distinct absorption regions: near-ultraviolet and visible regions, giving these compounds their striking colours.

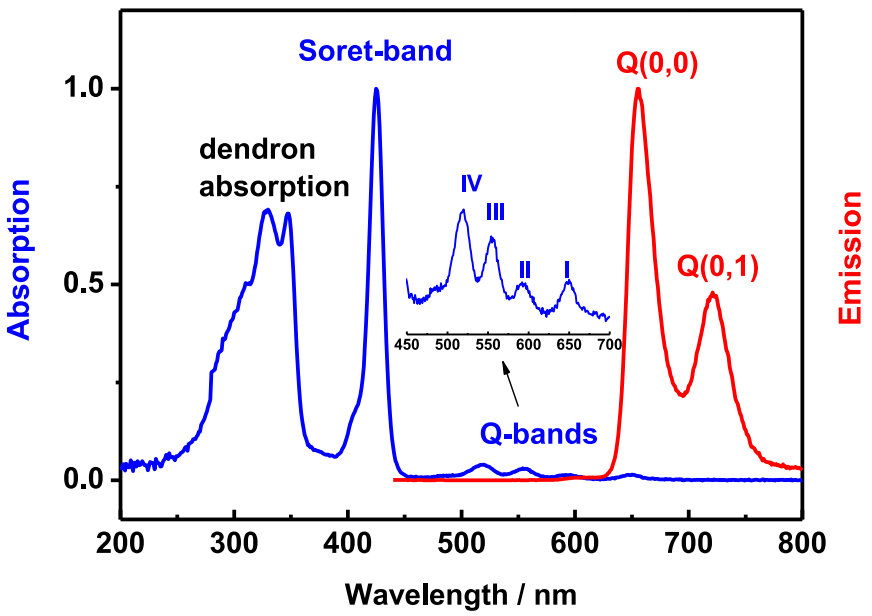

Figure 1.4 Absorption and emission spectra of a free-based *meso*-porphyrin dendrimer.

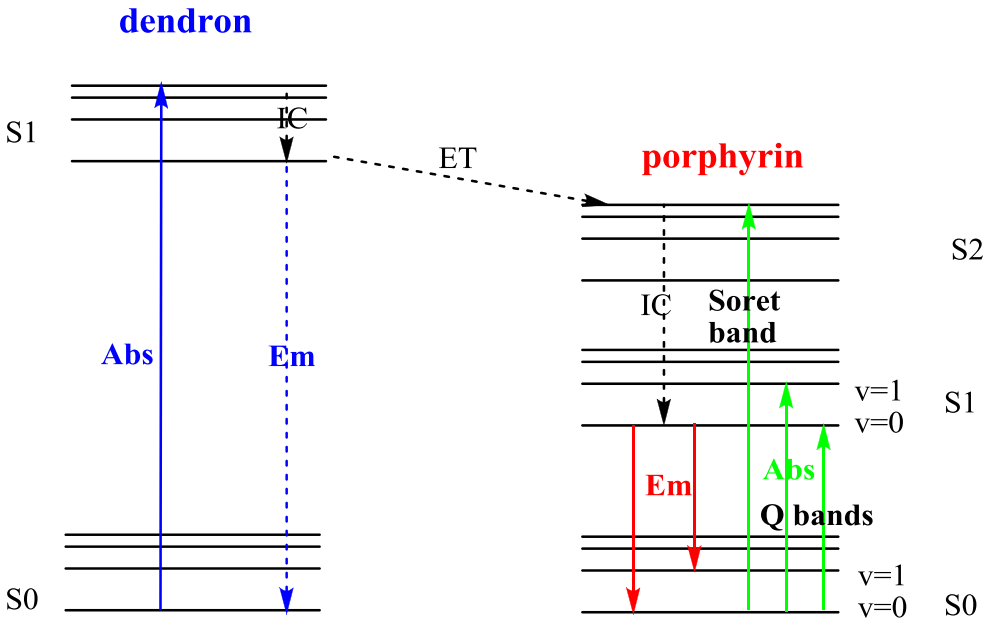

Figure 1.5 Jablonski energy-level diagram for a free-based porphyrin dendrimer.

1.3.1 Absorption spectrum of porphyrin

The electronic absorption spectrum of a typical porphyrin consists of two instric transitions (see Figure 1.4 and 1.5): (i) a strong transition from ground state to the second excited state (S0→S2) between 390-425 nm (depending on whether the porphyrin is β or *meso*- substituted), called the Soret band (or B band); and (ii) two to four weak transitions from ground state to the first excited state (S0→S1) situated between 480-700 nm, called Q bands.

The Soret band and the Q bands both arise from π-π* transitions, whereas, the former is strongly allowed (the extinction molar coefficient ε is in order of 10^5 $M^{-1}cm^{-1}$) and the later are only weakly allowed (the extinction molar coefficient ε is in order of 10^4 $M^{-1}cm^{-1}$). It can be explained by considering the Gouterman four orbitals model (HOMO and LUMO frontier orbitals).[41]

1.3.2 Q-bands and porphyrin structure

Q-bands are due to transitions to the vibrationless S1 state and higher vibrational levels in the S1 state. The number and intensity of them can give powerful clues to the substitution pattern of the porphyrin and whether it is metallized or not. This leads to classify porphyrin absorption spectra due to the number and relative intensity of the Q bands: a metal-free porphyrin or metalloporphyrin, a porphyrin with substituents on the pyrrole β or *meso*-positions, or, a protonated porphyrin.[42]

(a) Metal-free porphyrin, as free base, has four Q bands, denoted by increasing wavelength as Q_{IV}, Q_{III}, Q_{II} and Q_I, (or Qy(1,0), Qy(0,0), Qx(1,0), and Qx(0,0)).

IV>III>II>I, etio-porphyrin: the β-substituents are all alkyl groups.

III>IV>II>I, rhodo-porphyrin: the β-substituents are attached directly with π-electron (e.g. electron-withdrawing carbonyl or vinyl groups). Two π-electron groups on the neighbor pyrrole units in the macrocycle cancel each other out.

III>II>IV>I, oxo-rhodo-porphyrin: two π-electron groups are on opposite pyrrole units.

IV>II>III>I, phyllo-porphyrin: the β-positions are left unsubstituted (usually no less than four), or a *meso*-position is occupied.

(b) Metalloporphyrin, with metal cation, leads to reduction of two protons of the central nitrogens. Macrocycle is more symmetrical than free-base porphyrin so that its Q-bands spectrum generally consists only in two bands, denoting α- and β-bands (the former at longer wavelength than the latter):

α>β, the metal forms a stable square-planar porphyrin complex.

(e.g. Ni(II), Pd(II), Sn(IV), Cd(II))

α<β, the metal is easily displaced by protons.

(c) Protonation of the porphyrin, with two more protons in central nitrogens, also has more symmetrical macrocycle than free base porphyrin. It produces a simplification of Q band spectrum that can lead to profound color changes and the four Q bands collapse to two.

1.3.3 Emission spectrum of porphyrin

Internal conversion from S2 to S1 is rapid, so the emission of the free-base porphyrin is only detected from S1. It shows two peaks: one strong peak around 600 nm corresponding to the 0-0 transition, and a weaker peak around 700 nm due to the 0-1 transition. (See Figure 1.4 and Figure 1.5)

1.3.4 Energy transfer in porphyrin cored dendrimer

Energy transfer process could take place via the interaction between an excited donor group (D*) and a ground-state acceptor group (A), without emitting a photon when transferring energy. To realize the energy transfer, the spectral overlap of donor emission and acceptor absorption is necessary (see Figure 1.6), so that the energy lost from excited donor to ground state could turn to excite the acceptor group. Therefore, to enhance the energy transfer efficiency, the donor group should firstly have good abilities to absorb photons and emit photons, that is, with a high extinction coefficient and a high quantum yield. Generally, the more spectral overlap of donor emission and acceptor absorption is observed, the more efficient energy transfer occurs from this donor to the acceptor.

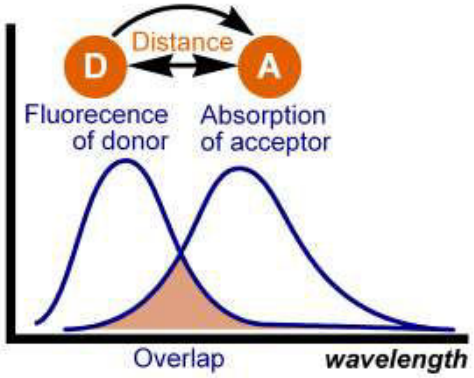

Figure 1.6 Spectral overlap between donor emission and acceptor absorption.

During photoinduced energy transfer process, the distance between donor and acceptor is also an important dependent factor, developing two mechanisms involved frequently in scientific literatures: **Dexter energy transfer** and **Förster resonance energy transfer**, as shown in Figure 1.7 and Figure 1.8.

(a) **Dexter energy transfer (DET)**

This mechanism is described as short-range, collisional or exchange energy transfer which is a non-radiative process with electron exchange, and it was first theoretically proposed by David L. Dexter in 1953.[43] Besides the overlap of emission spectra of D and absorption spectra of A, the exchange energy transfer needs the overlap of wavefunctions, that is, the overlap of the electron cloud. It means it can only occur at short distances, typically within 10 Å. The short distance making energy transfer happen is almost comparable to the collisional diameter.

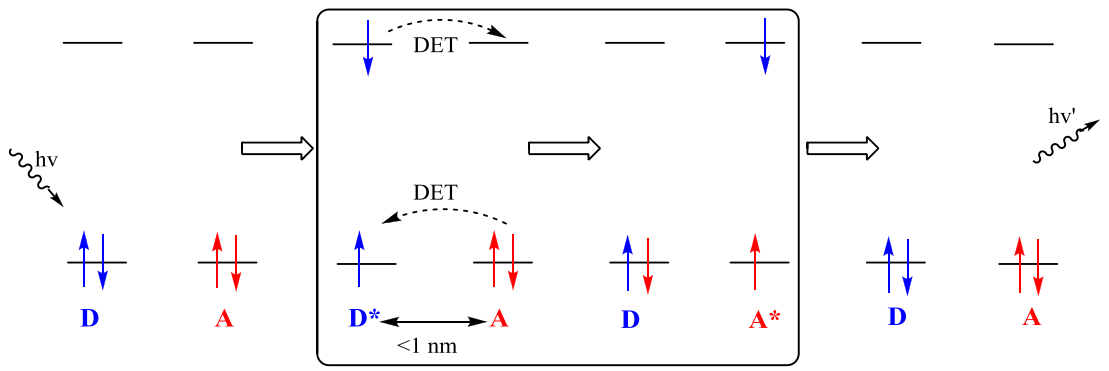

Figure 1.7 Schematic diagram for Dexter energy transfer.

(b) **Förster resonance energy transfer (FRET)**

The Förster resonance energy transfer is the discovery of a german physical chemist Theodor Förster.[44] This mechanism is described that an excited donor (D*) could transfer energy (not an electron) to excite a ground-state acceptor (A) through a non-radiative dipole-dipole coupling.[45] In other words, it bases on the Coulombic interaction between donor and acceptor. This process is highly distance-dependent, and it is effective only when the relative distance of Coulombic interaction between D-A pair is longer than the electron exchange energy transfer but smaller than 100 Å. The resonance energy transfer mechanism is also affected by the orientations of the emission transition dipole of D and the absorption dipole of A.

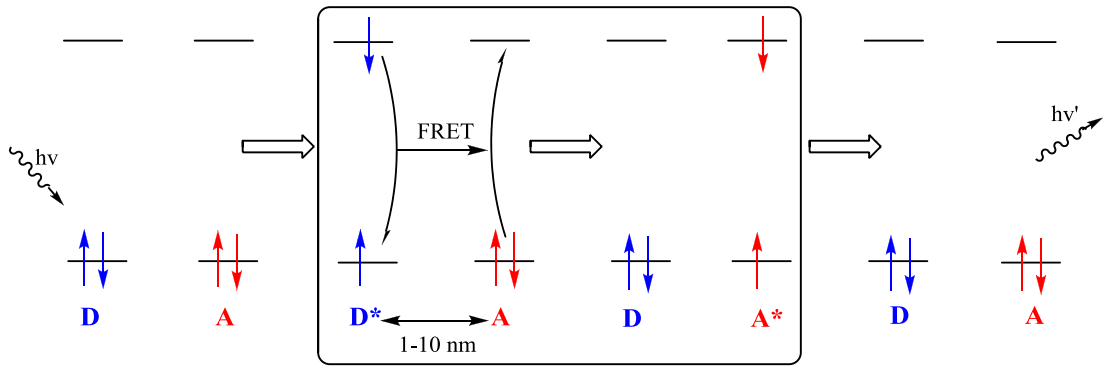

Figure 1.8 Schematic diagram for Förster energy transfer.

The process also could be shown in Jablonski diagram (Figure 1.9): A donor group D is excited by a photon and then relaxes to the lowest excited singlet state S1(D*). If the distance allows energy transfer, then the S1(D*) energy releases to the ground state S0(D), and simultaneously excites the acceptor group A to the lowest excited singlet state S1(A*) through non-radiative process. After excitation, the excited acceptor emits a photon and returns to the ground state S0(A).

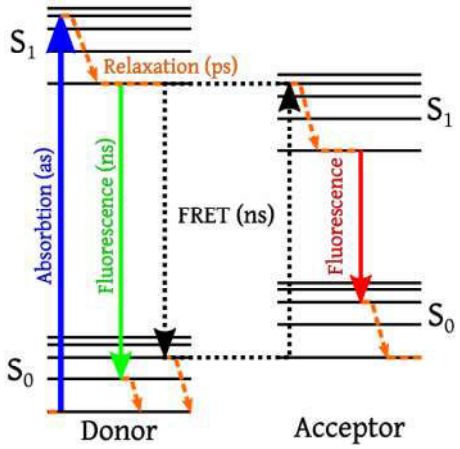

Figure 1.9 Jablonski diagram for Förster energy transfer.

Therefore, a suitable dendron chosen for a porphyrin-cored dendrimer could be benefit to transfer energy from dendron donor to porphyrin acceptor, when there are more spectral overlap between dendron emission and porphyrin core absorption.

1.4 Synthetic methods

1.4.1 Synthesis of porphyrin core

Rothemund in 1935 firstly obtained tetraarylporphyrins in one step by reaction of pyrrole and benzaldehyde in pyridine in a sealed flask at 150 °C for 24 h,[46] but the yield was very low and the experimental conditions were so severe.[47] From then on, the synthesis of porphyrin and its derivatives have undergone nearly 80 years. Nowadays, the synthesis of porphyrin core was mainly realized under two simple and practical conditions: **Adler-Longo's** [48] and **Lindsey's**[49] methods.

(a) **Adler-Longo's method**

Adler and Longo, in the 1960s, developed an alternative approach that the reaction were carried out by aromatic aldehyde and pyrrole under acid catalyzed condensation in a glassware open with air oxidation.[48] The conditions were optimized in different solvents and concentrations range of reactants, with the yields of porphyrins up to 20-40% (Figure 1.10).

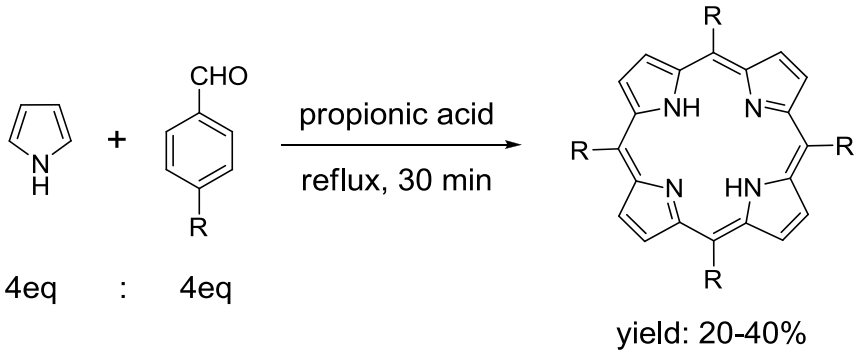

Figure 1.10 Adler-Longo's method for *meso*-substituted porphyrins.

(b) **Lindsey's method**

Over the period 1979-1986, Lindsey's group developed a new two-step synthetic strategy to form substituted porphyrins under more gentle conditions for condensation of aldehyde and pyrrole (Figure 1.11): in CH_2Cl_2 solvent with TFA or BF_3 etherate as acidic catalyst and *p*-chloranil as oxidant.[50] The Lindsey synthetic approach was more feasible for the larger scale synthesis[51] and obtained much higher yields of substituted tetraphenylporphyrins with the addition of salts.[52]

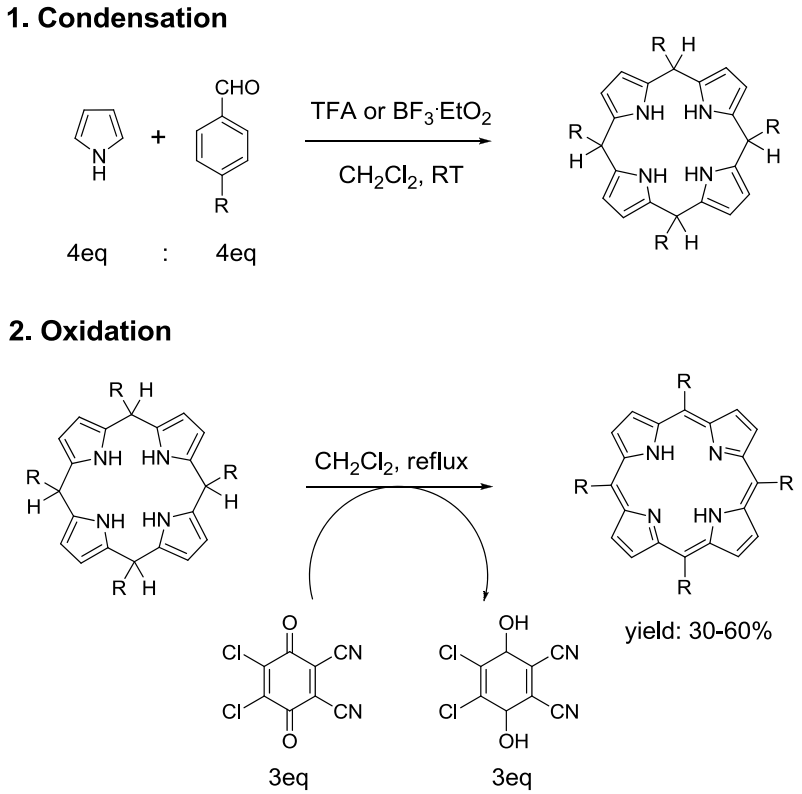

Figure 1.11 Lindsey's method for *meso*-substituted porphyrins.

1.4.2 Synthesis of dendrimer

Dendrimers are classified by generation, which refers to the number of repeated branching cycles that are performed during its synthesis. Each successive generation results in a dendrimer roughly twice the molecular weight of the previous generation. Higher generation dendrimers also have more exposed functional groups on the surface. Dendrimers can be considered to have three major portions: the core, the branches, and the end groups. Synthetic processes can also precisely control the size and number of branches on the dendrimer. There are two defined routes of dendrimer synthesis, **divergent** route and **convergent** route, as well as *meso*-porphyrin cored dendrimer synthesis (Figure 1.12).[53]

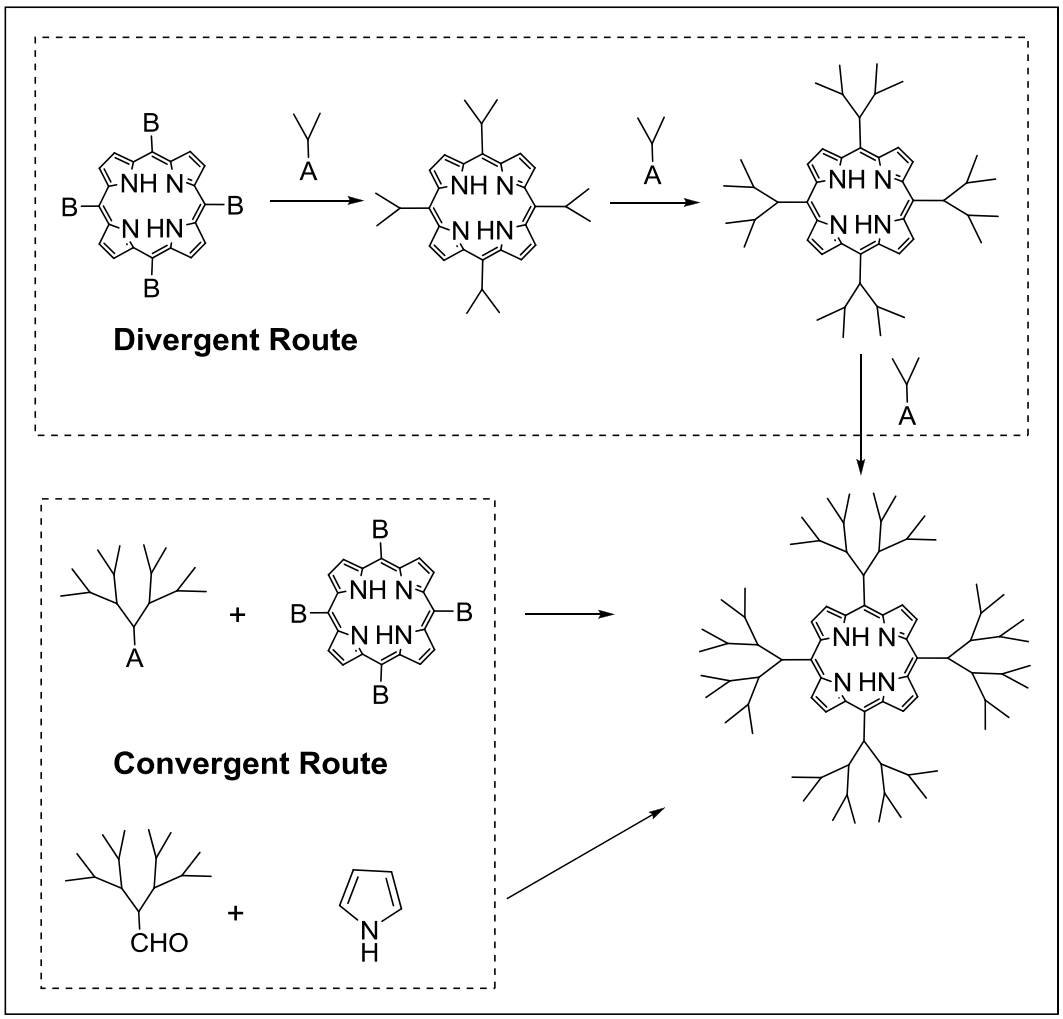

Figure 1.12 Synthetic routes of *meso*-porphyrin cored dendrimer.

(a) **Divergent route**

Dendrimer is assembled by generation, from a multifunctional core being extended outward by a series of repetitive reactions of active end group with new fragment. Each step of the reaction needs to overcome steric hindrance of end groups to prevent structural defects of dendrimer causing trailing generations (some branches are shorter than the others). Such impurities can impact the functionality and symmetry of the dendrimer, and they are extremely difficult to purify out because the relative size difference between perfect and imperfect dendrimers is very small.

(b) **Convergent route**

In this strategy, dendron should be formed firstly by repetitive inward reaction of active fragments, and subsequently final dendrimer can be created by reaction of a multifunctional core and this active dendron. For the high generation of dendrimer, firstly high generation of dendron is needed to be synthesized. This method makes it much easier to remove impurities and shorter branches along the way, so that the final dendrimer is more monodisperse. However dendrimers made by this route are not as large as those made by divergent one because crowding due to steric hindrance along the core still results in the difficulty to isolate mixtures with different numbers of dendrons.

In parallel, for *meso*-porphyrin cored dendrimers, there is another convergent route: using modified aldehyde dendron to react with pyrrole to create porphyrin core directly, resulting in the final *meso*-porphyrin cored dendrimer. This route would provide unique product easily, but the yield is usually low dependent on the generations of desired dendrimer and dendron.

1.5 Porphyrins in our group

These years in our group, many porphyrin-based derivatives were synthesized in different fields (see Figure 1.13): dendrimers,[54] supramolecular assemblies,[39] oligomers,[37,38] Pt and Pd complexes (OLEDs),[55] electropolymers,[56] organometallic Ru and Fe complexes (NLO properties).[57]

Here, we particularly focused on two important aspects as further study directions: porphyrin dendrimer and oligomer:

For porphyrin-based dendrimer, it was reported efficient light-harvesting systems in which 5,10,15,20-tetraphenylporphyrin (TPP) was linked, *via* ether bridges, to four, eight and sixteen fluorenyl donor moieties.[54c]

For porphyrin-based oligomer, some zinc or free-base linear dimer and trimer were obtained, and their steady-state optical properties,[37,38] energy transfer process[37,38] and two photons absorption measurements[58] have been studied recently.

Therefore, in our new attempts, we wondered to obtain more efficient π-extended conjugated porphyrin-based dendrimers and oligomers with new structures and to study the optical property-structure correlation.

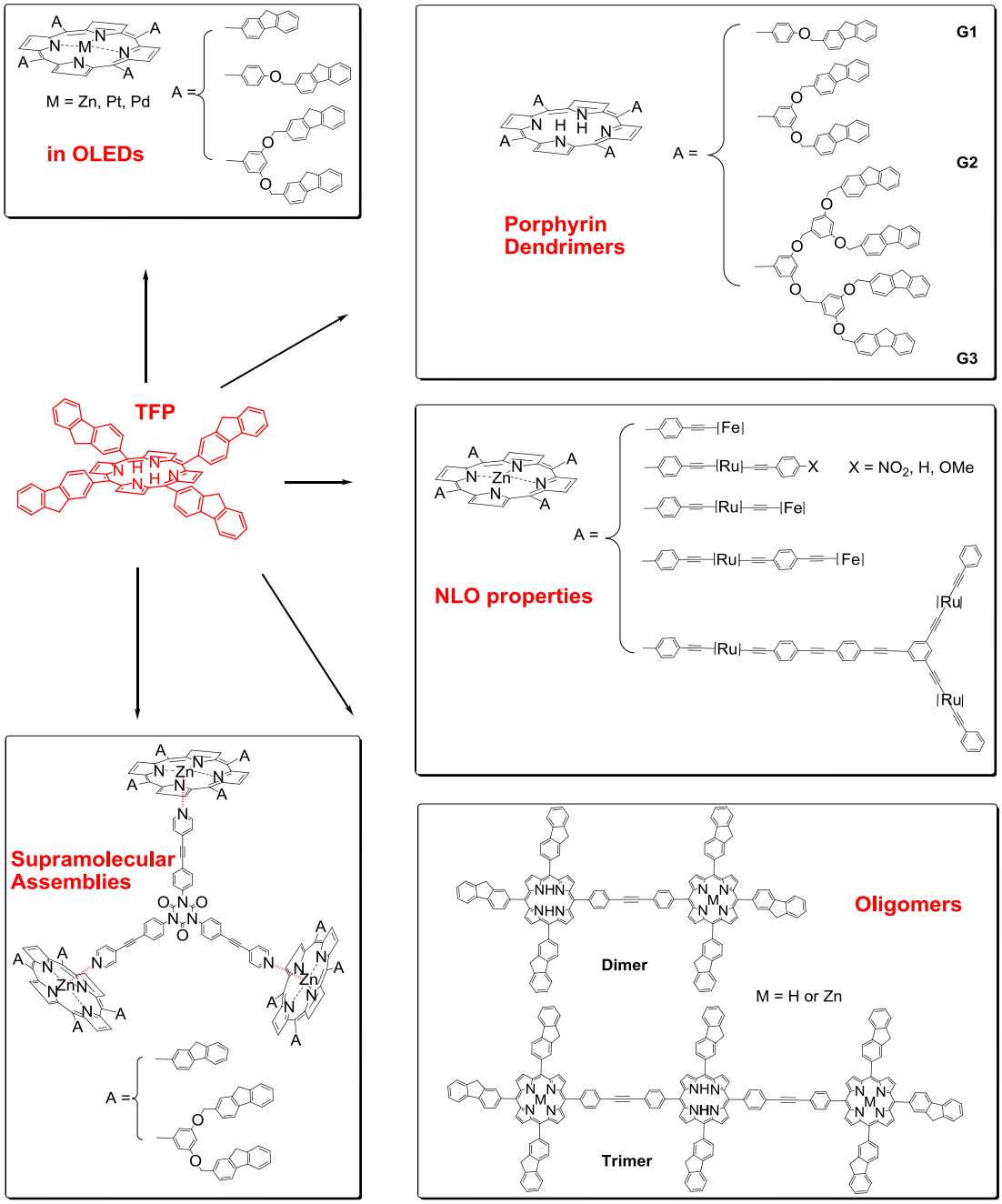

Figure 1.13 Porphyrin-based derivatives in our group.

1.6 Design of this PhD thesis

Fluorenyl group is a classic chromophore which absorbs around 300 nm ultra light and emits about 400 nm violet light, meanwhile, porphyrin core absorbs usually from 400 to 600 nm visible light. So connecting fluorenyl and porphyrin core could result in: firstly, there is obvious spectral overlap existing between fluorenyl and porphyrin core, in favour of proceeding energy transfer process from donor fluorenyl to acceptor porphyrin core; secondly, enlarge the absorption region of porphyrin, forming a light-harvesting system.

Along this line, we designed a series of conjugated *meso*-porphyrin cored dendrimers in different structures (see Figure 1.14) in order to study the influence on their optical properties:

(i) Fluorenyls in phenyl-alkynyl bridged dendron as terminated groups: the influence of dendron's structure

(ii) Fluorenyls in phenyl-alkynyl bridged dendron as cored, as bridged and as terminated groups: the influence of donor's positions

(iii) Dendron with alkynyl bridged or vinyl bridged: the influence of conjugated linkage

On the other hand, we designed as well two new porphyrin terminated oligomers with more fluorenyls in different structures (see Figure 1.15):

(i) Linear free-base dimer: two terminated tetrafluorenylporphyrin (TFP) linked and conjugated by fluorene

(ii) Star free-base trimer: three terminated TFP linked and conjugated by benzene.

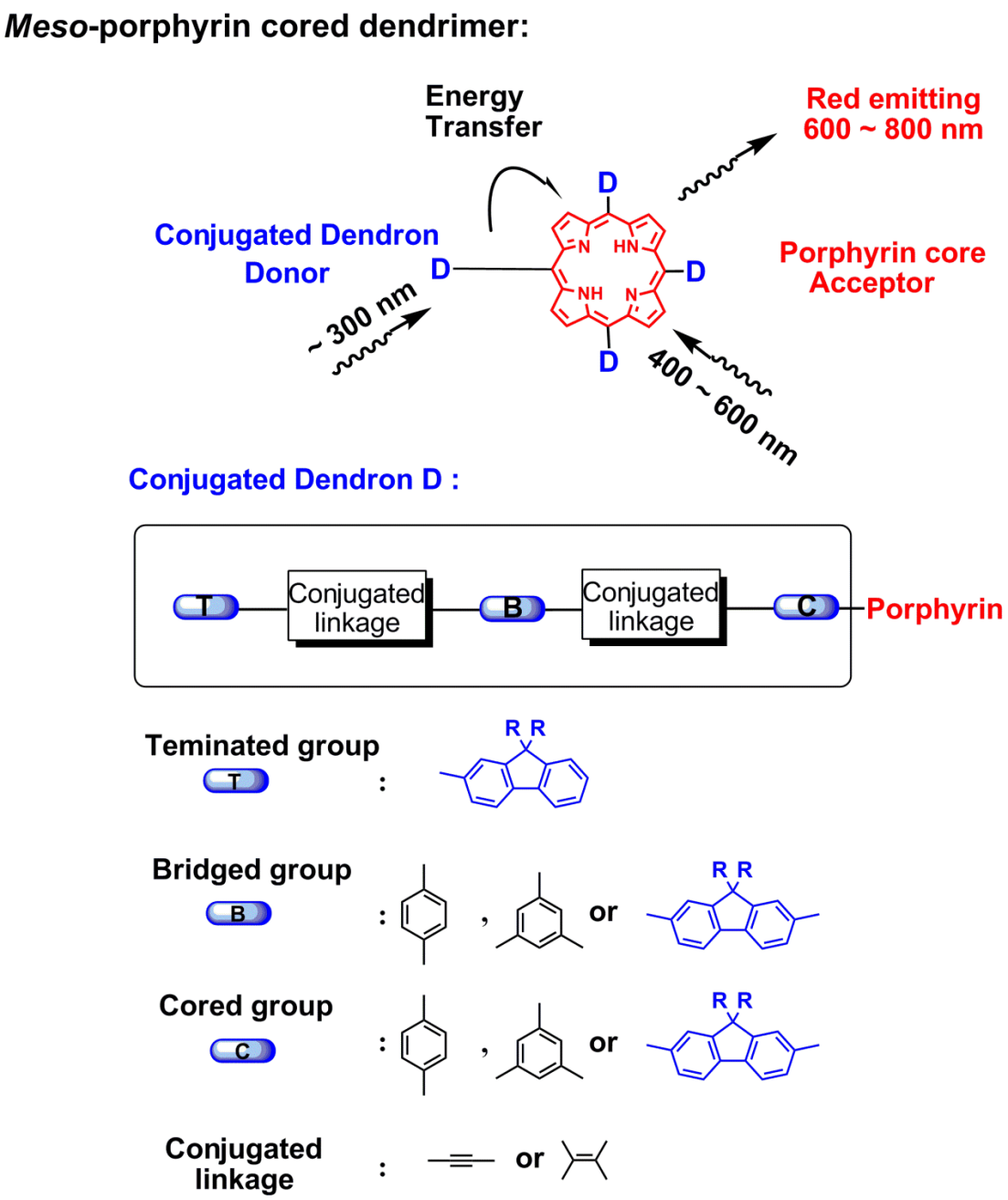

Figure 1.14 Structures of *meso*-porphyrin cored dendrimers.

Porphyrin-terminated oligomers:

Linear Dimer

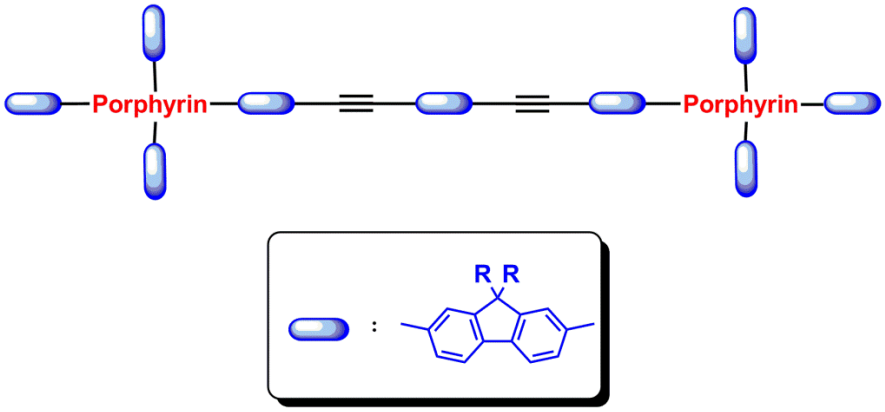

Star Trimer

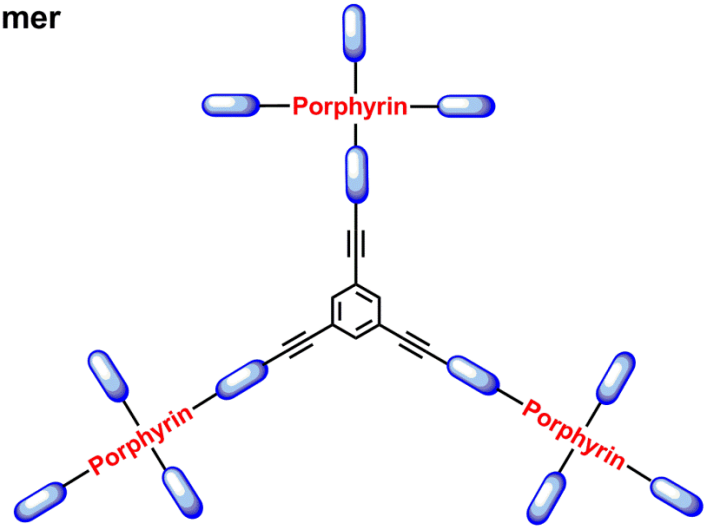

Figure 1.15 Structures of porphyrin-terminated oligomers.

General experimental procedure

^{1}H NMR spectra were recorded on BRUKER Ascend 400 at 298K.

^{13}C NMR spectra were recorded on two spectrometers: BRUKER Ascend 400 (for **TPP1-TPP6**), and BRUKER Ascend 500 (for **TFP1-TFP3** and **TPP-D**, **TFP-D**, **Monomer**, **Dimer** and **Trimer**).

High-resolution mass spectra were recorded on two different spectrometers: Bruker MicrOTOF-Q II, and a Thermo Fisher Scientific Q-Exactive in ESI positive mode.

Microanalysis was collected on Microanalyseur Flash EA1112 (for **TPP1-TPP6** and **TFP1**, **TFP2**).

UV-visible absorption and photoluminescence spectroscopy measurements for porphyrin dendrimers and oligomers in solvents (distilled CH_2Cl_2 and HPLC level toluene) were performed on BIO-TEK instrument UVIKON XL spectrometer and Edinburg FS920 Fluorimeter (Xe900) at room temperature, respectively.

Quantum yields were measured in toluene at room temperature, taking TPP (Φ =11%) as reference.

Fluorescence lifetime (for **TPP1-TPP6**) in toluene was measured on Edinburg FL920 Fluorescence Lifetime Spectrometer, and time-correlated single-photon counting using pulsed laser excitation at 426 nm was employed.

All the optical measurements were achieved in dilute solutions taking the same condition as standard: when porphyrin Soret-band maximum absorption intensity was near to 0.1 on UV-visible spectrometer.

Reaction reagents were purchased from commercial suppliers. Some solvents in reactions were distilled in common methods, except that DMF and $^{i}Pr_2NH$ were dried by 3 Å molecular sieves, and some solvents used without further purification were otherwise stated.

Chapter 2

The influence of substituted positions in cored group: TPP-cored porphyrin dendrimers with Bridged phenyl-alkynyl and terminated fluorenyl

2.1 Molecular design

5,10,15,20-tetraphenylporphyrin (**TPP**) was studied as a classic porphyrin for many years, in chemical-physics fields.[59] Many chemists were encouraged to design and synthesize some new structures of TPP-cored porphyrin and porphyrin dendrimers:[60] symmetric and asymmetric, conjugated and non-conjugated, free-based and metallic, covalent and coordinated, etc.

In our studies, we exploit that the phenyl unit substituent in TPP has mainly two positions easy to expand: *para*-position (A) and *meta*-position (B), as shown in Figure 2.1.

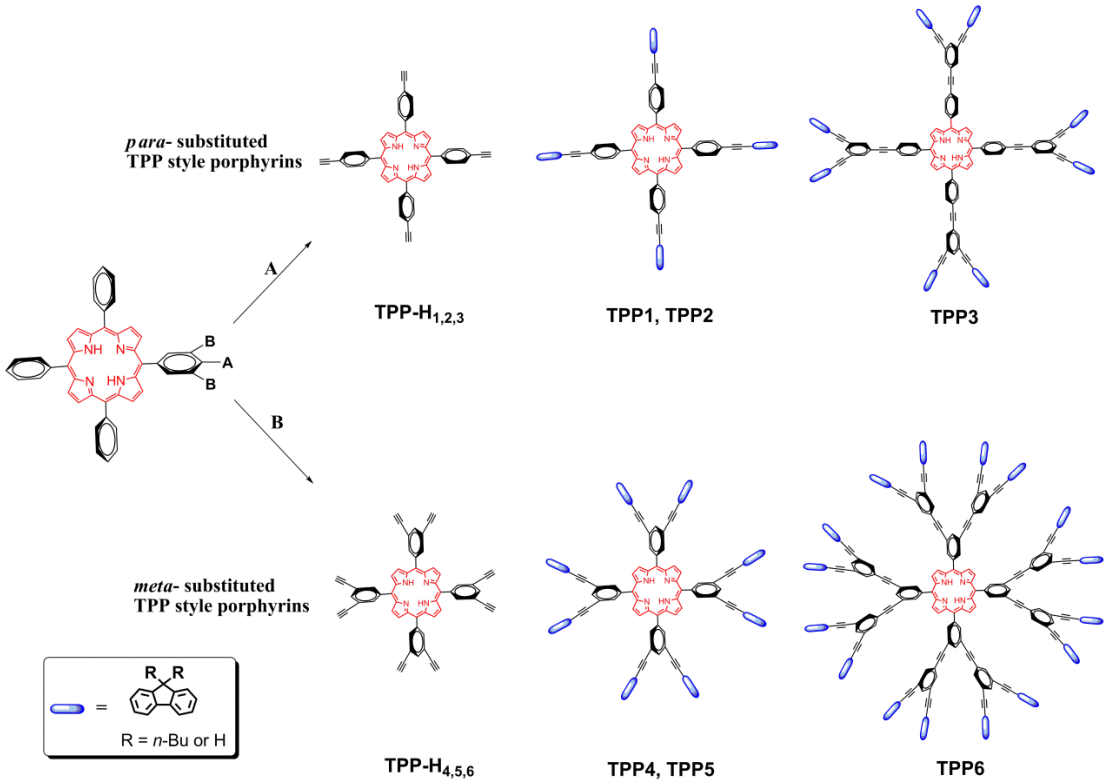

Figure 2.1 Molecular structures of TPP-cored porphyrin dendrimers **TPP1-TPP6** and their reference molecules **TPP-H$_{1,2,3}$** and **TPP-H$_{4,5,6}$**.

In consequence, expansion of conjugated dendron in these different positions would be discussed concerning the relationship between optical properties and structure. Based on parent porphyrin TPP, we designed and synthesized two groups of

new TPP-cored porphyrin dendrimers owning phenyl-alkynyl π conjugated dendron with fluorenyl terminals. We named them as *para*-substituted TPP-cored porphyrin dendrimers (**TPP1**, **TPP2** and **TPP3**) and *meta*-substituted TPP-cored porphyrin dendrimers (**TPP4**, **TPP5** and **TPP6**), respectively.

The second group of porphyrin dendrimers has more fluorenyl terminals because of two *meta*-substituted positions (B) on the phenyl, providing much denser ambient light absorbers as light-harvesting system. Dendrimers **TPP4** and **TPP5** have similar structure: they both possess 8 fluorenyl arms but **TPP5** has *n*-butyl substitutent on fluorenyl. **TPP6**, possessing 16 *n*-butyl substituted fluorenyl arms, is the second generation of **TPP4** and **TPP5**. For this *meta*-substituted family, porphyrin **TPP-H$_{4,5,6}$** is the reference.

2.2 Synthetic method design

2.2.1 ***Design 1****:* Divergent route, adding gradually active dendritic parts to porphyrin core to afford a new porphyrin dendrimer series.

At first, Design 1, the classic divergent route adopted in many publications, was considered to synthesize **TPP4**: a porphyrin possessing eight fluorenyl arms linked by triple-bonds. Triple-bond was introduced by Sonogashira coupling[61] and deprotection of TMS was achieved using K_2CO_3 in mixed solution of MeOH and CH_2Cl_2.

In this case, two different divergent routes, (I) and (II), were tried under similar reaction conditions (Figure 2.2): (I) bromo-porphyrin (8BrTPP) reacted with eight equiv of alkynyl-fluorene (**1**) and (II) alkynyl-porphyrin (**TPP-H$_{4,5,6}$**) reacted with eight equiv of bromo-fluorenyl. These two routes afforded a mixture of porphyrins which were difficult to separate and the target porphyrin was not detected by TLC (thin layer chromatography). This was probably due to the weak solubility of desired porphyrin **TPP4**, subsequently observed when we obtained this compound by Design 2.

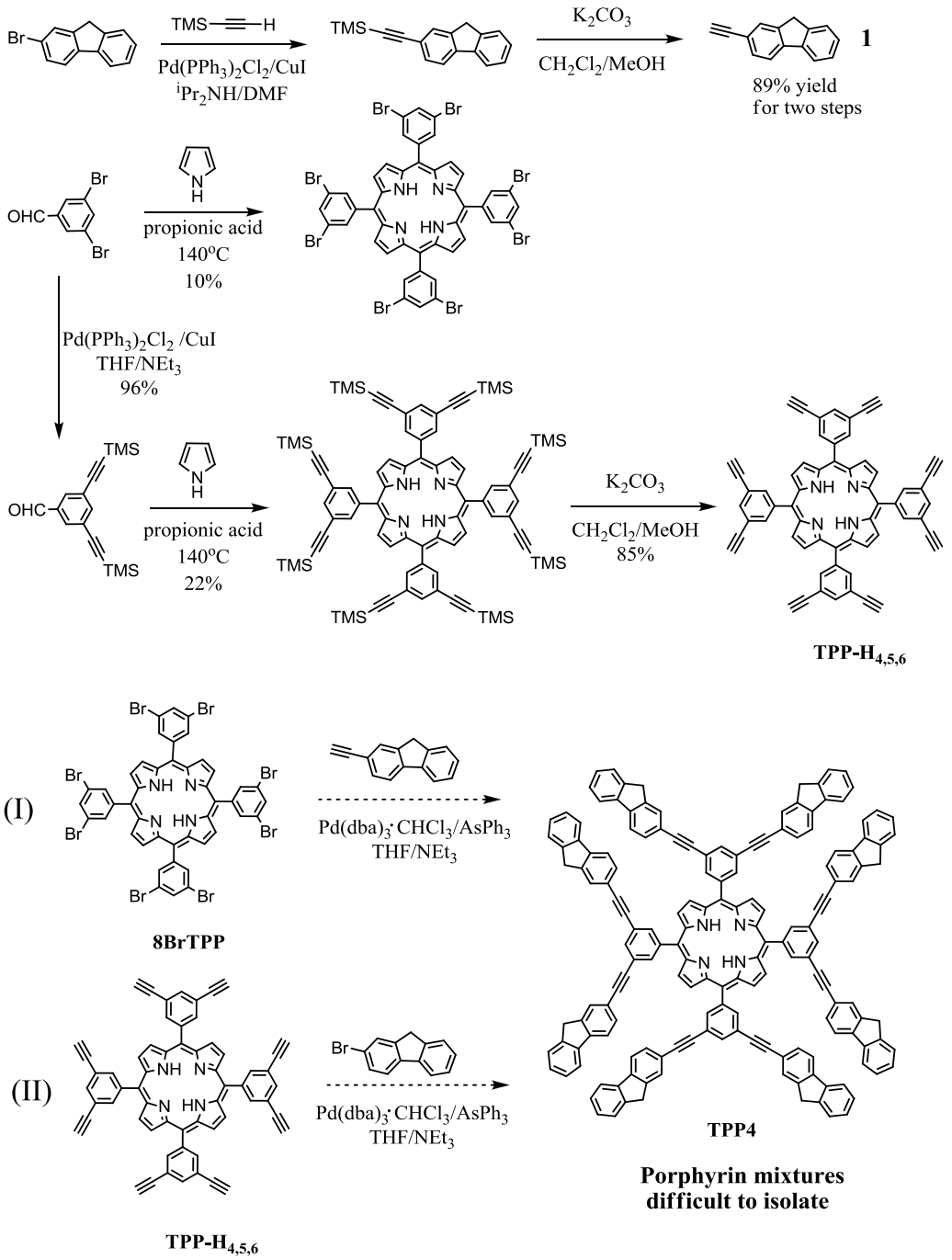

Figure 2.2 Two divergent routes (I) and (II), based on primary porphyrins to obtain **TPP4**. (Design 1)

Therefore, we abandoned this strategy for porphyrin dendrimers **TPP1-TPP6**. However, their reference analogue **TPP-H$_{1,2,3}$** for **TPP1-TPP3**, and **TPP-H$_{4,5,6}$** for **TPP4-TPP6**, respectively, were prepared successfully using Design 1 with good yields: porphyrin core synthesis has about 20-30% yield and deprotection of TMS is

up around 90% yield.

2.2.2 ***Design 2****:* Convergent route in two steps, (1) synthesis of modified aldehyde dendron, and (2) synthesis of porphyrin core.

(1) Synthesis of modified aldehyde dendron.

During the synthesis of aldehyde dendrons (Figure 2.3 and 2.4), we observed that aldehyde group could react with 9-*H* of fluorene in Sonogashira coupling conditions. So protection of the aldehyde was necessary (Figure 2.3): it was achieved using ethane-1,2-diol in toluene with 4-methylbenzenesulfonic acid (TsOH) as catalyst, and deprotection was realized in mixture solution of HCl (10%) and THF.[62]

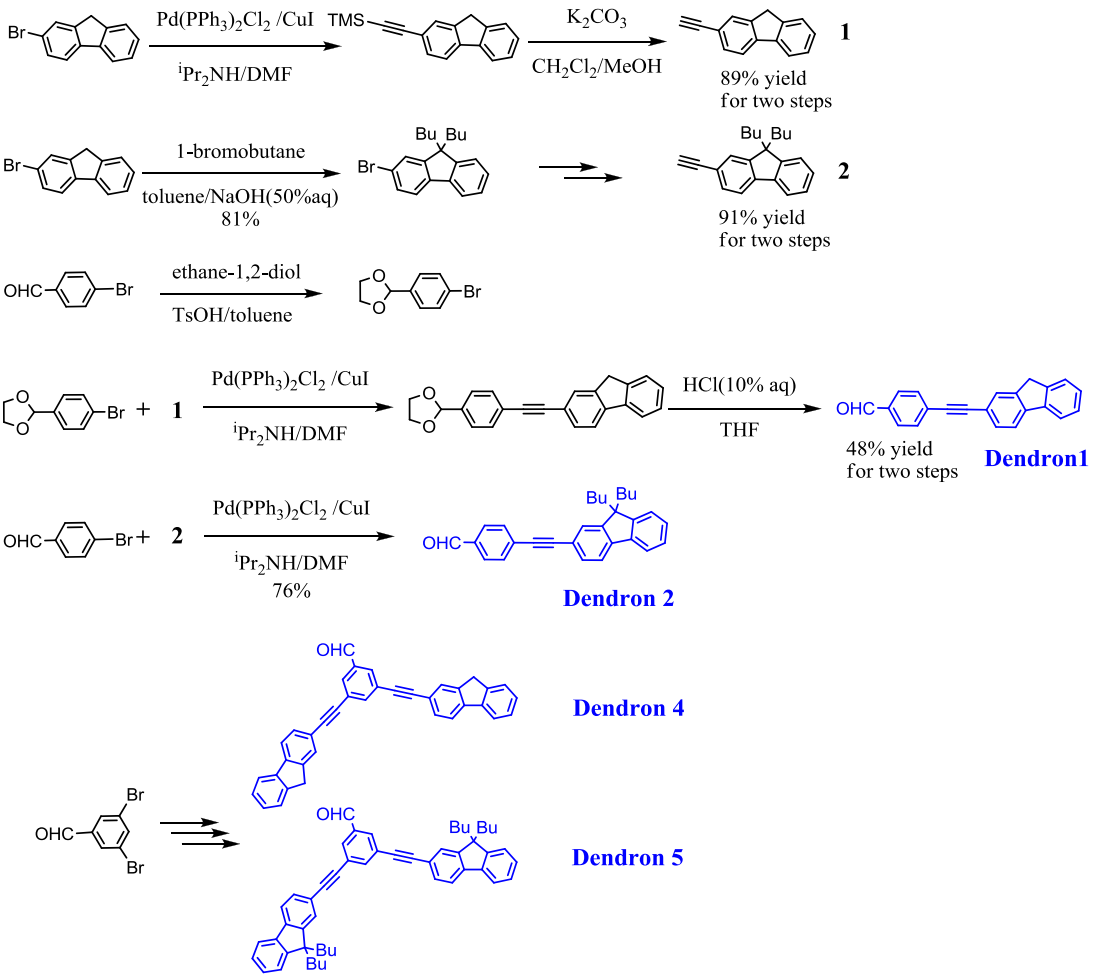

Figure 2.3 Synthesis of monofluorenyl **Dendron 1** and **2** and bisfluorenyl **Dendron 4** and **5**. (Design 2)

In parallel, 9-*H* of the fluorene group for **Dendron 1** and **4** were also replaced, with *n*-butyl to obtain corresponding **Dendron 2** and **5**, respectively. N-butyl substituted aldehydes and their final porphyrins have all better solubility. Later, during discussing the influence of carbon chains on optical properties, the spectra results showed no obvious changes.

The success for synthesizing **Dendron 3** and **6** was obtained by Corey-Fuchs reaction[63] and Sonogashira coupling.

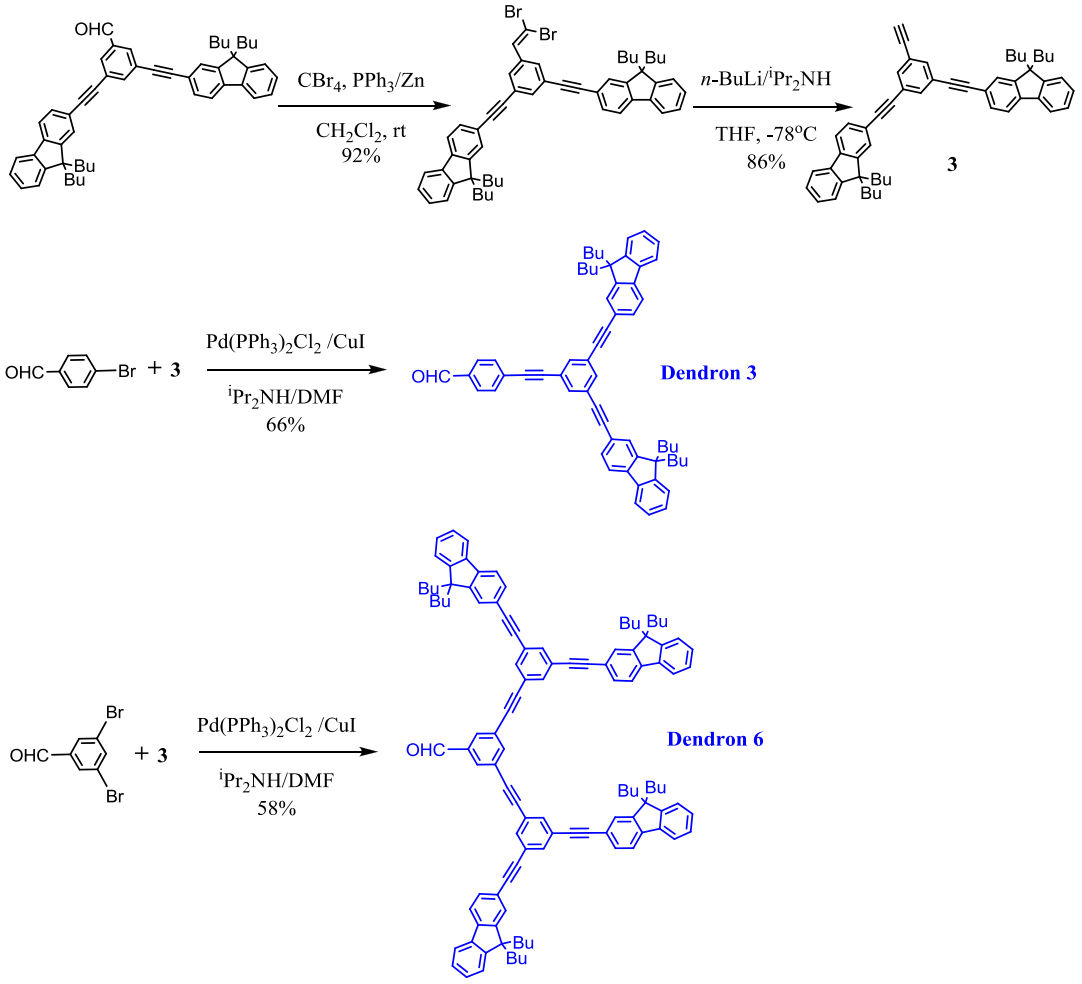

Figure 2.4 Synthesis of *n*-butyl substituted extended **Dendron 3** and tetrafluorenyl substituted **Dendron 6**. (Design 2)

(2) Synthesis of porphyrin core.

Porphyrin core syntheses are shown in Figure 2.5. Nowadays, two methods are the most used to synthesize porphyrin: Adler-Longo[48] and Lindsey[64], which are both efficient for synthesizing porphyrins substituted at the *meso* position. However, we noticed that our target porphyrins couldn't be obtained under Lindsey conditions and the reaction for synthesizing **TPP2** and **TPP5** both provided only black polymers.

Then Adler-Longo conditions were utilized successfully to synthesize target porphyrins but the yields were variable, mainly resulted from the different solubilities of modified aldehydes and generated porphyrins. For example, the non-substituted **Dendron 4**, used for **TPP4** synthesis, shows very weak solubility in propionic acid, even at high temperature, in consequence the yield for **TPP4** only reached 2%.

We must point that for purification: insoluble **TPP4** was absorbed on silica gel, on the top of the column, allowing to eliminate all byproducts and polymers by several washing with CH_2Cl_2. Finally, the pure product **TPP4** was collected by refluxing CH_2Cl_2 in an apparatus similar to Soxhlet extractor. Similar purification conditions were used to obtain **TPP1** owning 17% yield. But for corresponding **TPP5** and **TPP2** with carbon chains, the purification could be easily achieved by chromatography because of good solubility, and their overall yield raised to 18% and 28%, respectively.

For these reasons, π-extended porphyrins **TPP3** and **TPP6** were only prepared using *n*-butyl substituted **Dendron 3** and **6**. These porphyrins **TPP3** and **TPP6** were obtained in propionic acid at 140 ^{o}C for 5.5 h, yielding 22% and 13%, respectively. All the porphyrin dendrimers were further purified by recrystallization in distilled solutions of $CHCl_3$ and MeOH.

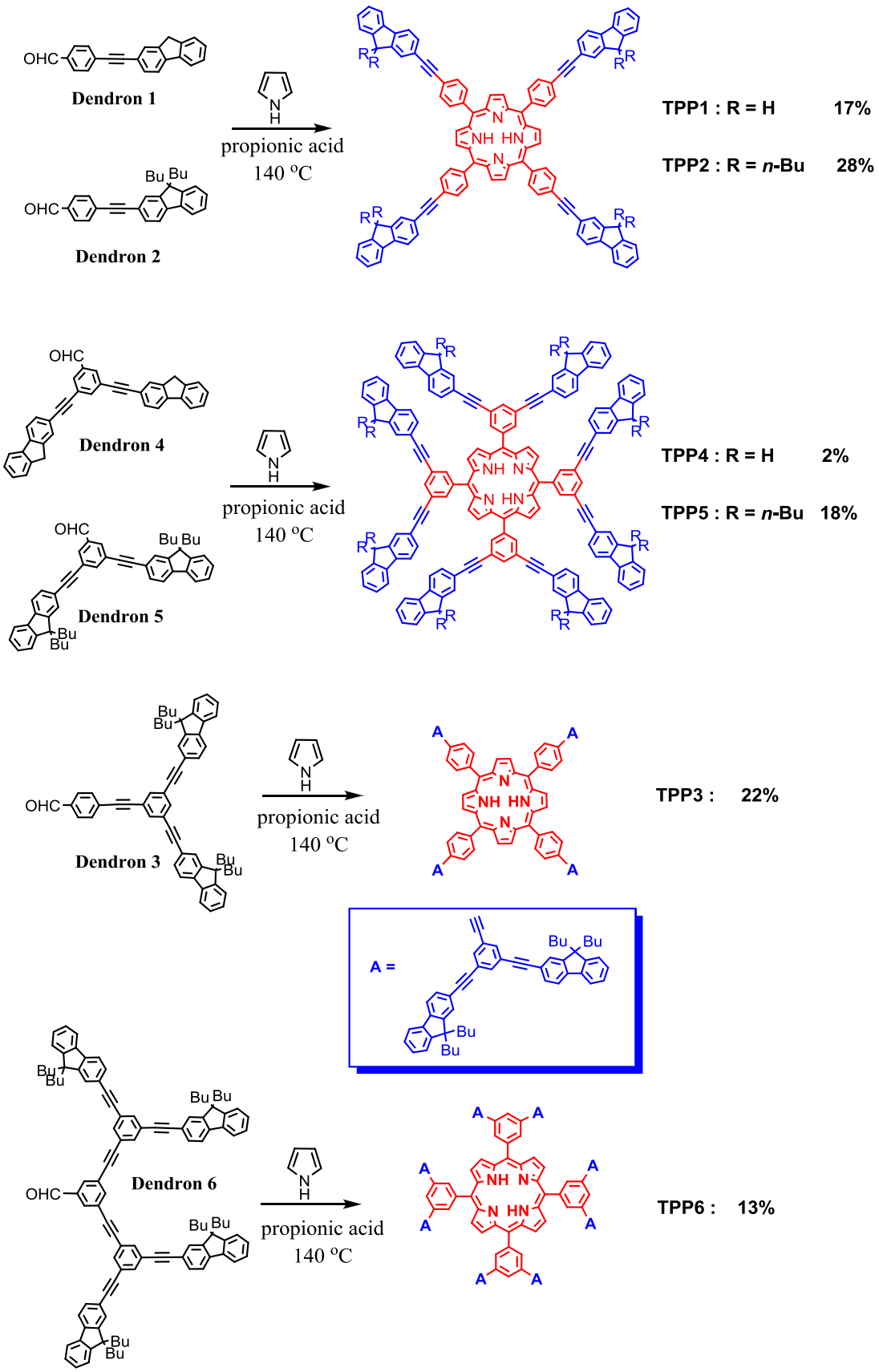

Figure 2.5 Synthesis of new porphyrin dendrimers by convergent route based on aldehyde dendrons. (Design 2)

2.2.3 ***Design 3****:* Divergent route to synthesize second generation of aldehyde **Dendron 3** and **6**.

It is worth to notice that, Design 2 for synthesizing **Dendron 3** and **6** belongs to convergent route. Then another divergent route was as well envisaged to obtain these dendrons, as shown in Figure 2.6.

1,3,5-tribromobenzene was used to synthesize desired double TMS substituted **4** under Sonogashira coupling conditions at room temperature, affording 88% yield. This product was easily isolated with few single TMS substituted byproduct by chromatography with heptane. Intermediate aldehydes **5** and **6** were synthesized in similar routes with 59% and 53% yield for two steps, respectively. But **Dendron 3** was not obtained successfully in the last step, and most of bromo-fluorene was remained and aldehyde **6** might react with itself in base solution at high temperature (75-95 ^{o}C). Very few new compound was collected, and observed to be aldehyde mixtures by ^{1}H NMR after isolation by chromatography. Therefore, rather than unsuccessful **Design 3**, for the preparation of **Dendron 3** and **6**, convergent route (**Design 2**) was definitively adopted.

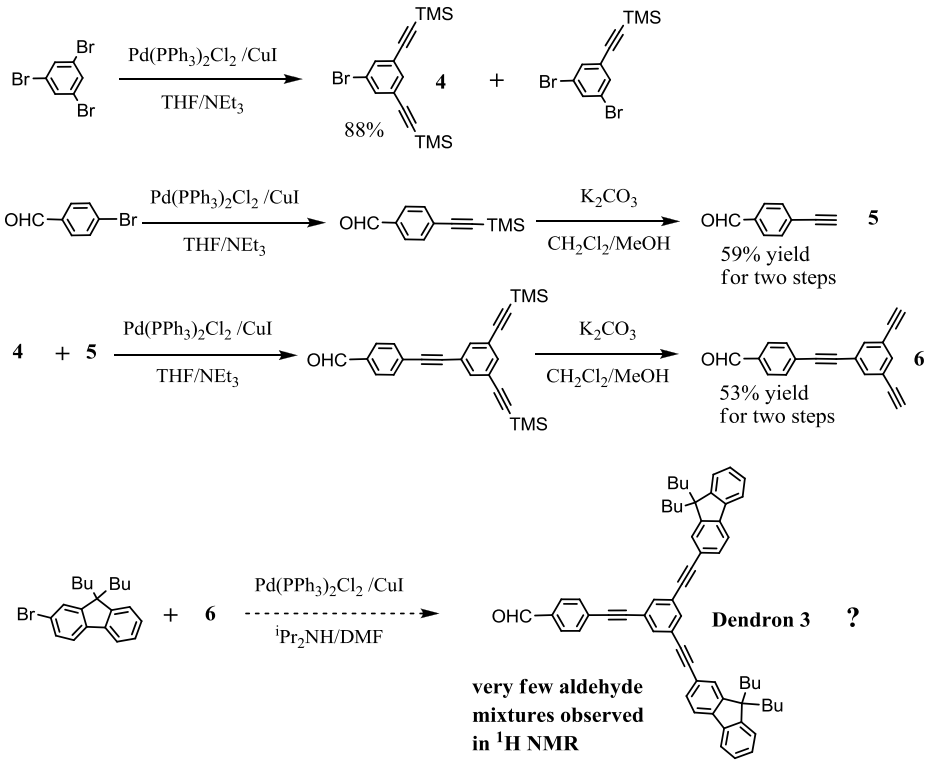

Figure 2.6 Unsuccessful divergent routes for synthesizing **Dendron 3**. (Design 3)

2.3 ^{1}H NMR analysis

Aldehyde **Dendron 1-6** and porphyrin dendrimers **TPP1-TPP6** were all well characterized by ^{1}H NMR in $CDCl_3$ (400 MHz).

2.3.1 ^{1}H NMR spectra of ***Dendron 1-6***

The protons of dendron have three components: (i) one aldehyde proton (-CHO), (ii) many aromatic protons (phenyl and fluorenyl), (iii) two 9-*H* protons in fluorenyl or four groups of protons in *n*-butyl.

Taking **Dendron 1** and **Dendron 2** as examples, fluorenyl of the former without *n*-butyl substitutent and that of the latter with *n*-butyl substitutent, their full spectra were shown in Figure 2.7. The single peak about 10 ppm is assigned to aldehyde proton. Protons around 7-8 ppm are belonging to aromatic moiety. Alkyl protons in fluorenyl, including four groups of protons in *n*-butyl around 0-2 ppm and 9-*H* around 4 ppm, are all well identified.

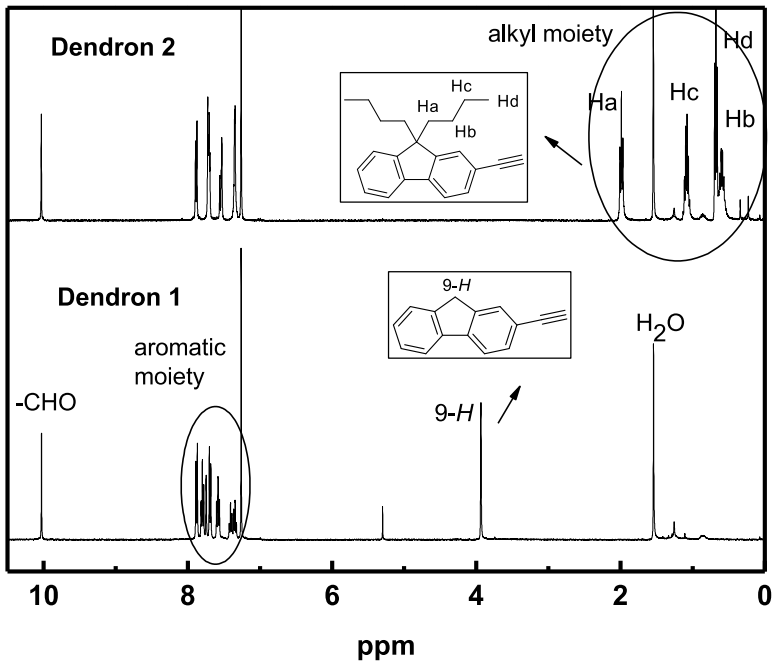

Figure 2.7 Detailed ^{1}H NMR spectra of **Dendron 1** and **Dendron 2**.

To compare protons around 7-10 ppm of **Dendron 1-6**, see Figure 2.8, the aldehyde protons have nearly no shift between **Dendron 1-6**, and the main differences focus on aromatic protons, which increase obviously with generation after normalizing the aldehyde proton signals.

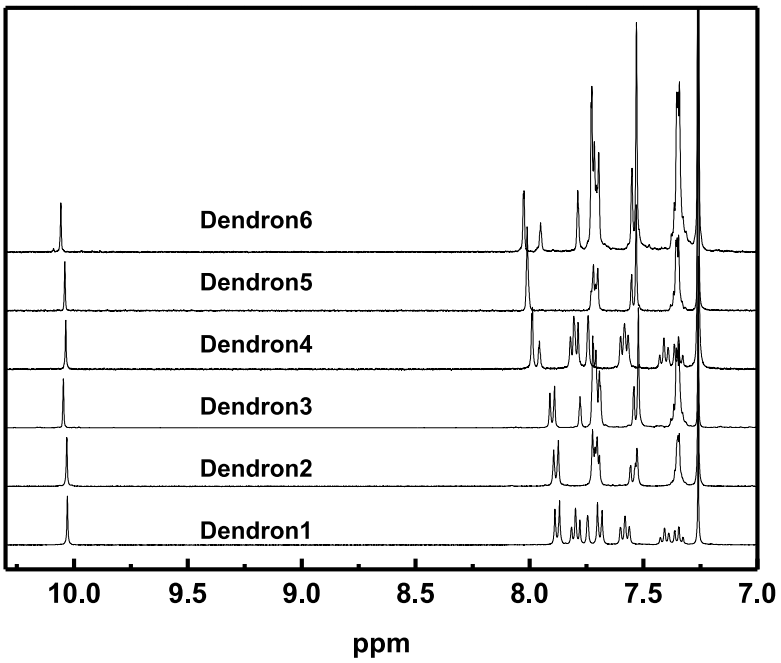

Figure 2.8 Partial ^{1}H NMR spectra of **Dendron 1-6**.

*2.3.2 ^{1}H NMR spectra of porphyrin dendrimers **TPP1-TPP6***

The protons of dendrimers **TPP1-TPP6** have four components: (i) eight protons of the pyrrole-β (porphyrin-Hβ), (ii) aromatic protons (phenyl and fluorenyl), (iii) 9-*H* protons in fluorenyl or four groups of protons in *n*-butyl, (iv) two protons in the heart of porphyrin (-NH).

Taking **TPP1** and **TPP5** as examples, fluorenyl of the former without *n*-butyl substituted and that of the latter with *n*-butyl substituted, their detailed ^{1}H NMR spectra are shown in Figure 2.9.

Two protons around -2.7 ppm and eight protons around 9 ppm are both characteristic peaks of the porphyrin macrocycle, the former belonging to hearted nitrogen atoms (-NH) and the latter assigned to pyrrole-β (Hβ). The regions between 7.2 and 8.5 ppm of **TPP1** and **TPP5** both respond to the aromatic protons from fluorenyl and phenyl. For **TPP1**, the 9-*H* protons are observed at 4.2 ppm; and for **TPP5** with *n*-butyl groups, the alkyl protons between 2.1 and 0.6 ppm could be well identified into four parts (see Figure 2.9B).

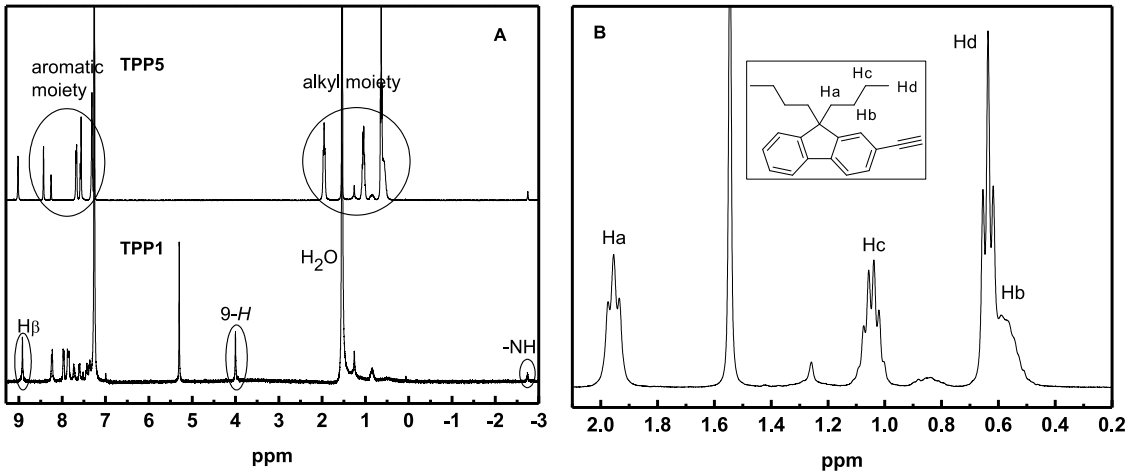

Figure 2.9 Detailed ^{1}H NMR spectra of **TPP1** and **TPP5**.

Partial ^{1}H NMR spectra of 7-9 ppm for *para*-substituted TPP-cored porphyrins (**TPP1**, **TPP2** and **TPP3**) and *meta*-substituted TPP-cored porphyrins (**TPP4**, **TPP5** and **TPP6**), are summarized in Figure 2.10, normalizing the single peak of Hβ. For *meta*-substituted TPP-cored porphyrins series, the Hβ presents a shift to the lower field compared to the *para*-substituted ones. The similar difference is also observed for the proton signals in the phenyl group of the TPP core: H_A and H_B for *para*-substituted porphyrins are located around δ = 8.2 and 8.0 ppm, and H_A and H_C for *meta*-substituted ones are located around δ = 8.4 and 8.2 ppm. The aromatic proton signals at 7.3-7.8 ppm increase obviously with generation as noticed for the dendrons.

Compared to Hβ and aromatic proton signals, alkyl protons, 9-*H* protons and -NH protons keep nearly no difference in shift between *para*-series and *meta*-ones.

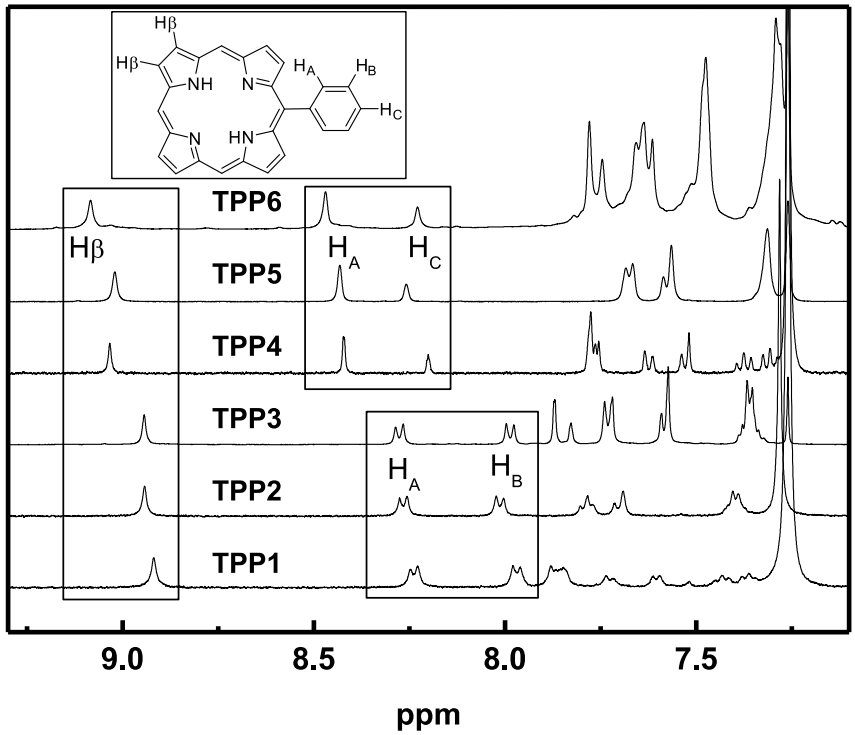

Figure 2.10 Partial ^{1}H NMR spectra of porphyrin dendrimers **TPP1**, **TPP2** and **TPP3** *versus* **TPP4**, **TPP5** and **TPP6**.

2.4 Optical properties of TPP1-TPP6

To better understand the relationships between structure and optical properties, **TPP**, **TPP-H$_{1,2,3}$**, and **TPP-H$_{4,5,6}$** are chosen as references. The molecular structures of all the porphyrins are summarized in Figure 2.11. The optical properties of the new dendrimers **TPP1-TPP6** are presented in Table 2.1.

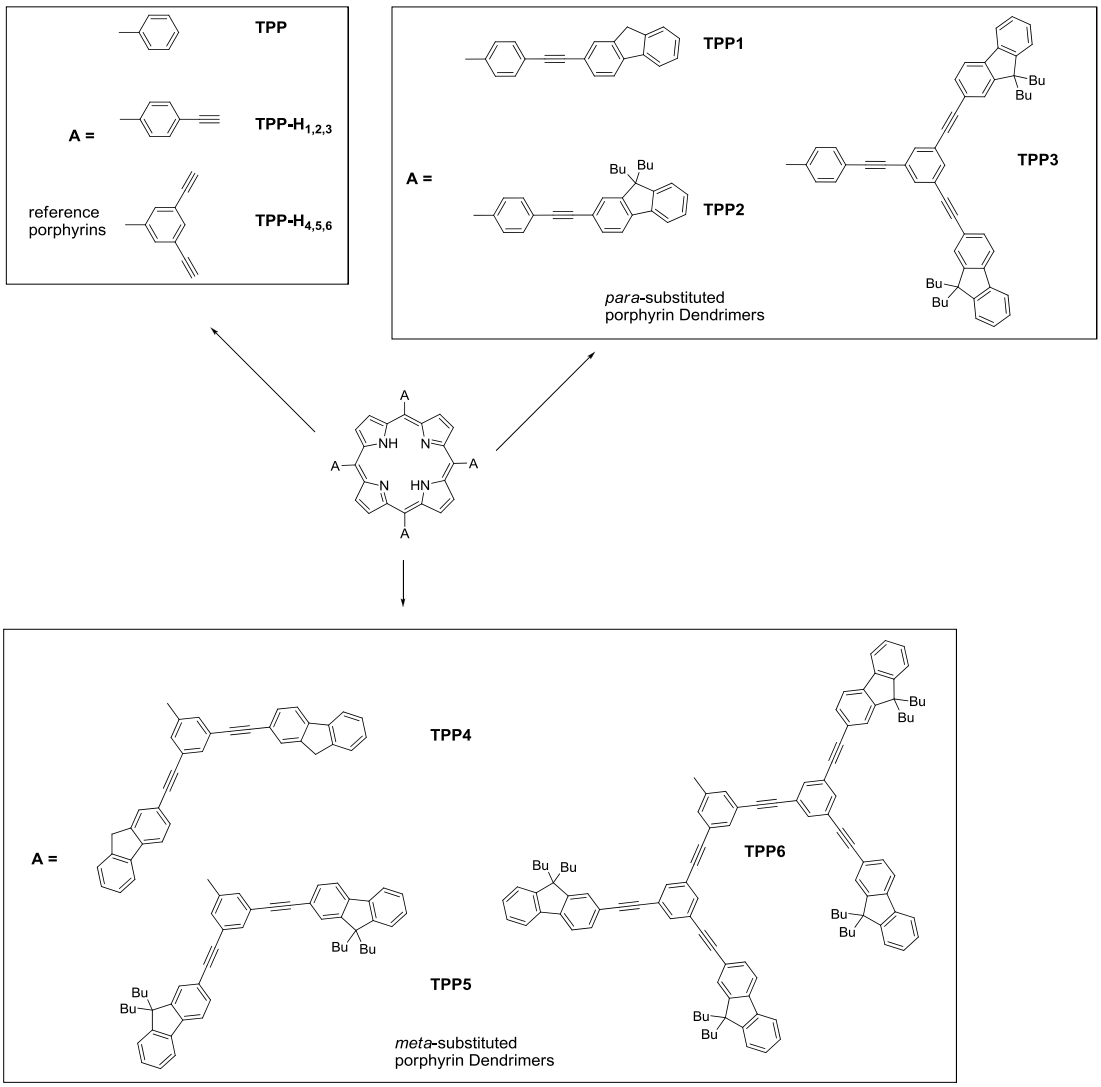

Figure 2.11 Molecular structures of reference porphyrins (**TPP**, **TPP-H$_{1,2,3}$** and **TPP-H$_{4,5,6}$**), *para*-substituted porphyrin dendrimers (**TPP1**, **TPP2** and **TPP3**) and *meta*-ones (**TPP4**, **TPP5** and **TPP6**).

2.4.1 Absorption and emission

Normalized absorption and emission spectra of reference compounds **TPP-H$_{1,2,3}$**, **TPP-H$_{4,5,6}$** and their parent molecule **TPP** are shown in Figure 2.12. Their absorption are typical for porphyrin with an intense Soret band around 420 nm, and four weaker Q-bands, Qy(1,0), Qy(0,0), Qx(1,0), and Qx(0,0), around 515, 550, 590, and 648 nm, respectively. Obvious differences concentrate on the relative intensities of Q(0,0) and Q(0,1) emission bands, which is dependent on the relative orbital energies of the excited state of the porphyrins, arising from the steric demands of rigid dendrons

causing the shape of the porphyrin core to deviate, to different degrees, from planarity.[24]

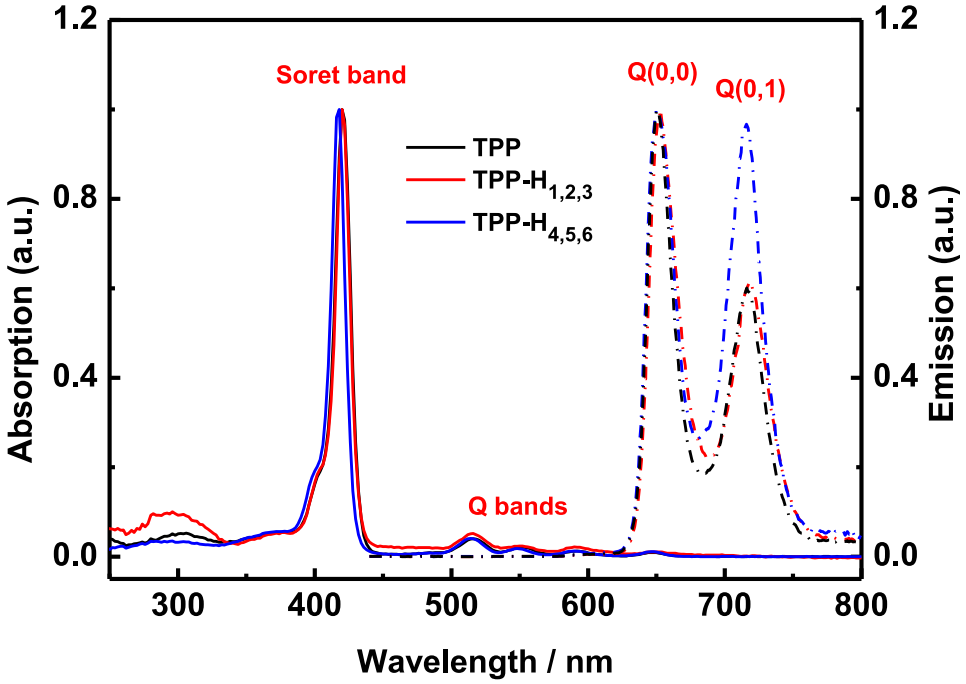

Figure 2.12 Normalized absorption and emission spectra of reference porphyrins **TPP**, **TPP-H$_{1,2,3}$** and **TPP-H$_{4,5,6}$**.

Figure 2.13 and Figure 2.14 exhibit normalized absorption and emission spectra of porphyrin dendrimers **TPP1-TPP6**, respectively. For their absorption, except the Soret-band and Q-bands, all these dendrimers show an additional band at 324-330 nm which corresponds to the absorption of the dendron with fluorenyl group.

For *para*-substituted TPP-cored porphyrin dendrimers: **TPP1**, **TPP2** and **TPP3**, possessing terminated fluorenyls in conjugated dendron, obvious absorption around 300 nm is observed, particularly compared to reference **TPP-H$_{1,2,3}$** without light absorber around porphyrin core. After respectively normalizing the intensity of Soret-band around 426 nm and emission peak Q(0,0) around 650 nm, see Figure 2.13, no change is observed between the two generations in the absorption and emission bands from porphyrin cores. It means introducing conjugated dendrons in the same

substituent position has the same influence on the planarity of cored porphyrin and so it does not have to change its shape significantly with generation.[24]

With the similar structure, **TPP2** possessing *n*-butyl chains, presents nearly no difference in the intensity of dendron absorption compared to **TPP1**. Dendrimer **TPP3**, with eight terminated fluorenyls in π-extended conjugated structure, exhibits two times stronger dendron absorption intensity than linear **TPP1** and **TPP2** with four fluorenyls, which could potentially increase energy transfer from dendron parts to porphyrin core.

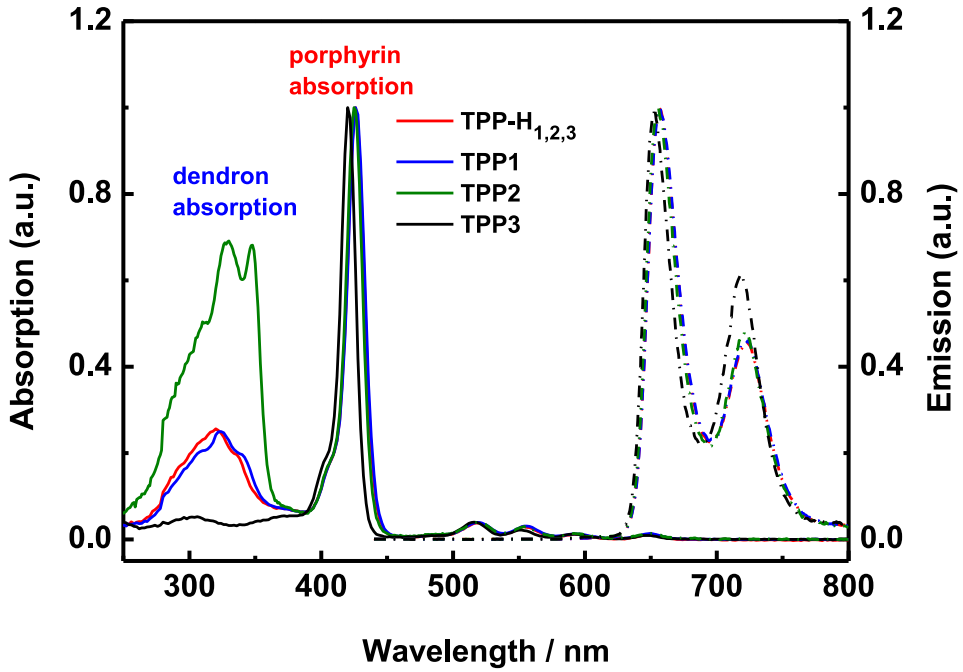

Figure 2.13 Normalized absorption and emission spectra of *para*-substituted TPP-cored porphyrins **TPP1**, **TPP2**, **TPP3** and their reference **TPP-H$_{1,2,3}$**.

The *meta*-substituted porphyrin series has denser conjugated structure and a larger number of terminated fluorenyls as light absorbers than *para*-ones. Similar phenomenon, as seen in Figure 2.14, occurs in absorption and emission spectra of *meta*-substituted TPP-style porphyrin dendrimers: **TPP4**, **TPP5** and **TPP6**. They keep similar absorption and emission of porphyrin core as **TPP-H$_{4,5,6}$** in normalized spectra,

and there is either no obvious difference between **TPP4** and **TPP5**. Surprisingly for **TPP6**, it exhibits higher dendron absorption than porphyrin core absorption. Moreover, the intensity of dendron absorption for **TPP6** is nearly three times stronger than those of **TPP4** and **TPP5**. This observation suggests that high dense array of terminated fluorenyls in conjugated dendron around porphyrin core would lead antenna absorption to become the main absorption of dendrimer, instead of porphyrin core.

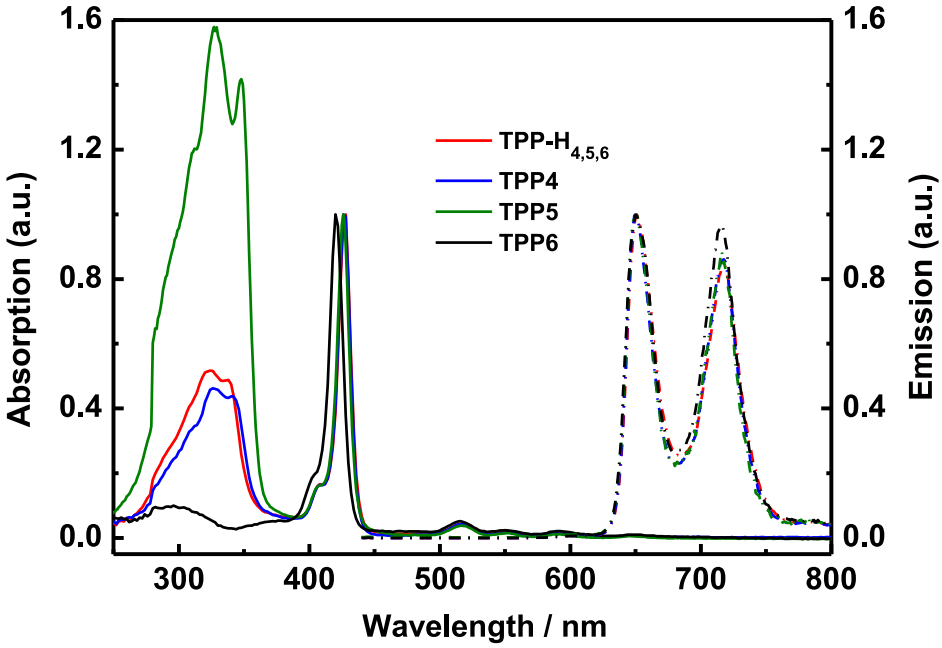

Figure 2.14 Normalized absorption and emission spectra of *meta*-substituted TPP-cored porphyrins **TPP4**, **TPP5**, **TPP6** and their reference **TPP-H$_{4,5,6}$**.

On the other hand, both **TPP3** and **TPP5** have eight substituted fluorenyl groups as light absorbers, but **TPP3** shows relatively higher dendron absorption compared to **TPP5**. This is probably due to the fact that **TPP3** has better light absorption, with a large dispersive structure decreasing the competition of terminals in space.

Table 2.1 Optical properties of dendrimers **TPP1-TPP6** in dilute CH_2Cl_2 at 298K.

	Absorption/nm[a]			Emission/nm[a] Ex=Soret-band	
	Dendron	Soret-band	Q-bands	Q(0,0)	Q(0,1)
TPP1	320	426	518,554,592,650	656	722
TPP2	324	426	518,555,592,650	657	722
TPP3	330	425	520,555,592,650	655	721
TPP4	324	427	517,552,589,646	651	718
TPP5	326	427	517,552,589,646	650	718
TPP6	327	427	517,552,590,646	651	716

a. Experiments were achieved in distilled CH_2Cl_2 with the UV-visble absorption region from 250 to 800 nm and emission region from 300 to 800 nm.

2.4.2 Energy transfer behaviors

The energy transfer (ET) from fluorenyl donors toward porphyrin acceptor is also discussed. Experiments for ET behavior were achieved at room temperature in dilute CH_2Cl_2 (distilled) solutions without degassed to eliminate intermolecular ET process.

Figure 2.15 presents the emission spectra of **TPP1-TPP6** using excitation wavelength at dendron absorption around 320 nm, compared to references **TPP-H$_{1,2,3}$** and **TPP-H$_{4,5,6}$.** These emission spectra are recorded from 300 nm to 800 nm. By taking dendron absorption as excitation wavelength, the emission spectra show only porphyrin core emission (650 nm and 720 nm) and no residual dendron emission. Meaning that, excitation of these dendrimers in the fluorenyl antennae (320 nm) only result in the red emission of porphyrins. Actually, the blue fluorenyl emission is completely quenched for all the series, and only red emission from the porphyrin is seen. This suggests that, for **TPP1-TPP6**, the absorbed dendron energy could be transferred efficiently to porphyrin core, and these dendrons could provide partly

contribution to porphyrin core emitting through this ET process.

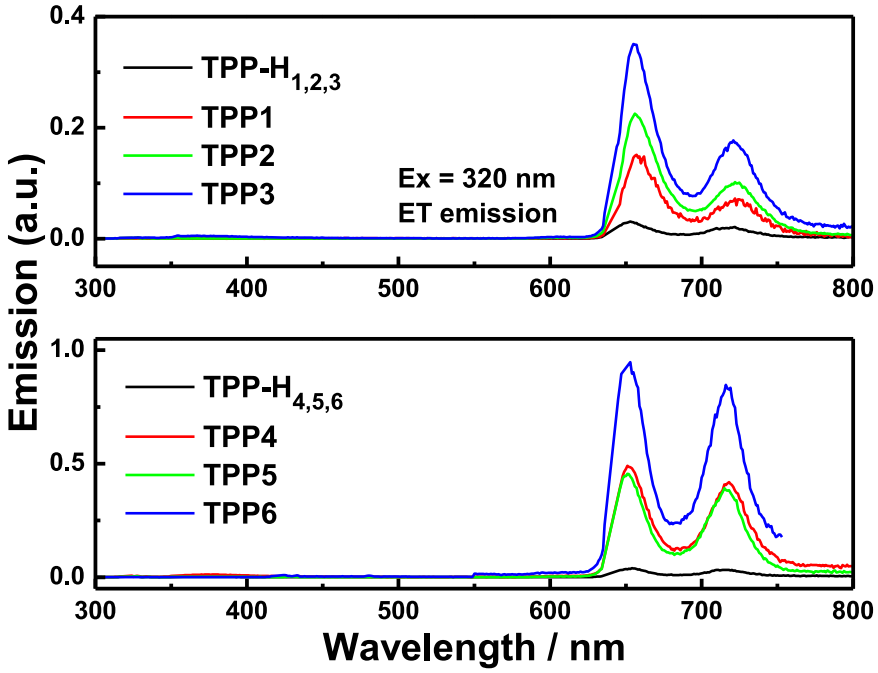

Figure 2.15 Energy Transfer behaviors exhibited in emission spectra for **TPP1-TPP6** using excitation wavelength: Ex = 320 nm.

Concerning the series *para*-substituted TPP-cored porphyrins - As expected, **TPP-H$_{1,2,3}$** presents almost no emission by 320 nm excitation, whereas **TPP1**, **TPP2** and **TPP3** exhibit obvious ET emission.

Similar properties are observed in *meta*-substituted TPP-cored porphyrins series, and they have obvious higher ET emission intensities. Especially for **TPP6**, with more terminated fluorenyls in π-extended dendron linkage, this dendrimer was observed the highest ET emission intensity by exciting at the highest dendron absorption (Ex = 327 nm).

2.4.3 Quantum yield and life time

The fluorescence quantum yields of these compounds were measured in dilute toluene (HPLC level) solutions by taking TPP ($\Phi_{TPP} = 0.11$) as calibration standard, the quantum yields of **TPP1-TPP6** are calculated by the following equation:

$$\Phi_s = \Phi_{TPP} \times (A_s/A_{TPP}) \times (I_{TPP}/I_s) \times (n_{TPP}/n_s)^2 \qquad \text{where,}$$

Φ_s : quantum yield of sample, Φ_{TPP} : quantum yield of TPP;

A : integration of emission area

I : intensity of absorption peak as excitation wavelength

n : refractive index of solvent

The quantum yields (see Table 2.2) show dependence on dendrimers' structures: *para*-substituted TPP-cored porphyrins series have quantum yield around 20%, higher than their parent molecule TPP, whereas *meta*-substituted porphyrins have quantum yields similar to TPP.

In an attempt to determine the origin of emission efficiency accompanying substituted dendron on *para* or *meta* position, in particular, whether it is due to an increase in the radiative rate constant or reduced non-radiative decay, the fluorescence lifetime τ of the compounds in dilute toluene solution was measured. The values obtained are given in Table 2.2.

For *para*-substituted TPP-cored porphyrins series, lifetimes around 9.7 ns are observed lower than for TPP. In contrary, for *meta*-substituted series, lifetimes are about 10.7 ns, higher than for TPP.

Table 2.2 Photophysical properties of the dendrimers **TPP1-TPP6**.

Porphyrin	$\Phi_s(\%)^a$	$\tau(ns)^b$	k_{obs} ($10^7 s^{-1}$)	$k_f(10^7\ s^{-1})^c$	$\sum k_{nr}(10^7\ s^{-1})^c$
TPP	11	9.95	10.0	1.10	8.94
TPP1	20	9.79	10.2	2.04	8.17
TPP2	20	9.75	10.2	2.05	8.20
TPP3	19	9.72	10.3	1.95	8.33
TPP4	13	10.65	9.4	1.22	8.17
TPP5	11	10.77	9.3	1.02	8.26
TPP6	13	10.74	9.3	1.21	8.10

a. Experiments for fluorescence quantum yields were achieved in distilled toluene by Soret band (426 nm) excition.

b. Fluorescence lifetime was measured in dilute toluene, using pulsed excitation at 426 nm.

c. k_f and $\sum k_{nr}$ are the radiative rate constant and the sum of non-radiative decay constants respectively.

Assuming that the emissive state is formed with unitary efficiency for each case when excited directly into the porphyrin at 426 nm, then:

$$\Phi_s = k_f/k_{obs} \quad \text{where} \quad k_{obs} = (k_f + \sum k_{nr}) = \tau^{-1}$$

allowing estimates of the radiative rate constant k_f and the sum of the non-radiative decay constants $\sum k_{nr}$ to be obtained from the measured lifetime τ and the quantum yield Φ_s.[65]

The rate constants estimated are collected in Table 2.2. It is seen that introductions of the substituted dendron in different positions both decrease the rate of non-radiative decay processes ($\sum k_{nr}$) compared to TPP, but little dependence exists on positions. Their radiative rate constant k_f show more dependence on substituent

positions, and k_f decreases by a factor of 2 upon going from first series **TPP1-TPP3** to second ones **TPP4-TPP6**.

Therefore, for the *para*-series **TPP1-TPP3**, the enhanced quantum yields could be attributed almost exclusively to an influence of substituted dendron on *para* position, increasing the oscillator strength of the radiative transition. For the *meta*-series **TPP4-TPP6**, their quantum yields are a bit higher than TPP probably due to significant lower in $\sum k_{nr}$, even though with similar radiative rate constant k_f as TPP.

2.5 Conclusions

1. Two groups of new TPP-cored porphyrin dendrimers were designed according to different substituted positions in cored phenyl: *para*-substituted series **TPP1**, **TPP2** and **TPP3**, and *meta*-substituted ones **TPP4**, **TPP5** and **TPP6**; they all have conjugated dendrons with bridged phenyl-alkynyl and terminated fluorenyls.

2. Three different strategies were described to synthesize these porphyrin dendrimers **TPP1-TPP6**, and they were finally synthesized by modified aldehyde dendrons under Adler-Longo's conditions.

3. Aldehyde **Dendron 1-6** and dendrimers **TPP1-TPP6** were all well characterized and analysed by ^{1}H NMR spectra.

4. Optical properties of **TPP1-TPP6** have obvious dependence on their structures:

(i) Porphyrins with the same substituted position in cored phenyl exhibit the same normalized absorption and emission peaks from porphyrin core.

(ii) With the structure of dendron expanding, dendrimers have obviously intense dendron absorption, and the intensity of dendron absorption refers to the proportion of ET emission.

(iii) The same substituted position in cored phenyl of porphyrin also results in similar quantum yield, life time and relative kinetics data.

Experimental Section

2-ethynylfluorene (1):

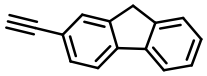

(1) In a schlenk, a mixture of 2-bromofluorene (5.0 g, 20.40 mmol, 1 eq), $Pd(PPh_3)_2Cl_2$ (86 mg, 0.122 mmol, 0.6% eq) and CuI (12 mg, 0.063 mmol, 0.3% eq) was added DMF (12 mL), $^{i}Pr_2NH$ (12 mL) and ethynyltrimethylsilane (4.4 mL, 30.60 mmol, 1.5 eq) under argon, respectively. The system was degassed by freeze-pump-thaw twice and heated for 2 days at 95 ^{o}C. After being evaporated, residue was farther purified by chromatography (heptane), and yellow crude powder (((fluoren-2-yl)ethynyl)trimethylsilane) was obtained.

^{1}H NMR (400 MHz, $CDCl_3$, ppm): δ 7.77 (d, *J* = 7.6 Hz, 1H), 7.71 (d, *J* = 7.6 Hz, 1H), 7.66 (s, 1H), 7.54 (d, *J* = 7.2 Hz, 1H), 7.50 (d, *J* = 7.6 Hz, 1H), 7.38 (t, *J* = 7.2 Hz, 1H), 7.31 (t, *J* = 7.2 Hz, 1H), 3.88 (s, 2H), 0.27 (s, 9H).

(2) Crude ((fluoren-2-yl)ethynyl)trimethylsilane was added into a mixture solvents of CH_2Cl_2 (60 mL) and MeOH (20 mL), together with K_2CO_3 (4.22 g, 30.60 mmol, 1.5 eq). The mixture was stirred overnight at room temperature. After being evaporated, residue was farther purified by chromatography (heptane), getting yellow powder (3.1 g, 89% yield for two steps).

^{1}H NMR (400 MHz, $CDCl_3$, ppm): δ 7.78 (d, *J* = 7.6 Hz, 1H), 7.73 (d, *J* = 7.6 Hz, 1H), 7.67 (s, 1H), 7.55 (d, *J* = 7.2 Hz, 1H), 7.52 (d, *J* = 8.0 Hz, 1H), 7.39 (t, *J* = 7.2 Hz, 1H), 7.33 (t, *J* = 7.2 Hz, 1H), 3.90 (s, 2H), 3.11 (s, 1H).

2-bromo-9,9-dibutyl-9*H*-fluorene

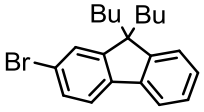

A mixture of 2-bromofluorene (5.0 g, 20.40 mmol, 1 eq) and Bu_4NBr (329 mg, 1.02 mmol, 5% eq) was added with toluene (25 mL, not dry) and 50% NaOH (25 mL), respectively. After 1-bromobutane (11 mL, 102 mmol, 5 eq) was added into the solution, the reaction was stirred for 24 h at 75-85 ^{o}C. The reaction was extracted with

water and ethyl acetate. After being evaporated, residue was farther purified by chromatography (heptane), getting colorless crystal (5.9 g, 81% yield).

^{1}H NMR (400 MHz, $CDCl_3$, ppm): δ 7.68-7.65 (m, 1H), 7.55 (d, *J* = 8.4 Hz, 1H), 7.46-7.44 (m, 2H), 7.34-7.32 (m, 3H), 2.00-1.88 (m, 4H), 1.12-1.03 (m, 4H), 0.68 (t, *J* = 7.2 Hz, 6H), 0.63-0.53 (m, 4H).

9,9-dibutyl-2-ethynyl-9*H*-fluorene (2):

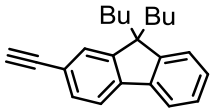

(1) The procedure of ethynyltrimethylsilane substituted is the same to that for ((fluoren-2-yl)ethynyl)trimethylsilane and the mixture was heated for 2 days at 95 ^{o}C. The TMS-compound can be purified by chromatography (heptane).

^{1}H NMR (400 MHz, $CDCl_3$, ppm): δ 7.69-7.66 (m, 1H), 7.62 (d, *J* = 8.0 Hz, 1H), 7.46 (d, *J* = 7.8 Hz, 1H), 7.43 (s, 1H), 7.33-7.31 (m, 3H), 1.95 (t, *J* = 8.6 Hz, 4H), 1.11-1.02 (m, 4H), 0.66 (t, *J* = 7.2 Hz, 6H), 0.62-0.48 (m, 4H), 0.29 (s, 9H).

(2) The procedure of deprotecting trimethylsilane is same to that for 2-ethynylfluorene and the purification of reaction was completed by chromatography (heptane), getting yellow oil (91% yield for two steps).

^{1}H NMR (400 MHz, $CDCl_3$, ppm): δ 7.70-7.68 (m, 1H), 7.64 (d, *J* = 7.6 Hz, 1H), 7.49-7.47 (m, 2H), 7.36-7.33 (m, 3H), 3.14 (s, 1H), 1.96 (t, *J* = 8.4 Hz, 4H), 1.12-1.03 (m, 4H), 0.67 (t, *J* = 7.4 Hz, 6H), 0.62-0.51 (m, 4H).

2-(4-bromophenyl)-1,3-dioxolane:

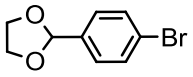

A mixture of 4-bromobenzaldehyde (4 g, 21.62 mmol, 1 eq), 4-methylbenzenesulfonic acid (14 mg, 0.09 mmol, 0.4% eq), and ethane-1,2-diol (1.81 mL, 32.43 mmol, 1.5 eq) in toluene (15 mL) were refluxed in a Dean-Stark apparatus for 2 days under argon. After evaporating the solvents, the residue was farther purified by chromatography

(heptane : CH_2Cl_2 = 1 : 1), getting colorless oil (4.51 g, 91% yield).

^{1}H NMR (400 MHz, DMSO-d6, ppm): δ 7.59 (d, *J* = 8.4 Hz, 2H), 7.39 (d, *J* = 8.4 Hz, 2H), 5.72 (s, 1H), 4.06-3.92 (m, 4H).

4-((fluoren-2-yl)ethynyl)benzaldehyde (Dendron 1):

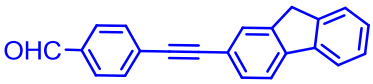

(1) In a schlenk, a mixture of 2-(4-bromophenyl)-1,3-dioxolane (1.04 g, 4.54 mmol, 1 eq), **1** (1.0 g, 5.26 mmol, 1.15 eq), $Pd(PPh_3)_2Cl_2$ (18.4 mg, 0.026 mmol, 0.6% eq) and CuI (2.5 mg, 0.013 mmol, 0.3% eq) was added DMF (6 mL) and $^iPr_2NH$ (6 mL) under argon, respectively. Then the system was degassed by freeze-pump-thaw twice and heated for 2 days at 95 ^oC. After being evaporated, residue was farther purified by chromatography (heptane : CH_2Cl_2 = 5 : 1), and yellow crude powder (2-(4-((fluoren-2-yl)ethynyl)phenyl)-1,3-dioxolane) was obtained.

(2) Crude 2-(4-((fluoren-2-yl)ethynyl)phenyl)-1,3-dioxolane was added into a mixture solvents of THF (20 mL) and HCl (5 mL, 10% aq). The mixture was stirred overnight at room temperature. The reaction was neutralized by $NaHCO_3$ and extracted with CH_2Cl_2 and water. After solvents was evaporated, residue was farther purified by chromatography (heptane : CH_2Cl_2 = 4 : 1), getting yellow powder (613 mg, 48% yield for two steps).

^{1}H NMR (400 MHz, $CDCl_3$, ppm): δ 10.03 (s, 1H), 7.88 (d, *J* = 8.4 Hz, 2H), 7.80 (t, *J* = 7.4 Hz, 2H), 7.75 (s, 1H), 7.69 (d, *J* = 8.4 Hz, 2H), 7.58 (t, *J* = 7.6 Hz, 2H), 7.41 (t, *J* = 7.2 Hz, 1H), 7.34 (t, *J* = 7.4 Hz, 1H), 3.94 (s, 2H).

4-((9,9-dibutyl-fluoren-2-yl)ethynyl)benzaldehyde (Dendron 2):

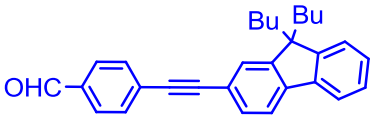

In a schlenk, a mixture of 4-bromobenzaldehyde (673 mg, 3.64 mmol, 1 eq), **2** (1.2 g, 3.97 mmol, 1.1 eq), $Pd(PPh_3)_2Cl_2$ (15 mg, 0.02 mmol, 0.6% eq) and CuI (2 mg, 0.01

mmol, 0.3% eq) was added DMF (5 mL) and $^{i}Pr_2NH$ (5 mL) under argon, respectively. Then the system was degassed by freeze-pump-thaw twice and heated for 2 days at 95 ^{o}C. After being evaporated, residue was farther purified by chromatography (heptane : CH_2Cl_2 = 4 : 1), showing yellow powder (1.12 g, 76% yield).

^{1}H NMR (400 MHz, $CDCl_3$, ppm): δ 10.03 (s, 1H), 7.88 (d, *J* = 8.0 Hz, 2H), 7.72-7.69 (m, 4H), 7.55 (d, *J* = 8.0 Hz, 1H), 7.53 (s, 1H), 7.36-7.34 (m, 3H), 1.99 (t, *J* = 8.4 Hz, 4H), 1.13-1.04 (m, 4H), 0.68 (t, *J* = 7.2 Hz, 6H), 0.64-0.55 (m, 4H).

2-(3,5-dibromophenyl)-1,3-dioxolane:

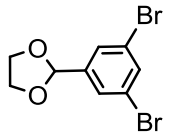

The procedure for protection of alkynyl is the same to that for 2-(4-bromophenyl)-1,3-dioxolane and the purification was completed by chromatography (heptane : CH_2Cl_2 = 10 : 1), showing colorless oil (88% yield).

^{1}H NMR (400 MHz, DMSO-d6, ppm): δ 7.86-7.86 (m, 1H), 7.62 (d, *J* = 1.6 Hz, 2H), 5.76 (s, 1H), 4.08-3.91 (m, 4H).

3,5-bis((fluoren-2-yl)ethynyl)benzaldehyde (Dendron 4):

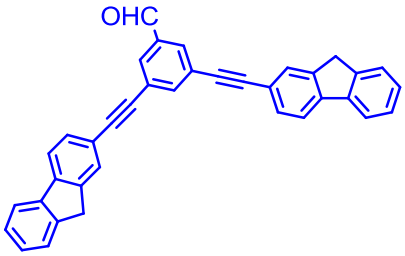

(1) In a schlenk, a mixture of 2-(3,5-dibromophenyl)-1,3-dioxolane (1.02 g, 3.31 mmol, 1 eq), **1** (1.58 g, 8.28 mmol, 2.5 eq), $Pd(PPh_3)_2Cl_2$ (28 mg, 0.040 mmol, 1.2% eq) and CuI (4 mg, 0.021 mmol, 0.6% eq) was added DMF (5 mL) and $^{i}Pr_2NH$ (5 mL) under argon, respectively. Then the system was degassed by freeze-pump-thaw twice and heated for 2 days at 95 ^{o}C. After being evaporated, residue was farther purified by chromatography (heptane : CH_2Cl_2 = 5 : 1), and yellow crude powder

(2-(3,5-bis((fluoren-2-yl)ethynyl)phenyl)-1,3-dioxolane) was obtained.

(2) Crude (2-(3,5-bis((fluoren-2-yl)ethynyl)phenyl)-1,3-dioxolane) was added into a mixture solvents of THF (40 mL) and HCl (10 mL, 10% aq). The mixture was stirred for 10 h at room temperature. The reaction was neutralized by $NaHCO_3$ and extracted with CH_2Cl_2 and water. After solvents was evaporated, residue was farther purified by chromatography (heptane : CH_2Cl_2 = 1 : 1), getting yellow powder (900 mg, 56% yield for two steps).

^{1}H NMR (400 MHz, $CDCl_3$, ppm): δ 10.04 (s, 1H), 7.99 (d, *J* = 1.6 Hz, 2H), 7.96 (t, *J* = 1.2 Hz, 1H), 7.81 (t, *J* = 6.8 Hz, 4H), 7.74 (s, 2H), 7.58 (t, *J* = 6.4 Hz, 4H), 7.41 (t, *J* = 7.4 Hz, 2H), 7.35 (t, *J* = 7.4 Hz, 2H), 3.95 (s, 4H).

3,5-bis((9,9-dibutyl-9*H*-fluoren-2-yl)ethynyl)benzaldehyde (Dendron 5):

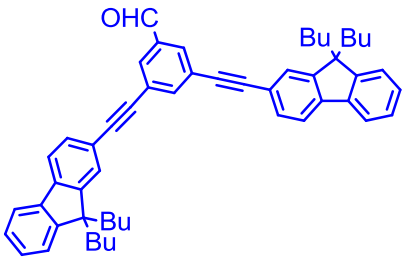

In a schlenk, a mixture of 3,5-dibromobenzaldehyde (569 mg, 2.16 mmol, 1 eq), **2** (1.63 g 5.39 mmol, 2.5 eq), $Pd(PPh_3)_2Cl_2$ (18 mg, 0.026 mmol, 1.2% eq) and CuI (2.5 mg, 0.013 mmol, 0.6% eq) was added DMF (5 mL) and $^iPr_2NH$ (5 mL) under argon, respectively. Then the system was degassed by freeze-pump-thaw twice and heated for 2 days at 95 ^oC. After being evaporated, residue was farther purified by chromatography (heptane : CH_2Cl_2 = 5 : 1), showing white powder (1.22 g, 80% yield).

^{1}H NMR (400 MHz, $CDCl_3$, ppm): δ 10.04 (s, 1H), 8.01 (s, 3H), 7.73-7.70 (m, 4H), 7.55-7.53 (m, 4H), 7.37-7.33 (m, 6H), 2.00 (t, *J* = 8.2 Hz, 8H), 1.14-1.05 (m, 8H), 0.69 (t, *J* = 7.4 Hz, 12H), 0.64-0.57 (m, 8H).

2,2'-(5-(2,2-dibromovinyl)-1,3-phenylene)bis(ethyne-2,1-diyl)bis(9,9-dibutyl-9H-fluorene):

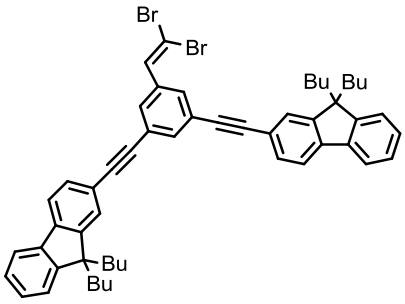

In a schlenk, a mixture of PPh_3 (2.45 g, 9.34 mmol, 2 eq) and Zn powder (0.61 g, 9.34 mmol, 2 eq) was added dry CH_2Cl_2 (45 mL). After the solution was cooled to 0 ^oC in ice-water bath, CBr_4 was put into schlenk under argon protection and the reaction was kept at low temperature for 2 min. After the bath removing and the mixture was stirred overnight at room temperature. Then the mixture was cooled to 0 ^oC again and added **6** (3.3 g, 4.67 mmol, 1 eq) in 20 mL CH_2Cl_2 to the schlenk under argon protection. Kept the low temperature for 10 min and stirred it in dark at room temperature for 4 h. Filtered the solution and evaporate CH_2Cl_2, then the residue was absorbed in silica and farther purified by chromatography (heptane : CH_2Cl_2 = 100 : 5), showing white powder (3.71 g, 92% yield).

^1H NMR (400 MHz, $CDCl_3$, ppm): δ 7.75 (s, 1H), 7.72-7.70 (m, 3H), 7.69 (s, 1H), 7.67 (s, 2H), 7.54 (s, 1H), 7.51 (s, 3H), 7.47 (s, 1H), 7.37-7.31 (m, 6H), 1.99 (t, *J* = 8.4 Hz, 8H), 1.14-1.05 (m, 8H), 0.69 (t, *J* = 7.2 Hz, 12H), 0.65-0.52 (m, 8H).

2,2'-(5-ethynyl-1,3-phenylene)bis(ethyne-2,1-diyl)bis(9,9-dibutyl-9H-fluorene) (3):

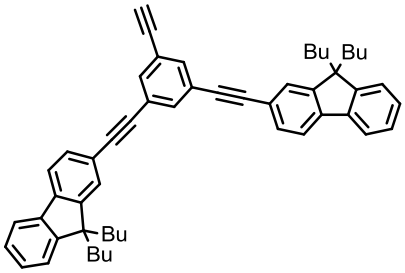

N-BuLi (3.24 mL, 5.181 mmol, 3 eq) was added to a cold (-78 ^oC) solution of $^iPr_2NH$ (0.73 mL, 5.181 mmol, 3 eq) in dry THF (13 mL). After warming up to room

temperature, the mixture was injected dropwise into the solution of 2,2'-(5-(2,2-dibromovinyl)-1,3-phenylene)bis(ethyne-2,1-diyl)bis(9,9-dibutyl-9H-fluorene) (1.49 g, 1.727 mmol, 1 eq) in dry THF (32 mL) at -78 ^{o}C in liquid nitrogen-acetone bath. Kept the low temperature for 1 h, then quenched the reaction with saturated NH_4Cl (5 mL). Removed the bath, the reaction was stirred until the temperature was up to room temperature. Extracted it with ethyl acetate and dried it with $MgSO_4$. Evaporated solvents, then the residue was absorbed in silica and farther purified by chromatography (heptane : CH_2Cl_2 = 100 : 5), showing white powder (1.05 g, 86% yield).

^{1}H NMR (400 MHz, $CDCl_3$, ppm): δ 7.75 (s, 1H), 7.72-7.68 (m, 4H), 7.64 (s, 2H), 7.53-7.51 (m, 4H), 7.35-7.31 (m, 6H), 3.13 (s, 1H), 1.99 (t, *J* = 8.0 Hz, 8H), 1.14-1.05 (m, 8H), 0.68 (t, *J* = 7.2 Hz, 12H), 0.65-0.54 (m, 8H).

4-((3,5-bis((9,9-dibutyl-9H-fluoren-2-yl)ethynyl)phenyl)ethynyl)benzaldehyde (Dendron 3):

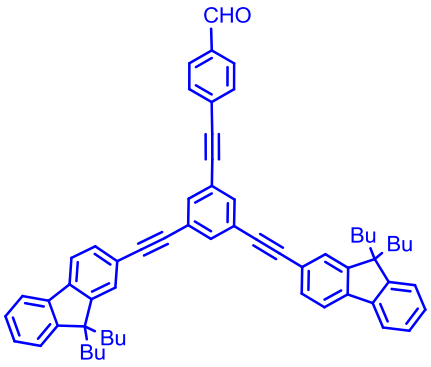

In a schlenk, a mixture of 4-bromobenzaldehyde (123 mg, 0.67 mmol, 1 eq), **7** (515 mg, 0.732 mmol, 1.1 eq), $Pd(PPh_3)_2Cl_2$ (28 mg, 0.04 mmol, 6% eq) and CuI (4 mg, 0.02 mmol, 3% eq) was added DMF (5 mL) and $^{i}Pr_2NH$ (10 mL) under argon, respectively. Then the system was degassed by freeze-pump-thaw twice and heated for 2 days at 95 ^{o}C. After being evaporated, residue was absorbed in silica and farther purified by chromatography (heptane : CH_2Cl_2 = 5 : 1), showing white powder (357 mg, 66% yield).

^{1}H NMR (400 MHz, $CDCl_3$, ppm): δ 10.05 (s, 1H), 7.90 (d, *J* = 8.4 Hz, 2H), 7.78 (s, 1H), 7.72-7.69 (m, 8H), 7.54-7.52 (m, 4H), 7.38-7.33 (m, 6H), 1.99 (t, *J* = 8.0 Hz,

8H), 1.14-1.05 (m, 8H), 0.69 (t, J = 7.2 Hz, 12H), 0.64-0.54 (m, 8H).

3,5-bis((3,5-bis((9,9-dibutyl-9H-fluoren-2-yl)ethynyl)phenyl)ethynyl) benzaldehyde (Dendron 6):

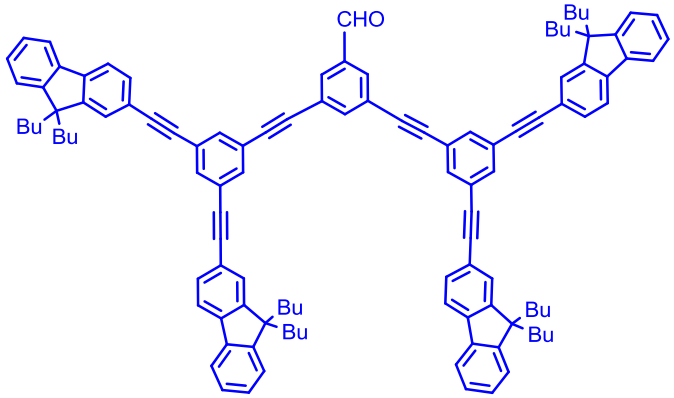

In a schlenk, a mixture of 3,5-dibromobenzaldehyde (160 mg, 0.61 mmol, 1 eq), **7** (900 mg, 1.28 mmol, 2.1 eq), $Pd(PPh_3)_2Cl_2$ (51 mg, 0.07 mmol, 6% eq) and CuI (7 mg, 0.04 mmol, 3% eq) was added DMF (15 mL) and $^{i}Pr_2NH$ (20 mL) under argon, respectively. Then the system was degassed by freeze-pump-thaw twice and heated for 2 days at 95 ^{o}C. After being evaporated, residue was absorbed in silica and farther purified by chromatography (heptane : CH_2Cl_2 = 5 : 1), showing white powder (530 g, 58% yield).

^{1}H NMR (400 MHz, $CDCl_3$, ppm): δ 10.06 (s, 1H), 8.02 (s, 2H), 7.95 (s, 1H), 7.79 (s, 2H), 7.73-7.70 (m, 11H), 7.55-7.53 (m, 9H), 7.38-7.31 (m, 12H), 2.00 (t, J = 8.0 Hz, 16H), 1.13-1.05 (m, 16H), 0.69 (t, J = 8 Hz, 24H), 0.64-0.55 (m, 16H).

4-((trimethylsilyl)ethynyl)benzaldehyde:

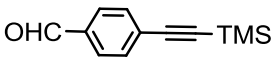

In a schlenk, a mixture of 4-bromobenzaldehyde (3.51 g, 18.97 mmol, 1 eq), $Pd(PPh_3)_2Cl_2$ (80 mg, 0.11 mmol, 0.6% eq) and CuI (11 mg, 0.06 mmol, 0.3% eq) was added NEt_3 (10 mL), THF (10 mL) and ethynyltrimethylsilane (3.24 mL, 22.77 mmol, 1.2 eq) under argon, successively. Then the system was degassed by freeze-pump-thaw twice and heated overnight at 45 ^{o}C. After being evaporated, residue was absorbed in silica and farther purified by chromatography (heptane :

CH_2Cl_2 = 2 : 1), showing white powder (3.66 g, 95% yield).

^{1}H NMR (400 MHz, $CDCl_3$, ppm): δ 10.00 (s, 1H), 7.82 (d, *J* = 8.4 Hz, 2H), 7.60 (d, *J* = 8.4 Hz, 2H), 0.27 (s, 9H).

3,5-bis((trimethylsilyl)ethynyl)benzaldehyde :

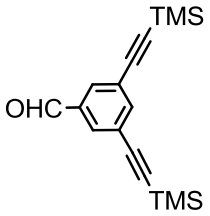

In a schlenk, a mixture of 3,5-dibromobenzaldehyde (2 g, 7.58 mmol, 1 eq), $Pd(PPh_3)_2Cl_2$ (64 mg, 0.09 mmol, 0.6% eq) and CuI (8.7 mg, 0.05 mmol, 0.3% eq) was added NEt_3 (2 mL), THF (15 mL) and ethynyltrimethylsilane (2.7 mL, 18.9 mmol, 2.5 eq) under argon, successively. Then the system was degassed by freeze-pump-thaw twice and heated overnight at 45 ^{o}C. After being evaporated, residue was absorbed in silica and farther purified by chromatography (heptane : CH_2Cl_2 = 2 : 1), showing white powder (2.08 g, 92% yield).

^{1}H NMR (400 MHz, $CDCl_3$, ppm): δ 9.94 (s, 1H), 7.88 (s, 2H), 7.79 (s, 1H), 0.25 (s, 18H).

TPP1:

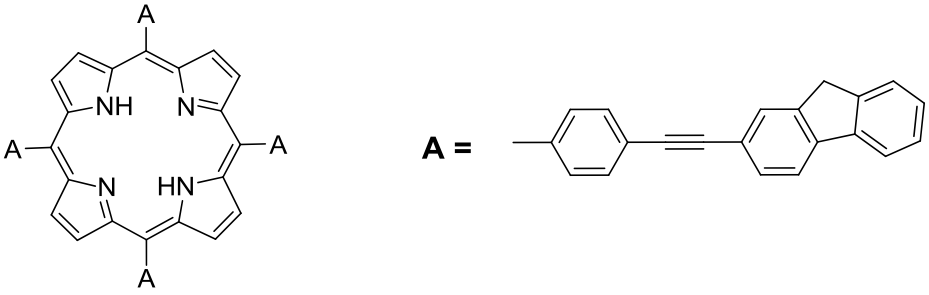

The mixture of **3** (400 mg, 1.36 mmol, 1 eq) and propionic acid (5 mL) was heated to 120 ^{o}C. After pyrrole (0.095 mL, 1.36 mmol, 1 eq) in propionic acid (1 mL) was added into the mixture dropwise, the reaction was kept refluxing (140 ^{o}C) for 1.5 h. After cooling to room temperature, MeOH was added to the reaction mixture and the precipitate was filtered. The residue could be purified by chromatography (petroleum ether : CH_2Cl_2 = 5 : 1), getting purple powder (80 mg, 17% yield).

^{1}H NMR (400 MHz, $CDCl_3$, ppm): δ 8.92 (s, 8H), 8.24 (d, *J* = 7.2 Hz, 8H), 7.97 (d, *J* = 7.2 Hz, 8H), 7.88-7.85 (m, 12H), 7.73 (d, *J* = 8.0 Hz, 4H), 7.60 (d, *J* = 7.2 Hz, 4H), 7.43 (t, *J* = 6.8 Hz, 4H), 7.36 (t, *J* = 6.8 Hz, 4H), 4.00 (s, 8H), -2.74 (s, 2H).

HRMS-ESI: m/z = 1367.5200 $[M+H]^+$ (calcd: 1366.4974).

Anal. Calcd. (%) for $C_{104}H_{62}N_4$: C, 91.33; H, 4.57; N, 4.10. Found: C, 91.06; H, 4.39; N, 4.08.

TPP2:

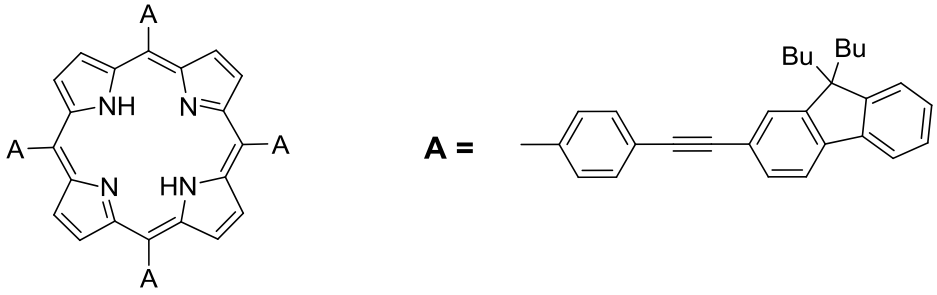

The mixture of **4** (700 mg, 1.72 mmol, 1 eq) and propionic acid (6.5 mL) was heated to 120 ^{o}C. After pyrrole (0.12 mL, 1.72 mmol, 1 eq) in propionic acid (1 mL) was added into the mixture dropwise, the reaction was kept refluxing (140 ^{o}C) for 1.5 h. After cooling to room temperature, MeOH was added to the reaction mixture and the precipitate was filtered. The residue could be purified by chromatography (petroleum ether : CH_2Cl_2 = 1 : 1), getting rose-purple powder (220 mg, 28% yield).

^{1}H NMR (400 MHz, $CDCl_3$, ppm): δ 8.92 (s, 8H), 8.24 (d, *J* = 7.6 Hz, 8H), 7.99 (d, *J* = 7.6 Hz, 8H), 7.78-7.75 (m, 8H), 7.69-7.67 (m, 8H), 7.40-7.35 (m, 12H), 2.05 (t, *J* = 8.0 Hz, 16H), 1.19-1.10 (m, 16H), 0.73 (t, *J* = 7.2 Hz, 24H), 0.69-0.60 (m, 16H), -2.74 (s, 2H).

^{13}C NMR (100 MHz, $CDCl_3$, ppm): δ 151.1, 150.9, 141.9, 141.7, 140.4, 134.6, 130.8, 130.0, 127.6, 126.9, 126.1, 123.1, 122.9, 121.4, 120.1, 119.7, 91.9, 89.3, 55.1, 40.2, 26.0, 23.1, 13.9.

HRMS-ESI: m/z = 1816.0055 $[M+H]^+$ (calcd: 1814.9982).

Anal. Calcd. (%) for $C_{136}H_{126}N_4$: C, 89.92; H, 6.99; N, 3.08. Found: C, 89.65; H, 6.59; N, 3.12.

TPP3:

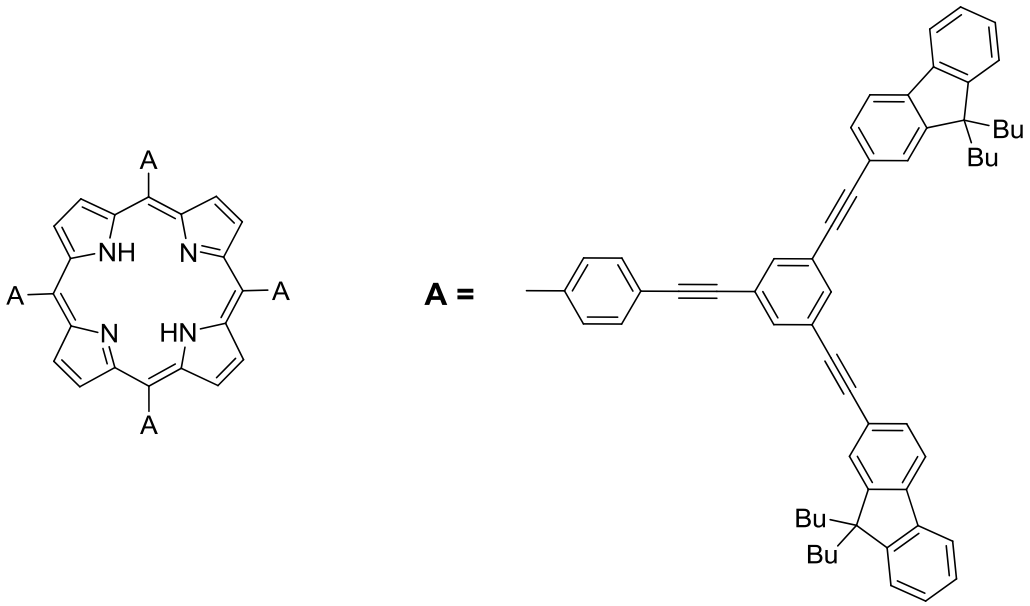

The mixture of **8** (312 mg, 0.39 mmol, 1 eq) and propionic acid (2 mL) was heated to 120 ^{o}C. After pyrrole (0.03 mL, 0.39 mmol, 1 eq) in propionic acid (0.5 mL) was added into the mixture dropwise, the reaction was kept refluxing (140 ^{o}C) for 5.5 h. After cooling to room temperature, MeOH was added to the reaction mixture and the precipitate was filtered. The residue could be purified by chromatography (petroleum ether : CH_2Cl_2 = 5 : 1), showing red powder, and recrystallized by refluxing $CHCl_3$ and MeOH, getting dark purple powder (72 mg, 22% yield).

^{1}H NMR (400 MHz, $CDCl_3$, ppm): δ 8.94 (s, 8H), 8.28 (d, *J* = 8.0 Hz, 8H), 7.99 (d, *J* = 8.0 Hz, 8H), 7.87 (s, 8H), 7.83 (s, 4H), 7.73 (d, *J* = 8.0 Hz, 16H), 7.59-7.57 (m, 16H), 7.39-7.32 (m, 24H), 2.02 (t, *J* = 8.0 Hz, 32H), 1.17-1.08 (m, 32H), 0.71 (t, *J* = 7.2 Hz, 48H), 0.67-0.58 (m, 32H), -2.72 (s, 2H).

^{13}C NMR (100 MHz, $CDCl_3$, ppm): δ 151.1, 150.8, 142.4, 141.8, 140.3, 134.7, 134.2, 134.0, 130.7, 130.2, 127.6, 126.9, 126.1, 124.4, 124.1, 124.0, 122.9, 122.6, 120.9, 120.1, 119.7, 91.9, 90.4, 89.3, 87.9, 55.1, 40.2, 25.9, 23.1, 13.8.

HRMS-ESI: m/z = 3416.8821 $[M+H]^+$ (calcd: 3415.8746).

Anal. Calcd. (%) for $C_{260}H_{238}N_4$: C, 91.34; H, 7.02; N, 1.64. Found: C, 91.05; H, 6.93; N, 1.77.

TPP4:

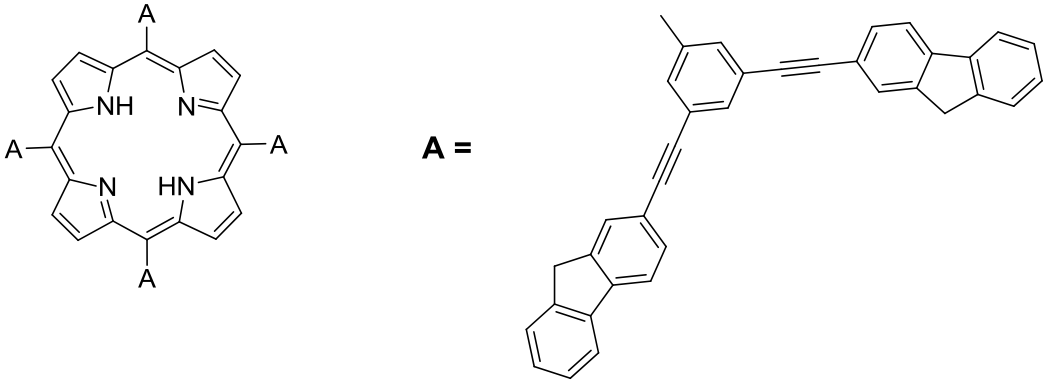

The mixture of **5** (850 mg, 1.76 mmol, 1 eq) and propionic acid (40 mL) was heated to 120 ^{o}C. After pyrrole (0.12 mL, 1.76 mmol, 1 eq) in propionic acid (1 mL) was added into the mixture dropwise, the reaction was kept refluxing (140 ^{o}C) for 3 h. After cooling to room temperature, MeOH was added to the reaction mixture and the precipitate was filtered. The residue could be recrystallized by CH_2Cl_2, getting light brown powder (20 mg, 2% yield).

^{1}H NMR (400 MHz, $CDCl_3$, ppm): δ 9.03 (s, 8H), 8.42 (s, 8H), 8.20 (s, 4H), 7.78-7.76 (m, 24H), 7.62 (d, *J* = 8.0 Hz, 8H), 7.54-7.52 (m, 8H), 7.38 (t, *J* = 7.6 Hz, 8H), 7.31 (t, *J* = 7.4 Hz, 8H), 3.90 (s, 16H), -2.75 (s, 2H).

HRMS-ESI: m/z = 2119.7510 $[M+H]^+$ (calcd: 2118.7478).

Anal. Calcd. (%) for $C_{164}H_{94}N_4$: C, 92.89; H, 4.47; N, 2.64. Found: C, 92.48; H, 4.44; N, 2.59.

TPP5:

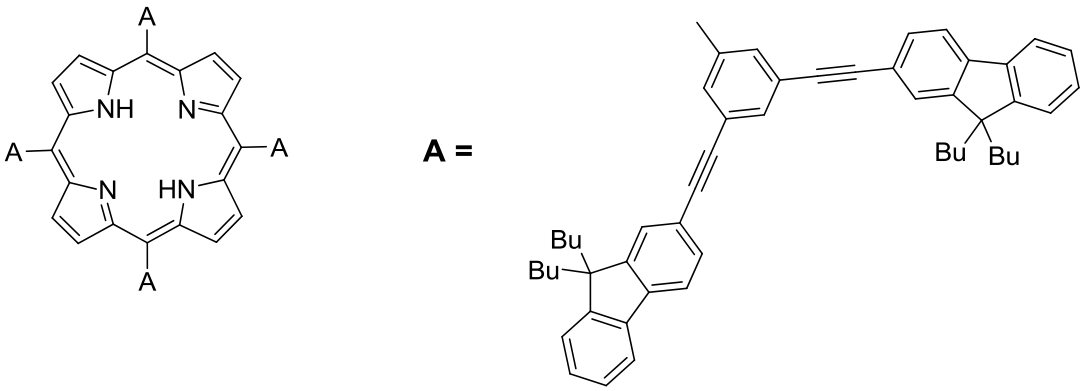

The mixture of **6** (860 mg, 1.22 mmol, 1 eq) and propionic acid (6 mL) was heated to 120 ^{o}C. After pyrrole (0.085 mL, 1.22 mmol, 1 eq) in propionic acid (1 mL) was added into the mixture dropwise, the reaction was kept refluxing (140 ^{o}C) for 3 h. After cooling to room temperature, MeOH was added to the reaction mixture and the precipitate was filtered. The residue could be purified by chromatography (petroleum ether : CH_2Cl_2 = 5 : 1), showing red powder, and recrystallized by refluxing $CHCl_3$ and MeOH, getting red powder (165 mg, 18% yield).

^{1}H NMR (400 MHz, $CDCl_3$, ppm): δ 9.02 (s, 8H), 8.43 (s, 8H), 8.26 (s, 4H), 7.67 (d, *J* = 7.2 Hz, 16H), 7.59-7.57 (m, 16H), 7.31 (broad, 24H), 1.95 (t, *J* = 8.0 Hz, 32H), 1.07-1.02 (m, 32H), 0.65-0.48 (m, 80H), -2.75 (s, 2H).

^{13}C NMR (100 MHz, $CDCl_3$, ppm): δ 151.1, 150.8, 142.5, 141.8, 140.3, 136.7, 134.0, 130.8, 127.6, 126.9, 126.2, 122.9, 122.6, 121.0, 120.0, 119.7, 118.7, 91.6, 88.6, 55.1, 40.1, 25.9, 23.0, 13.8.

HRMS-ESI: m/z = 3016.7047 $[M+H]^+$ (calcd: 3015.7494).

Anal. Calcd. (%) for $C_{228}H_{222}N_4$: C, 90.73; H, 7.41; N, 1.86. Found: C, 90.39; H, 7.38; N, 1.93.

TPP6:

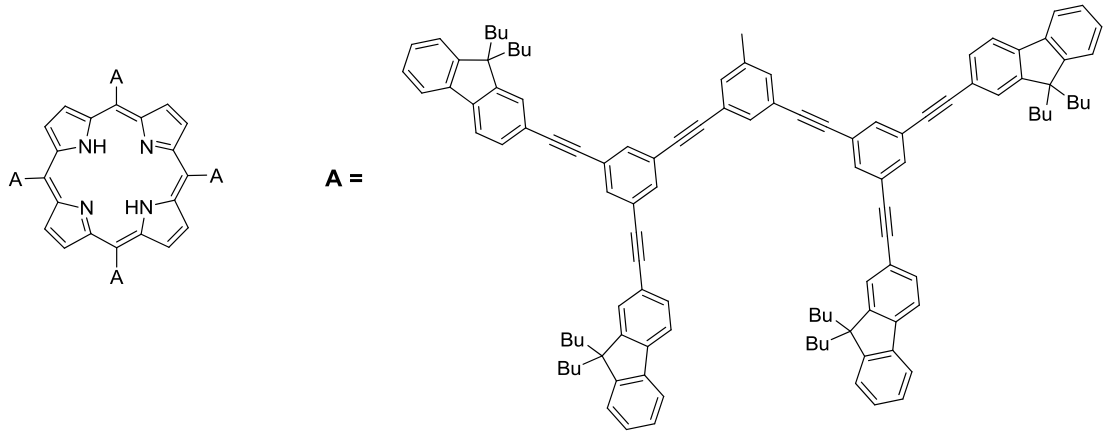

The mixture of **9** (500 mg, 0.33 mmol, 1 eq) and propionic acid (3 mL) was heated to 120 ^{o}C. After pyrrole (0.02 mL, 0.33 mmol, 1 eq) in propionic acid (0.5 mL) was added into the mixture dropwise, the reaction was kept refluxing (140 ^{o}C) for 5.5 h. After cooling to room temperature, MeOH was added to the reaction mixture and the precipitate was filtered. The residue could be purified by chromatography (petroleum ether : CH_2Cl_2 = 5 : 1), showing red powder, and recrystallized by refluxing $CHCl_3$ and MeOH, getting dark purple powder (66 mg, 13% yield).

^{1}H NMR (400 MHz, $CDCl_3$, ppm): δ 9.08 (s, 8H), 8.46 (s, 8H), 8.22 (s, 4H), 7.77-7.74 (m, 20H), 7.65-7.61 (m, 32H), 7.52-7.47 (m, 36H), 7.36-7.28 (m, 48H), 1.91 (t, *J* = 8.0 Hz, 64H), 1.05-0.99 (m, 64H), 0.63-0.52 (m, 160H), -2.70 (s, 2H).

^{13}C NMR (100 MHz, $CDCl_3$, ppm): δ 151.0, 150.8, 141.8, 140.3, 134.4, 134.0, 130.7, 127.6, 126.8, 126.1, 124.4, 124.0, 123.6, 122.9, 122.2, 120.8, 120.0, 119.6, 91.9, 89.4, 89.1, 87.8, 55.0, 40.1, 25.8, 23.0, 13.8.

HRMS-ESI: m/z = 3109.7570 $[M+2H]^{2+}$ (calcd: 3109.7584).

Anal. Calcd. (%) for $C_{476}H_{446}N_4$: C, 91.88; H, 7.22; N, 0.90. Found: C, 91.67; H, 7.17; N, 0.72.

TPP-H$_{1,2,3}$:

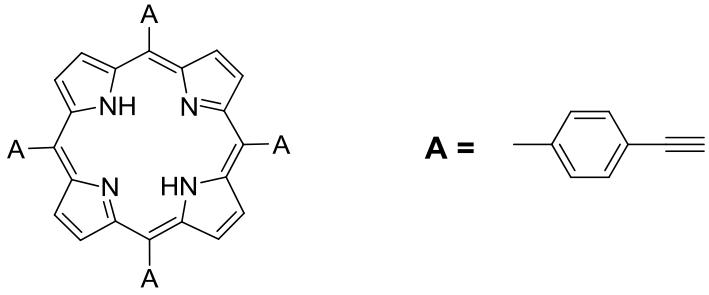

(1) The mixture of 4-((trimethylsilyl)ethynyl)benzaldehyde (650 mg, 3.21 mmol, 1 eq) and propionic acid (10 mL) was heated to 120 ^{o}C. After pyrrole (0.22 mL, 3.21 mmol, 1 eq) in propionic acid (1 mL) was added into the mixture dropwise, the reaction was kept refluxing for 1.5 h. After cooling to room temperature, MeOH was added to the reaction mixture and the precipitate was filtered. The residue could be purified by chromatography (heptane : CH_2Cl_2 = 5 : 1), getting purple powder (255 mg, 32% yield).

^{1}H NMR (400 MHz, $CDCl_3$, ppm): δ 8.82 (s, 8H), 8.14 (d, *J* = 8.0 Hz, 8H), 7.87 (d, *J* = 8.0 Hz, 8H), 0.38 (s, 36H), -2.83 (s, 2H).

(2) **TPP-TMS$_{1,2,3}$** (250 mg, 0.25 mmol, 1 eq) was added into a mixture solvents of CH_2Cl_2 (36 mL) and MeOH (12 mL), together with K_2CO_3 (553 mg, 4 mmol, 16 eq). The mixture was stirred overnight at room temperature. After being evaporated, residue was farther purified by chromatography (heptane : CH_2Cl_2 = 2 : 1), getting purple powder (168 mg, 94% yield).

^{1}H NMR (400 MHz, $CDCl_3$, ppm): δ 8.84 (s, 8H), 8.17 (d, *J* = 8.0 Hz, 8H), 7.90 (d, *J* = 8.0 Hz, 8H), 3.33 (s, 4H), -2.83 (s, 2 H).

TPP-$H_{4,5,6}$:

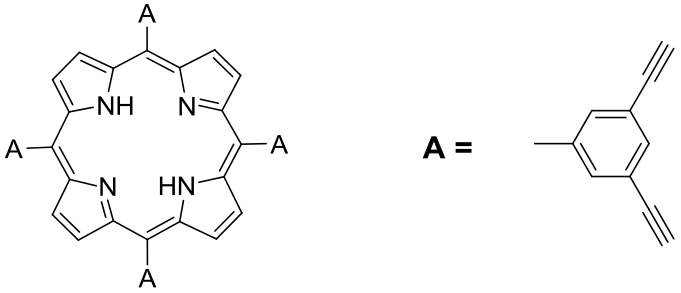

(1) The mixture of 3,5-bis((trimethylsilyl)ethynyl)benzaldehyde (1 g, 3.35 mmol, 1 eq) and propionic acid (15 mL) was heated to 120 ^{o}C. After pyrrole (0.23 mL, 3.35 mmol, 1 eq) in propionic acid (1 mL) was added into the mixture dropwise, the reaction kept refluxing for 3.3 h. After cooling to room temperature, MeOH was added to the reaction mixture and the precipitate was filtered. The residue could be purified by chromatography (heptane : CH_2Cl_2 = 5 : 1), getting red powder (260 mg, 22% yield).
^{1}H NMR (400 MHz, $CDCl_3$, ppm): δ 8.86 (s, 8H), 8.27 (s, 8H), 8.07 (s, 4H), 0.30 (s, 72H), -2.91 (s, 2H).

(2) **TPP-$TMS_{4,5,6}$** (550 mg, 0.40 mmol, 1 eq) was added into a mixture solvents of CH_2Cl_2 (90 mL) and MeOH (30 mL), together with K_2CO_3 (877 mg, 6.36 mmol, 16 eq). The mixture was stirred for 1 day at room temperature. After being evaporated, residue was farther purified by chromatography (heptane : CH_2Cl_2 = 2 : 1), getting purple powder (274 mg, 86% yield).
^{1}H NMR (400 MHz, $CDCl_3$, ppm): δ 8.85 (s, 8H), 8.31 (s, 8H), 8.06 (s, 4H), 3.20 (s, 8H), -2.93 (s, 2H).

Chapter 3

The influence of light absorber positions: TFP-cored porphyrin dendrimers with Cored, bridged and terminated fluorenyls

3.1 Molecular design

As described in the introduction, 5,10,15,20-tetrafluorenylporphyrin (**TFP**) showed obvious higher quantum yield (23-24%), than **TPP** (11-12%). There are as well many porphyrin dendrimers, taking TFP as core reported in the literatures.[16,66]

After synthesizing a series of TPP-cored porphyrin with terminated fluorenyl, as described in chapter 2, we noticed that they all had interesting light-harvesting properties with conjugated dendron and terminated fluorenyl. Along this line, we attempted to obtain porphyrin dendrimers with fluorenyl group inserted in different positions of conjugated dendrons: as terminated group, bridged group and cored group connected directly in *meso* position of porphyrin, named **TFP1**, **TFP2** and **TFP3** (as shown in Figure 3.1).

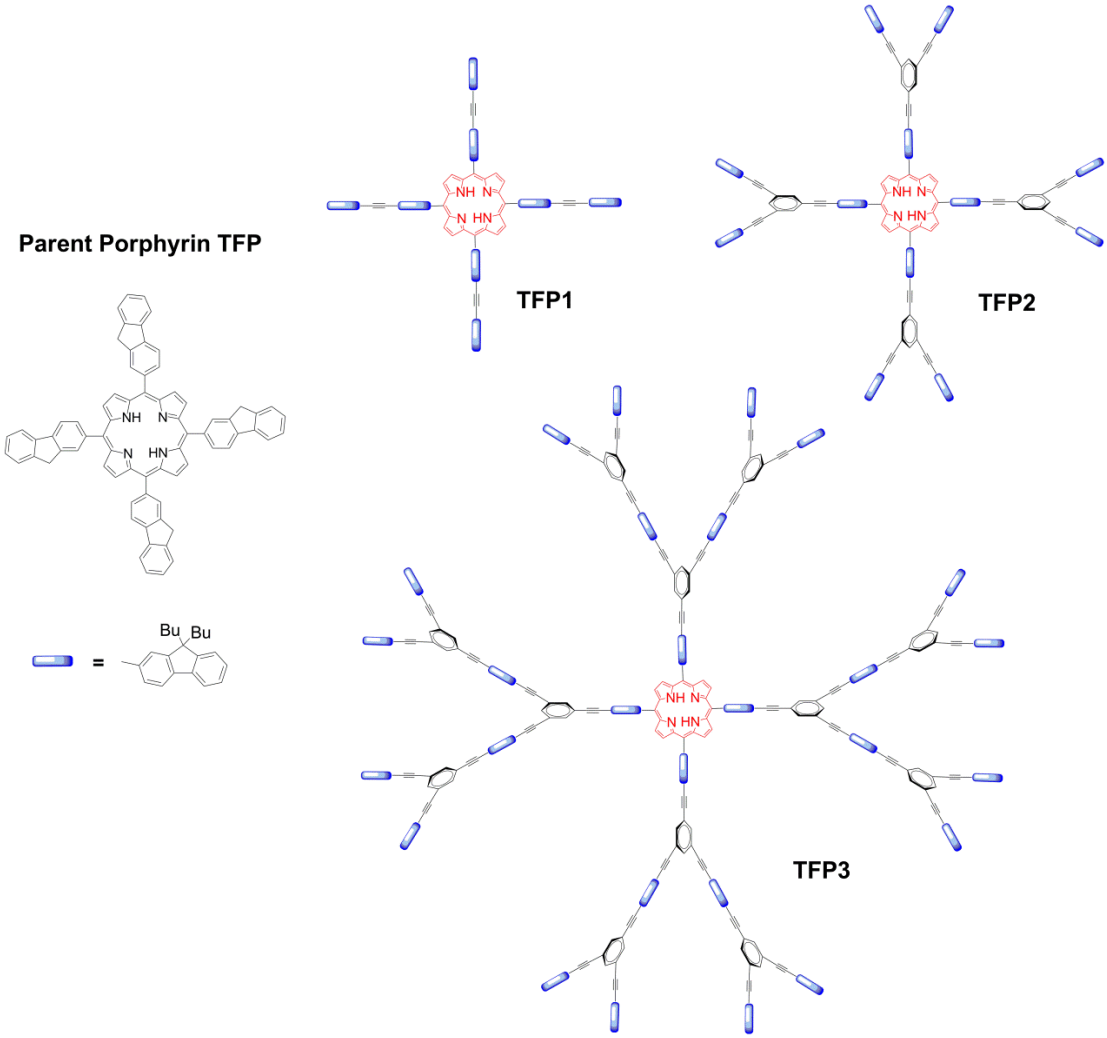

Figure 3.1 TFP-cored porphyrin dendrimers **TFP1**, **TFP2** and **TFP3**.

As for TPP series in chapter 2, *n*-butyl was added on the fluorenyl group to increase the solubility of final porphyrin dendrimers. All these three new porphyrin dendrimers have four cored fluorenyl units in common: (i) **TFP1** has four terminated fluorenyls; (ii) **TFP2** increases up to eight terminated fluorenyls utilizing expanded conjugated dendron with phenyl-alkynyl linkage; (iii) **TFP3**, has eight bridged fluorenyls inserted in further expanded conjugated dendron, as well as sixteen terminated fluorenyls.

3.2 Synthetic method design

For gaining this new family of porphyrin dendrimers, the successful strategy used for TPP-cored porphyrin dendrimers was also adopted for TFP-cored series, described as two steps (Figure 3.2): (i) the first step for forming modified aldehyde dendron, (ii) next step for forming porphyrin core.

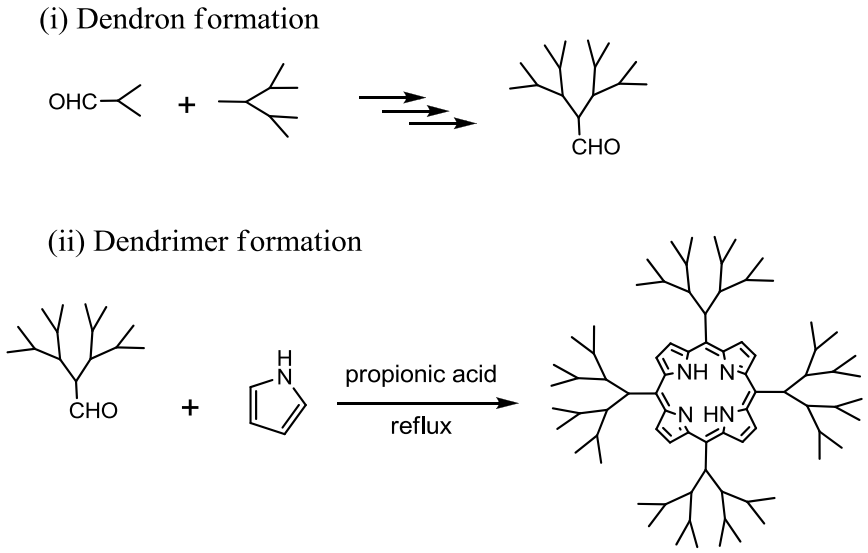

Figure 3.2 Synthetic strategy used for TFP-cored porphyrin dendrimers.

3.2.1 Dendron formation

The detailed synthetic methods of conjugated aldehyde dendron were shown in Figure 3.3 and Figure 3.4. As illustrated, the increase generation of dendron was realized mainly from repetitive reactions of Sonogashira coupling and Corey-Fuchs

reaction.

To gain these rigid **Dendron 1-3** with good solubilities (same for final dendrimer), *n*-butyl group was added in 9*H* of 2-bromofluorene with about 80% yield.

The synthesis of molecules **1** and **3** were already described in chapter 2 for TPP-cored porphyrin dendrimers. Then **1** and **3** reacted with bromo-aldehyde **2** under similar conditions, yielding respectively **Dendron 1** and **Dendron 2**.

Dendron 1 has linear conjugated structure and small molecular weight, and the yield could be up to 90%.

The second generation **Dendron 2** has an extended conjugated structure in space and higher molecular weight so that the reaction between alkynyl **3** and bromo **2** had the difficulty to overcome the steric hindrance, and in consequence only 60% yield is obtained under higher temperature and longer reaction time.

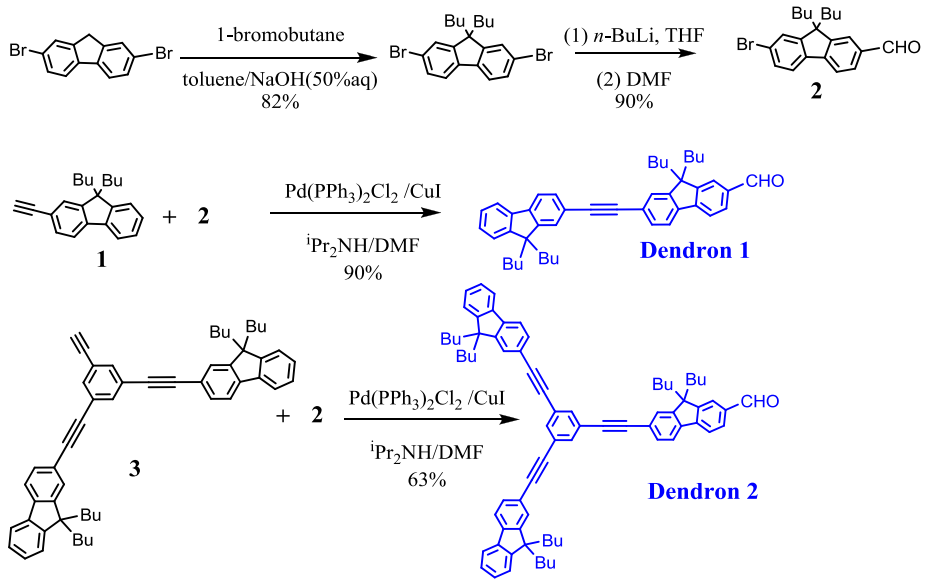

Figure 3.3 Synthesis of **Dendron 1** and **Dendron 2**.

Dendron 3 is the third generation of dendron with the largest conjugated structure and it has three layers of fluorenyl groups near to aldehyde function. Taking **Dendron 2** as starting material, **Dendron 3** was obtained by two times repetitive reactions of Sonogashira coupling and Corey-Fuchs reactions. From a series of reactions for **5** to **9**, the yields of Corey-Fuchs reaction could still keep 70% to 90%. Unfortunately the continually growing structure obviously increased the difficulty of

Sonogashira coupling between two active groups: alkynyl and bromo. So in the last step, for **Dendron 3**, we used iodo-aldehyde **4** instead of bromo-aldehyde **2** in order to promote reaction activity. We prepared **4** by two substitution reactions: from bromo to iodo yielding 96%, and from iodo to aldehyde yielding 73%. It is noticed that, for the first step from bromo to iodo, the reaction time of *n*-BuLi and bromo should be enough to gain disubstituted product instead of monosubstituted byproduct; for the second step from iodo to aldehyde, the reaction of *n*-BuLi and iodo only cost 20 min and long reaction time could decrease the yield.

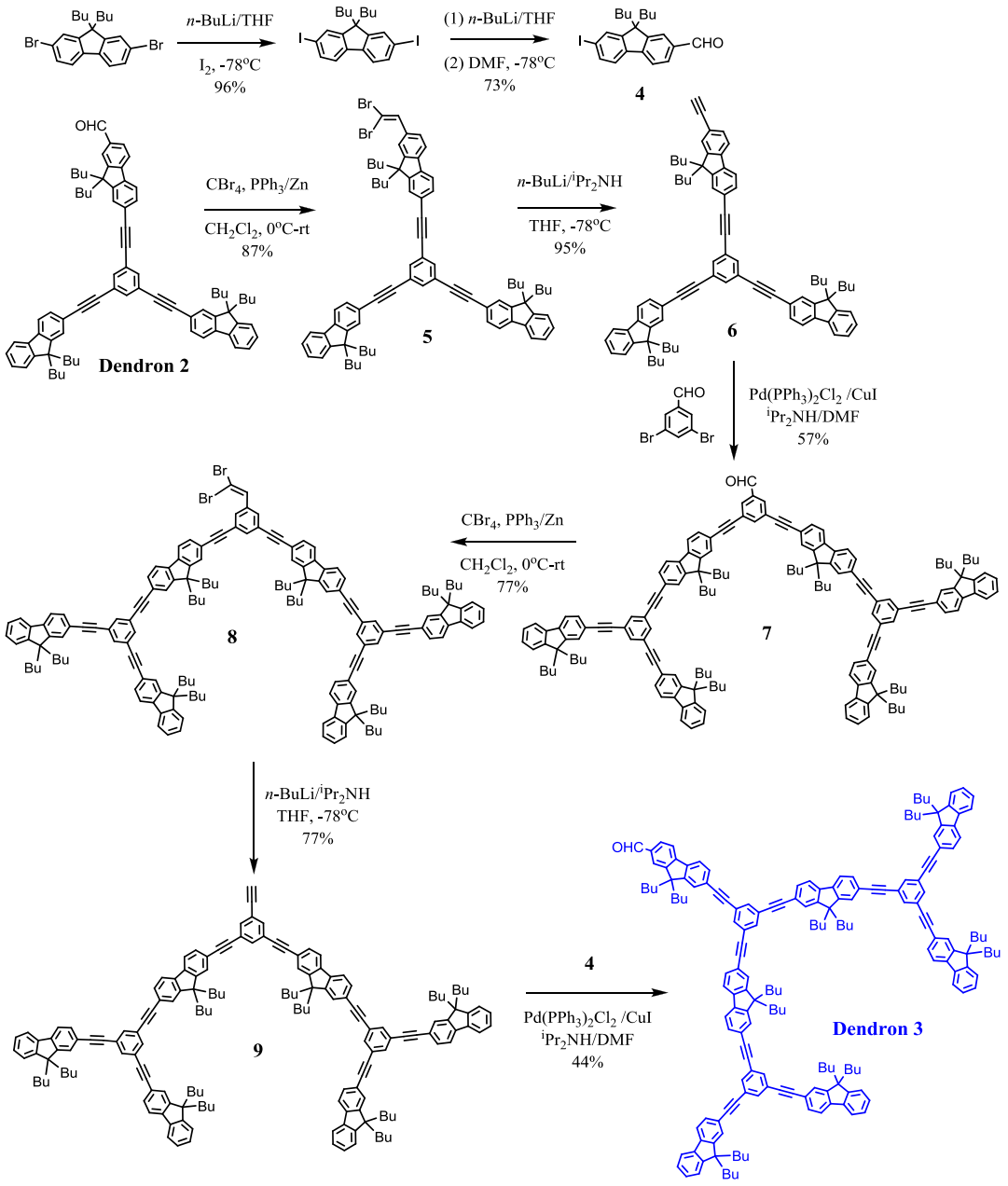

Figure 3.4 Synthesis of **Dendron 3**.

3.2.2 Dendrimer formation

To form the porphyrin core, Adler-Longo's method was adopted for condensation of **Dendron 1-3** and pyrrole in refluxing propionic acid about 5.5 h, yielding the desired TFP-cored porphyrin dendrimers **TFP1**, **TFP2** and **TFP3** (see Figure 3.5). After the reactions, **TFP1** and **TFP2** were obtained by chromatography as red powders about 19% yields, and farther recrystallization in refluxing $CHCl_3$ and MeOH gave dark purple powders.

While under similar conditions, **TFP3** only had 1% yield after chromatography, and the red product with pretty good solubility was very hard to undergo farther recrystallization. The low yield of **TFP3** is probably due to the large rigid structure of **Dendron 3** which increases the steric hindrance effect and decreases the active condensation of aldehyde and pyrrole, and the reaction showed many blue luminescent byproducts and black polymers by thin-layer chromatography (TLC) monitoring.

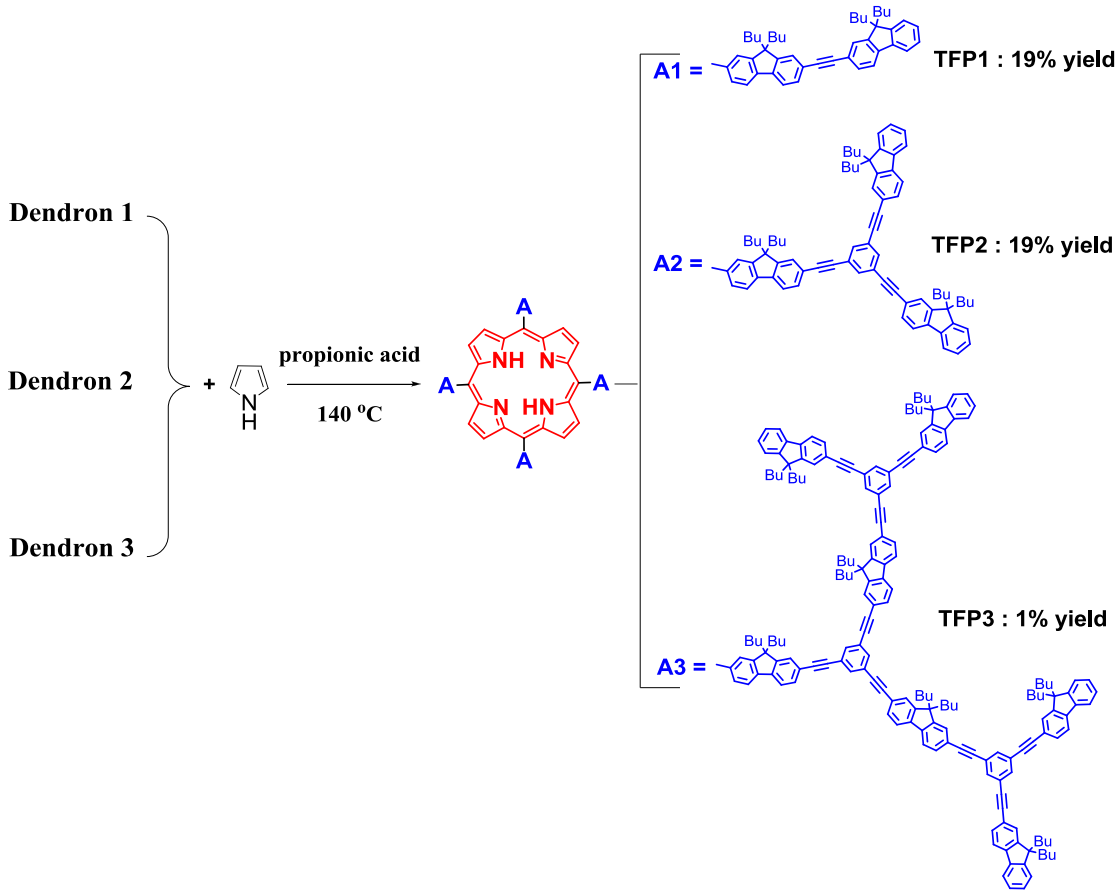

Figure 3.5 Synthesis of TFP-cored porphyrin dendrimers **TFP1**, **TFP2** and **TFP3**.

3.3 ^{1}H NMR analysis

The aldehyde **Dendron 1-3** and TFP-cored porphyrin dendrimers **TFP1**, **TFP2** and **TFP3** were all well characterized by ^{1}H NMR in $CDCl_3$ (400 MHz).

*3.3.1 ^{1}H NMR spectra of **Dendron 1-3***

The protons of this type of dendron have three components: (i) aldehyde proton around 10 ppm, (ii) aromatic protons around 7-8 ppm and (iii) alkyl ones around 0-2 ppm.

Taking **Dendron 2** as example, its full spectrum was showed in Figure 3.6. One proton around 10 ppm responds to aldehyde function, four groups of protons Ha,b,c,d around 0-2 ppm are assigned to butyl of fluorenyl, and they are all well identified (see Figure 3.6B). Protons around 7-8 ppm belong to protons of phenyl and fluorenyl. By comparing protons around 7-10 ppm of **Dendron 1-3**, as shown in Figure 3.7, the proportion of aldehyde function in the whole molecule decreases obviously, particularly for **Dendron 3**, and it probably explains the low yield of forming porphyrin macrocycle.

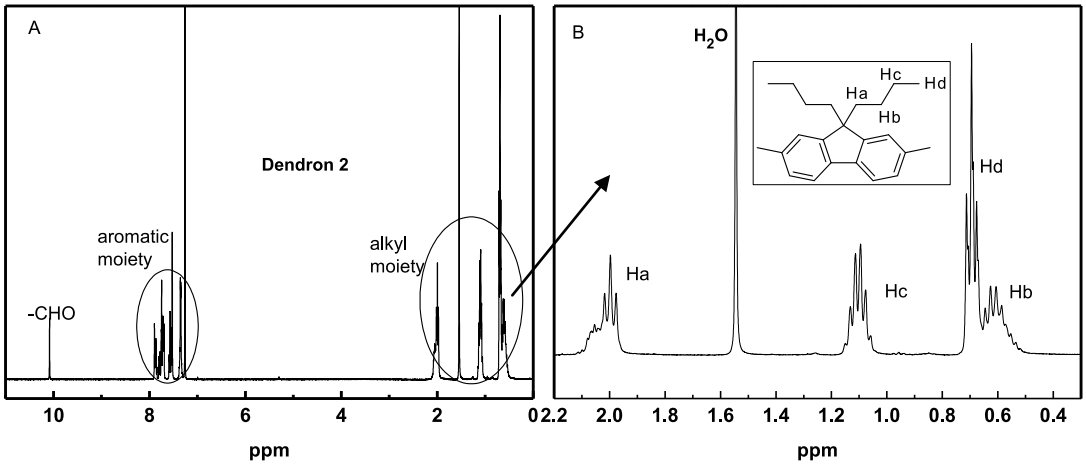

Figure 3.6 ^{1}H NMR spectrum of **Dendron 2**.

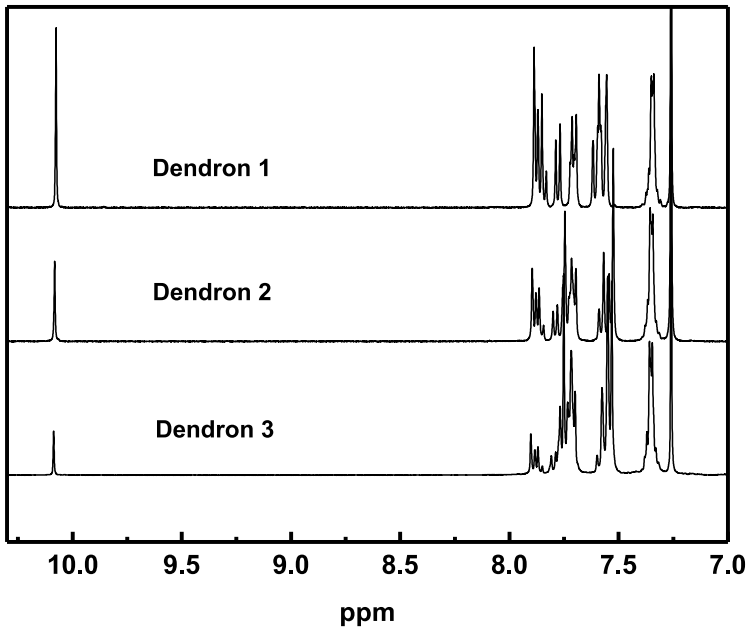

Figure 3.7 Partial ^{1}H NMR spectra of **Dendron 1-3**.

*3.3.2 ^{1}H NMR spectra of porphyrin dendrimers **TFP1**, **TFP2** and **TFP3***

The ^{1}H NMR spectra of dendrimers **TFP1-TFP3** have four components: (i) pyrrole-β protons of porphyrin (Hβ) around 8.9 ppm, (ii) aromatic protons around 7.3-8.3 ppm, (iii) alkyl protons around 0.5-2.2 ppm and (iv) –NH proton in porphyrin heart around -2.5 ppm.

Figure 3.8 shows the full spectrum of **TFP2**. (i) Eight protons at δ = 8.94 ppm are assigned to proton pyrrole-β of porphyrin. (ii) For the aromatic moiety: three proton peaks $H_{A,B,C}$ around 7.9-8.3 ppm could be identified to partial protons in the cored fluorenyl, other aromatic protons around 7.3-7.8 ppm belong to protons of phenyl and fluorenyl. (iii) According to the ratio of integration, the alkyl moiety could be identified into two parts (see Figure 3.8B): four groups of butyl protons in cored fluorenyl have a little shifts to the lower field, and the shifts of butyl protons in terminated fluorenyl exhibit at higher field; especially for **TFP3**, its butyl protons in terminated and bridged fluorenyl have the same shift at high field compared to butyl protons in cored fluorenyl. (iv) Two protons observed around -2.5 ppm belong to the

nitrogen atoms in the heart of the porphyrin (-NH).

In Figure 3.9, the partial ^{1}H NMR spectra of dendrimers (7.2-9.0 ppm), by taking 8 pyrrole-β protons of porphyrin (Hβ) as standard, it is clear that the signal of dendron for **TFP3** is much higher than **TFP2** and **TFP1**, corresponding to the largest molecular structure of **TFP3** among these dendrimers.

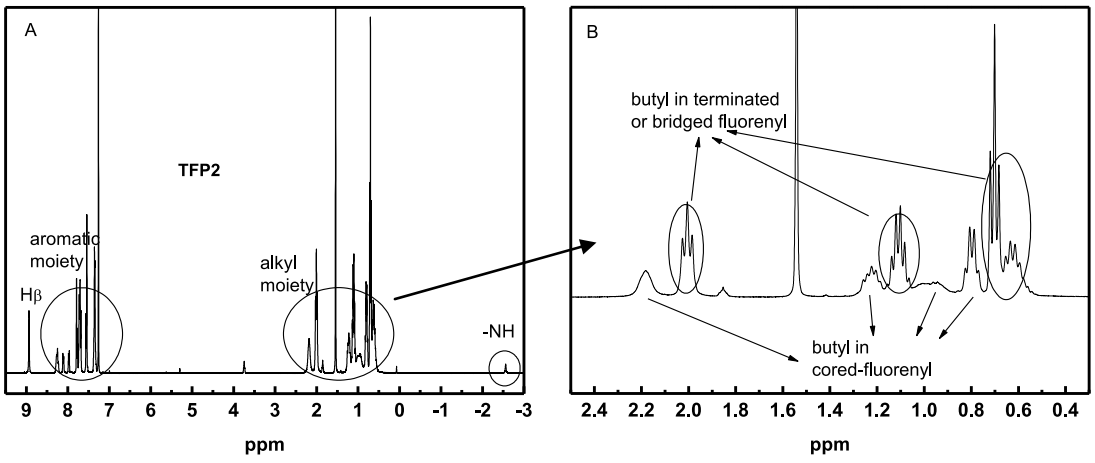

Figure 3.8 ^{1}H NMR spectrum of **TFP2**.

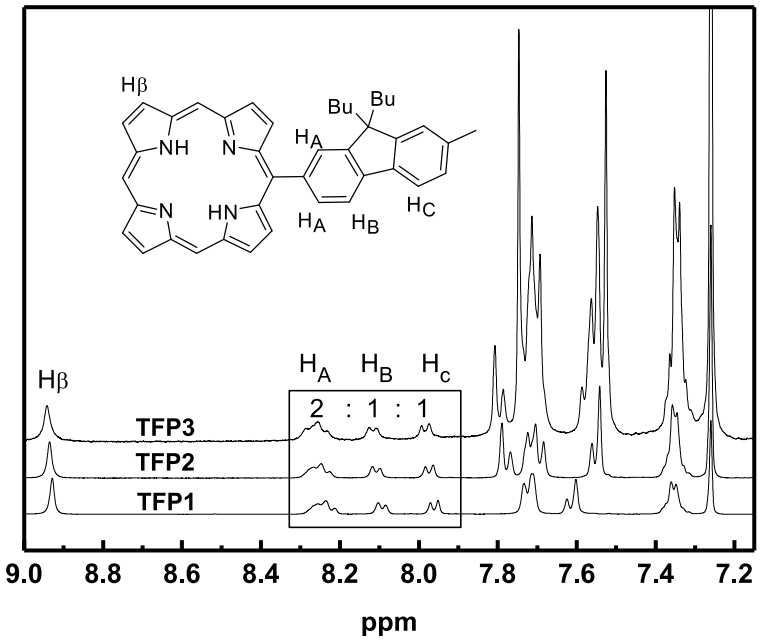

Figure 3.9 Partial ^{1}H NMR spectra of **TFP1**, **TFP2** and **TFP3**.

3.4 Optical properties

UV-visible absorption and photoluminescence spectra measurements for new TFP-cored porphyrin dendrimers **TFP1-TFP3** in dilute toluene (HPLC level) were performed at room temperature.

To better investigate the influence of fluorenyl on optical properties of dendrimers **TFP1-TFP3**, some molecules with similar structures such as **TFP-Bu**, **TPP**, **TPP1** and **TPP2** were chosen as references, as shown in Figure 3.10.

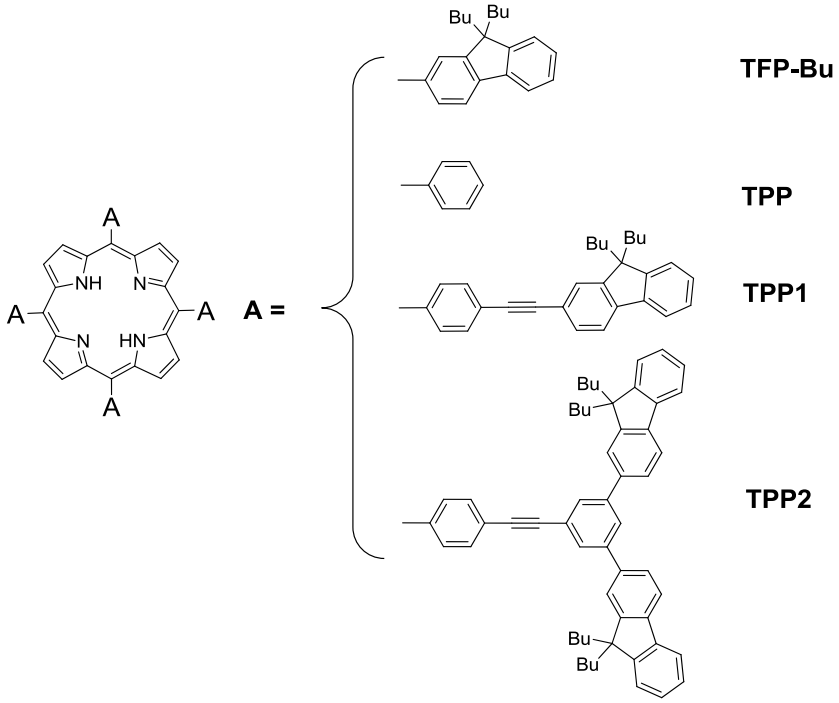

Figure 3.10 Molecular structures of reference porphyrins.

3.4.1 Absorption and emission

Dendrimers **TFP1-TFP3** all have two components in their UV-visible absorption spectra (Figure 3.11): (i) intense Soret-band around 430 nm and four Q-bands from 520-650 nm, are typically free base porphyrin absorptions; (ii) extra absorption, around 300-400 nm, is due to dendron absorption. In this region, it is absent for **TFP-Bu** possessing only cored fluorenyls (around 280 nm). It suggests that cored fluorenyls might have no contribution in dendron absorption for dendrimers **TFP1-TFP3**.

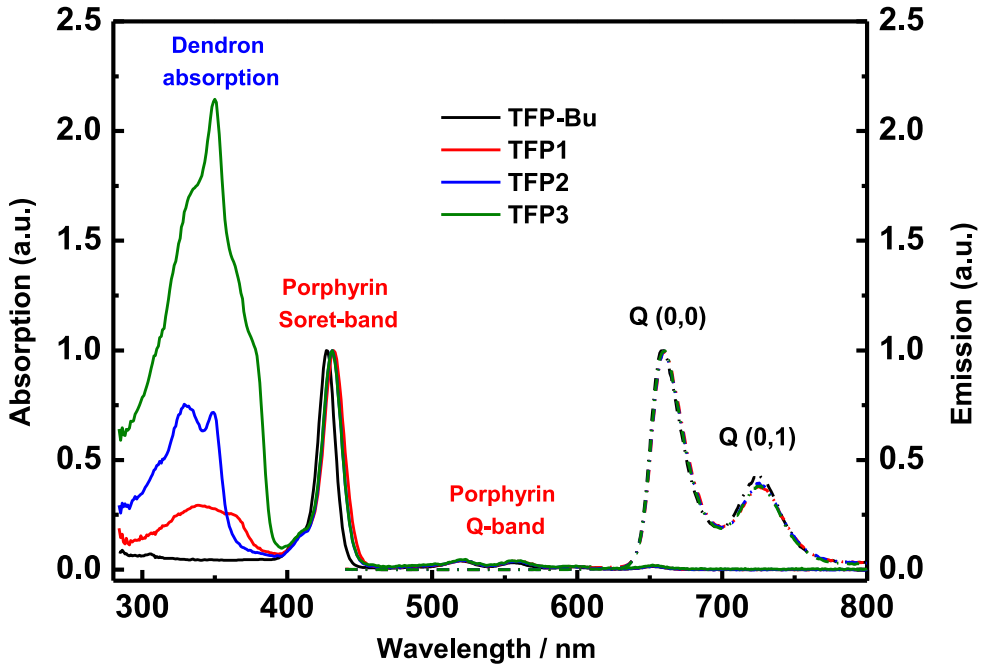

Figure 3.11 UV-visible absorption and emission spectra of **TFP1-TFP3** and their reference **TFP-Bu**.

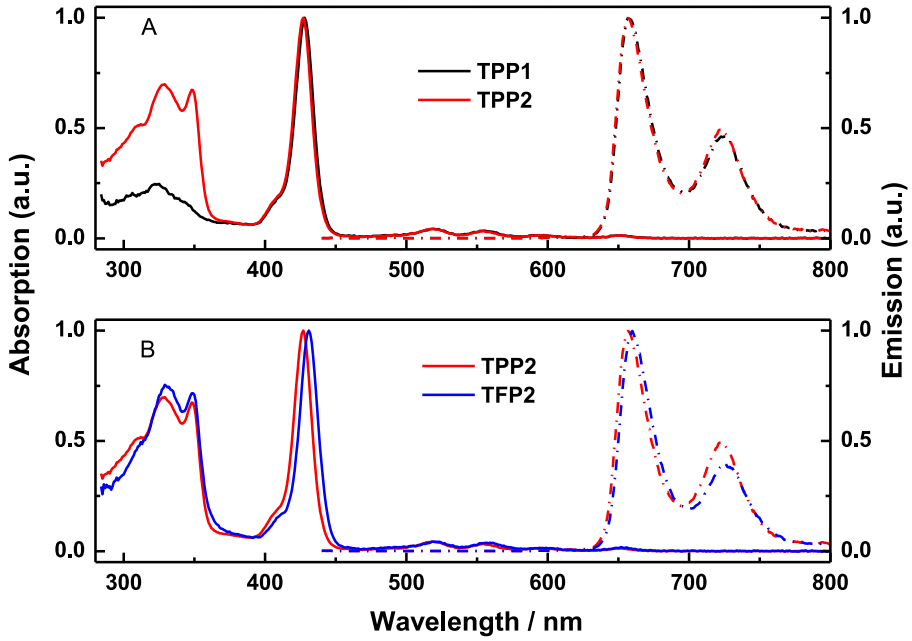

Figure 3.12 UV-visible absorption and emission spectra of reference TPP-cored porphyrin dendrimers (A) and contrastive spectra of **TFP2** and **TPP2** (B).

By comparing Figure 3.11 and Figure 3.12A, the spectra of **TFP1-TFP3** with cored fluorenyl, present similar properties to reference TPP-cored porphyrin dendrimers with cored phenyl: (i) dendron absorption increases regularly with dendron generation growing, and (ii) normalized porphyrin core absorption (Soret-band and Q-bands) has no shift between generations. The comparison of **TFP2** and **TPP2** spectra (see Figure 3.12B) shows obvious spectral shifts between these two dendrimers with similar structure but different cored groups: **TFP2** has slightly higher dendron absorption and its Soret-band has a 3 nm red shift compared to **TPP2**.

After normalizing the intensity of Soret-band, it is clear that dendron absorptions increase obviously from **TFP1** to **TFP3**.

By Soret-band excitation, the dendrimer **TFP1-TFP3** and reference **TFP-Bu** all show porphyrin emission peaks Q(0,0) and Q(0,1). After normalizing to the emission intensity Q(0,0), they all exhibit similar emission spectra as their reference **TFP-Bu**. For these dendrimers **TFP1-TFP3**, the intensity ratios of Q(0,0) and Q(0,1) keep constant, and the same phenomenon also occurs in TPP-cored porphyrin dendrimers (Figure 3.12A). It means that dendrimers **TFP1-TFP3** also have the same relative orbital energies of the excited state of the porphyrins and the steric demands of rigid dendrons.[24] So, for these fluorenyl-cored porphyrin dendrimers, by introducing three different conjugated dendrons, they have the same influence on the planarity of porphyrin ring and do not have to change its shape significantly with generations.

On the other hand, **TFP2** shows 2-3 nm red shift for Q(0,0) and Q(0,1) compared to **TPP2**. For these two dendrimers, the different ratios of Q(0,0) and Q(0,1) further evidence that cored group (fluorenyl and phenyl) is the main factor concerning the planarity of porphyrin ring.

Table 3.1 Optical properties of TFP-cored porphyrin dendrimers and their reference porphyrins.

	Absorption[a]			Emission[a] Ex = Soret-band		Quantum yield[b](%)
	Dendron	Soret-band	Q-bands	Q(0,0)	Q(0,1)	
TFP-Bu	-	427	519,555,596,652	659	725	20
TFP1	339	432	520,557,598,652	660	725	24
TFP2	333	431	520,557,597,652	660	725	24
TFP3	350	431	521,557,598,652	660	725	23
TPP	-	419	514,548,590,649	652	719	11
TPP1	324	427	519,555,597,650	657	724	20
TPP2	328	428	518,555,594,651	657	723	19

a. Experiments were achieved in toluene (HPLC level) in the UV-visible region from 285 to 800 nm and emission region from 440 to 800 nm.

b. Experiments for fluorescence quantum yields were achieved in toluene (HPLC level) using TPP (Φ =11%) as standard, by excitation of Soret band (419-431 nm).

Table 3.1 shows relative optical data of TFP-cored porphyrin dendrimers and their reference porphyrins. Dendrimers **TFP1-TFP3** show similar quantum yields (~24%) and the similar phenomenon occurred in TPP-cored porphyrin dendrimers **TPP1** and **TPP2** (~20%). The quantum yields of porphyrin dendrimers all increase significantly compared to **TFP-Bu** and **TPP** without conjugated dendrons, but it doesn't change with the dendron growing and generation increasing.

In conclusion, we assumed that, for symmetric *meso*-substituted porphyrin dendrimers, (i) the same cored groups connection on porphyrin has the same effect on porphyrin ring planarity, which could further influence the emission spectrum (the ratio of Q(0,0) and Q(0,1)) and quantum yield. (ii) Bridged and terminated groups mainly play a major role in light harvesting, through increasing the dendron

absorption. (i) and (ii) observed are corresponding for TFP-cored porphyrin dendrimers, as well as respectively for *para*-TPP cored series and *meta*-TPP cored ones in chapter 2.

However, we should notice that, this conclusion is limited to small molecular porphyrin: such as **TFP-Bu**, which has the same cored groups as **TFP1-TFP3**, but no further peripheral modification, resulting in different emission spectrum and quantum yield.

3.4.2 Energy transfer behaviors

Their energy transfer behaviors (ET) were also studied from absorption and emission spectra at steady state, and the method of spectral measurement is the same as TPP-cored porphyrin dendrimers. Figure 3.13 presents the emission spectra of **TFP1-TFP3** using excitation wavelength at dendron absorption around 330-350 nm**,** compared to reference **TFP-Bu** as well. These emission spectra were recorded from 250 to 800 nm.

By dendron excitation (~330 nm), the emission spectra of **TFP1** and **TFP2** show only porphyrin core red emission (660 and 725 nm) and no dendron emission in blue-light emitting region. In this condition, the blue emissions from conjugated dendrons are completely quenched through the ET process from dendron to porphyrin core, and red emission is seen exclusively.

The porphyrin **TFP3**, with the largest dendron, shows two emission components: (i) The energy transfer emission at 660 and 725 nm as **TFP1** and **TFP2**. (ii) Residual dendron emission appears around 400 nm. It means that the dendron emission was not totally quenched when ET process occurred through long enough distance of conjugated linkage. On the other hand, **TFP3** has more ET red emission than porphyrin core emission, which is due to its very strong dendron absorption compared to Soret-band.

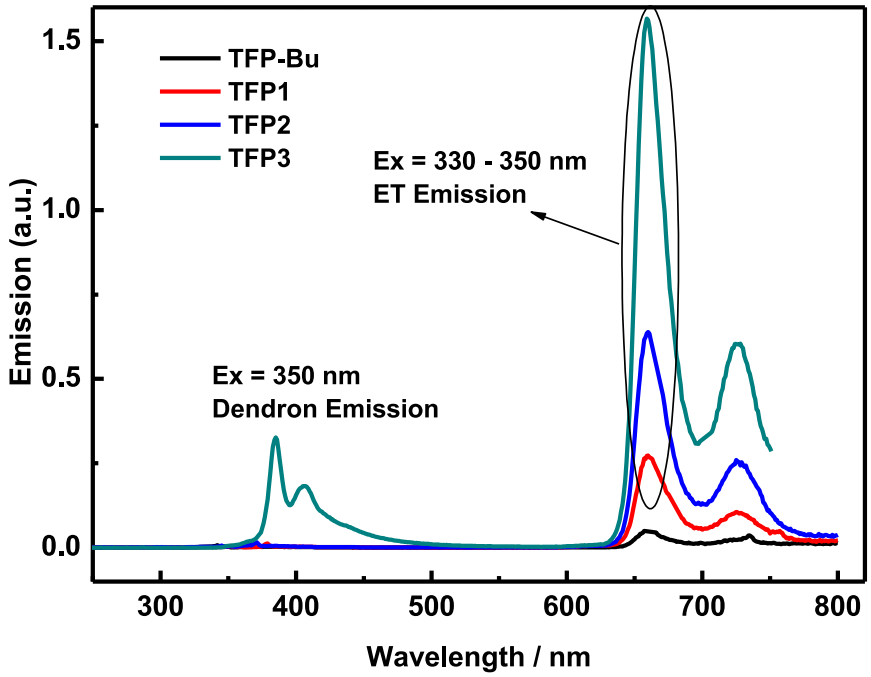

Figure 3.13 Energy transfer behaviors exhibited in emission spectra for **TFP1-TFP3** using excitation wavelengths: Ex = 330-350 nm. (Normalizing the intensity of porphyrin core emission at 660 nm)

To study the energy transfer efficiency of **TFP3**, excitation spectra from two emission peaks (Em = 660 and 725 nm) were measured as shown in Figure 3.14, and compared with absorption spectrum. These spectra are all normalized at the porphyrin absorption Soret-band (431 nm).

Obviously, excitation spectra of Q(0,0) at 660 nm and Q(0,1) at 725 nm are both similar to absorption spectrum, further proves that (i) **TFP3** emissions Q(0,0) and Q(0,1) could both root in two processes: directly exciting porphyrin core and indirectly exciting dendron through ET process; (ii) the energy transfer efficiency of **TFP3** is near to 100%.

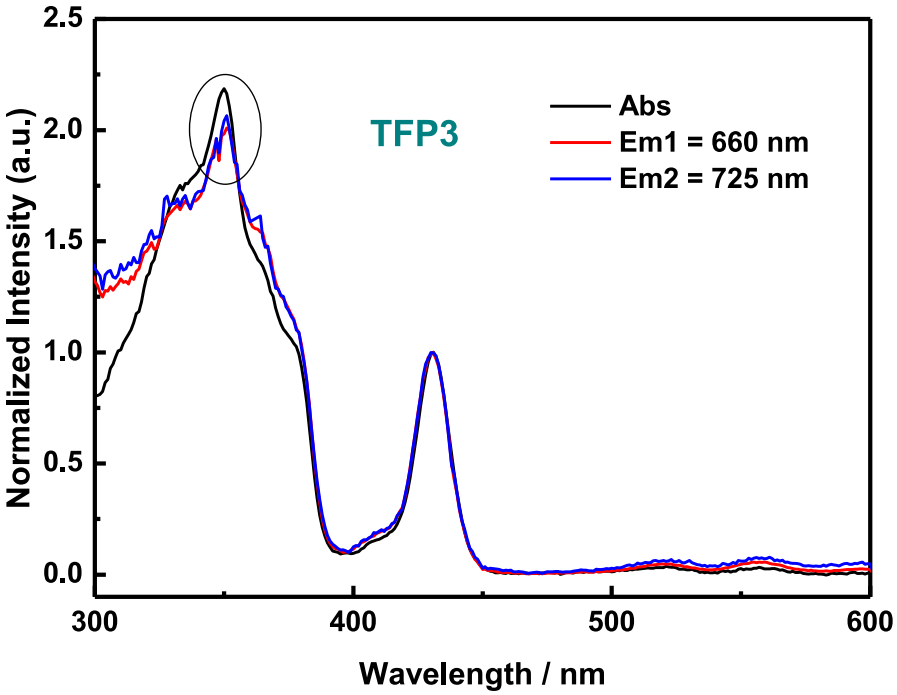

Figure 3.14 Corrected excitation spectra of **TFP3** comparing to absorption spectrum. (Normalizing the intensity of Soret-band at 431 nm)

3.5 Conclusions

1. According to different positions of fluorenyls in conjugated dendrons: cored fluorenyl, bridged fluorenyl and terminated fluorenyl, we designed a series of TFP-cored porphyrin dendrimers **TFP1**, **TFP2** and **TFP3**.

2. These porphyrin dendrimers were synthesized via modified aldehyde dendrons under Adler-Longo's conditions, and these modified dendrons were mainly obtained through repetitive reactions of Sonogashira coupling and Corey-Fuchs reactions.

3. Aldehyde **Dendron 1-3** and dendrimers **TFP1-TFP3** were all well characterized and analysed by ^{1}H NMR spectra.

4. Optical properties of TFP-cored porphyrin dendrimers have obvious dependence on their structures:

(i) Cored fluorenyl mainly influences emission peaks and quantum yield.

(ii) Bridged fluorenyl and terminated fluorenyl have great effect on dendron absorption and energy transfer.

(iii) Dendron emission is not totally quenched by long distance energy transfer process by exciting dendron of **TFP3**.

Experimental section

2,7-dibromo-9,9-dibutyl-9*H*-fluorene:

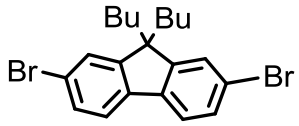

A mixture of 2,7-dibromofluorene (5.0 g, 15.43 mmol, 1 eq) and Bu_4NBr (249 mg, 0.77 mmol, 5% eq) was added with toluene (20 mL, not dry) and 50% NaOH (12 mL, aq), respectively. After 1-bromobutane (5 mL, 46.30 mmol, 3 eq) was added into the solution, the reaction was stirred for 40 h at 75-85 ^oC. The reaction was extracted with water and ethyl acetate. After being evaporated, residue was farther purified by chromatography (heptane), getting colorless crystal (5.5 g, 82% yield).

^1H NMR (400 MHz, $CDCl_3$, ppm): δ 7.53-7.51 (m, 2H), 7.46-7.47 (m, 4H), 1.94-1.90 (m, 4H), 1.14-1.04 (m, 4H), 0.69 (t, J = 7.6 Hz, 6H), 0.61-0.53 (m, 4H).

7-bromo-9,9-dibutyl-9*H*-fluorene-2-carbaldehyde (2):

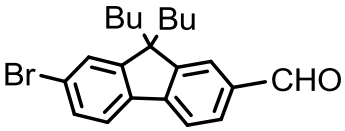

In a Schlenk , a solution of 2,7-dibromo-9,9-dibutyl-9*H*-fluorene (2.5 g, 5.73 mmol, 1 eq) in dry THF (60 mL) was cooled to -78 ^oC in liquid nitrogen-acetone bath. At low temperature, *n*-BuLi (3.58 mL, 5.73 mmol, 1 eq) was added to the solution dropwise for 30 min. Kept it stirring at -78 ^oC for 1 h, then injected dry DMF (1 mL) into the reaction, stirring it at -78 ^oC for another 1 h. Removed the bath and stirred the reaction overnight at room temperature. Added saturated NH_4Cl (aq) and extracted it with ethyl acetate. Evaporated the solvents and the residue was farther purified by chromatography (heptane : CH_2Cl_2 = 7 : 1), getting white powder (2 g, 90% yield).

^1H NMR (400 MHz, $CDCl_3$, ppm): δ 10.06 (s, 1H), 7.87-7.86 (m, 2H), 7.81 (d, J = 8.4 Hz, 1H), 7.64 (d, J = 8.8 Hz, 1H), 7.52-7.50 (m, 2H), 2.07-1.92 (m, 4H), 1.13-1.04 (m, 4H), 0.67 (t, J = 7.2 Hz, 6H), 0.62-0.47 (m, 4H).

9,9-dibutyl-7-((9,9-dibutyl-9*H*-fluoren-2-yl)ethynyl)-9*H*-fluorene-2-carbaldehyde (Dendron 1):

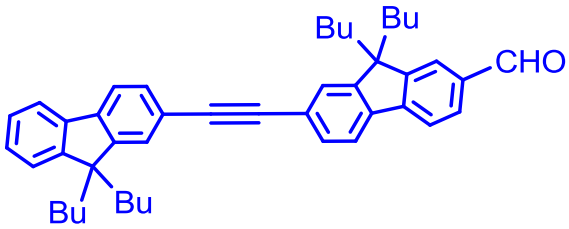

In a schlenk, a mixture of **2** (310 mg, 0.80 mmol, 1 eq), **1** (365 mg, 1.21 mmol, 1.5 eq), $Pd(PPh_3)_2Cl_2$ (17 mg, 0.02 mmol, 3% eq) and CuI (2.3 mg, 0.01 mmol, 1.5% eq) was added DMF (5 mL) and $^{i}Pr_2NH$ (5 mL) under argon, respectively. And the system was degassed by freeze-pump-thaw twice and heated for 2 days at 95 ^{o}C. After being evaporated, residue was absorbed in silica and farther purified by chromatography (heptane : CH_2Cl_2 = 5 : 1), showing white powder (442 mg, 90% yield).

^{1}H NMR (400 MHz, $CDCl_3$, ppm): δ 10.08 (s, 1H), 7.89-7.83 (m, 3H), 7.78 (d, J = 7.6 Hz, 1H), 7.72-7.69 (m, 2H), 7.62-7.56 (m, 4H), 7.37-7.31 (m, 3H), 2.11-1.98 (m, 8H), 1.14-1.05 (m, 8H), 0.68 (td, J_1 = 7.4 Hz, J_2 = 2.8 Hz, 12H), 0.63-0.48 (m, 8H).

7-((3,5-bis((9,9-dibutyl-9*H*-fluoren-2-yl)ethynyl)phenyl)ethynyl)-9,9-dibutyl-9*H*-fluorene-2-carbaldehyde (Dendron 2):

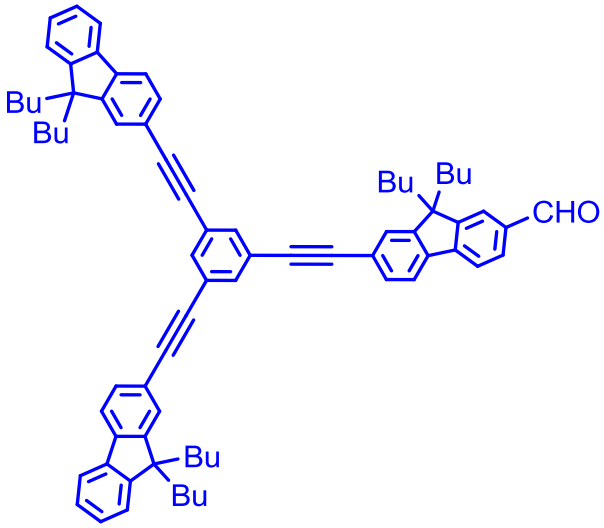

In a schlenk, a mixture of **2** (1.48 g, 3.84 mmol, 1 eq), **3** (2.97 g, 4.22 mmol, 1.1 eq), $Pd(PPh_3)_2Cl_2$ (32 mg, 0.046 mmol, 1.2% eq) and CuI (4.4 mg, 0.023 mmol, 0.6% eq) was added DMF (10 mL) and $^{i}Pr_2NH$ (20 mL) under argon, respectively. And the

system was degassed by freeze-pump-thaw twice and heated for 60 h at 100 °C. After being evaporated, residue was absorbed in silica and farther purified by chromatography (petroleum ether : CH_2Cl_2 = 5 : 1), showing white powder (2.46 g, 63% yield).

^{1}H NMR (400 MHz, $CDCl_3$, ppm): δ 10.08 (s, 1H), 7.90-7.84 (m, 3H), 7.79 (d, J = 7.6 Hz, 1H), 7.75-7.70 (m, 7H), 7.59-7.57 (m, 2H), 7.54-7.52 (m, 4H), 7.38-7.32 (m, 6H), 2.10-1.98 (m, 12H), 1.15-1.06 (m, 12H), 0.69 (td, J_1 = 7.2 Hz, J_2 = 2.4 Hz, 18H), 0.65-0.52 (m, 30H).

9,9-dibutyl-2,7-diiodo-9*H*-fluorene:

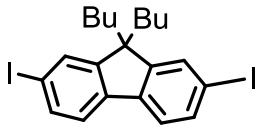

In a Schlenk , a solution of 2,7-dibromo-9,9-dibutyl-9*H*-fluorene (2.06 g, 4.72 mmol, 1 eq) in dry THF (20 mL) was cooled to -78 °C in liquid nitrogen-acetone bath under argon. At low temperature, *n*-BuLi (7.08 mL, 11.33 mmol, 2.4 eq) was added to the solution dropwise for 30 min. Kept it stirring at -78 °C for 2 h, then slowly injected a solution of I_2 (2.88 g, 11.33 mmol, 2.4 eq) dissolved in THF (10 mL) and stirred it at -78 °C for another 2 h. Removed the bath and stirred the reaction overnight at room temperature. Added saturated $Na_2S_2O_3$ (aq) to reduce excess of I_2 and extracted it with ethyl acetate. Evaporated the solvents and the residue was farther purified by chromatography (petroleum ether), getting white crystal (2.4 g, 96% yield).

^{1}H NMR (400 MHz, $CDCl_3$, ppm): δ 7.67-7.64 (m, 4H), 7.41 (d, J = 8.0 Hz, 2H), 1.92-1.88 (m, 4H), 1.14-1.04 (m, 4H), 0.69 (t, J = 7.2 Hz, 6H), 0.60-0.52 (m, 4H).

9,9-dibutyl-7-iodo-9*H*-fluorene-2-carbaldehyde (4):

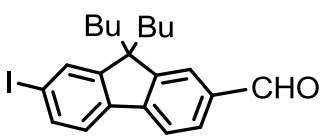

In a Schlenk , a solution of 9,9-dibutyl-2,7-diiodo-9*H*-fluorene (523 mg, 0.99 mmol, 1

eq) in dry THF (40 mL) was cooled to -78 ^{o}C in liquid nitrogen-acetone bath. At low temperature, *n*-BuLi (0.62 mL, 0.99 mmol, 1 eq) was added to the solution dropwise for 10 min. Kept it stirring at -78 ^{o}C for 20 min, then injected dry DMF (1 mL) into the reaction, stirring it at -78 ^{o}C for another 1 h. Removed the bath and stirred the reaction for 2 h at room temperature. Added saturated NH_4Cl (aq) and extracted it with ethyl acetate. Evaporated the solvents and the residue was farther purified by chromatography (petroleum ether : CH_2Cl_2 = 5 : 1), getting white powder (310 g, 73% yield).

^{1}H NMR (400 MHz, $CDCl_3$, ppm): δ 10.06 (s, 1H), 7.87-7.85 (m, 2H), 7.82-7.80 (m, 1H), 7.72-7.71 (m, 2H), 7.52 (d, *J* = 8.4 Hz, 1H), 2.06-1.91 (m, 4H), 1.13-1.04 (m, 4H), 0.67 (t, *J* = 7.2 Hz, 6H), 0.62-0.46 (m, 4H).

2,2'-(5-((9,9-dibutyl-7-(2,2-dibromovinyl)-9*H*-fluoren-2-yl)ethynyl)-1,3-phenylene) bis(ethyne-2,1-diyl)bis(9,9-dibutyl-9*H*-fluorene) (5):

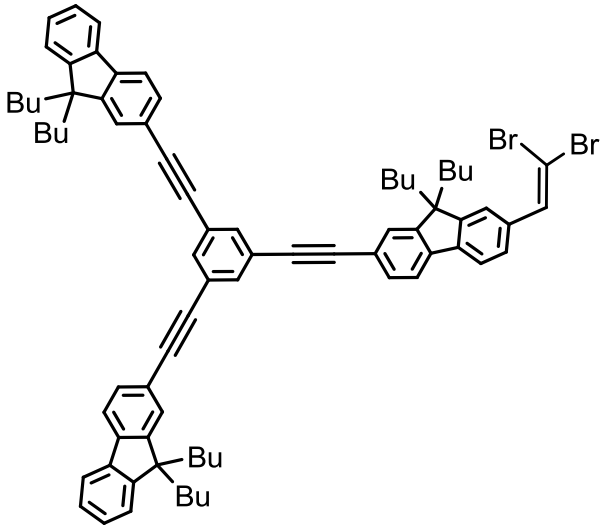

In a schlenk, a mixture of PPh_3 (1.28 g, 4.88 mmol, 2 eq) and Zn powder (317 mg, 4.88 mmol, 2 eq) was added dry CH_2Cl_2 (15 mL). After the solution was cooled to 0 ^{o}C in ice-water bath, put CBr_4 (1.62 g, 4.88 mmol, 2 eq) into schlenk under argon protection and kept low temperature for 2 min. Removed the bath and stirred the mixture overnight at room temperature. Cooled the mixture to 0 ^{o}C again, and injected the solution of **Dendron 2** (2.46 g, 2.44 mmol, 1 eq) dissolved in dry CH_2Cl_2 (15 mL) into the schlenk under argon protection. Kept the low temperature (0 ^{o}C) for 10 min

and stirred it overnight in dark at room temperature. Filtered the solution and evaporated CH_2Cl_2, then the residue was absorbed in silica and farther purified by chromatography (heptane : CH_2Cl_2 = 100 : 5), showing white powder (2.46 g, 87% yield).

^{1}H NMR (400 MHz, $CDCl_3$, ppm): δ 7.74-7.69 (m, 9H), 7.58 (d, *J* = 6.8 Hz, 2H), 7.54-7.52 (m, 7H), 7.35-7.31 (m, 6H), 2.00 (t, *J* = 8.0 Hz, 12H), 1.15-1.06 (m, 12H), 0.69 (t, *J* = 7.2 Hz, 18H), 0.64-0.54 (m, 12H).

2,2'-(5-((9,9-dibutyl-7-ethynyl-9*H*-fluoren-2-yl)ethy4nyl)-1,3-phenylene)bis (ethyne-2,1-diyl)bis(9,9-dibutyl-9*H*-fluorene) (6):

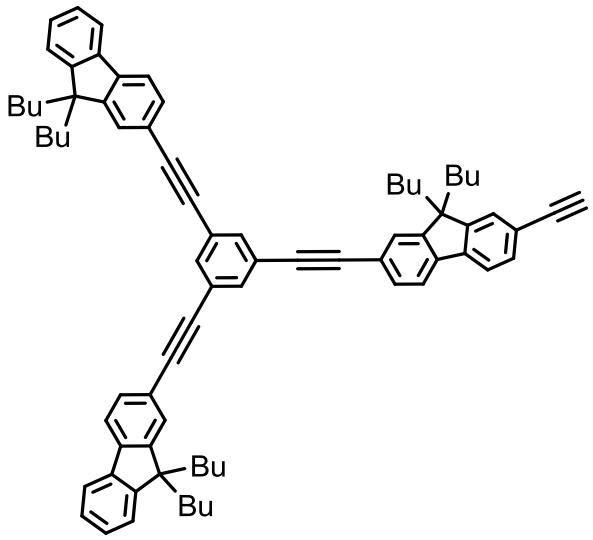

N-BuLi (1.1 mL, 1.75 mmol, 3 eq) was added to a cold (-78^{o}C) solution of ^{i}Pr$_2$NH (0.25 mL, 1.75 mmol, 3 eq) in dry THF (5 mL). After warming up to room temperature carefully, the mixture was injected dropwise into the solution of **5** (680 mg, 0.58 mmol, 1 eq) in dry THF (10 mL) at -78 ^{o}C in liquid nitrogen-acetone bath. Kept the low temperature for 1 h, then quenched the reaction with saturated NH_4Cl (5 mL, aq). Removed the bath, stirred it until the temperature was up to room temperature. Extracted it with ethyl acetate and dried it with $MgSO_4$. Evaporated solvents, then the residue was absorbed in silica and farther purified by chromatography (heptane : CH_2Cl_2 = 100 : 5), showing white powder (560 mg, 95% yield).

^{1}H NMR (400 MHz, $CDCl_3$, ppm): δ 7.74-7.65 (m, 9H), 7.54-7.49 (m, 8H), 7.35-7.34 (m, 6H), 3.17 (s, 1H), 2.00 (t, *J* = 8.0 Hz, 12H), 1.15-1.06 (m, 12H), 0.70 (t, *J* = 7.4 Hz, 18H), 0.65-0.54 (m, 12H).

3,5-bis((7-((3,5-bis((9,9-dibutyl-9*H*-fluoren-2-yl)ethynyl)phenyl)ethynyl)-9,9-dibutyl-9*H*-fluoren-2-yl)ethynyl)benzaldehyde (7):

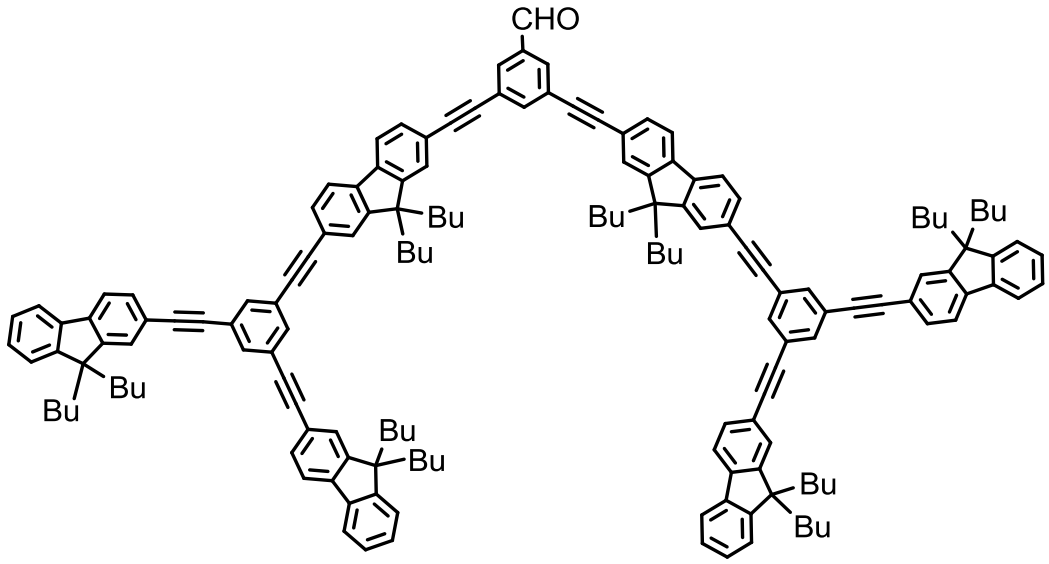

In a schlenk, a mixture of 3,5-dibromobenzaldehyde (263 mg, 1.00 mmol, 1 eq), **6** (2 g, 2.00 mmol, 2 eq), $Pd(PPh_3)_2Cl_2$ (28 mg, 0.04 mmol, 2% eq) and CuI (3.8 mg, 0.02 mmol, 1% eq) was added DMF (12 mL) and $^iPr_2NH$ (12 mL) under argon, respectively. And the system was degassed by freeze-pump-thaw twice and heated for 60 h at 100 ^oC. After being evaporated, residue was farther purified by chromatography (heptane : CH_2Cl_2 = 5 : 1), showing light yellow powder (1.2 g, 57% yield).

^{1}H NMR (400 MHz, $CDCl_3$, ppm): δ 10.05 (s, 1H), 8.03 (s, 3H), 7.75-7.70 (m, 18H), 7.57-7.53 (m, 16H), 7.35-7.31 (m, 12H), 2.05-1.98 (m, 24H), 1.17-1.06 (m, 24H), 0.74-0.55 (m, 60H).

2,2',2'',2'''-(5,5'-(7,7'-(5-(2,2-dibromovinyl)-1,3-phenylene)bis(ethyne-2,1-diyl) bis(9,9-dibutyl-9*H*-fluorene-7,2-diyl))bis(ethyne-2,1-diyl)bis(benzene-5,3,1-triyl)) tetrakis(ethyne-2,1-diyl)tetrakis(9,9-dibutyl-9*H*-fluorene) (8) :

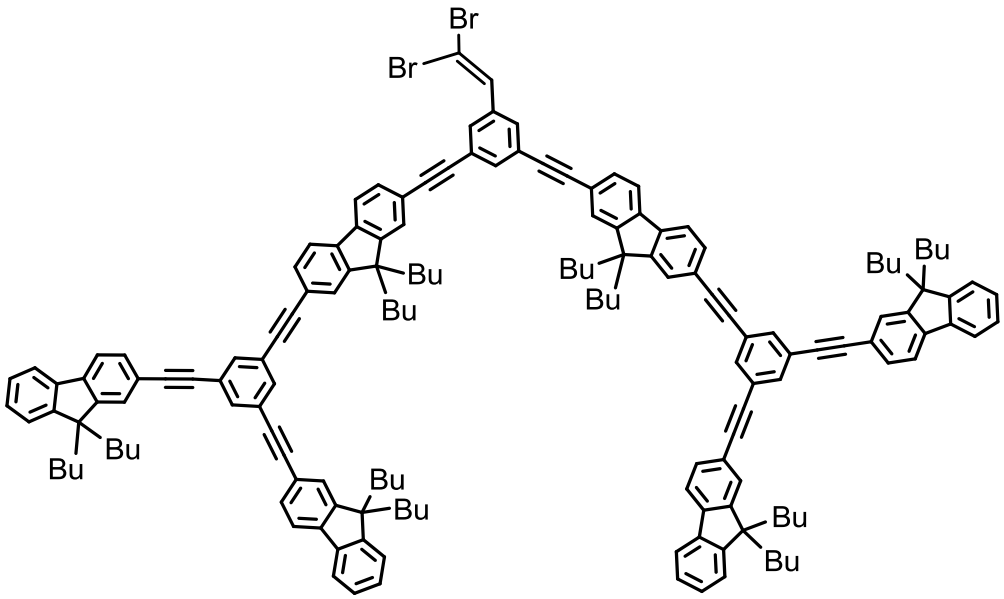

In a schlenk, a mixture of PPh_3 (299 mg, 1.14 mmol, 2 eq) and Zn powder (74 mg, 1.14 mmol, 2 eq) was added dry CH_2Cl_2 (6 mL). After the solution was cooled to 0 ^oC in ice-water bath, put CBr_4 (378 mg, 1.14 mmol, 2 eq) into schlenk under argon protection and kept low temperature for 2 min. Removed the bath and stirred the mixture overnight at room temperature. Cooled the mixture to 0 ^oC again, and injected the solution of **7** (1.2 g, 0.57 mmol, 1 eq) dissolved in dry CH_2Cl_2 (30 mL) into the schlenk under argon protection. Kept the low temperature (0 ^oC) for 10 min and stirred it overnight in dark at room temperature. Filtered the solution and evaporated CH_2Cl_2, then the residue was absorbed in silica and farther purified by chromatography (petroleum ether : CH_2Cl_2 = 20 : 1 to 10 : 1), showing white powder (1.0 g, 77% yield).

^1H NMR (400 MHz, $CDCl_3$, ppm): δ 7.81-7.69 (m, 21H), 7.56-7.48 (m, 17H), 7.38-7.32 (m, 12H), 2.05-1.98 (m, 24H), 1.16-1.06 (m, 24H), 0.74-0.54 (m, 60H).

2,2',2'',2'''-(5,5'-(7,7'-(5-ethynyl-1,3-phenylene)bis(ethyne-2,1-diyl)bis(9,9-dibutyl-9*H*-fluorene-7,2-diyl))bis(ethyne-2,1-diyl)bis(benzene-5,3,1-triyl))tetrakis(ethyne-2,1-diyl)tetrakis(9,9-dibutyl-9*H*-fluorene) (9):

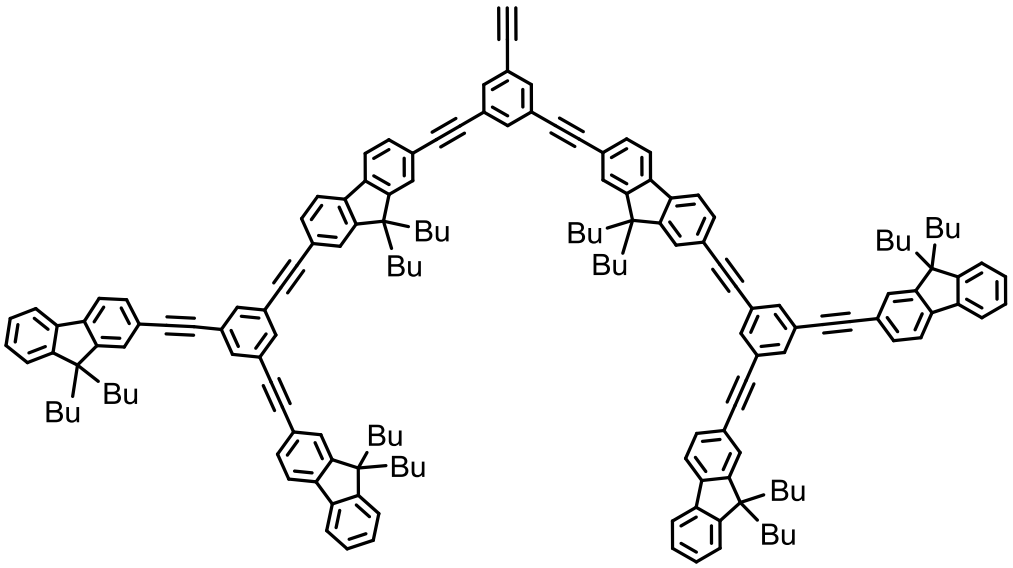

N-BuLi (0.83 mL, 1.33 mmol, 3 eq) was added to a cold (-78 ^{o}C) solution of $^{i}Pr_2NH$ (0.20 mL, 1.33 mmol, 3 eq) in dry THF (5 mL). After warming up to room temperature carefully, the mixture was injected dropwise into the solution of **8** (1.0 g, 0.44 mmol, 1 eq) in dry THF (10 mL) at -78 ^{o}C in liquid nitrogen-acetone bath. Kept the low temperature for 1 h, then quenched the reaction with saturated NH_4Cl (5 mL, aq). Removed the bath, and stirred it until the temperature was up to room temperature. Extracted it with ethyl acetate and dried it with $MgSO_4$. Evaporated solvents, then the residue was absorbed in silica and farther purified by chromatography (petroleum ether : CH_2Cl_2 = 100 : 5), showing green white powder (720 mg, 77% yield).

^{1}H NMR (400 MHz, $CDCl_3$, ppm): δ 7.77-7.67 (m, 21H), 7.57-7.53 (m, 16H), 7.38-7.32 (m, 12H), 3.14 (s, 1H), 2.05-1.98 (m, 24H), 1.17-1.06 (m, 24H), 0.74-0.54 (m, 60H).

7-((3,5-bis((7-((3,5-bis((9,9-dibutyl-9*H*-fluoren-2-yl)ethynyl)phenyl)ethynyl)-9,9-dibutyl-9*H*-fluoren-2-yl)ethynyl)phenyl)ethynyl)-9,9-dibutyl-9*H*-fluorene-2-carbaldehyde (Dendron 3):

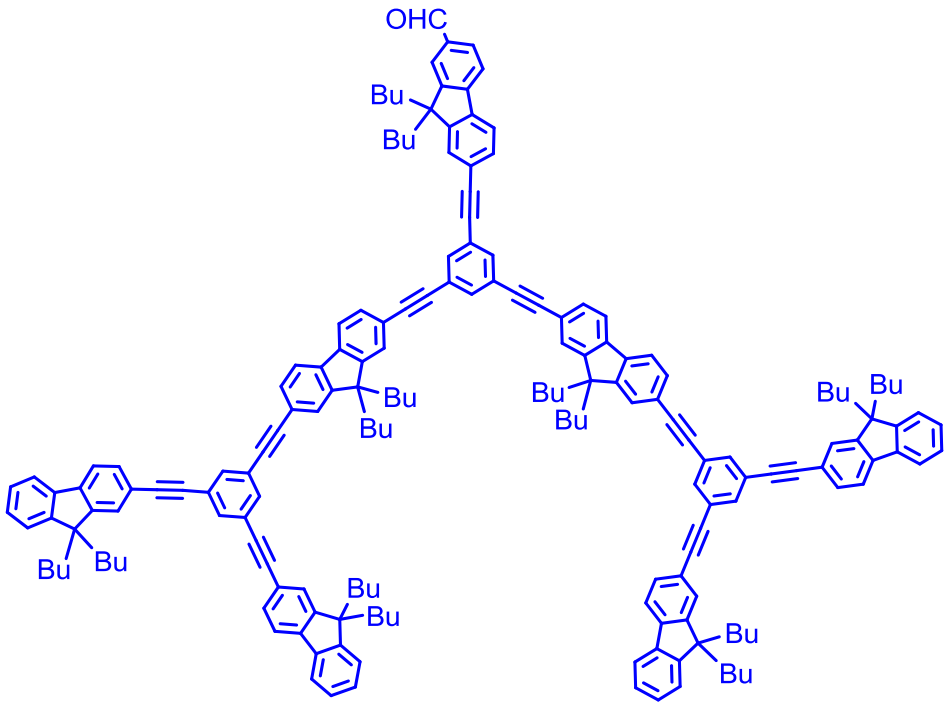

In a schlenk, a mixture of **4** (102 mg, 0.24 mmol, 1 eq), **9** (500 mg, 0.24 mmol, 1 eq), $Pd(PPh_3)_2Cl_2$ (10 mg, 0.14 mmol, 6% eq) and CuI (1.5 mg, 0.07 mmol, 3% eq) was added DMF (10 mL) and $^{i}Pr_2NH$ (10 mL) under argon, respectively. And the system was degassed by freeze-pump-thaw twice and heated for 90 h at 95 ^{o}C. After being evaporated, residue was absorbed in silica and farther purified by chromatography (petroleum ether : CH_2Cl_2 = 5 : 1 to 3 : 1), showing light yellow powder (250 mg, 66% yield).

^{1}H NMR (400 MHz, $CDCl_3$, ppm): δ 10.09 (s, 1H), 7.90-7.85 (m, 3H), 7.81-7.70 (m, 21H), 7.60-7.53 (m, 19H), 7.38-7.32 (m, 12H), 2.09-1.98 (m, 28H), 1.17-1.06 (m, 28H), 0.75-0.54 (m, 70H).

TFP1:

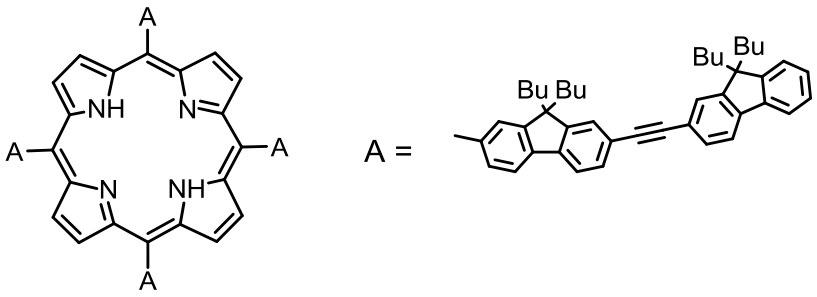

The mixture of **Dendron 1** (300 mg, 0.49 mmol, 1 eq) and propionic acid (4 mL) was heated to 120 ^{o}C. After pyrrole (0.03 mL, 0.49 mmol, 1 eq) in propionic acid (0.6 mL) was added into the mixture dropwise, the reaction kept refluxing for 5.5 h. After cooling to room temperature, MeOH was added to the reaction mixture to obtain precipitate and the precipitate was filtered. The residue could be purified by chromatography (petroleum ether : CH_2Cl_2 = 5 : 1), showing red powder, and recrystallized by refluxing $CHCl_3$ and MeOH, getting purple powder (60 mg, 19% yield).

^{1}H NMR (400 MHz, $CDCl_3$, ppm): δ 8.93 (s, 8H), 8.26-8.21 (m, 8H), 8.09 (d, *J* = 7.6 Hz, 4H), 7.96 (d, *J* = 8.0 Hz, 4H), 7.73-7.71 (m, 16H), 7.62-7.60 (m, 8H), 7.36-7.32 (m, 12H), 2.17 (broad, 16H), 2.02 (t, *J* = 8.0 Hz, 16H), 1.25-1.17 (m, 16H), 1.14-1.08 (m, 16H), 0.99-0.94 (m, broad, 16H), 0.81-0.76 (m, 24H), 0.70 (t, *J* = 7.2 Hz, 24H), 0.66-0.55 (m, 16H), -2.56 (s, 2H).

^{13}C NMR (125 MHz, $CDCl_3$, ppm): δ 151.3, 150.0, 150.8, 149.6, 141.5, 141.4, 141.2, 140.5, 140.1, 133.8, 131.0, 130.6, 129.4, 127.5, 126.9, 126.1, 126.0, 122.9, 122.1, 121.5, 120.7, 120.1, 120.0, 119.7, 118.2, 90.9, 90.5, 55.4, 55.1, 40.3, 26.4, 25.9, 23.1, 14.1, 14.0, 13.8.

HRMS-ESI: m/z = 2616.6227 $[M+H]^+$ (calcd: 2616.6315).

Anal. Calcd. (%) for $C_{196}H_{206}N_4$: C, 89.93; H, 7.93; N, 2.14. Found: C, 89.68; H, 7.90; N, 2.06.

TFP2:

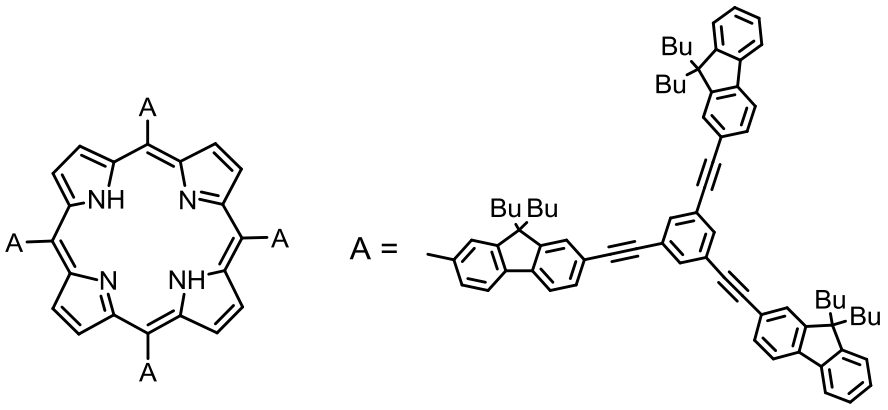

The mixture of **Dendron 2** (200 mg, 0.20 mmol, 1 eq) and propionic acid (3 mL) was heated to 120 ^{o}C. After pyrrole (0.01 mL, 0.2 mmol, 1 eq) in propionic acid (0.3 mL) was added into the mixture dropwise, the reaction kept refluxing for 5.5 h. After cooling to room temperature, MeOH was added to the reaction mixture to obtain precipitate and the precipitate was filtered. The residue could be purified by chromatography (petroleum ether : CH_2Cl_2 = 5 : 1), showing red powder, and recrystallized by refluxing $CHCl_3$ and MeOH, getting purple powder (40 mg, 19% yield).

^{1}H NMR (400 MHz, $CDCl_3$, ppm): δ 8.94 (s, 8H), 8.27-8.23 (m, 8H), 8.11 (d, *J* = 7.2 Hz, 4H), 7.97 (d, *J* = 7.6 Hz, 4H), 7.79-7.77 (m, 12H), 7.72-7.68 (m, 24H), 7.56-7.54 (m, 16H), 7.36-7.32 (m, 24H), 2.18 (broad, 16H), 2.01 (t, *J* = 8.0 Hz, 32H), 1.26-1.19 (m, 16H), 1.16-1.06 (m, 32H), 1.03-0.93 (m, broad, 16H), 0.83-0.77 (m, 24H), 0.70 (t, *J* = 7.4 Hz, 48 H), 0.65-0.54 (m, 32H), -2.56 (s, 2H).

^{13}C NMR (125 MHz, $CDCl_3$, ppm): δ 151.4, 151.1, 150.8, 149.6, 141.8, 141.6, 141.5, 140.3, 140.0, 133.9, 131.1, 130.7, 129.4, 127.6, 126.9, 126.3, 126.1, 124.3, 124.2, 122.9, 121.5, 120.9, 120.7, 120.2, 120.1, 119.7, 118.3, 91.7, 88.3, 88.0, 55.4, 55.1, 40.3, 40.2, 26.4, 25.9, 23.1, 14.1, 14.0, 13.8.

HRMS-ESI: m/z = 4217.5189 $[M+H]^+$ (calcd: 4217.5079).

Anal. Calcd. (%) for $C_{320}H_{318}N_4$: C, 91.08; H, 7.60; N, 1.33. Found: C, 90.88; H, 7.53; N, 1.20.

TFP3:

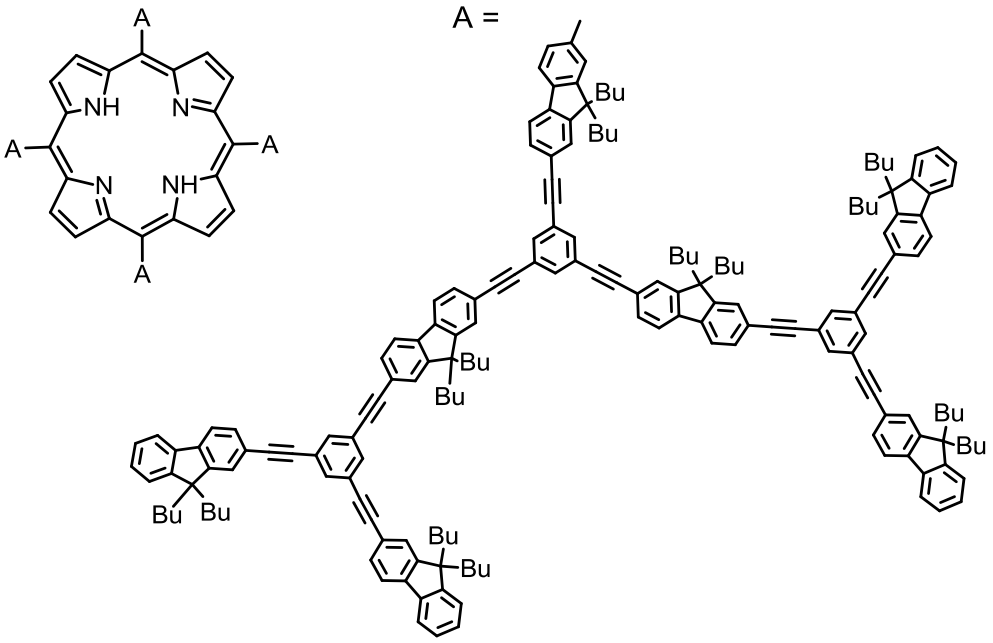

The mixture of **Dendron 3** (240 mg, 0.1 mmol, 1 eq) and propionic acid (4 mL) was heated to 120 ^{o}C. After pyrrole (0.007 mL, 0.1 mmol, 1 eq) in propionic acid (0.5 mL) was added into the mixture dropwise, the reaction kept refluxing for 5.5 h. After being evaporated, residue was absorbed in silica and farther purified by chromatography (petroleum ether : CH_2Cl_2 = 5 : 1), showing red powder (2 mg, 1% yield).

^{1}H NMR (400 MHz, $CDCl_3$, ppm): δ 8.94 (s, 8H), 8.29-8.23 (m, 8H), 8.12 (d, *J* = 8.4 Hz, 4H), 7.98 (d, *J* = 7.6 Hz, 4H), 7.81-7.79 (m, 12H), 7.75-7.69 (m, 76H), 7.59-7.53 (m, 68H), 7.36-7.32 (m, 48H), 2.19 (broad, 16H), 2.09-1.98 (m, 96H), 1.26-1.22 (m, 16H), 1.16-1.06 (m, 96H), 0.99-0.94 (broad, 16H), 0.85-0.80 (m, 24H), 0.75-0.67 (m, 144H), 0.65-0.55 (m, 96H), -2.55 (s, 2H).

^{13}C NMR (125 MHz, $CDCl_3$, ppm): δ 151.2, 151.0, 150.8, 148.8, 143.2, 141.8, 141.0, 140.9, 140.3, 140.0, 133.9, 133.8, 131.1, 130.9, 130.7, 127.6, 126.9, 126.1, 124.3, 124.1, 124.0, 122.9, 121.6, 120.9, 120.7, 120.1, 120.0, 119.7, 91.7, 91.6, 91.5, 88.4, 87.9, 55.4, 55.2, 55.0, 40.2, 26.3, 25.9, 23.0, 14.1, 14.0, 13.8.

HRMS-ESI: m/z = 9832.8390 $[M+H]^+$ (calcd: 9828.9364).

Chapter 4

The influence of linkages in dendron: Porphyrin dendrimers with Bridged vinyl and alkynyl

4.1 Molecular design

To construct a conjugated molecule, vinyl and alkynyl are usually used as bridged group: vinyl creates local planar conjugated structure with *trans*- or *cis*-configuration; alkynyl provides local linear conjugated structure which owns higher rigid properties. In reported publications, there are many porphyrin dendrimers designed and synthesized containing bridged vinyl and alkynyl units by chemists.[23-25,67]

In our project, we have synthesized different triple bonded porphyrin dendrimers with bridged alkynyl, then we devoted to conjugated double bonded series with bridged vinyl. We wonder that different bridged groups would result in what effects on optical properties of porphyrin dendrimers.

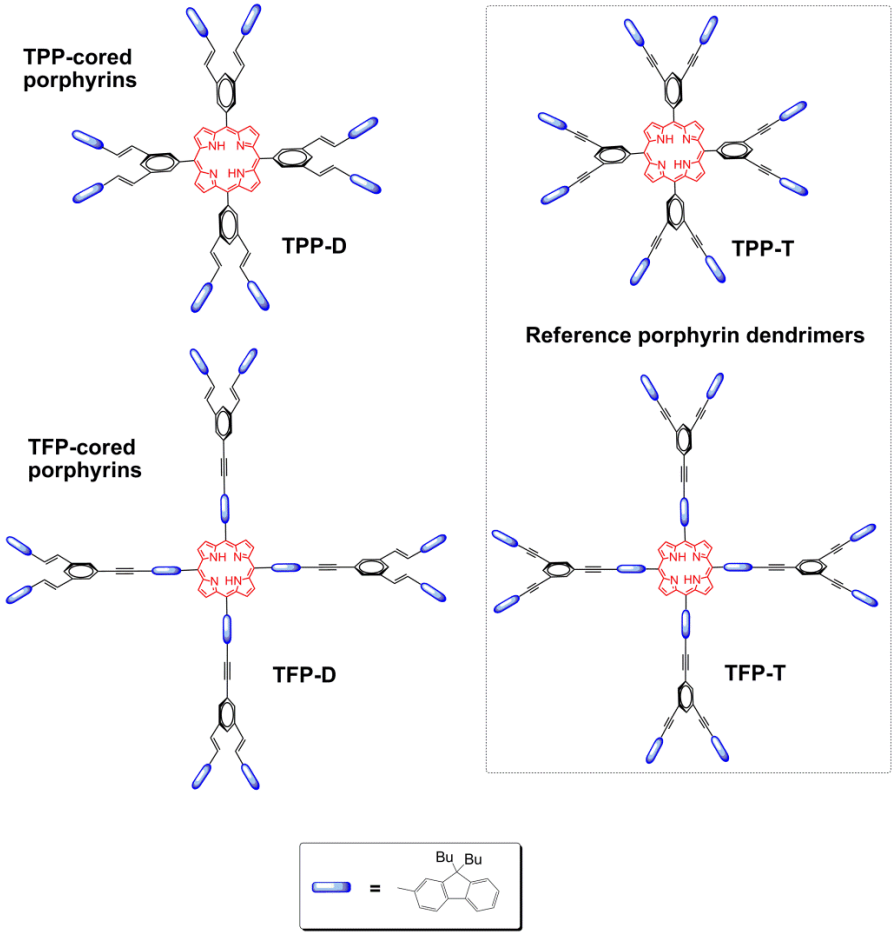

Figure 4.1 Molecular structures of porphyrin dendrimers with bridged vinyl (D) and their reference series with bridged alkynyl (T).

Along this line, we respectively designed TPP-cored and TFP-cored porphyrin dendrimers with bridged vinyl, named **TPP-D** and **TFP-D**. Then we compared these new double bonded (D) dendrimers to relative triple bonded (T) ones, named **TPP-T** and **TFP-T**, presented before as TPP5 (chapter 2) and TFP2 (chapter 3) respectively. For clarity, their molecular structures were drawn in Figure 4.1.

4.2 Synthetic method design

The successful methods of triple bonded series, **TPP-T** and **TFP-T**, were described in detail in former chapters, and herein we will synthesize the new double bonded series **TPP-D** and **TFP-D** in similar procedures:

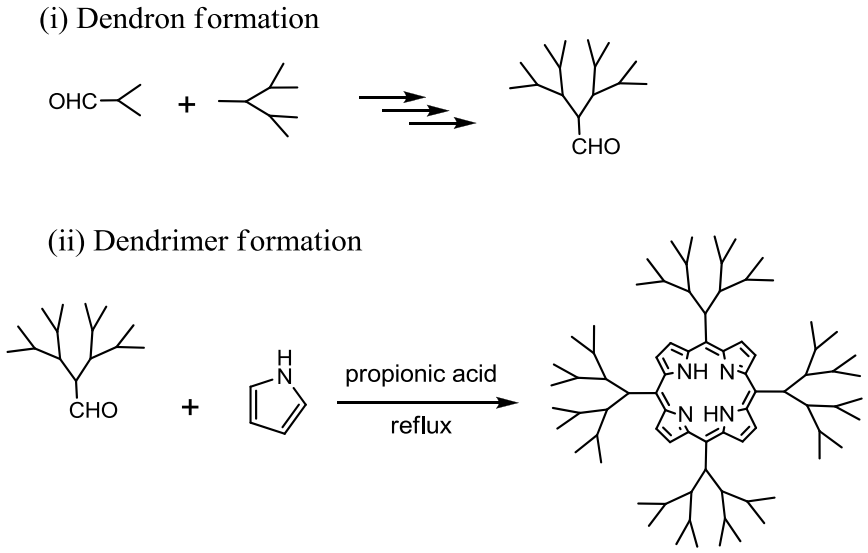

Figure 4.2 Synthetic strategy used for porphyrin dendrimers with bridged vinyl.

4.2.1 Dendron formation

The synthesis of vinyl-bridged aldehyde dendrons **D-PhCHO** and **D-FlCHO** was achieved in Figure 4.3. As illustrated, double bond was formed by classic associative reactions of Michaelis-Arbuzov reaction[68] and Horner-Wadsworth-Emmons reaction[68].

First, 1-bromo-3,5-bismethylbenzene was chosen as the starting material, and halogenation occurred in benzyl by NBS (*N*-bromosuccinimide) in dichloromethane

using AIBN (azobisisobutyronitrile) as radical initiator. Normally, this reaction yields about 20-30% target product usually together with multi-substituted components.[68bc,69] Therefore, the reaction conditions were simply optimized from temperature, time and solvent; the adopted conditions (as shown in experimental section) gave the product including monobromo-substituted and tribromo-substituted byproducts: the former could be isolated by chromatography (heptane), the latter was mixed in dibromo-substituted product (ratio tri- : di- = 1 : 4 in ^{1}H NMR spectrum) calculating the 49% yield of target product in halogenation.

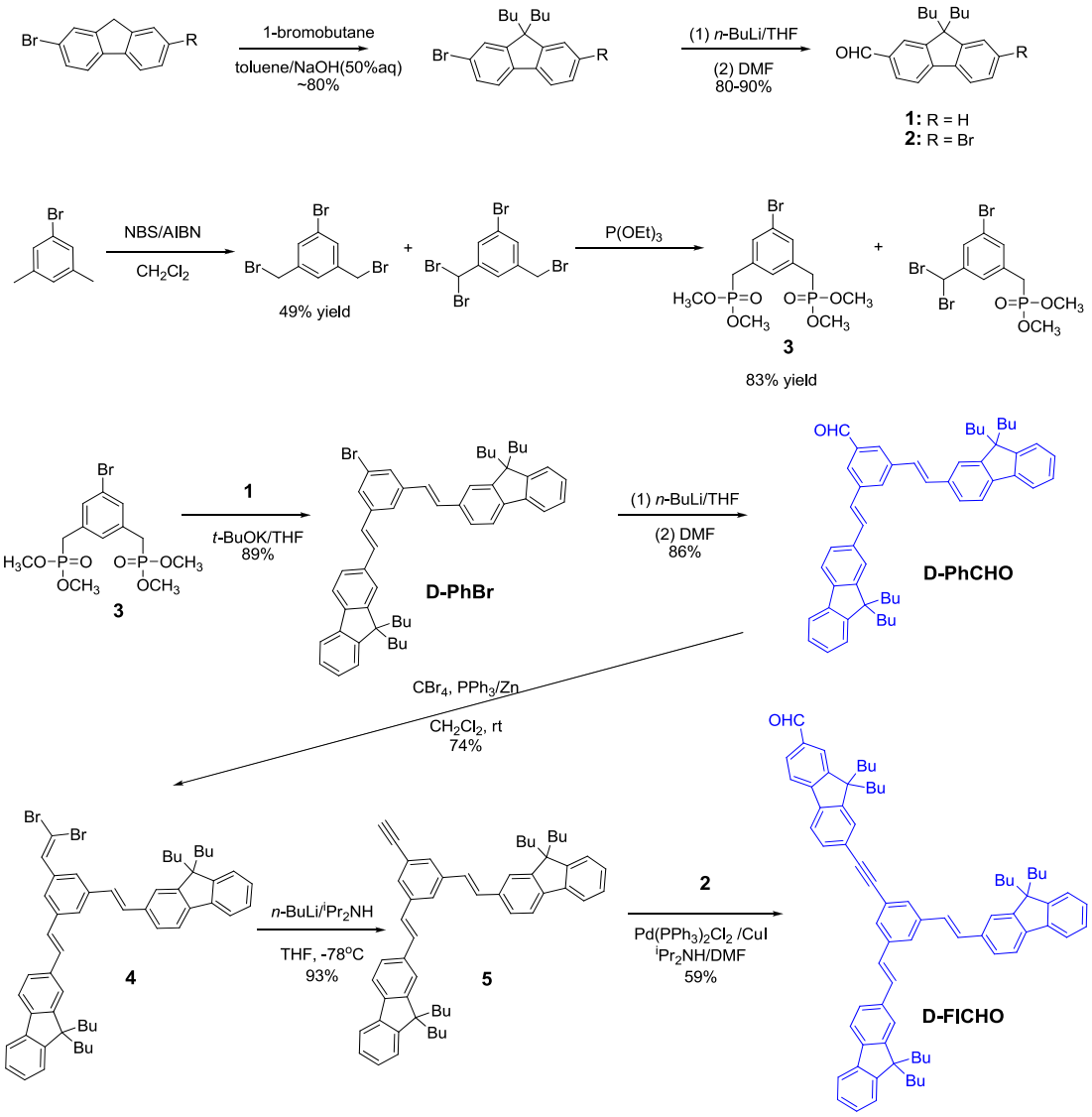

Figure 4.3 Synthetic routes of vinyl-bridged aldehydes **D-PhCHO** and **D-FlCHO**.

In the next step, Michaelis-Arbuzov reaction, the mixed bromo-substituted material reacted directly with refluxed excess of $P(OEt)_3$. The result components also included desired di-substituted product **3** and mono-substituted byproduct which could be isolated by chromatography. In details, at first the byproduct was washed easily using CH_2Cl_2, subsequently the target product was collected by ethyl acetate giving colorless oil as 83% yield.

In Horner-Wadsworth-Emmons reaction, compound **3** reacting with aldehyde **1** under *t*-BuOK/THF condition created double-bond linked **D-PhBr** with 89% yield as the intermediate. Then the aldehyde **D-PhCHO** could be synthesized from **D-PhBr** through two steps: (1) *n*-BuLi/THF (2) DMF, showing 86% yield in totally.

Taking the former dendron **D-PhCHO** as starting material, dendron **D-FlCHO** was prepared by associative reactions of Corey-Fuchs reaction (74% yield for first step, 93% yield for the second one) and Sonogashira coupling (59% yield), giving mixed conjugated aldehyde dendron (see Figure 4.3).

Another two alkynyl-bridged dendrons **T-PhCHO** and **T-FlCHO**, synthesized in chapter 2 (named Dendron 5) and chapter 3 (named Dendron 2) respectively, are represented in Figure 4.4. They are dendron analogues, used to prepare relative alkynyl-bridged porphyrin dendrimers as reference porphyrins in the following discussion.

4.2.2 Dendrimer formation

The synthesis of vinyl-bridged porphyrin dendrimers **TPP-D** and **TFP-D** was shown in Figure 4.4, and we adopted the same Adler-Longo's conditions as for alkynyl-bridged porphyrin dendrimers **TPP-T** and **TFP-T** (chapter 2 and 3). In more details, the condensation of dendron **D-PhCHO** and pyrrole in refluxing propionic acid for 5.5 h yielded **TPP-D** about 8%, and dendron **D-FlCHO** formed **TFP-D** about 1% yield. Compared to triple bonded analogues, the yields for double bonded dendrimers are obviously lower.

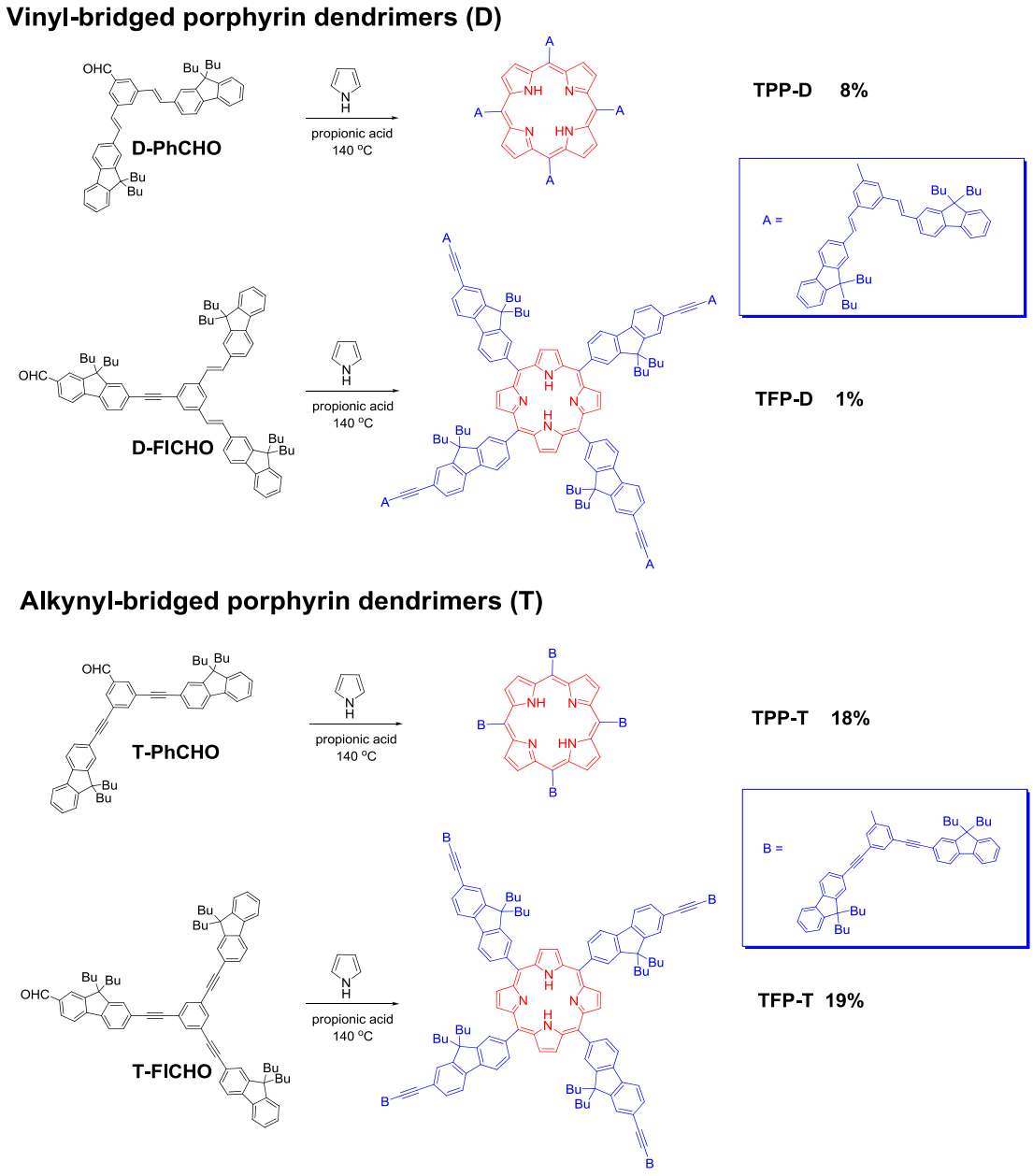

Figure 4.4 Synthesis of vinyl-bridged porphyrin dendrimers **TPP-D**, **TFP-D** and alkynyl-bridged ones **TPP-T**, **TFP-T** for comparison.

4.3 ^{1}H NMR analysis

Vinyl-bridged dendrons **D-PhCHO**, **D-FlCHO** and dendrimers **TPP-D** and **TFP-D** were all well characterized by ^{1}H NMR in $CDCl_3$ (400 MHz). Their ^{1}H NMR spectra were compared with ones of alkynyl-bridged dendrons **T-PhCHO**, **T-FlCHO** and dendrimers **TPP-T** and **TFP-T** previously analyzed (chapter 2 and 3).

*4.3.1 ^{1}H NMR spectra of dendrons **D-PhCHO**, **T-PhCHO**, **D-FlCHO** and **T-FlCHO***

Figure 4.5 shows the full ^{1}H NMR spectra of dendrons **D-PhCHO**, **T-PhCHO**, **D-FlCHO** and **T-FlCHO**: one proton for aldehyde group is around 10 ppm, protons situated 7-8 ppm belong to aromatic moiety (phenyl and fluorenyl groups), and four groups of protons in alkyl moiety are located 0.5-2.1 ppm. Specially for double bonded dendrons **D-PhCHO** and **D-FlCHO**, four protons of vinyl are involved in broad peak around 7.18-7.40 ppm.

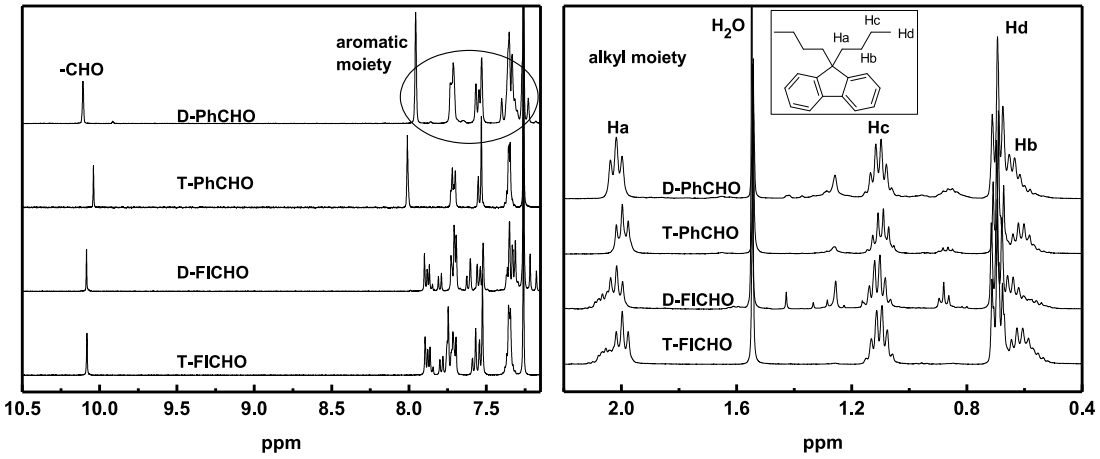

Figure 4.5 ^{1}H NMR spectra of dendrons **D-PhCHO**, **T-PhCHO**, **D-FlCHO** and **T-FlCHO**.

As Figure 4.5 shows, different conjugated bridged groups influence more on the shifts of some near protons, such as some aromatic protons, and aldehyde protons in **D-PhCHO** and **T-PhCHO**. But for long-distanced protons, alkyl moiety of fluorenyl

and aldehyde protons in **D-FlCHO** and **T-FlCHO**, the shifts keep no change. The similar phenomenon also occurred in the proton shifts of their relative porphyrin dendrimers, Hβ and –NH (see Figure 4.6).

*4.3.2 ^{1}H NMR spectra of porphyrin dendrimers **TPP-D**, **TPP-T**, **TFP-D** and **TFP-T***

As Figure 4.6 shows, (i) eight protons Hβ of porphyrin ring are located around 9 ppm, and (ii) protons in aromatic moiety and four vinyl protons are around 7.2-8.4 ppm. Only some of protons in cored phenyl and cored fluorenyl can be assigned: H_A and H_B in phenyl, and H_A, H_B and H_C in fluorenyl. Protons of vinyl in porphyrin dendrimers **TPP-D** and **TFP-D**, are also involved in broad peak around 7.20-7.31 ppm.

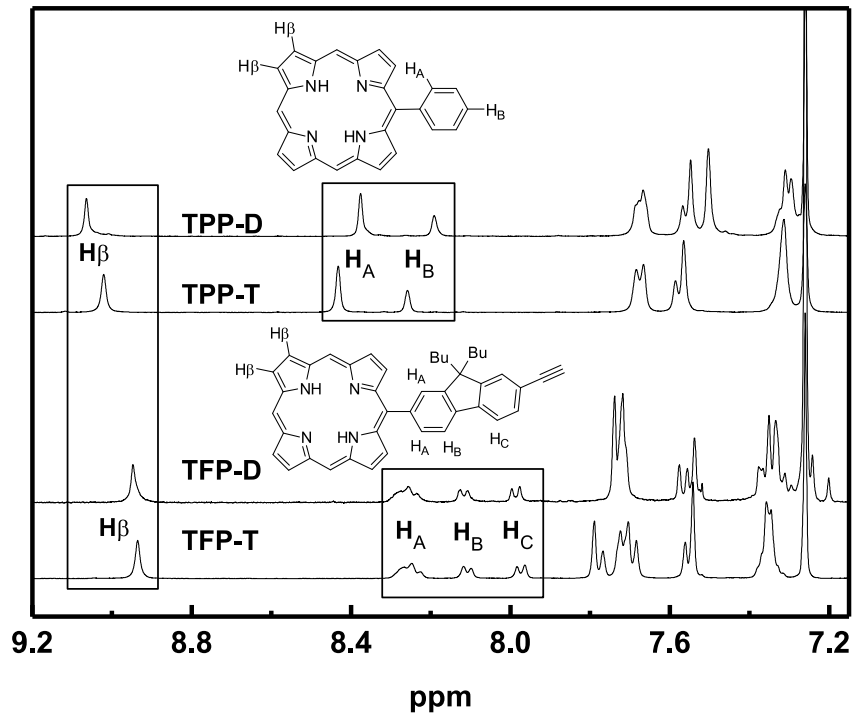

Figure 4.6 Partial ^{1}H NMR spectra of porphyrin dendrimers (7.15 to 9.2 ppm).

For the butyl protons of fluorenyl, the signals also show no difference between **TPP-D** and **TPP-T**, **TFP-D** and **TFP-T** as their relative aldehyde dendrons.

Therefore, in Figure 4.7, we only exhibit proton Ha in butyl of fluorenyl and two –NH protons in porphyrin heart.

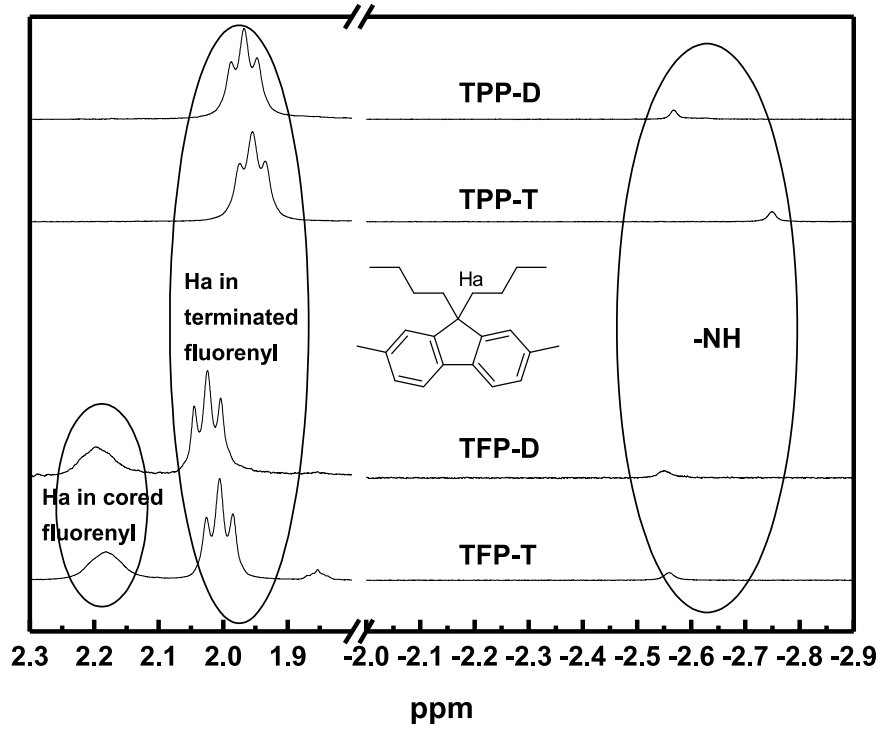

Figure 4.7 Partial ^{1}H NMR spectra of porphyrin dendrimers (-2.9 to 2.3 ppm).

By comparison of **TPP-D** and **TPP-T** spectra, bridged vinyl or alkynyl connected in cored groups, (i) influences strongly on the proton shifts of porphyrin (Hβ and –NH) and cored group (H_A and H_B), but (ii) do not change the signal of some aromatic protons and butyl protons in fluorenyl because of long distance.

By comparison of **TFP-D** and **TFP-T** spectra, the same bridged alkynyl connected in cored fluorenyl, results in no change in proton shifts of porphyrin (Hβ and –NH), cored group (H_A, H_B and H_C), and butyl in fluorenyl; the peripheral bridged vinyl and alkynyl only influence some near aromatic protons.

4.4 Optical properties

UV-visible absorption and photoluminescence spectroscopy measurements for porphyrin dendrimers **TPP-D**, **TPP-T**, **TFP-D** and **TFP-T** in toluene (HPLC level) were performed at room temperature.

In this chapter, we compared **TPP-D** and **TPP-T**, **TFP-D** and **TFP-T**, respectively. **TPP** and **TFP-Bu** with the same cored phenyl and cored fluorenyl, as parent molecules, are also used to be discussed (see Figure 4.8).

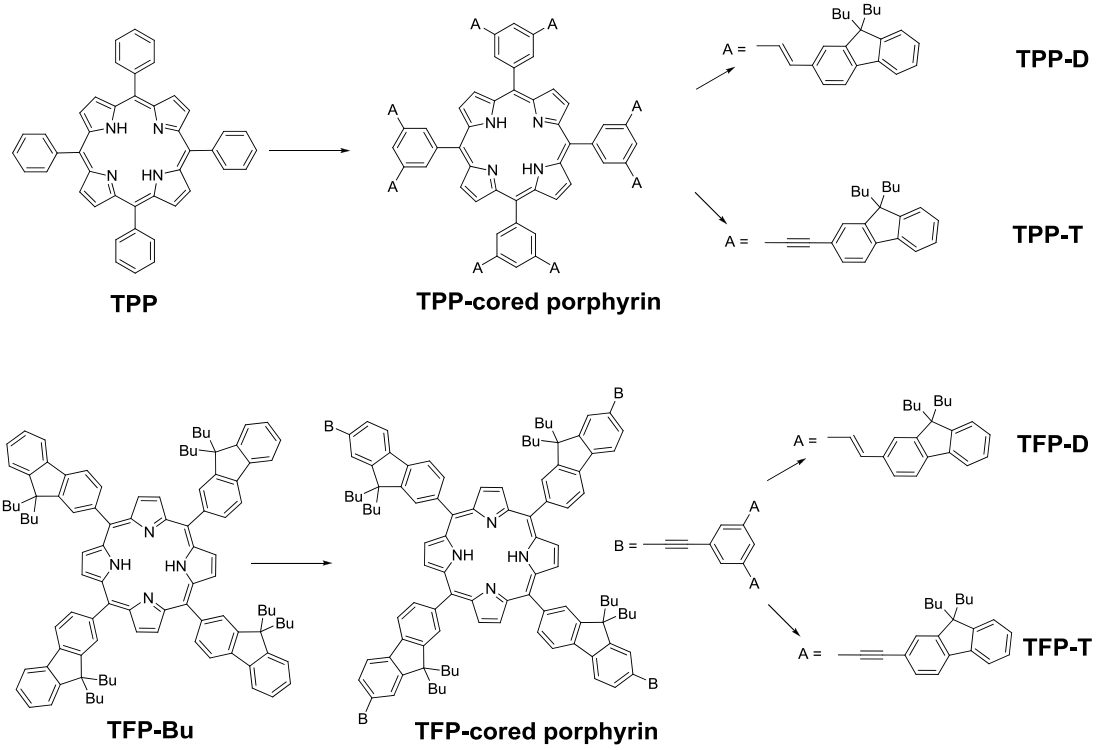

Figure 4.8 Molecular structures of porphyrin dendrimers.

4.4.1 Absorption and emission

Normalized absorption and emission spectra were exhibited in Figure 4.9, and their emission spectra were obtained by Soret-band excitation.

In absorption spectra of TPP-cored porphyrins, **TPP-D** and **TPP-T** have mainly two parts of absorption: (i) Soret-band around 430 nm and four Q-bands from 520 to

650 nm are due to characteristic absorptions of porphyrin, (ii) extra intense absorption from 300 to 400 nm are from light-harvesting of conjugated dendron.

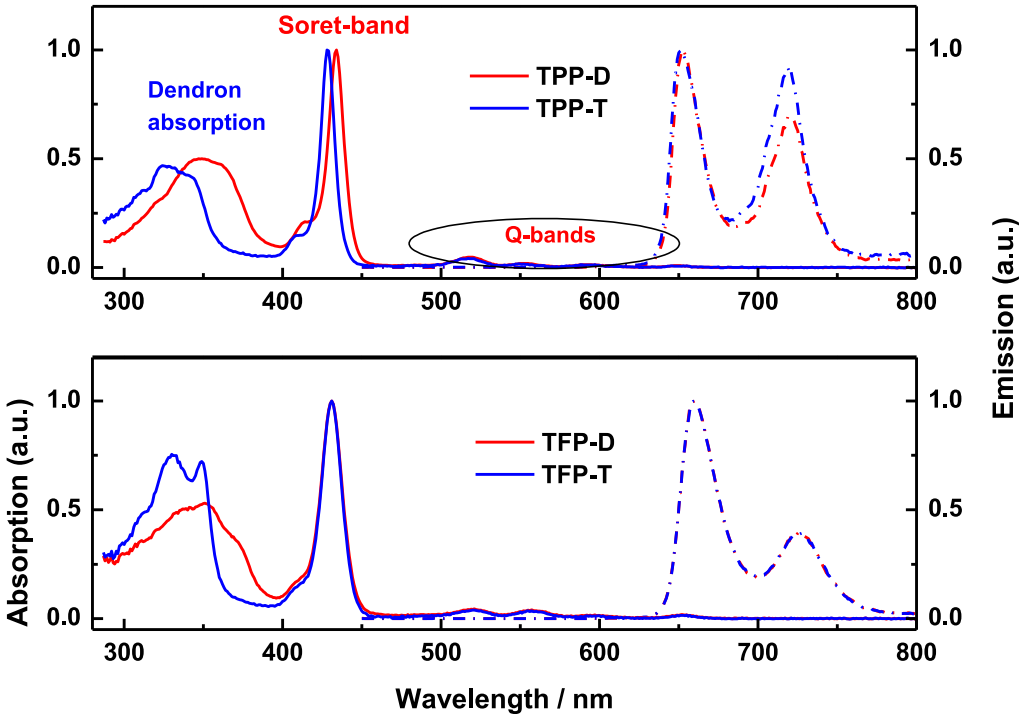

Figure 4.9 UV-visible absorption and emission spectra of double bonded series **TPP-D** and **TFP-D**, and their reference triple bonded ones **TPP-T** and **TFP-T**.

Compared dendrimers **TPP-D** and **TPP-T**, **TPP-D** has 6 nm red shifts in Soret-band, this is due to different planar torsion of porphyrin ring resulting from cored phenyl connecting different conjugated linkages. But for the Q-bands absorption, **TPP-D** and **TPP-T** keep approximately the same intensities and shifts. Refer to their dendron absorption parts, the intensities for two dendrimers are almost the same, and it might results in their similar energy transfer emission which would be discussed in the next section.

In chapter 2, we ever discussed the influence of cored group connected directly to porphyrin on emission. The results showed that the same substituted position in cored group could keep the same planarity of the porphyrin ring leading to the same

normalized emission (the ratio of Q(0,0) and Q(0,1)).

Here, after comparing **TPP-D** and **TPP-T**, we further observed that different conjugated linkages connected to cored phenyl in the same substituted position could also change the planarity of the porphyrin ring in a certain extent, showing a little difference in the ratio of Q(0,0) and Q(0,1). Obviously, the rigidity and conjugation of vinyl and alkynyl is important for the planarity of the macrocycle. Of course, this does not eliminate certain long-distance effect on the planarity of the porphyrin ring, from large dendron in more complicated structures.

Based on the analysis above, it would be easier to understand the normalized absorption and emission spectra of TFP-cored porphyrin dendrimers. With the same cored fluorenyl-alkynyl connected to porphyrin ring directly, **TFP-D** and **TFP-T** both keep the same Soret-band shift and the same emission ratio of Q(0,0) and Q(0,1). This suggests the later connected double bonded dendron and triple bonded dendron have small effect on porphyrin planarity. We noticed that, **TFP-T** has more intense dendron absorption than **TFP-D**, and it corresponds to their energy transfer emissions.

Their quantum yields were measured in toluene at room temperature, and all detailed optical data were listed in Table 4.1. **TPP-D** has similar quantum yield as **TPP-T**, showing about 0.13-0.14 near to TPP; however, for **TFP-D**, it has obvious lower quantum yield than **TFP-T**, suggesting more flexible bridged vinyl in peripheral dendron might increase the nonradiative transition to some extent resulting in the decrease in quantum yield.

Table 4.1 Optical data of vinyl-bridged porphyrin dendrimers and their reference alkynyl bridged porphyrin dendrimers.

	Absorption[a]			Emission[a] Ex = Soret-band		Quantum yield[b](%)
	Dendron	Soret-band	Q-bands	Q (0,0)	Q(0,1)	
TPP	-	419	514,548,590,649	652	719	11
TPP-D	349	434	518,552,593,649	652	719	14
TPP-T	325	428	518,552,593,649	652	719	13
TFP-Bu	-	427	519,555,596,652	659	725	20
TFP-D	351	431	520,557,597,652	659	725	18
TFP-T	349	431	520,557,597,652	659	725	24

a. Experiments were achieved in toluene (HPLC level) with the UV-visible absorption region from 287 to 800 nm and emission region from 450 to 800 nm.

b. Experiments for fluorescence quantum yields were achieved in toluene (HPLC level) using TPP (Φ =11%) as standard, by Soret band excitation.

4.4.2 Energy transfer behaviors

We continued to study their energy transfer behaviors (ET) from absorption and emission spectra at steady state, and the method of spectral measurement has been described in chapter 2 and 3. Figure 4.10 presents the emission spectra of **TPP-D** and **TPP-T**, **TFP-D** and **TFP-T**, using excitation wavelengths at dendron absorption 325-351 nm. These emission spectra were recorded from 300 to 800 nm.

As expected, all these dendrimers show only porphyrin core red emission around 650-750 nm by the dendron excitation, and there is no residual dendron emission observed from 300 to 600 nm, suggesting these dendrimers could efficiently transfer energy from dendron to porphyrin core and all the dendron emission could be totally quenched.

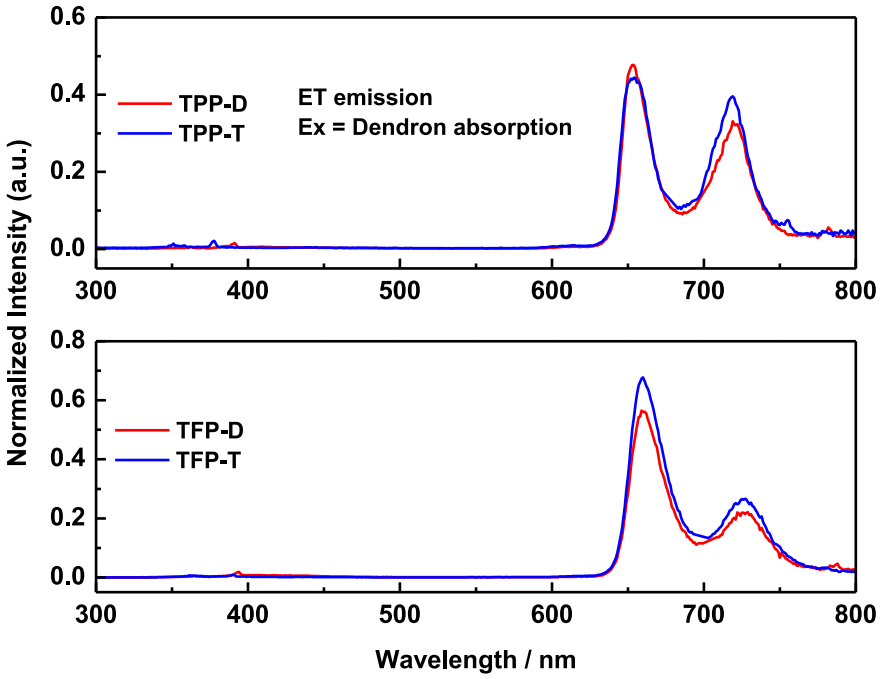

Figure 4.10 Energy transfer behaviors exhibited in emission spectra using excitation wavelengths: Ex = dendron absorption. (Normalizing the intensity of porphyrin core emission at Q(0,0))

4.5 Conclusions

1. To investigate the influence of different conjugated linkages on dendrimer's optical properties, we designed and synthesized two new porphyrin dendrimers with bridged vinyl: **TPP-D** and **TFP-D**, and considered corresponding alkynyl bridged ones **TPP-T** and **TFP-T** as references for discussion.

2. Classic associative reactions of Michaelis-Arbuzov reaction and Horner-Wadsworth -Emmons reaction were used for vinyl formation. The synthetic method of porphyrin dendrimer still followed two steps: (i) formation of modified aldehyde dendron (ii) formation of porphyrin dendrimer under Adler-Longo's conditions.

3. New double bonded aldehyde dendrons (**D-PhCHO** and **D-FlCHO**) and relative porphyrin dendrimers (**TPP-D** and **TFP-D**) were all well characterized by ^{1}H NMR analysis, and compared to references triple bonded dendrons (**T-PhCHO** and **T-FlCHO**) and dendrimers (**TPP-T** and **TFP-T**).

4. Bridged vinyl and alkynyl could influence optical properties of porphyrin dendrimers in certain extent according to substituted positions:

(i) In absorption and emission spectra: with cored group involved different conjugated linkages, **TPP-D** and **TPP-T** have obvious changes in Soret-band and in the ratio of emission Q(0,0) and Q(0,1); while, for **TFP-D** and **TFP-T**, the conjugated linkages in peripheral dendron induces no changes in their porphyrin absorption and emission spectra.

(ii) For their quantum yield: **TPP-D** and **TPP-T** have similar yields; while for **TFP-D** and **TFP-T**, flexibility of conjugated linkages in peripheral dendron as well could change the quantum yield by influencing nonradiative transition.

(iii) Energy transfer behavior: bridged vinyl and alkynyl could both transfer energy efficiently; ET emission intensities, respectively for **TPP-D** and **TPP-T**, **TFP-D** and **TFP-T**, show similar according to emission and absorption spectra in steady state.

4.6 Synthesis and characterization of second generation of TPP-D style porphyrin dendrimer with bridged vinyl

We ever attempted to design and synthesize the second generation of TPP-D style porphyrin dendrimer with bridged vinyl, named **TPP-D2**, see Figure 4.11.

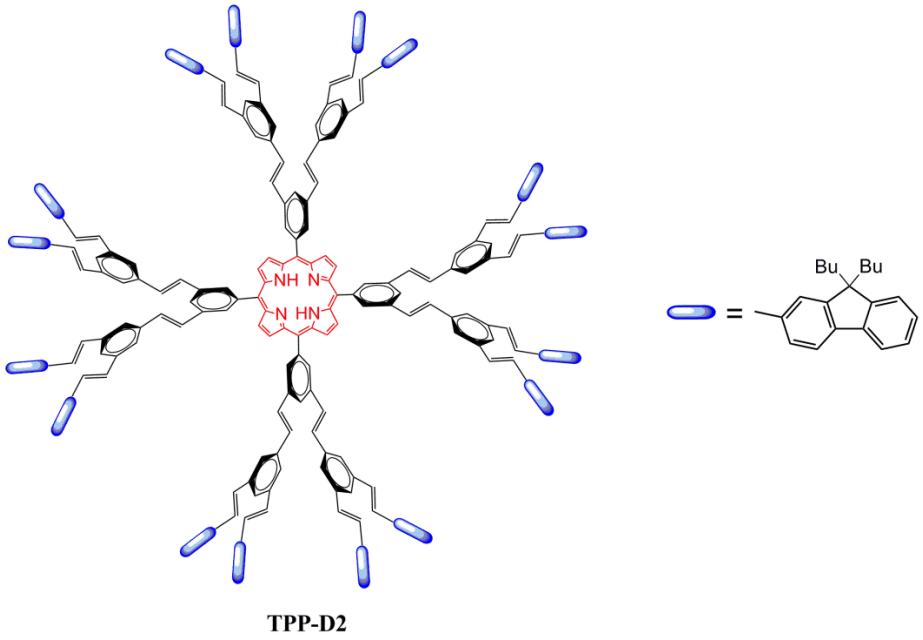

Figure 4.11 Molecular structure of porphyrin dendrimer **TPP-D2**.

During synthesizing the target porphyrin dendrimer **TPP-D2**, unfortunately, synthetic conditions and molecular structure limited the yield seriously, so in this chapter, we only introduce the synthetic routes for **TPP-D2**, and no more repetition of the reactions for further investigation of its optical properties. The detailed synthesis routes are described as follow.

*4.6.1 Formation of dendron **D2-PhCHO***

The synthetic method was described in Figure 4.12, which was similar to the preparation of dendron **D-PhCHO**. After repetition of Horner-Wadsworth-Emmons reaction, the second generation intermediate **D2-PhBr** was obtained by 93% yield,

and subsequently the second generation of double bonded aldehyde **D2-PhCHO** has the yield of 65% in next two steps.

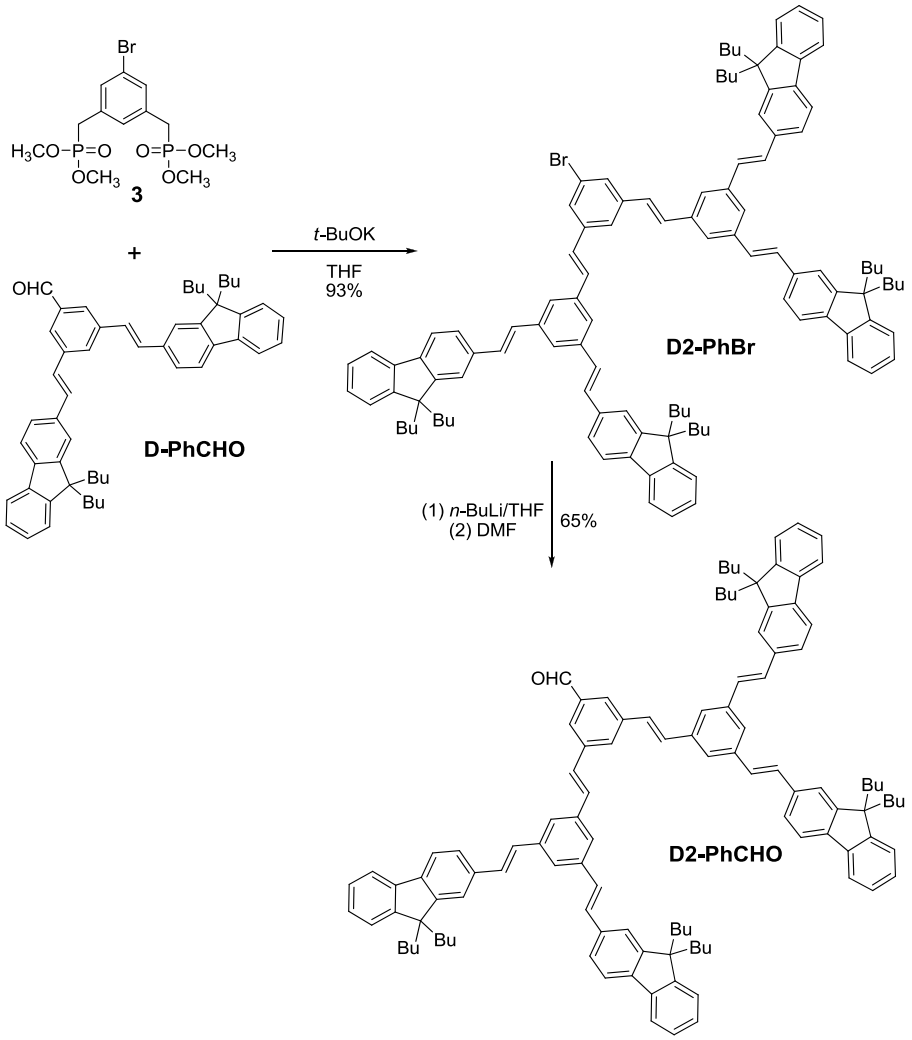

Figure 4.12 Synthetic route of vinyl-bridged aldehyde **D2-PhCHO**.

*4.6.2 Formation of porphyrin dendrimers **TPP-D2** and **ZnTPP-D2***

The conditions for preparing **TPP-D** were also adopted for second generation double bonded porphyrin **TPP-D2**: the condensation of dendron **D2-PhCHO** and pyrrole in refluxing propionic acid for 5.5 h gave 4% yield of **TPP-D2** mixed with amount of red polymer or oligomer which showed many broad signals in ^{1}H NMR spectrum.

For purification, then metallization of porphyrin mixture with $Zn(OAc)_2$ had been done in mixed solvents of CH_2Cl_2 and MeOH at 40 ^{o}C overnight, giving very

few pink product **ZnTPP-D2** which could be isolated from red polymer or oligomer byproducts. Considering such low yield of **TPP-D2**, we supposed that vinyl group might be unstable in propionic acid at high temperature (140 ^{o}C) so that some red polymer or oligomer with high molecular weight formed so fast leaving few target porphyrin **TPP-D2**.

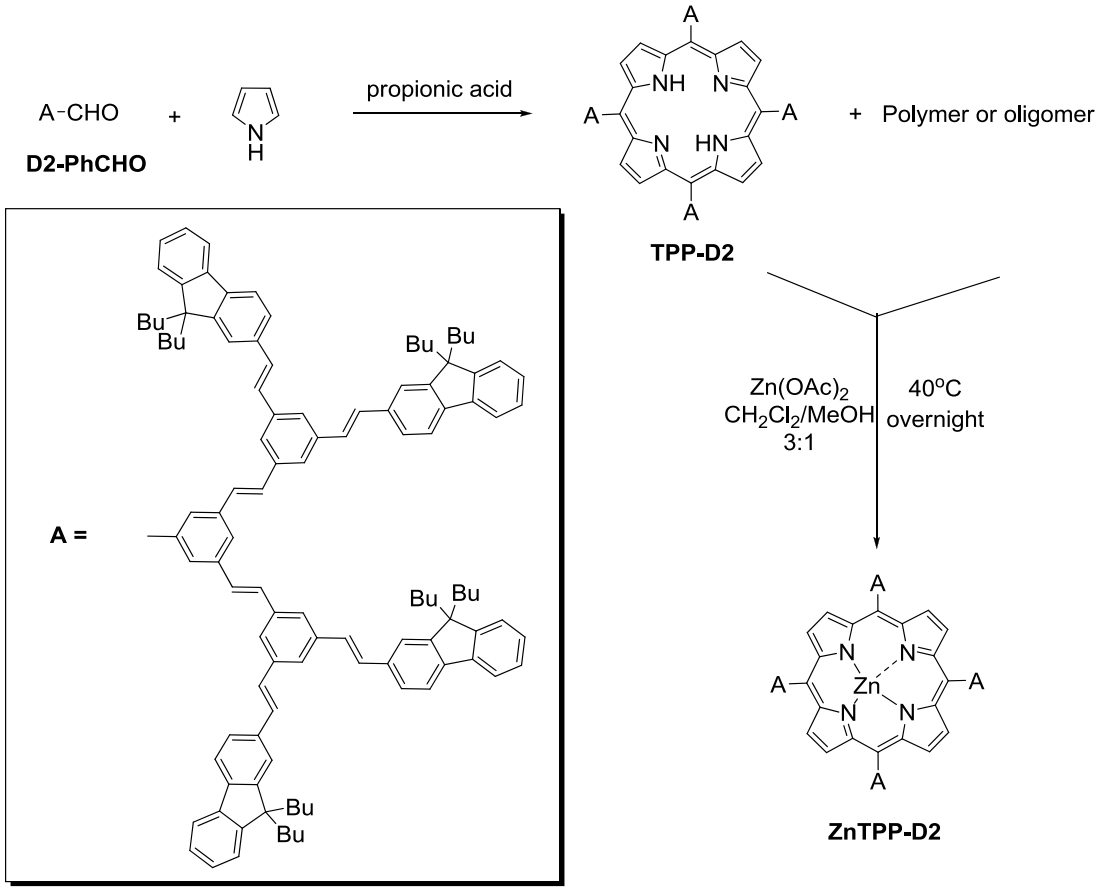

Figure 4.13 Synthetic methods of porphyrin dendrimers **TPP-D2** and **ZnTPP-D2**.

*4.6.3 ^1H NMR spectra of dendron **D2-PhCHO** and porphyrin dendrimer **ZnTPP-D2***

The ^1H NMR measurements of dendron **D2-PhCHO** and porphyrin dendrimer **ZnTPP-D2**, were performed in CD_2Cl_2 because the signal of $CDCl_3$ has a large overlap with the peaks of aromatic moiety. Their partial ^1H NMR spectra of dendron and dendrimer were showed in Figure 4.14.

Some characteristic proton signals could be identified, but most of aromatic protons are still mixed together because of larger molecular structures.

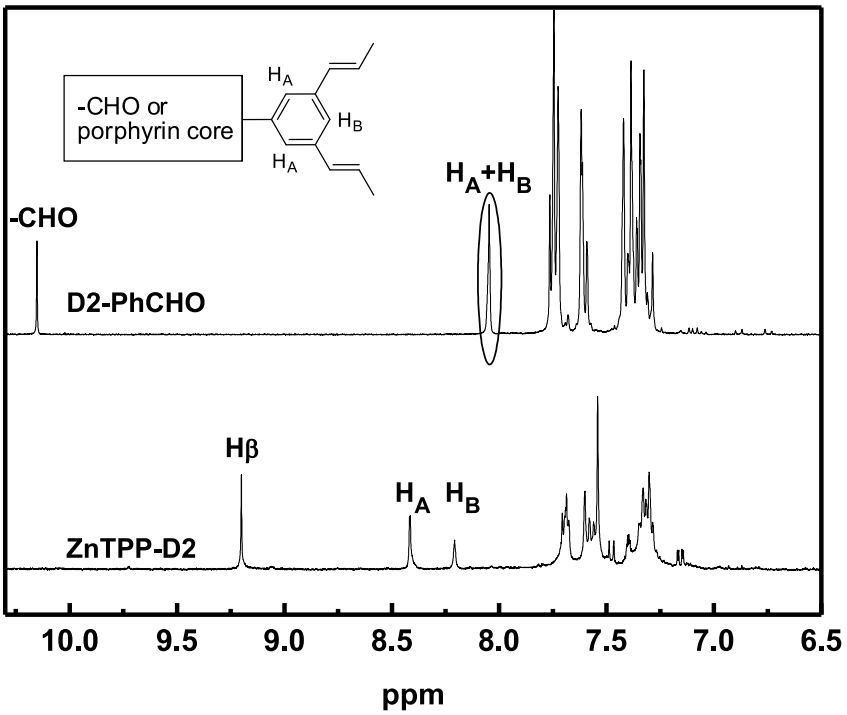

Figure 4.14 Partial ^1H NMR of dendron **D2-PhCHO** and porphyrin dendrimer **ZnTPP-D2**.

Experimental section

7-bromo-9,9-dibutyl-9*H*-fluorene-2-carbaldehyde (2):

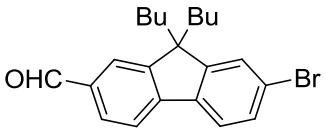

(1) A mixture of 2,7-dibromofluorene (5.0 g, 15.43 mmol, 1 eq) and Bu_4NBr (249 mg, 0.77 mmol, 5% eq) was added with toluene (20 mL, not dry) and 50% NaOH (12 mL), respectively. After 1-bromobutane (5 mL, 46.30 mmol, 3 eq) was added into the solution, the reaction was stirred for 40 h at 75-85 ^oC. The reaction was extracted with water and ethyl acetate. After being evaporated, residue was farther purified by chromatography (heptane), getting 2,7-dibromo-9,9-dibutyl-9*H*-fluorene as colorless crystal (5.5 g, 82% yield).

^1H NMR (400 MHz, $CDCl_3$, ppm): δ 7.53-7.51 (m, 2H), 7.46-7.47 (m, 4H), 1.94-1.90 (m, 4H), 1.14-1.04 (m, 4H), 0.69 (t, J = 7.6 Hz, 6H), 0.61-0.53 (m, 4H).

(2) In a Schlenk, a solution of 2,7-dibromo-9,9-dibutyl-9*H*-fluorene (2.5 g, 5.73 mmol, 1 eq) in dry THF (60 mL) was cooled to -78 ^oC in liquid nitrogen-acetone bath. At low temperature, *n*-BuLi (3.58 mL, 5.73 mmol, 1 eq) was added dropwise to the solution for 30 min. Kept it stirring at -78 ^oC for 1 h, then injected dry DMF (1 mL) into the reaction, stirring it at -78 ^oC for another 1 h. Removed the bath and stirred the reaction overnight at room temperature. Added saturated NH_4Cl and extracted it with ethyl acetate. Evaporated the solvents and the residue was farther purified by chromatography (heptane : CH_2Cl_2 = 7 : 1), getting white powder (2 g, 90% yield).

^1H NMR (400 MHz, $CDCl_3$, ppm): δ 10.06 (s, 1H), 7.87-7.86 (m, 2H), 7.81 (d, J = 8.4 Hz, 1H), 7.64 (d, J = 8.8 Hz, 1H), 7.52-7.50 (m, 2H), 2.07-1.92 (m, 4H), 1.13-1.04 (m, 4H), 0.67 (t, J = 7.2 Hz, 6H), 0.62-0.47 (m, 4H).

9,9-dibutyl-9*H*-fluorene-2-carbaldehyde (1):

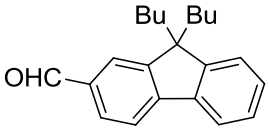

The same procedure as **2** was adopted.

^{1}H NMR (400 MHz, $CDCl_3$, ppm): δ 10.06 (s, 1H), 7.88 (s, 1H), 7.85-7.83 (m, 2H), 7.80-7.77 (m, 1H), 7.42-7.36 (m, 3H), 2.08-1.96 (m, 4H), 1.11-1.02 (m, 4H), 0.66 (t, *J* = 7.4 Hz, 6H), 0.60-0.52 (m, 4H).

1-bromo-3,5-bis(bromomethyl)benzene:

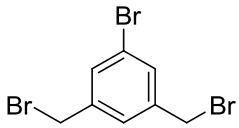

1-bromo-3,5-bismethylbenzene (5 g, 3.67 mL, 27.02 mmol, 1 eq) was added into CH_2Cl_2 (100 mL, distilled), together with NBS (9.6 g, 54.04 mmol, 2 eq) and AIBN (220 mg, 1.351 mmol, 0.05 eq). The mixture was stirred for 30 min at room temperature then refluxed for 30 h. Cooled it in ice-water bath and filtered it, washing residue with heptane. Evaporated the solvents and further purified it by chromatography (heptane) collecting target product (4.56 g, 49% yield) as white powder, as well as monobromo-substituted byproduct (3.55 g) and tribromo-substituted byproduct (1.4 g).

^{1}H NMR (400 MHz, $CDCl_3$, ppm): δ 7.47 (s, 2H), 7.34 (s, 1H), 4.41 (s, 4H).

Tetraethyl (5-bromo-1,3-phenylene)bis(methylene)diphosphonate (3):

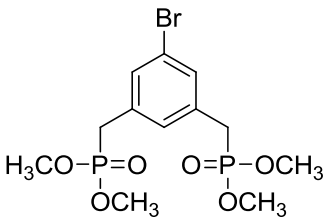

In a flask, 1-bromo-3,5-bis(bromomethyl)benzene (2.4 g, 7 mmol, 1 eq) and $P(OEt)_3$ (2.4 mL, 14 mmol, 2 eq) were added respectively. The mixture was refluxed for 4 h at

140 °C. The excess of $P(OEt)_3$ was removed under reduced pressure. Then the product could be purified by chromatography using CH_2Cl_2 to remove other byproduct and then collected by ethyl acetate, giving colorless oil (2.66 g, 83% yield).

^{1}H NMR (400 MHz, $CDCl_3$, ppm): δ 7.34 (s, 2H), 7.16 (s, 1H), 4.07-4.00 (m, 8H), 3.08 (d, *J* = 22.0 Hz, 4H), 1.26 (t, *J* = 7.0 Hz, 12 H).

D-PhBr:

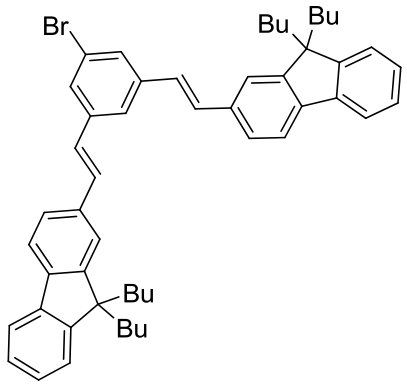

In a schlenk, **1** (1.69 g, 5.51 mmol, 2.2 eq) and **3** (1.146 g, 2.51 mmol, 1 eq) were added, then THF (100 mL, dried) was inserted. Put schlenk into ice-water bath (0 °C), added *t*-BuOK (1.2 g, 10.69 mmol, 4.4 eq) into schlenk under Argon. Kept the reaction stirring for 1 h at 0 °C. Removed the bath and added NH_4Cl saturated solution (aq) and extracted it with ethyl acetate. Evaporated the solvents and further purified by chromatography (CH_2Cl_2 : heptane = 1 : 10), giving white powder(1.7 g, 89% yield).

^{1}H NMR (400 MHz, $CDCl_3$, ppm): δ 7.71 (d, *J* = 7.6 Hz, 4H), 7.61 (s, 1H), 7.60 (s, 2H), 7.52 (d, *J* = 8.4 Hz, 2H), 7.50 (s, 2H), 7.37-7.31 (m, 6H), 7.27 (d, *J* = 16.0 Hz, 2H), 7.12 (d, *J* = 16.4 Hz, 2H), 2.01 (t, *J* = 8.0 Hz, 8H), 1.15-1.06 (m, 8 H), 0.71-0.58 (m, 20H).

D-PhCHO:

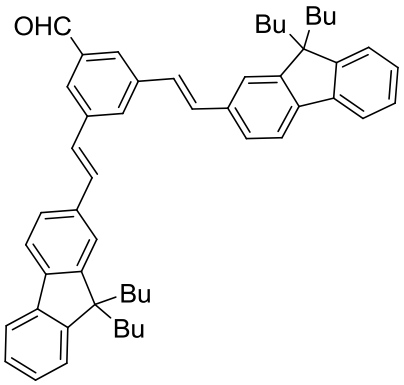

In a schlenk, **D-PhBr** (720 mg, 0.94 mmol, 1 eq) was dissolved in THF (60 mL) and inserted *n*-BuLi (0.59 mL, 0.94 mmol, 1.6 M, 1 eq) dropwise at -78 ^{o}C for 15 min. The reaction was stirred for additional 40 min at low temperature. Then added DMF (1 mL, dried), continued to stir the reaction for 1 h at -78 ^{o}C. Removed the bath and added NH_4Cl saturated solution (aq) and extracted it with ethyl acetate. Evaporated the solvents and further purified by chromatography (CH_2Cl_2 : heptane = 1 : 5), giving light yellow powder (580 mg, 86% yield).

^{1}H NMR (400 MHz, $CDCl_3$, ppm): δ 10.11 (s, 1H), 7.96 (s, 3H), 7.73-7.71 (m, 4H), 7.56 (d, *J* = 8.0 Hz, 2H), 7.53 (s, 2H), 7.40-7.23 (m, 10H), 2.02 (t, *J* = 8.0 Hz, 8H), 1.15-1.06 (m, 8 H), 0.71-0.56 (m, 20H).

2,2'-(5-(2,2-dibromovinyl)-1,3-phenylene)bis(ethene-2,1-diyl)bis(9,9-dibutyl-9*H*-fluorene) (4):

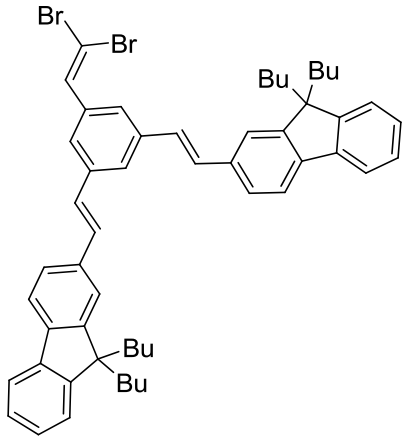

In a schlenk, a mixture of PPh_3 (221 mg, 0.84 mmol, 2 eq) and Zn powder (55 mg, 0.84 mmol, 2 eq) was added dry CH_2Cl_2 (4 mL). After the solution was cooled to 0 ^oC in ice-water bath, put CBr_4 (280 mg, 0.84 mmol, 2 eq) into schlenk under argon protection and kept low temperature for 2 min. Removed the bath and stirred the mixture overnight at room temperature. Cooled the mixture to 0 ^oC again, and injected the solution of **D-PhCHO** (300 mg, 0.42 mmol, 1 eq) which was dissolved in dry CH_2Cl_2 (4 mL) into the schlenk under argon protection. Kept the low temperature (0 ^oC) for 10 min and stirred it for 4 h in dark at room temperature. Filtered the solution and evaporated CH_2Cl_2, then the residue was absorbed in silica and farther purified by chromatography (heptane : CH_2Cl_2 = 100 : 5), collecting white powder (270 mg, 74% yield).

^1H NMR (400 MHz, $CDCl_3$, ppm): δ 7.71 (d, *J* = 7.6 Hz, 5H), 7.60 (s, 2H), 7.56 (s, 1H), 7.54 (d, *J* = 7.6 Hz, 2H), 7.51 (s, 2H), 7.37-7.30 (m, 7H), 7.27 (s, 1H), 7.22-7.18 (m, 2H), 2.02 (t, *J* = 8.0 Hz, 8H), 1.15-1.06 (m, 8H), 0.71-0.54 (m, 20H).

2,2'-(1E,1'E)-2,2'-(5-ethynyl-1,3-phenylene)bis(ethene-2,1-diyl)bis(9,9-dibutyl-9H-fluorene) (5):

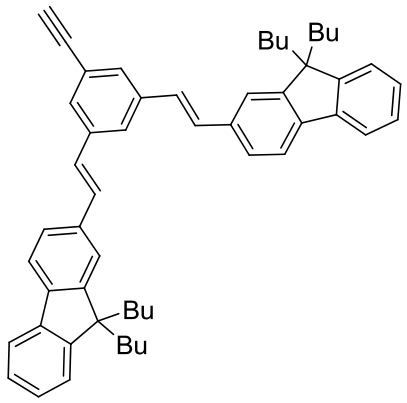

N-BuLi (0.58 mL, 0.93 mmol, 3 eq) was added to a cold (-78 ^{o}C) solution of $^{i}Pr_2NH$ (0.13 mL, 0.93 mmol, 3 eq) in dry THF (4 mL). After warming up to room temperature, the mixture was injected dropwise into the solution of **4** (270 mg, 0.31 mmol, 1 eq) in dry THF (8 mL) at -78 ^{o}C in liquid nitrogen-acetone bath. Kept the low temperature for 1 h, then quenched the reaction with saturated NH_4Cl (2 mL). Removed the bath, it was stirred until the temperature was up to room temperature. Extracted it with ethyl acetate and evaporated solvents, then the residue was absorbed in silica and farther purified by chromatography (heptane : CH_2Cl_2 = 100 : 5), showing white powder (205 mg, 93% yield).

^{1}H NMR (400 MHz, $CDCl_3$, ppm): δ 7.71 (d, *J* = 7.6 Hz, 5H), 7.60 (s, 2H), 7.53 (d, *J* = 7.6 Hz, 2H), 7.50 (s, 2H), 7.37-7.29 (m, 7H), 7.27 (s, 1H), 7.17-7.13 (m, 2H), 3.12 (s, 1H), 2.01 (t, *J* = 8.0 Hz, 8H), 1.15-1.06 (m, 8H), 0.71-0.58 (m, 20H).

D-FlCHO:

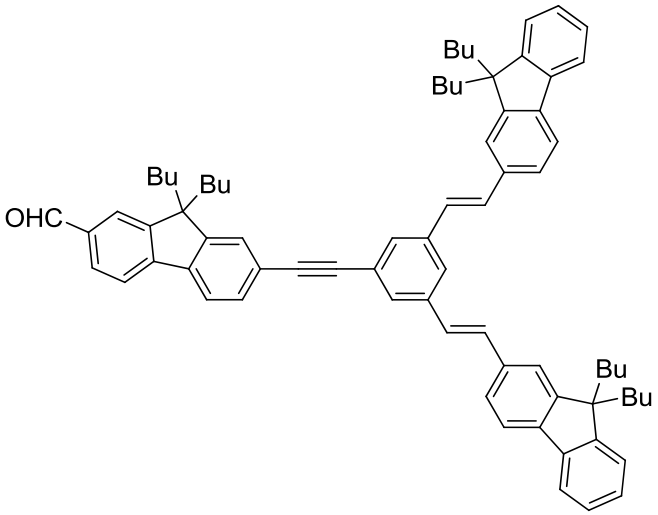

In a schlenk, a mixture of **2** (101 mg, 0.26 mmol, 1 eq), **5** (205 mg, 0.29 mmol, 1.1 eq), $Pd(PPh_3)_2Cl_2$ (12 mg, 0.017 mmol, 6% eq) and CuI (1.6 mg, 0.009 mmol, 3% eq) was added DMF (10 mL) and $^{i}Pr_2NH$ (10 mL) under argon, respectively. Then the system was degassed by freeze-pump-thaw twice and heated for 90 h at 95 ^{o}C. After being evaporated, residue was absorbed in silica and farther purified by chromatography (petroleum ether : CH_2Cl_2 = 4 : 1), showing white powder (170 mg, 65% yield).

^{1}H NMR (400 MHz, $CDCl_3$, ppm): δ 10.08 (s, 1H), 7.90-7.87 (m, 3H), 7.80 (d, *J* = 8.0 Hz, 1H), 7.73-7.69 (m, 6H), 7.63-7.60 (m, 2H), 7.55 (d, *J* = 7.6 Hz, 2H), 7.52 (s, 2H), 7.37-7.30 (m, 9H), 7.22-7.18 (m, 2H), 2.09-2.00 (m, 12H), 1.16-1.07 (m, 12H), 0.72-0.51 (m, 30H).

TPP-D:

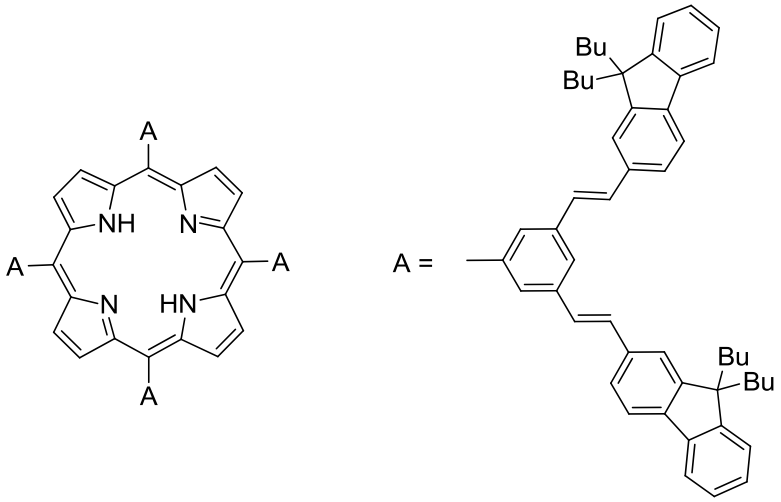

The mixture of **D-PhCHO** (230 mg, 0.32 mmol, 1 eq) and propionic acid (2 mL) was heated to 120 ^{o}C. After pyrrole (0.02 mL, 0.32 mmol, 1 eq) in propionic acid (1 mL) was added into the mixture dropwise, the reaction kept refluxing for 5.5 h. After cooling to room temperature, MeOH was added to the reaction mixture and the precipitate was filtered. The residue could be purified by chromatography (petroleum ether : CH_2Cl_2 = 5 : 1), showing red powder, and recrystallized by refluxing $CHCl_3$ and MeOH, getting dark red powder (19 mg, 8% yield).

^{1}H NMR (400 MHz, $CDCl_3$, ppm): δ 9.06 (s, 8H), 8.38 (s, 8H), 8.19 (s, 4H), 7.69-7,67 (m, 16H), 7.57 (s, 4H), 7.55 (s, 12H), 7.50 (s, 16H), 7.31-7.28 (m, 24H), 1.97 (t, *J* = 8.0 Hz, 32H), 1.08-1.02 (m, 32H), 0.65-0.54 (m, 80H), -2.57 (s, 2H).

^{13}C NMR (125 MHz, $CDCl_3$, ppm): δ 151.3, 151.0, 142.9, 141.2, 140.8, 136.3, 136.1, 131.9, 130.7, 127.6, 127.1, 126.8, 125.8, 124.0, 122.8, 120.8, 119.9, 119.7, 54.9, 40.3, 25.9, 23.0, 13.8.

HRMS-ESI: m/z = 3032.8723 $[M+H]^+$ (calcd: 3032.8819).

TFP-D:

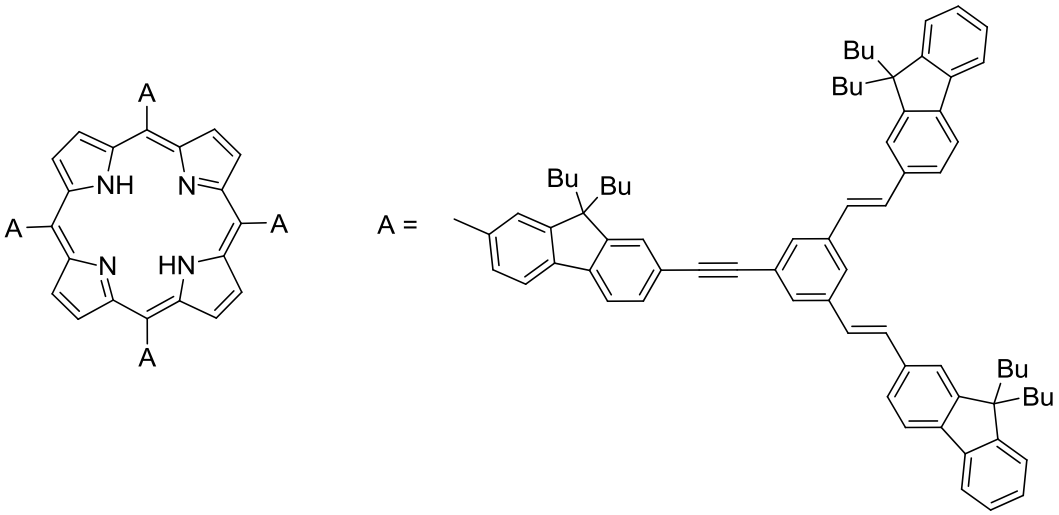

The mixture of **D-FlCHO** (170 mg, 0.19 mmol, 1 eq) and propionic acid (5 mL) was heated to 120 ^{o}C. After pyrrole (0.01 mL, 0.19 mmol, 1 eq) in propionic acid (0.5 mL) was added into the mixture dropwise, the reaction kept refluxing for 5 h. After cooling to room temperature, MeOH was added to the reaction mixture and the precipitate was filtered. The residue could be purified by chromatography (petroleum ether : CH_2Cl_2 = 5 : 1), showing red powder (2 mg, 1% yield).

^{1}H NMR (400 MHz, $CDCl_3$, ppm): δ 8.95 (s, 8H), 8.27-8.24 (m, 8H), 8.12 (d, *J* = 7.2 Hz, 4H), 7.99 (d, *J* = 8.0 Hz, 4H), 7.74-7.72 (m, 32H), 7.57 (d, *J* = 8.0 Hz, 8H), 7.54 (s, 8H), 7.38-7.30 (m, 36H), 7.24-7.20 (m, 8H), 2.20 (broad, 16H), 2.02 (t, *J* = 8.0 Hz, 32H), 1.26-1.22 (m, 16H), 1.16-1.07 (m, 32H), 1.03-0.95 (m, broad, 16H), 0.84-0.78 (m, 24H), 0.70 (t, *J* = 7.2 Hz, 48H), 0.67-0.58 (m, 32H), -2.55 (s, 2H).

^{13}C NMR (125 MHz, $CDCl_3$, ppm): δ 151.3, 151.0, 141.5, 141.3, 140.7, 138.2, 136.0, 133.9, 130.5, 128.4, 127.1, 126.8, 125.7, 124.2, 124.0, 123.1, 122.9, 121.0, 119.9, 119.7, 92.1, 55.0, 40.3, 26.0, 23.1, 14.1, 14.0, 13.8.

HRMS-ESI: m/z = 4233.71 $[M+H]^+$ (calcd: 4233.6331).

D2-PhBr:

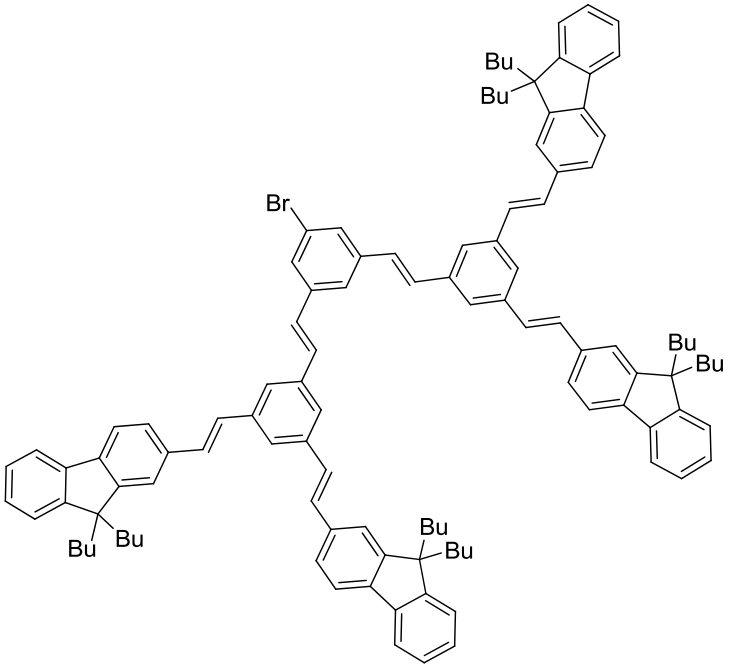

The synthesis procedure is similar to **D-PhBr** and the purification was completed by chromatography (heptane : CH_2Cl_2 = 10 : 1), showing white powder (93% yield).

^{1}H NMR (400 MHz, $CDCl_3$, ppm): δ 7.72-7.71 (m, 10H), 7.64 (s, 7H), 7.57 (d, *J* = 8.0 Hz, 4H), 7.55 (s, 4H), 7.37-7.31 (m, 16H), 7.30-7.18 (m, 8H), 2.03 (t, *J* = 8.0 Hz, 16H), 1.16-1.07 (m, 16 H), 0.72-0.57 (m, 40H).

D2-PhCHO:

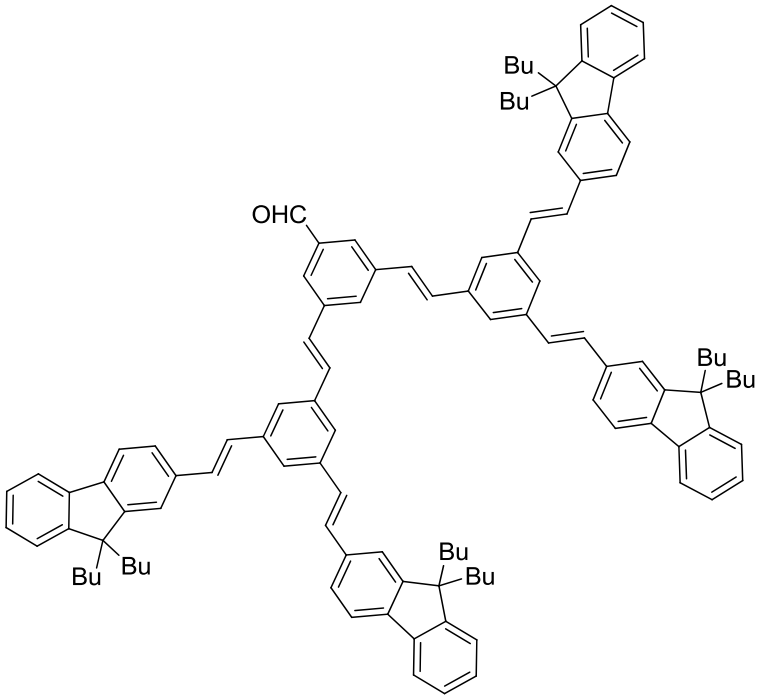

The synthesis procedure is similar to **D-PhCHO** and the purification was completed by chromatography (heptane : CH_2Cl_2 = 5 : 1), showing yellow powder (65% yield). ^{1}H NMR (400 MHz, CD_2Cl_2, ppm): δ 10.15 (s, 1H), 8.05 (s, 3H), 7.76-7.73 (m, 13H), 7.62-7.59 (m, 8H), 7.42-7.29 (m, 25H), 2.06 (t, *J* = 8.0 Hz, 16H), 1.17-1.08 (m, 16 H), 0.72-0.54 (m, 40H).

TPP-D2:

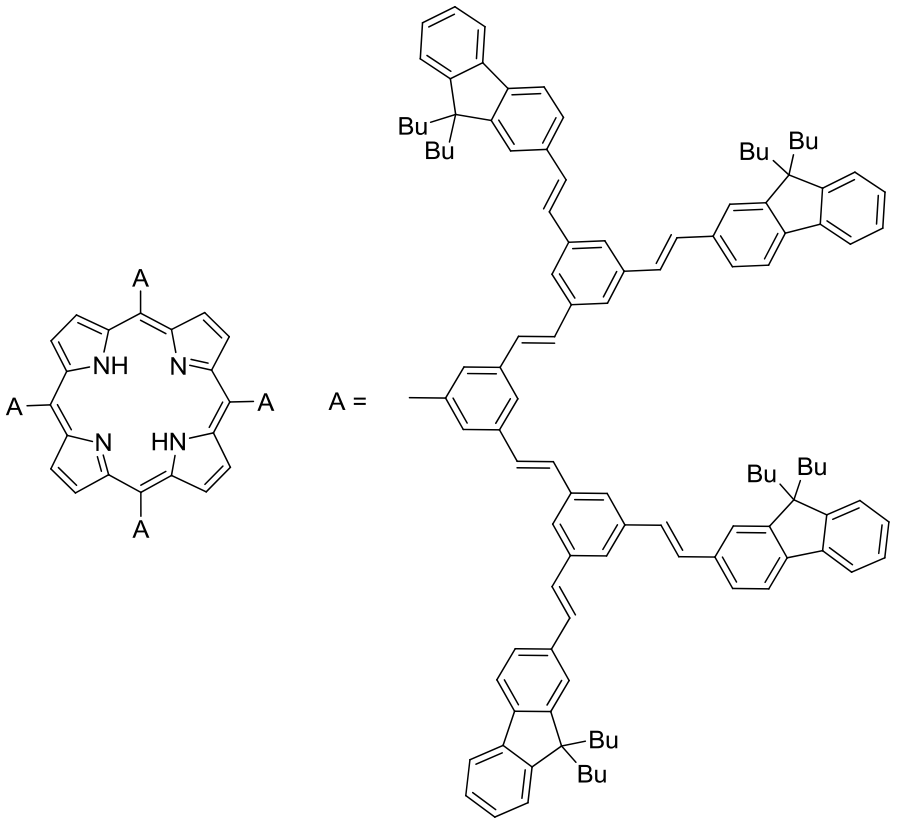

The mixture of **D2-PhCHO** (250 mg, 0.16 mmol, 1 eq) and propionic acid (4 mL) was heated to 120 ^{o}C. After pyrrole (0.01 mL, 0.16 mmol, 1 eq) in propionic acid (1 mL) was added into the mixture dropwise, the reaction kept refluxing for 5.5 h. After cooling to room temperature, MeOH was added to the reaction mixture and the precipitate was filtered. The residue could be purified by chromatography (petroleum ether : CH_2Cl_2 = 5 : 1), showing red powder mixtures (10 mg, 4% yield).

ZnTPP-D2:

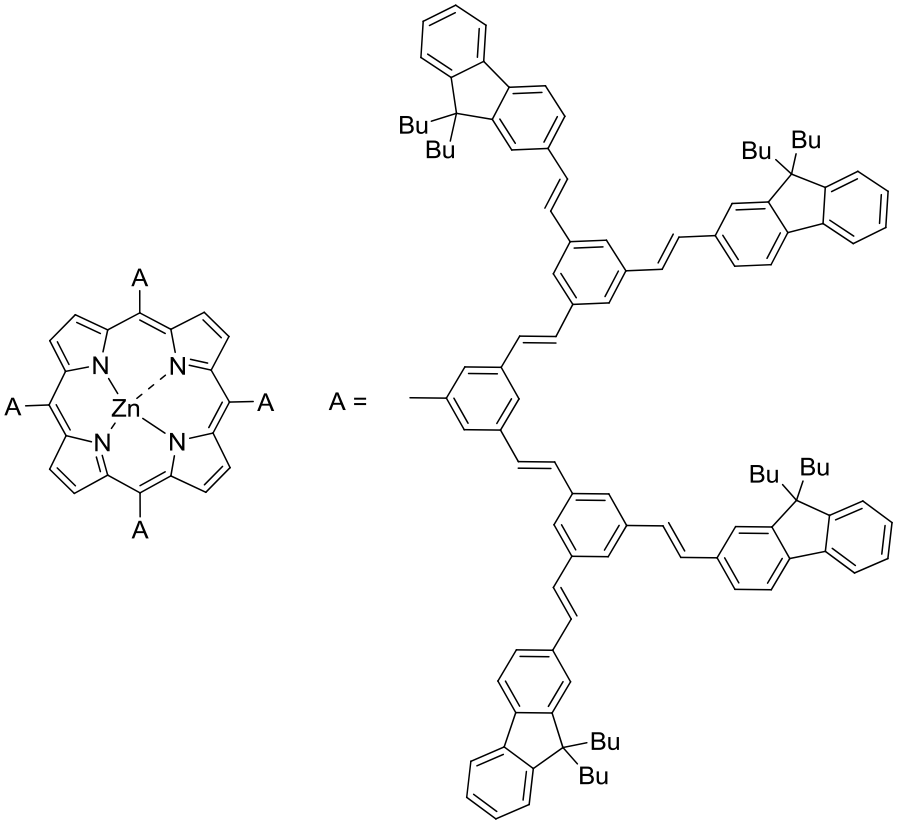

Crude **TPP-D2** mixture reacted with excess of $Zn(OAc)_2$ in mixed solvents of CH_2Cl_2 and MeOH (3 : 1) at 40 ^oC overnight. After evaporating the solvents, the Zn complex could be isolated by chromatography (petroleum ether : CH_2Cl_2 = 5 : 1), collecting very few pink product.

^1H NMR (400 MHz, CD_2Cl_2, ppm): δ 9.20 (s, 8H), 8.42 (s, 8H), 8.21 (s, 4H), 7.71-7.68 (m, 32H), 7.60-7.54 (m, 60H), 7.48 (d, J = 8.4 Hz, 8H), 7.42-7.27 (m, 80H), 7.15 (dd, J_1 = 8.4 Hz, J_2 = 2.4 Hz, 4H), 2.01 (t, J = 7.2 Hz, 64H), 1.12-1.01 (m, 64H), 0.65-0.52 (m, 160H).

Chapter 5

Porphyrin oligomers:
Linear Dimer and star Trimer

5.1 Molecular design

Many chemists have prepared some polymers,[12,70] oligomers[9,10b,71] and some porphyrin assemblies,[72] by taking porphyrin unit as light-harvesting group. For these macromolecules, they focused on molecular construction, light harvesting, and energy, charge or electron transfer.

Previously in our group, two linear dimer[37] and trimer[38] were synthesized and their optical properties were mainly studied from energy transfer process and two-photon absorption properties. As shown in Figure 5.1A, **Monomer A**, **B** and **C** were prepared to form linear Dimer AB and Trimer ACA, as well as their free corresponding based oligomers. On this line, we investigated a new series of oligomers: linear dimer and star trimer (Figure 5.1B).

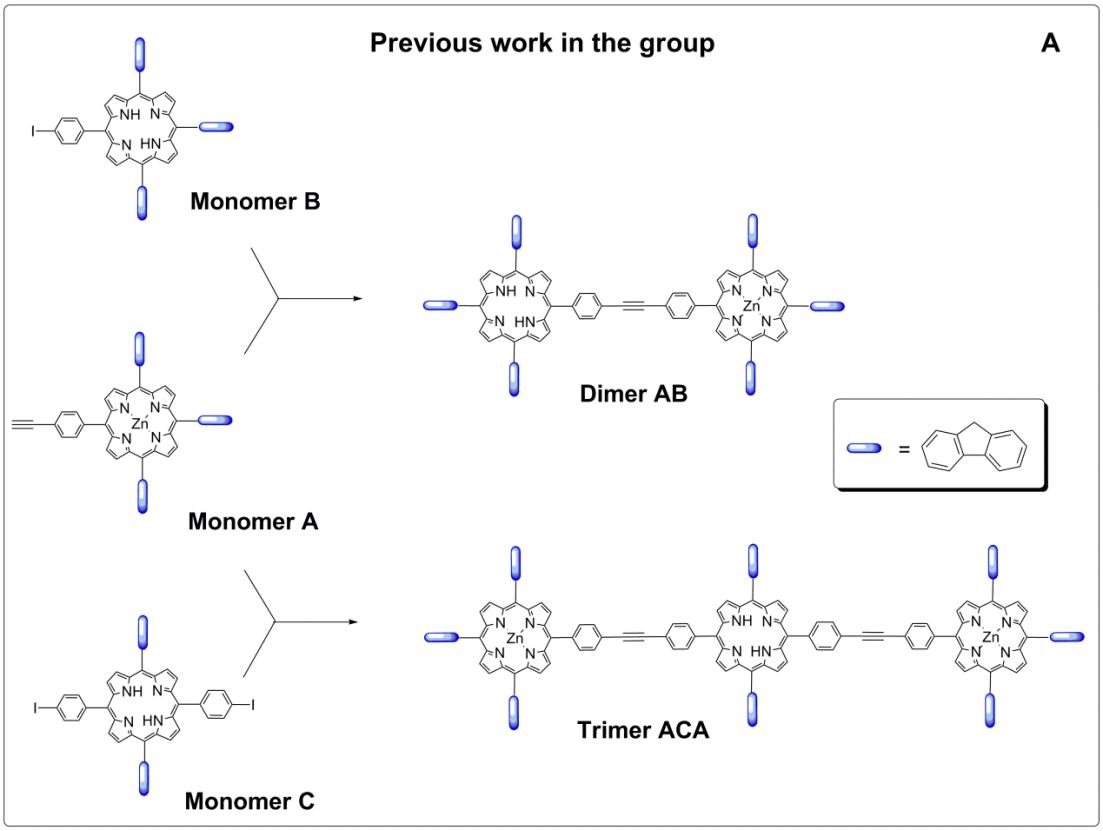

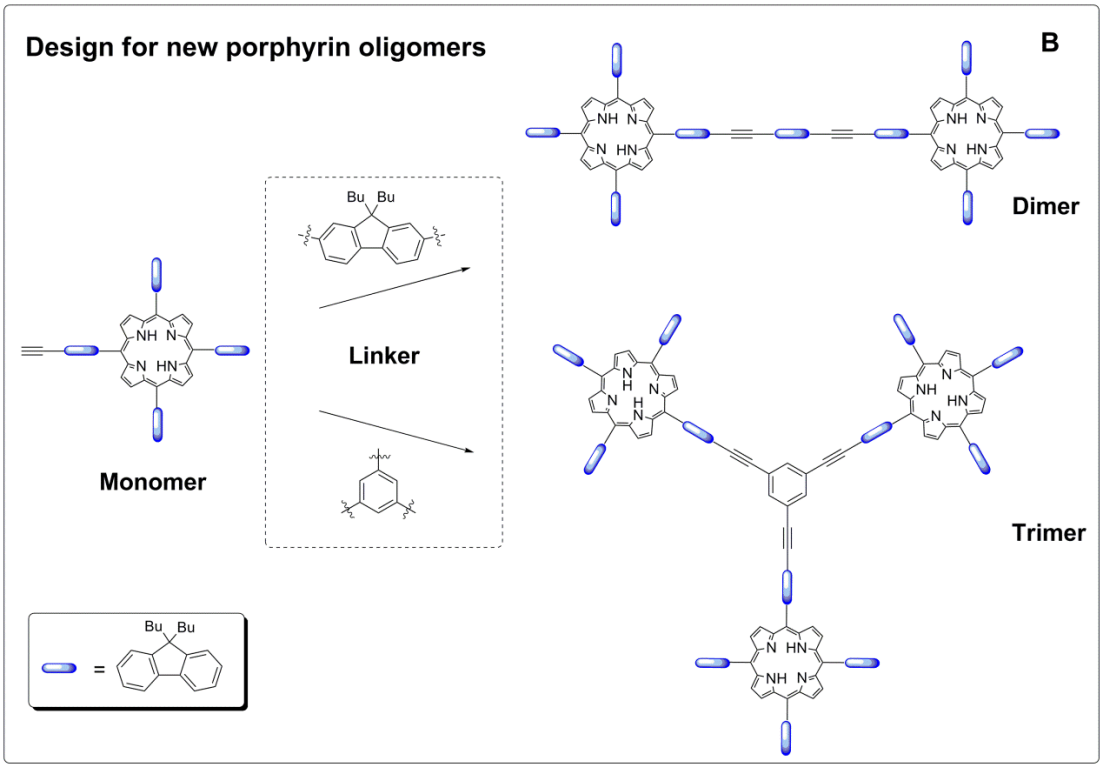

Figure 5.1 Previous work (A) and new design (B) for porphyrin oligomers.

For these new designed molecules, we chose TFP-cored monomer keeping high quantum yield as TFP: on one hand, more fluorenyls as light absorbers could be inserted in these oligomers; on another hand, the possibility of byproducts could also be potentially decreased, because this coupling is done by using only one type of monomer. To obtain oligomers with good solubility, we added as well *n*-butyl chains in fluorenyl.

For the new dimer, 2,7-fluorenyl linker was chosen to form linear conformation with in totally 9 fluorenyls: one bridged and 8 cored fluorenyls. Whereas, for the trimer, 1,3,5-benzene linker was used to obtain star conformation with in totally 12 cored fluorenyls.

5.2 Synthetic method design

5.2.1 Monomer formation

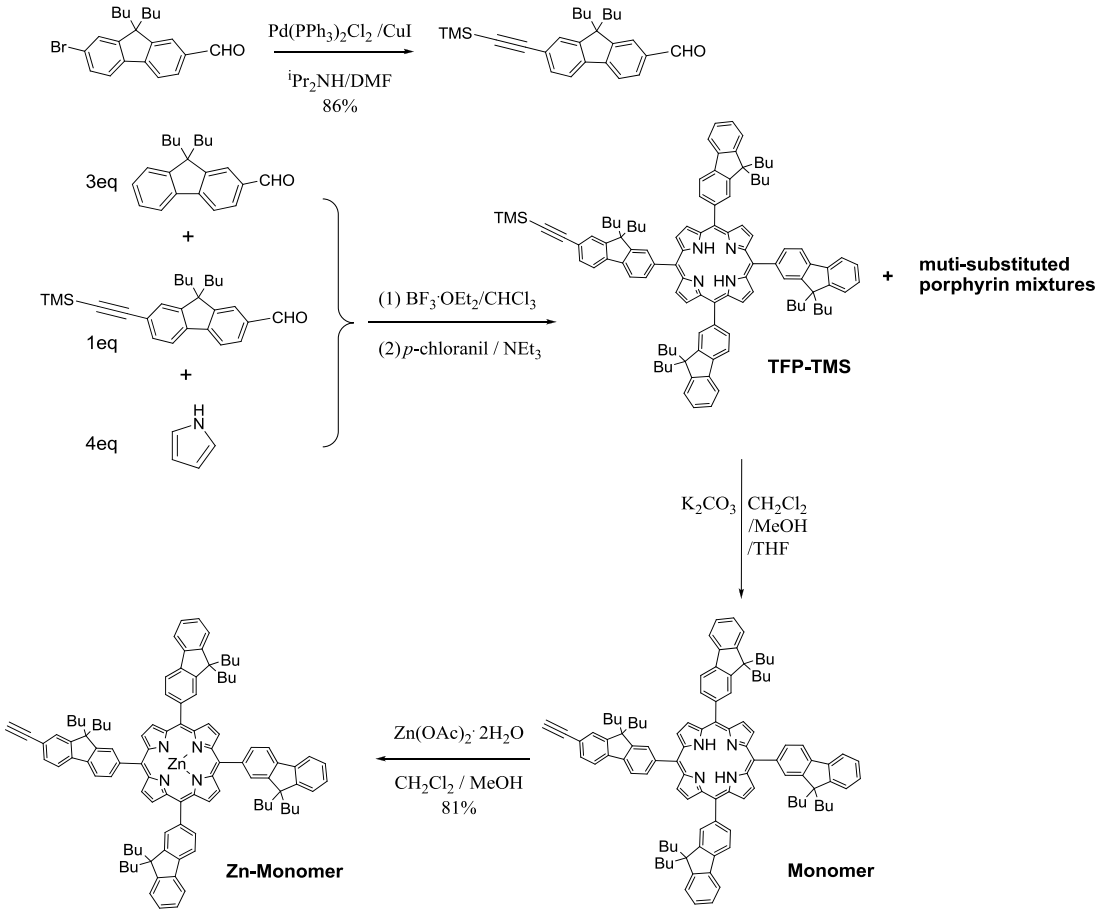

Figure 5.2 Synthetic strategies used for porphyrin **Monomer** and **Zn-Monomer**.

The synthetic method for porphyrin monomers is shown in Figure 5.2. To form the asymmetric porphyrin TFP-TMS, we adopted Lindsey conditions: (1) In the first step, starting materials were added in stoichiometric ratio of 3 : 1 : 4, and dissolved in distilled $CHCl_3$; After degassing the system with argon for 30 min, $BF_3{\cdot}OEt_2$ was injected to start the reaction and the mixture was stirred in dark for 3 h, under argon protection. (2) In the second step, oxidant *p*-chloranil was added to quench the cyclization of porphyrinogen, and dehydrogenation began in refluxing system for another 2 h without argon protection. After cooling to room temperature, controlled amount of NEt_3 was injected to neutralize the protonated porphyrin. Chromatography

had been done to purify the product, but unfortunately, porphyrin mixtures (Figure 5.3) were collected simultaneously because of their similar polarities, showing 68% yield as red powders.

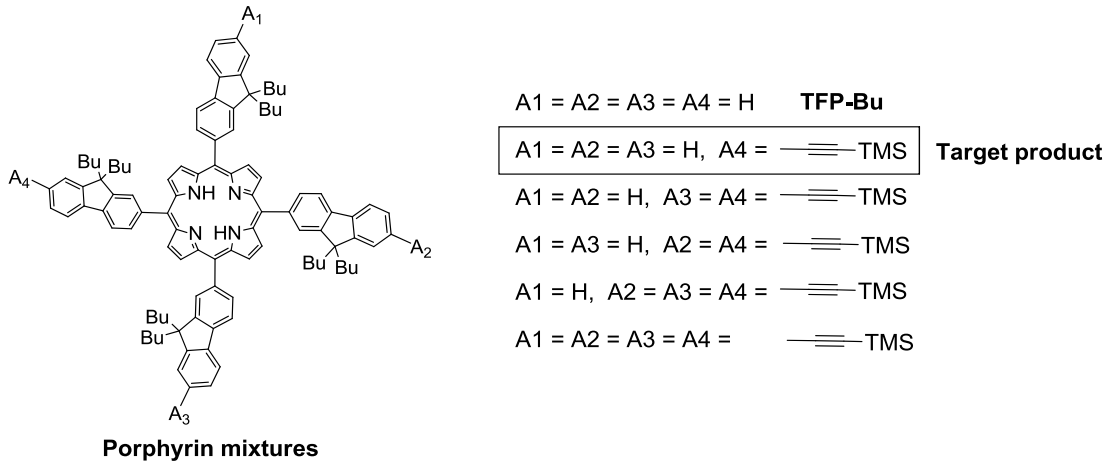

Figure 5.3 Statistical distributions of components in porphyrin mixtures.

Subsequently, deprotection of TMS was achieved directly in solvents mixture of CH_2Cl_2 and MeOH using excess of K_2CO_3, to dissolve all the porphyrin mixtures, controlled amount of THF was added as well. The reaction was heated at 45 ^oC for 30 h by TLC monitoring. Then chromatography was used to isolate **Monomer**: different eluents were tried, showing the mixture solvents of heptane and THF (4 : 1) could separate every component in TLC. We found that the purification could not be done even adding only a little CH_2Cl_2 in eluent. Therefore, lower polar eluent (heptane : THF = 10 : 1) was adopted in column chromatography, giving pure mono-substituted product **Monomer** as red powder (15% yield for two steps). We have to notice that, for the mixtures before deprotection of TMS, they still could not be isolated in TLC using this eluent (heptane : THF = 4 : 1).

To avoid the insertion of copper ion during Sonogashira catalytical coupling, metallization was done in advance to protect the heart of **Monomer** using Zn ion: $Zn(OAc)_2$ reacted with **Monomer** in mixed solvents of CH_2Cl_2 and MeOH at 45 ^oC overnight, giving 81% yield of **Zn-Monomer** as purple powder.

5.2.2 Oligomers formation

(1) Dimer formation

The synthetic method for porphyrin oligomers is shown in Figure 5.4. Considering the large rigid building block: **Zn-Monomer**, more active catalysts $Pd(PPh_3)_4$/CuI were used in Sonogashira coupling, and the proportion of solvents DMF and $^{i}Pr_2NH$ was chosen as 10:1 to increase the solubility of starting materials and products. The reaction time and temperature were optimized, so heating the reaction for 70 h at 140 ^{o}C was finally adopted. After reaction, the products were also shown as muti-components: starting material, mono-substituted byproduct, homo-coupling byproduct and target product, etc. Likewise, Zn porphyrin derivatives had the same difficulties to be separated because of their similar polarities.

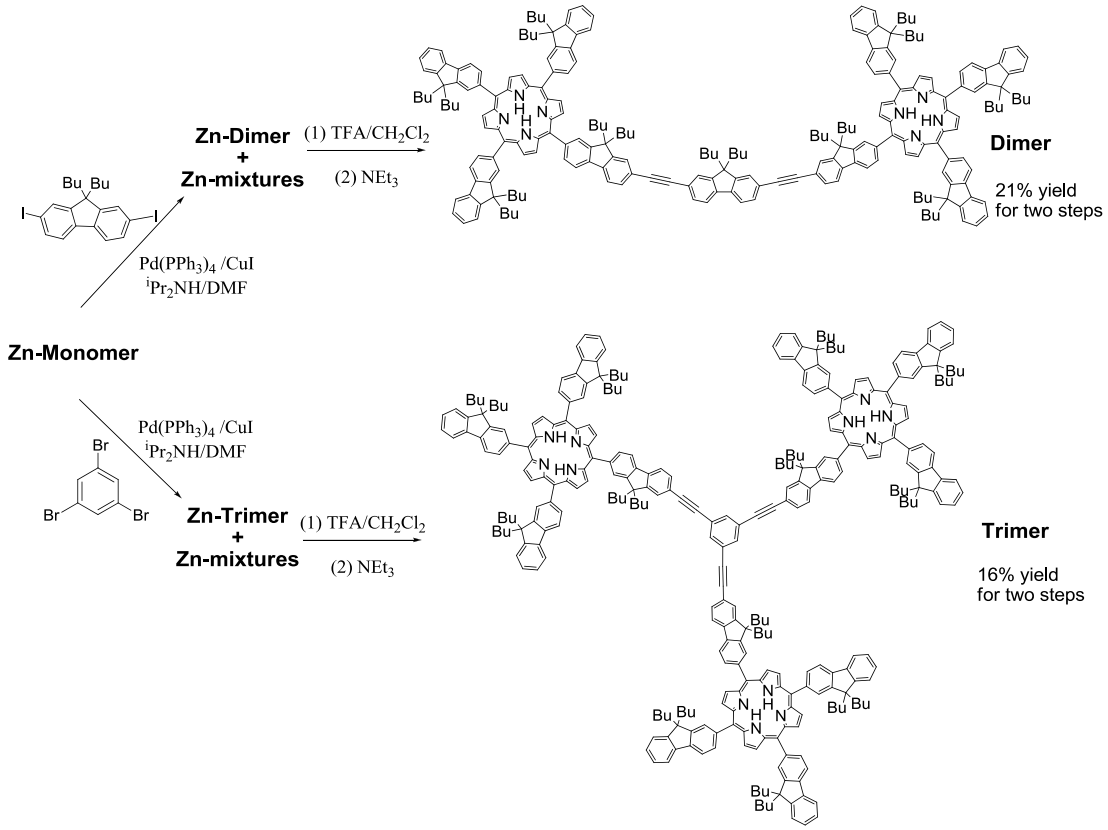

Figure 5.4 Synthetic strategies used for porphyrin **Dimer** and **Trimer**.

Then, demetallization was done in two steps: (1) A small excess of TFA (Trifluoroacetic Acid) was added dropwise in CH_2Cl_2 solution of Zn complexes, showing the color of solution changing from red to green gradually. The formation of protonated porphyrins was observed in UV-visible absorption spectrum. We kept the protonation reaction stirring at room temperature overnight to be sure all the porphyrins are demetallized. (2) Then controlled amount of NEt_3 was added to neutralize the protonated porphyrin derivatives, and the color of solution changed progressively green to red-brown. After 1 h of neutralization, CH_2Cl_2 was evaporated easily under reduced pressure, and enough MeOH was added subsequently to precipitate all the neutral porphyrin derivatives. We filtered the MeOH solution and did further purification of residue by column chromatography with eluent of heptane and THF (4 : 1). MALDI-Mass was used to check the target product: free-based **Dimer**.

(2) Trimer formation

The preparation procedures and conditions of free-based **Trimer** are similar to **Dimer**, also using Sonogashira coupling and de-metalization reactions. The yield for **Trimer** was lower than **Dimer**, resulting from larger steric hindrance of target tri-substituted product and probably more multi-substituted oligomers are obtained as byproducts.

5.3 ^{1}H NMR analysis

*5.3.1 ^{1}H NMR spectra of **Monomer** and **Zn-Monomer***

Figure 5.5 exhibits full ^{1}H NMR spectra of **Monomer** and **Zn-Monomer**. For **Monomer**: (i) 8 protons of porphyrin ring Hβ locate around 9 ppm; (ii) 27 protons, around 8.3-7.4 ppm, are assigned to aromatic protons of fluorenyl groups; (iii) one alkynyl proton lies at 3.21 ppm; (iv) *n*-butyl protons Ha,b,c,d could be identified very well from 2.2 to 0.7 ppm, particularly 16 protons of Hc are separated into two broad peaks with the same integrations; (v) two protons at -2.58 ppm are -NH of porphyrin

heart.

After the Zn ion insertion, **Zn-Monomer** still keeps most similar shifts and integrations of protons as **Monomer**: aromatic protons in fluorenyls, alkynyl proton and *n*-butyl protons. For Hβ of porphyrin ring, **Zn-Monomer** has a slight shift to lower field. Because of Zn chelation in porphyrin ring, there is no -NH signal in high field.

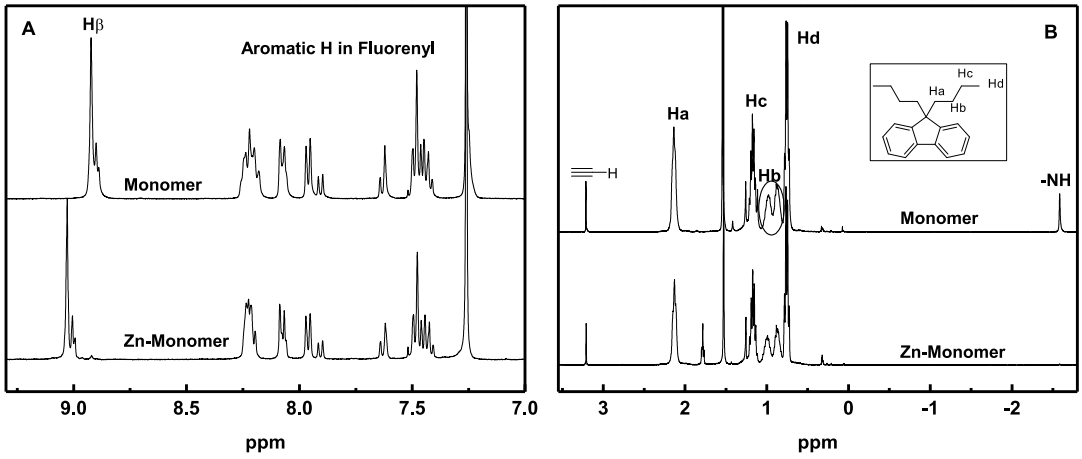

Figure 5.5 ^{1}H NMR spectra of **Monomer** and **Zn-Monomer**.

*5.3.2 ^{1}H NMR spectra of **Dimer** and **Trimer***

Comparing to free-based **Monomer**, Figure 5.6 shows ^{1}H NMR spectra of **Dimer** and **Trimer**. In Figure 5.6A, protons Hβ of these three compounds all locate around 8.92 ppm; their aromatic protons from fluorenyl or phenyl mainly distribute from 8.3 to 7.4 ppm, and some multi-peaks of **Dimer** and **Trimer** are obviously similar to **Monomer** but with slight differences in integration.

In Figure 5.6B, the signals of *n*-butyl protons and -NH protons in high field could be very well identified and their shifts for **Dimer** and **Trimer** both correspond to **Monomer**.

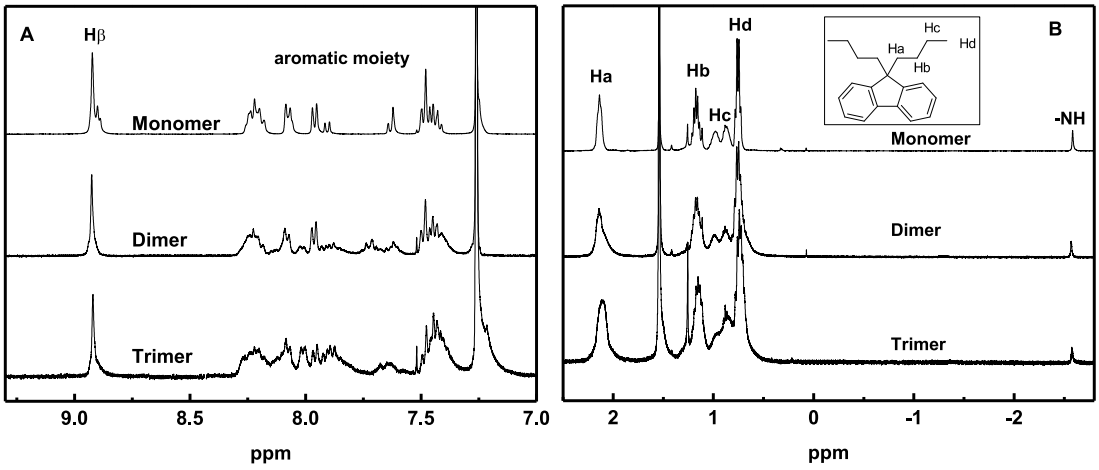

Figure 5.6 ^{1}H NMR spectra of **Monomer**, **Dimer** and **Trimer**.

5.4 Optical properties

UV-visible absorption and photoluminescence spectroscopy measurements for porphyrin oligomers **Dimer** and **Trimer** in toluene (HPLC) were performed at room temperature, as well as for **Monomer** as reference. Their relative optical data are summarized in Table 5.1.

5.4.1 Absorption and emission

Normalized absorption spectra of **Monomer**, **Dimer** and **Trimer** are shown in details, in Figure 5.7. These three compounds all keep two intrinsic absorption regions of porphyrin: Soret-band locates at 428 nm and other four Q-bands distribute from 519 to 653 nm. Between **Monomer** and the two oligomers, they show the same shift of Soret-band, but for Q-bands, oligomers have a little red shift compared to **Monomer**. Interestingly, **Dimer** and **Trimer**, with different structures, present the same Soret-band and Q-bands shifts, and the differences exist in the intensities of Q-bands. After normalizing at Soret-band, **Trimer** presents more intense Q-bands absorption compared to **Dimer** and **Monomer**, specially for Qx(0,0), and the similar change also occurs in emission peaks Q(0,0).

All the dilute toluene solutions were prepared with similar Soret-band intensity (near to 0.1 on UV-visible spectrometer), while measuring, their emission spectra also exhibited similar intensity at Q(0,1) peaks, therefore, the emission spectra of **Monomer**, **Dimer** and **Trimer** are also summarized at normalizing the intensities of Q(0,1).

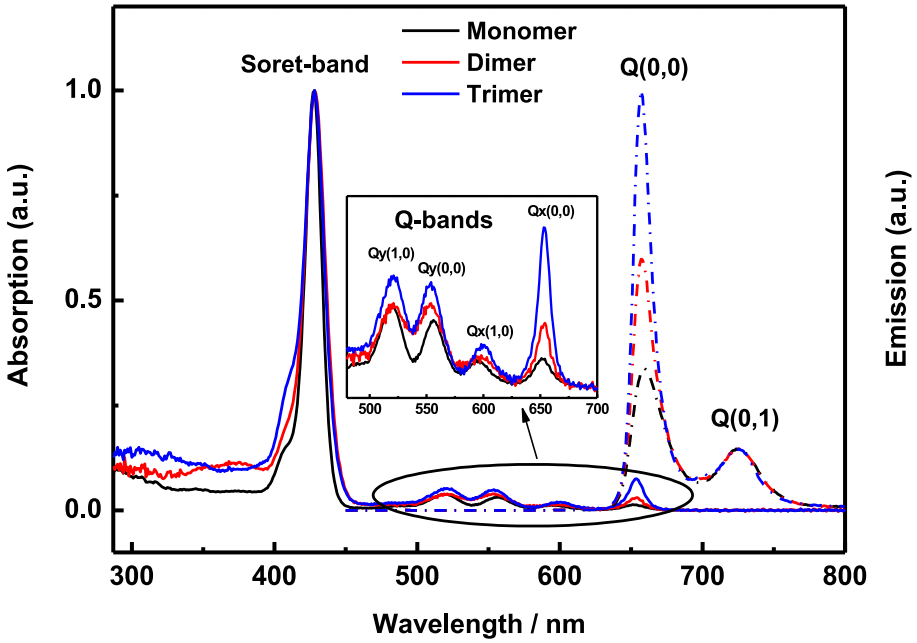

Figure 5.7 UV-visible absorption and emission spectra of **Monomer**, **Dimer** and **Trimer**.

In Figure 5.7, the emission peaks Q(0,0) have the similar change tendency as Qx(0,0), and from **Monomer** to **Trimer**, the intensities of Q(0,0) increase obviously. We integrated the emission areas of Q(0,0) and Q(0,1), noted as $S_{Q(0,0)}$ and $S_{Q(0,1)}$, the area integration ratios of $S_{Q(0,0)}$: $S_{Q(0,1)}$ for **Monomer**, **Dimer** and **Trimer** are 1.6, 2.2 and 3.0, respectively. It suggests that, with the numbers of terminated porphyrin increasing, Q(0,0) of **Trimer** becomes the predominant red-lighting resource.

5.4.2 Quantum yield

The fluorescence quantum yields of these compounds were listed in Table 5.1, taking TPP (Φ =11% in toluene) as reference. **Monomer** has 20% quantum yield similar to the analogue TFP-Bu without alkynyl (Figure 5.3). **Dimer** with two terminated porphyrins shows as well about 20% quantum yield, but still higher than linear free-based Dimer AB in previous work which shows 17% quantum yield,[37] suggesting terminated porphyrin is also an important factor for quantum yield. It is worth noticed that, **Trimer** with star-shaped construction, exhibit the highest quantum yield of 33%. Therefore, along this line, it encourages us to design 3D expanded conjugated oligomer with terminated TFP porphyrin in future.

Table 5.1 Optical data of porphyrin **Monomer**, **Dimer** and **Trimer**.

	Absorption[a]		Emission[a] Ex = Soret-band			Quantum yield[b](%)
	Soret-band	Q-bands	Q(0,0)	Q(0,1)	$S_{Q(0,0)}$: $S_{Q(0,1)}$	
TPP	419	514,548,590,649	652	719	-	11
Monomer	428	519,556,596,652	659	726	1.6	20
Dimer	428	521,554,598,653	657	726	2.2	20
Trimer	428	521,554,598,653	657	726	3.0	33

a. Experiments were achieved in toluene (HPLC level) with the UV-visible absorption region from 287 to 800 nm and emission region from 450 to 800 nm.

b. Experiments for fluorescence quantum yields were achieved in toluene (HPLC level) using TPP (Φ =11%) as standard, by Soret-band excitation.

5.5 Conclusions

1. Taking *n*-butyl substituted TFP as terminated group, designed and synthesized one porphyrin **Monomer** and two oligomers: linear **Dimer** and star **Trimer**.

2. The formation of **Monomer** was achieved under Lindsey conditions and the purification could be achieved after deprotection of TMS. The formation of oligomers is done successively by metallization, Sonogashira coupling and de-metallization reactions, and the purification needs MALDI-Mass monitoring.

3. By ^{1}H NMR analysis, these two oligomers keep many similar proton signals as **Monomer**, but it is difficult to identify the assignation of aromatic protons.

4. For their optical properties:

(i) **Dimer** and **Trimer** have the same Soret-band shift as **Monomer**, but the intensities of Q-bands show more differences, especially for Qx(0,0).

(ii) The emission area ratios of Q(0,0) and Q(0,1) enhance obviously with the numbers of terminated porphyrin increasing, and for **Trimer**, it shows Q(0,0) as predominated red emission.

(iii) **Dimer** keeps similar quantum yield as **Monomer**, while **Trimer** with star-shaped construction has the highest quantum yield of 33%.

Experimental section

9,9-dibutyl-7-((trimethylsilyl)ethynyl)-9*H*-fluorene-2-carbaldehyde:

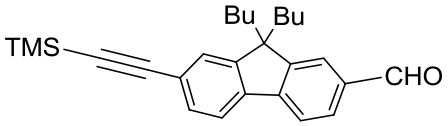

In a schlenk, a mixture of 7-bromo-9,9-dibutyl-9*H*-fluorene-2-carbaldehyde (2.07 g, 5.37 mmol, 1 eq), $Pd(PPh_3)_2Cl_2$ (23 mg, 0.032 mmol, 0.6% eq) and CuI (3 mg, 0.016 mmol, 0.3% eq) was added DMF (5 mL), $^{i}Pr_2NH$ (5 mL) and ethynyltrimethylsilane (1.15 mL, 8.06 mmol, 1.5 eq) under argon, successively. The system was degassed by freeze-pump-thaw twice and heated for 2 days at 95 ^{o}C. After being evaporated, residue was farther purified by chromatography (heptane), and yellow white powder was obtained (1.86 g, 86% yield).

^{1}H NMR (400 MHz, $CDCl_3$, ppm): δ 10.06 (s, 1H), 7.87-7.85 (m, 2H), 7.82-7.80 (m, 1H), 7.71 (d, *J* = 8 Hz, 1H), 7.50 (d, *J* = 8 Hz, 1H), 7.47 (s, 1H), 2.07-1.94 (m, 4H), 1.11-1.02 (m, 4H), 0.65 (t, *J* = 8 Hz, 6H), 0.60-0.44 (m, 4H), 0.29 (s, 9H).

TFP-TMS:

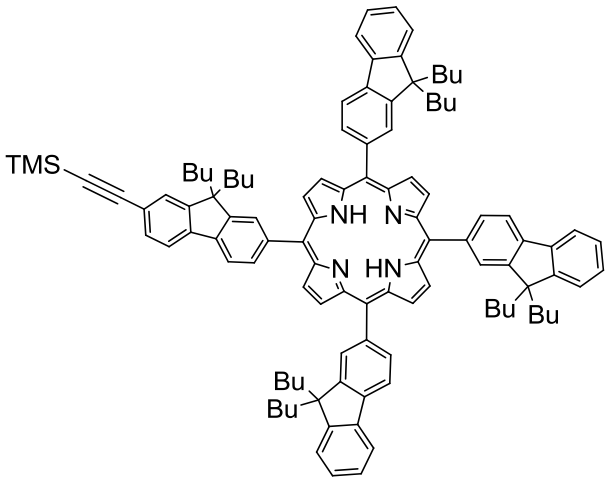

In a two-neck flask , a mixture of 9,9-dibutyl-9*H*-fluorene-2-carbaldehyde (2.05 g, 6.71 mmol, 3 eq), 9,9-dibutyl-7-((trimethylsilyl)ethynyl)-9*H*-fluorene-2-carbaldehyde (900 mg, 2.23 mmol, 1 eq) and pyrrole (0.62 mL, 8.94 mmol, 4 eq) were dissolved in dry chloroform (550 mL) under argon. After degassing the mixture with argon for 30

min, $BF_3 \cdot OEt_2$ (0.2 mL) was injected and the reaction was stirred in dark for 3 h under argon at room temperature. Then oxidant *p*-chloranil (1.5 g) was added, and the reaction was heated at 60 ^oC for another 2 h without argon protection. After cooling the reaction to room temperature, NEt_3 (2 mL) was added to the mixture and then continue stirred for 10 min. Evaporated the solvents and the residue was absorbed in silica. Purification was done by chromatography (CH_2Cl_2 : heptane = 1 : 3), getting porphyrin mixture as red powder (2.3 g, 68% yield).

Monomer:

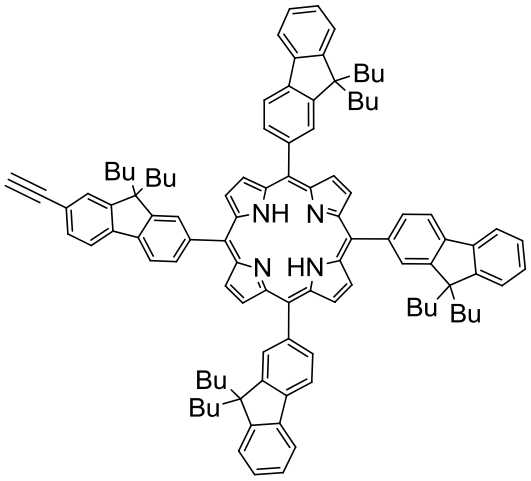

In a mixture solvents of CH_2Cl_2 (300 mL), MeOH (100 mL) and THF (60 mL), porphyrin mixture TFP-TMS (2.3 g, 1.52 mmol, 1 eq) was added together with K_2CO_3 (840 mg, 6.08 mmol, 4 eq). The mixture was stirred at 45 ^oC for 30 h. After filtering excess of K_2CO_3, the residue was washed by CH_2Cl_2. Evaporated the solvents, farther purification was done by chromatography (heptane : THF = 10 : 1), getting pure target porphyrin as red powder (470 mg, 15% yield for two steps).

^1H NMR (400MHz, $CDCl_3$, ppm): δ 8.92-8.89 (m, 8H), 8.24-8.18 (m, 8H), 8.08-8.07 (m, 4H), 7.96 (d, *J* = 8 Hz, 3H), 7.91 (d, *J* = 8 Hz, 1H), 7.64-7.62 (m, 2H), 7.52-7.41 (m, 9H), 3.21 (s, 1H), 2.14 (m, broad, 16H), 1.21-1.14 (m, 16H), 0.98 (m, broad, 8H), 0.88 (m, broad, 8H), 0.78-0.73 (m, 24H), -2.58 (s, 2H).

^{13}C NMR (125 MHz, $CDCl_3$, ppm): δ 151.2, 149.5, 149.2, 141.8, 141.7, 141.0, 140.9,

140.7, 139.8, 133.8, 133.6, 131.5, 129.4, 127.4, 127.0, 126.7, 123.1, 120.9, 120.8, 120.6, 120.4, 120.1, 118.3, 117.8, 84.8, 55.3, 40.3, 26.3, 23.1, 13.9.

HRMS-ESI: m/z = 1439.8802 $[M+H]^+$ (calcd:1439.8803).

Zn-Monomer:

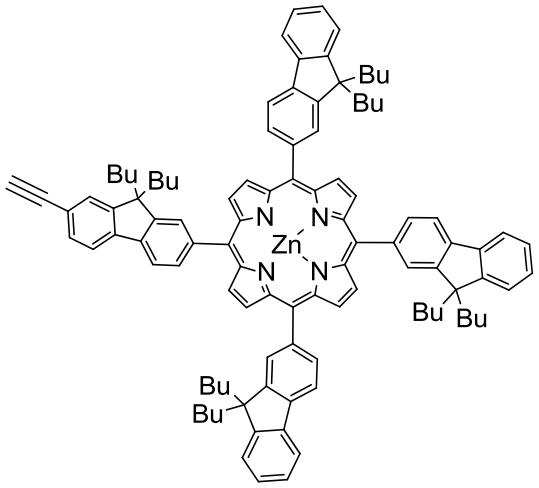

Monomer (270 mg, 0.19 mmol, 1 eq) and $Zn(OAc)_2{\cdot}2H_2O$ (123 mg, 0.75 mmol, 4 eq) were added into a mixture solvents of CH_2Cl_2 (90 mL) and MeOH (30 mL). The reaction was stirred overnight at 45 ^oC. Evaporated the solvents and the residue was farther purified by chromatography (heptane : CH_2Cl_2 = 1 : 1), collecting Zn-porphyrin as red powder (228 mg, 81% yield).

^1H NMR (400 MHz, $CDCl_3$, ppm): δ 9.03-8.99 (m, 8H), 8.24-8.20 (m, 8H), 8.09-8.06 (m, 4H), 7.96 (d, *J* = 8 Hz, 3H), 7.91 (d, *J* = 8 Hz, 1H), 7.64-7.62 (m, 2H), 7.52-7.41 (m, 9H), 3.21 (s, 1H), 2.13 (m, broad, 16H), 1.21-1.13 (m, 16H), 0.99 (m, broad, 8H), 0.88 (m, broad, 8H), 0.78-0.73 (m, 24H).

Zn-Dimer:

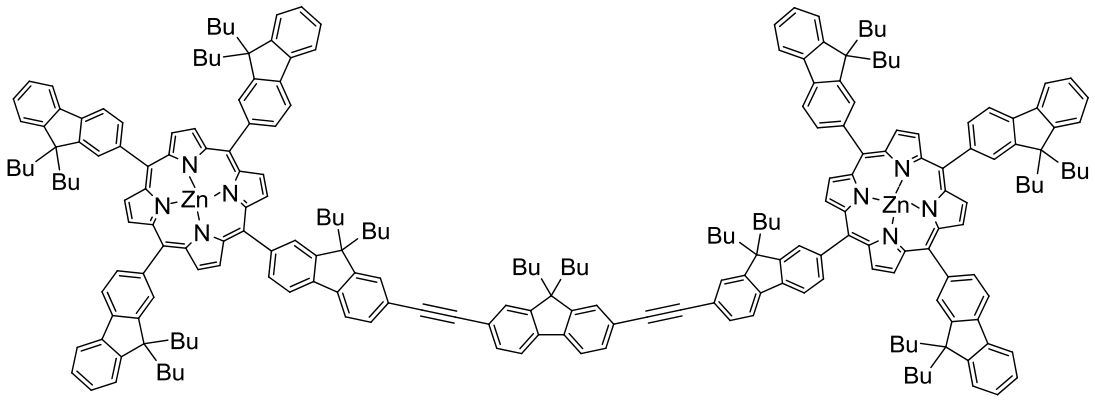

In a schlenk, a mixture of 9,9-dibutyl-2,7-diiodo-*9H*-fluorene (13 mg, 0.024 mmol, 1 eq), **Zn-Monomer** (80 mg, 0.053 mmol, 2.2 eq), $Pd(PPh_3)_4$ (12 mg, 0.011 mmol, 45% eq) and CuI (2 mg, 0.011 mmol, 45% eq) was added DMF (10 mL) and $^{i}Pr_2NH$ (1 mL) under argon, successively. The system was degassed by freeze-pump-thaw twice and heated at 140 ^{o}C for 70 h. After being evaporated, residue was farther purified by chromatography (heptane : THF = 4 : 1 to 2 : 1), and then the porphyrin mixtures of Zn complexes were obtained as red powder.

Dimer:

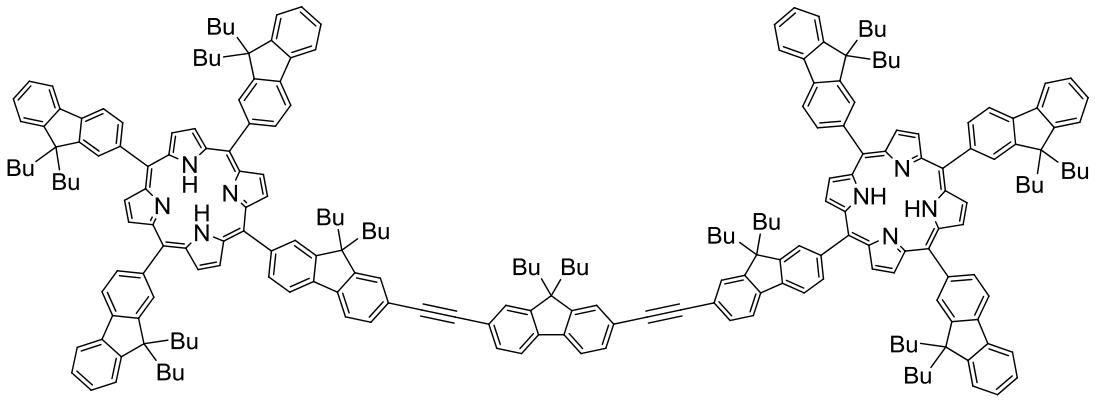

In a flask, all the Zn complexes were dissolved in CH_2Cl_2. A slight excess of TFA was added dropwise into the flask until the color of solution changing from red to green gradually. The protonation reaction was stirred at room temperature overnight. NEt_3 was added dropwise into the solution until the color changing from green to red-brown, and the neutralization was kept for another 1 h at room temperature. Evaporated all the CH_2Cl_2 under reduced pressure, leaving a certain volume of solvents with high boiling temperature, and MeOH was added subsequently to precipitate all the porphyrin derivatives. Filtered the MeOH solution and the red residue could be further purified by chromatography (heptanes : THF = 4 : 1). MALDI-Mass was used to test every component from column chromatography and **Dimer** was collected as red powder (16 mg, 21% yield from **Zn-Monomer**).

^{1}H NMR (400 MHz, $CDCl_3$, ppm): δ 8.93 (s, 8H), 8.25-8.19 (m, 11H), 8.15-8.07 (m, 6H), 8.01 (d, *J* = 8 Hz, 2H), 7.96 (d, *J* = 8 Hz, 5H), 7.93-7.83 (m, 6H), 7.76-7.67 (m, 5H), 7.65-7.56 (m, 4H), 7.52-7.39 (m, 21H), 2.14 (m, broad, 36H), 1.22-1.11 (m, 36H), 0.99-0.70 (m, 90H), -2.57 (s, 2H).

^{13}C NMR (125 MHz, $CDCl_3$, ppm): δ 151.4, 151.2, 149.2, 141.0, 140.9, 140.7, 133.6, 131.0, 130.8, 129.4, 127.4, 127.3, 127.1, 126.1, 126.0, 123.1, 123.0, 120.9, 120.1, 119.9, 118.2, 117.8, 55.4, 55.3, 40.3, 26.3, 26.0, 23.1, 14.1, 14.0.

HRMS-ESI: m/z = 3152.9190 $[M+H]^+$ (calcd: 3152.9255), 1576.9671 $[M+2H]^{2+}$ (calcd: 1576.9664).

Zn-Trimer:

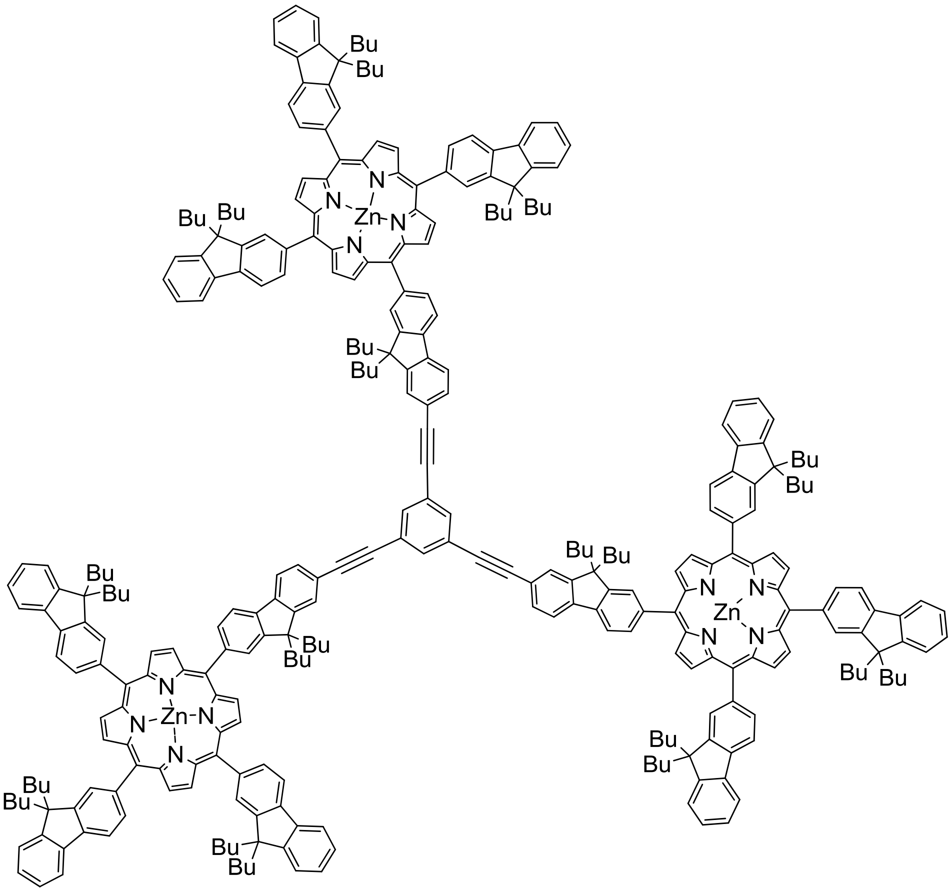

The synthesis procedure of **Zn-Trimer** is the same as **Zn-Dimer**, and the Zn complexes were also used in protonation reaction directly to obtain **Trimer**.

Trimer:

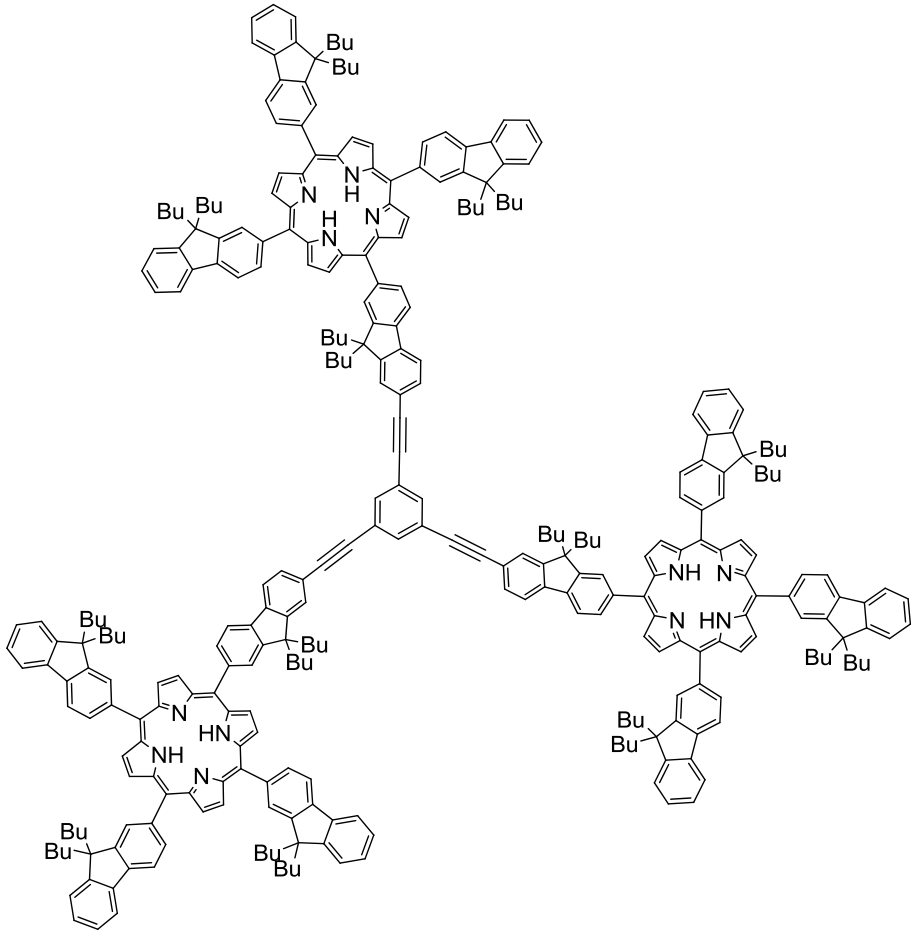

The synthesis procedure of **Trimer** is the same as **Dimer**, giving red powder with 16% yield from **Zn-Monomer**.

^{1}H NMR (400 MHz, $CDCl_3$, ppm): δ 8.92 (s, 8H), 8.27-8.16 (m, 14H), 8.14-8.05 (m, 11H), 8.01 (d, J = 8 Hz, 6H), 7.96 (d, J = 8 Hz, 4H), 7.93-7.81 (m, 15H), 7.68-7.58 (m, 7H), 7.52-7.38 (m, 27H), 2.11 (m, broad, 48H), 1.19-1.11 (m, 48H), 0.98-0.69 (m, 120H), -2.58 (s, 2H).

^{13}C NMR (125 MHz, $CDCl_3$, ppm): δ 151.2, 149.2, 141.1, 141.0, 140.9, 133.7, 131.0, 127.5, 127.3, 127.0, 123.1, 123.0, 120.9, 120.1, 120.0, 117.9, 55.3, 40.3, 26.3, 23.1, 14.0.

HRMS-ESI: m/z = 1463.8832 $[M+3H]^{3+}$ (calcd: 1463.8803).

References

1. Mcdermott, G.; Prince, S. M.; Free, A. A.; et al, *Nature* **1995**, *374*, 517-521.

2. Severance, S.; Hamza, I. *Chem. Rev.* **2009**, *109*, 4596-4616.

3. (a) Juan, O.; Helqe, M.-B.; Martin, A. *Chem. Commun.* **2014**, *50*, 3488-3490. (b) Ema, T.; Miyazaki, Y.; Shimonishi, J.; Maeda, C.; Hasegawa, J.-Y. *J. Am. Chem. Soc.* **2014**, *136*, 15270-15279. (c) Jiang,Q.; Sheng, W.; Tian, M.; Tang, J.; Guo, C. *Eur. J. Org. Chem*. **2013**, 1861-1866.

4. (a) Ethirajan, M.; Chen, Y.; Joshi, P.; Pandey, R. *Chem. Soc. Rev.* **2011**, *40*, 340-362. (b) Josefsen, L. B.; Boyle, R. W. *Theranostics* **2012**, *2*, 916-966. (c) Pushpan, S. K.; Venkatraman, S.; Anand, V. G.; Sankar, J.; Parmeswaran, D.; Ganesan, S.; Chandrashekar, T. K. *Curr. Med. Chem. Anticancer Agents* **2002**, *2*, 187-207. (d) Pandey,R. K.; Smith, K. M.; Dougherty, T. J. *J. Med. Chem.* **1990**, *33*, 2032-2038

5. (a) Koszelewski, D.; Nowak-Król, A.; Drobizhev, M.; Wilson, C. J.; Haley, J. E.; Cooper, T. M.; Romiszewski, J.; Górecka, E.; Anderson, H. L.; Rebane, A.; Gryko, D. T. *J. Mater. Chem. C* **2013**, *1*, 2044-2053. (b) Graham, K. R.; Yang Y.; Sommer J. R.; Shelton, A. H.; Schanze, K. S.; Xue, J.; Reynolds, J. R. *Chem. Mater.* **2011**, *23*, 5305-5312. (c) Zhu, L.-G.; Wang, J.; Reng, T.-G.; Li, C.-Y.; Guo, D.-C.; Guo, C.-C. *J. Phys. Org. Chem.* **2010**, *23*, 190-194.

6. (a) Li, C.; Ly, J.; Lei, B.; Fan, W.; Zhang, D.; Han, J.; Meyyappan, M.; Thompson, M.; Zhou, C. *J. Phys. Chem. B* **2004**, *108*, 9646-9649. (b) Bussetti, G.; Campione, M.; Ferraro, L.; Raimondo, L.; Bonanni, B.; Goletti, C.; Palummo, M.; Hogan, C.; Duò, L.; Finazzi, M.; Sassella, A. *J. Phys. Chem. C*, **2014**, *118*, 15649-15655.

7. (a) Li, L.-L.; Diau, E. W.-G. *Chem. Soc. Rev.* **2013**, *42*, 291-304. (b) Huang, X.; Zhu, C.; Zhang, S.; Li, W.; Guo, Y.; Zhan, X.; Liu, Y.; Bo, Z. *Macromolecules* **2008**, *41*, 6895-6902.

8. (a) Kozaki, M.; Uetomo, A.; Suzuki, S.; Okada, K. *Org. Lett.* **2008**, *10*, 4477-4480. (b) Uetomo, A.; Kozaki, M.; Suzuki, S.; Yamanaka, K.-i.; Ito, O.; Okada, K. *J. Am. Chem. Soc.* **2011**, *133*, 13276-13279.

9. (a) Harriman, A.; Hissler, M.; Trompette, O.; Ziessel, R. *J. Am. Chem. Soc*. **1999**, *121*, 2516-2525. (b) Fortage, J.; Boixel, J.; Blart, E.; Becker, H. C.; Odobel, F. *Inorg. Chem.* **2008**, *48*, 518-526.

10. (a) Mongin, O.; Papamicaël, C.; Hoyler, N.; Gossauer, A. *J. Org. Chem.* **1998**, *63*, 5568-5580. (b) Nakano, A.; Yasuda, Y.; Yamazaki, T.; Akimoto, S.; Yamazaki, I.; Miyasaka, H.; Itaya, A.; Murakami, M.; Osuka, A. *J. Phys. Chem. A* **2001**, *105*, 4822-4833.

11. (a) Singh, B. P.; Vigava, R.; Shetty, S. J.; Kandasamy, K.; Puntambekar, P. N.; Srivastava, T. S. *J. Porphyrins Phthalocyanines* **2000**, *4*, 659-664. (b) Rozhkov, V.; Wilson, D.; Vinogradov, S. *Macromolecules* **2002**, *35*, 1991-1993. (c) Jiang, D.-L.; Aida, T. *J. Am. Chem. Soc.* **1998**, *120*, 10895-10901.

12. (a) Li, B.; Fu, Y.; Han, Y.; Bo, Z. *Macromol. Rapid Commun.* **2006**, *27*, 1355-1361. (b) Fei, Z.; Han, Y.; Bo, Z. *J. Polym. Sci., Part A: Polym. Chem.* **2008**, *46*, 4030-4037.

13. (a) Kozaki, M.; Akita, K.; Suzuki, S.; Okada, K. *Org. Lett.* **2007**, *9*, 3315-3318. (b) Kimura, M.; Shiba, T.; Yamazaki, M.; Hanabusa, K.; Shirai, H.; Kobayashi, N. *J. Am. Chem. Soc.* **2001**, *123*, 5636-5642.

14. (a) Wang, L.; Jiang, Y.; Luo, J.; Zhou, Y.; Zhou, J. H.; Wang, J.; Pei, J. *Adv. Mater.* **2009**, *47*, 4854-4858. (b) Duan, X. F.; Wang, J. L.; Pei, J. *Org. Lett.* **2005**, *7*, 4071-4073.

15. (a) Kreyenschmidt, M.; Klaerner, G.; Fuhrer, T.; Aschenhurst, J.; Karg, S.; Chen, W. D.; Lee, V. Y.; Scott, J. C.; Miller, R. D. *Macromolecules* **1998**, *31*, 1099-1103. (b) Montgomery, N. A.; Denis, J.-C.; Schumacher, S.; Ruseckas, A.; Skabara, P. J.; Kanibolotsky, A.; Paterson, M. J.; Galbraith, I.; Turnbull, G. A.; Samuel, I. D. W. *J. Phys. Chem. A.* **2011**, *115*, 2913-2919.

16. (a) Li, B.; Xu, X.; Sun, M.; Fu, Y.; Yu, G.; Liu, Y.; Bo, Z. *Macromolecules* **2005**, *39*, 456-461. (b) Li, B.; Li, J.; Fu, Y.; Bo, Z. *J. Am. Chem. Soc.* **2004**, *126*, 3430-3431.

17. Fei, Z.; Li, B.; Bo, Z.; Lu, R. *Org. Lett.* **2004**, *6*, 4703-4706.

18. Sun, M.; Bo, Z. *J. Polym. Sci., Part A: Polym. Chem.* **2007**, *45*, 111-124.

19. Harth, E. M.; Hecht, S.; Helms, B.; Malmstrom, E. E.; Fréchet, J. M. J.; Hawker, C. J. *J. Am. Chem. Soc.* **2002**, *124*, 3926-3938.

20. (a) Oar, M. A.; Dichtel, W. R.; Serin, J. M.; Fréchet, J. M. J.; Rogers, J. E.; Slagle, J. E.; Fleitz, P. A.; Tan, L.-S.; Ohulchanskyy, T. Y.; Prasad, P. N. *Chem. Mater.* **2006**, *18*, 3682-3692. (b) Dichtel, W. R.; Serin, J. M.; Edder, C.; Fréchet, J. M. J.; Matuszewski, M.; Tan, L.-S.; Ohulchanskyy, T. Y.; Prasad, P. N. *J. Am. Chem. Soc.* **2004**, *126*, 5380-5381.

21. (a) Tavasli, M.; Bettington, S.; Bryce, M. R.; Al-Attar, H.; Dias, F. B.; King, S.; Monkman, A. P.; *J. Mater. Chem.* **2005**, *15*, 4963-4970. (b) Al-Attar, H.; Monkman, A. P.; Tavasli, M.; Bettington, S.; Bryce, M. R. *Appl. Phys. Lett.* **2005**, *86*, 121101.

22. Scherf, U.; List, E. J. W. *Adv. Mater.* **2002**, *14*, 477-487.

23. (a) Onitsuka, K.; Kitajima, H.; Fujimoto, M.; Iuchi, A.; Takei, F.; Takahashi, S. *Chem. Commun.* **2002**, 2576-2577. (b) Du, B.; Fortin, D.; Harvey, P. D. *Inorg. Chem.* **2011**, *50*, 11493-11505.

24. (a) Frampton, M. J.; Beavington, R.; Lupton, J. M.; Samuel, I. D. W.; Burn, P. L. *Synth. Met.* **2001**, *121*, 1671-1672. (b) Frampton, M. J.; Magennis, S. W.; Pillow, J. N. G.; Burn, P. L.; Samuel, I. D. W. *J. Mater. Chem.* **2003**, *13*, 235-242. (c) Pillow, J. N. G.; Halim, M.; Lupton, J. M.; Burn, P. L.; Samuel, I. D. W. *Macromolecules* **1999**, *32*, 5985-5993.

25. Kozaki, M.; Morita, S.; Suzuki, S.; Okada, K. *J. Org. Chem.* **2012**, *77*, 9447-9457.

26. Kumaresan, D.; Agarwal, N.; Ravikanth, M. *J. Chem. Soc., Perkin Trans. 1* **2001**, 1644-1648.

27. (a) Fan, J.; Whiteford, J. A.; Olenyuk, B.; Levin, M. D.; Stang, P. J.; Fleischer, E. B. *J. Am. Chem. Soc.* **1999**, *121*, 2741-2752. (b) Matano, Y.; Matsumoto, K.; Hayashi, H.; Nakao, Y.; Kumpulainen, T.; Chukharev, V.; Tkachenko, N. V.; Lemmetyinen, H.; Shimizu, S.; Kobayashi, N.; Sakamaki, D.; Ito, A.; Tanaka, K.; Imahori, H. *J. Am. Chem. Soc.* **2012**, *134*, 1825-1839. (c) Haumesser, J.; Gisselbrecht, J.-P.; Karmazin-Brelot, L.; Bailly, C.; Weiss, J.; Ruppert, R. *Organometallics* **2014**, *33*, 4923-4930.

28. Gao, Y.; Zhang, X.; Ma, C.; Li, X.; Jiang, J. *J. Am. Chem. Soc.* **2008**, *130*, 17044-17052.

29. (a) Aratani, N.; Osuka, A.; Kim, Y. H.; Jeong, D. H.; Kim, D. *Angew. Chem. Int.*

Ed. **2000**, *39*, 1458-1462. (b) Osuka, A.; Shimidzu, H. *Angew. Chem. Int. Ed. Engl.* **1997**, *36*, 135-137.

30. Hori, T.; Aratani, N.; Takagi, A.; Matsumoto, T.; Kawai, T.; Yoon, M.-C.; Yoon, Z. S.; Cho, S.; Kim, D.; Osuka, A. *Chem. Eur. J.* **2006**, *12*, 1319-1327.

31. (a) Hwang, I.-W.; Kamada, T.; Ahn, T. K.; Ko, D. M.; Nakamura, T.; Tsuda, A.; Osuka, A.; Kim, D. *J. Am. Chem. Soc.* **2004**, *126*, 16187-16198. (b) Hwang, I.-W.; Aratani, N.; Osuka, A.; Kim, D. *Bull. Korean Chem. Soc*. **2005**, *26*, 19-31.

32. Tanaka, T.; Osuka, A. *Chem. Soc. Rev.* **2015**, Advance Article DOI: 10.1039/C3CS60443H.

33. Nakamura, Y.; Aratani, N.; Osuka, A. *Chem. Soc. Rev.* **2007**, *36*, 831-845.

34. Durot, S.; Taesch, J.; Heitz, V. *Chem. Rev.* **2014**, *114*, 8542-8578.

35. (a) Zhu, B.; Chen, H.; Lin, W.; Ye, Y.; Wu, J.; Li, S. *J. Am. Chem. Soc.* **2014**, *136*, 15126-15129. (b) Nakamura, Y.; Aratani, N.; Osuka, A. *Chem. Soc. Rev.* **2007**, *36*, 831-845.

36. (a) Fan, J.; Whiteford, J. A.; Olenyuk, B.; Levin, M. D.; Stang, P. J.; Fleischer, E. B. *J. Am. Chem. Soc.* **1999**, *121*, 2741-2752. (b) Matano, Y.; Matsumoto, K.; Hayashi, H.; Nakao, Y.; Kumpulainen, T.; Chukharev, V.; Tkachenko, N. V.; Lemmetyinen, H.; Shimizu, S.; Kobayashi, N.; Sakamaki, D.; Ito, A.; Tanaka, K.; Imahori, H. *J. Am. Chem. Soc.* **2012**, *134*, 1825-1839. (c) Haumesser, J.; Gisselbrecht, J.-P.; Karmazin-Brelot, L.; Bailly, C.; Weiss, J.; Ruppert, R. *Organometallics* **2014**, *33*, 4923-4930.

37. Merhi A.; Drouet, S.; Kerisit, N.; Paul-Roth, C. O. *Tetrahedron* **2013**, *69*, 7112-7124.

38. Paul-Roth, C. O.; Merhi, A.; Yao, D.; Mongin, O. *Journal of Photochemistry and Photobiology A: Chemistry* **2014**, *288*, 23-33.

39. Drouet, S.; Merhi, A.; Argouarch, G.; Paul, F.; Mongin, O.; Blanchard-Desce, M.; Paul-Roth, C. O. *Tetrahedron* **2012**, *68*, 98-105.

40. (a) Quimby, D. J.; Longo, F. R. *J. Am. Chem. Soc.* **1975**, *97*, 5111-5117. (b) Uttamlal, M.; Sheila Holmes-Smith, A. *Chem. Phys. Lett.* **2008**, *454*, 223-228. (c) Retsek, J. L.; Medforth, C. J.; Nurco, D. J.; Gentemann, S.; Chirvony, V. S.; Smith, K.

M.; Holten, D. *J. Phys. Chem. B* **2001**, *105*, 6396-6411.

41. (a) Gouterman, M. *J. Mol. Spectroscopy* **1961**, *6*, 138-163. (b) Gouterman, M. *J. Chem. Phys.* **1959**, *30*, 1139-1161.

42. Milgrom, L. R. *The colours of Life: An Introduction to the Chemistry of Porphyrins and Related Compounds*, **1997**, OUP, Oxford.

43. Dexter, D. L. *J. Chem. Phys.* **1953**, *21*, 836-850.

44. Förster, T. *Zwischenmolekulare Energiewanderung und Fluoreszenz* (*Intermolecular energy migration and fluorescence*), Annalen der Physik (in German), **1948**, *437*, 55-75.

45. Helms, V. *Principles of Computational Cell Biology*, **2008**, Wiley-VCH, Weinheim.

46. Rothemund, P. *J. Am. Chem. Soc.* **1935**, *57*, 2010-2011.

47. (a) Rothemund, P. *J. Am. Chem. Soc.* **1936**, *58*, 625-627. (b) Rothemund, P.; Menotti, A. R. *J. Am. Chem. Soc.* **1941**, *63*, 267-270.

48. (a) Adler, A.D.; Longo, F.R.; Finarelli, J. D.; Assour, J.; Korsakoff, L. *J. Org. Chem.* **1967**, *32*, 476-476. (b) Adler, A.D.; Longo, F. R.; Shergalis, W. *J. Am. Chem. Soc.* **1964**, *86*, 3145-3149.

49. (a) Lindsey, J. S.; Hsu, H. C.; Schreiman, I. C. *Tetrahedron Lett.* **1986**, *27*, 4969-4970. (b) Lindsey, J. S.; Schreiman, I. C.; Hsu, H. C.; Kearney, P. C.; Marguerettaz, A. M. *J. Org. Chem.* **1987**, *52*, 827-836.

50. Lee, C.-H.; S. Lindsey, J. *Tetrahedron* **1994**, *50*, 11427-11440.

51. Lindsey, J. S.; MacCrum, K. A.; Tyhonas, J. S.; Chuang, Y. Y. *J. Org. Chem.* **1994**, *59*, 579-587.

52. Li, F. R.; Yang, K. X.; Tyhonas, J. S.; Maccrum, K. A.; Lindsey, J. S. *Tetrahedron* **1997**, *53*, 12339-12360.

53. Li, W.-S.; Aida, T. *Chem. Rev.* **2009**, *109*, 6047-6076.

54. (a) Drouet, S.; Paul-Roth, C. O.; Simonneaux, G. *Tetrahedron* **2009**, *65*, 2975-2981. (b) Drouet, S.; Paul-Roth, C. O. *Tetrahedron* **2009**, *65*, 10693-10700. (c) Merhi, A.; Drouet, S.; Kerisit, N.; Paul-Roth, C. O. *Tetrahedron* **2012**, *68*, 7901-7910.

55. (a) Drouet, S.; Paul-Roth, C. O.; Fattori, V.; Cocchi, M.; Williams, J. A. G. *New J.*

Chem. **2011**, *35*, 438-444. (b) Paul-Roth, C. O.; Drouet, S.; Merhi, A.; Williams, J. A. G.; Gildea, L. F.; Pearson, C.; Petty, M. C. *Tetrahedron* **2013**, *69*, 9625-9632.

56. (a) Paul-Roth, C.; Rault-Berthelot, J.; Simonneaux, G.; *Tetrahedron* **2004**, *60*, 12169-12175. (b) Drouet, S.; Ballut, S.; Rault-Berthelot, J.; Turban, P.; Paul-Roth, C. *Thin Solid Films* **2009**, *517*, 5474-5481.

57. (a) Drouet, S.; Merhi, A.; Grelaud, G.; Cifuentes, M. P.; Humphrey, M. G.; Matczyszyn, K.; Samoc, M.; Toupet, L.; Paul-Roth, C. O.; Paul, F. *New J. Chem.* **2012**, *36*, 2192-2195. (b) Drouet, S.; Merhi, A.; Yao, D.; Cifuentes, M. P.; Humphrey, M. G.; Wielgus, M.; Olesiak-Banska, J.; Matczyszyn, K.; Samoc, M.; Paul, F.; Paul-Roth, C. O. *Tetrahedron* **2012**, *68*, 10351-10359. (c) Merhi, A.; Grelaud, G.; Ripoche, N.; Barlow, A.; Cifuentes, M. P.; Humphrey, M. G.; Paul, F.; Paul-Roth, C. O. *Polyhedron* **2015**, *86*, 64-70.

58. Mongin, O.; Hugues, V.; Blanchard-Desce, M.; Mehri, A.; Drouet, S.; Yao, D.; Paul-Roth, C. O. *Photochemical & Photobiological Sciences* **2014**, submitted.

59. (a) Su, W.; Cooper, T. M.; Brant, M. C. *Chem. Mater.* **1998**, *10*, 1212-1213. (b) Verma, S.; Ghosh, H. N. *J. Phys. Chem. Lett.* **2012**, *3*, 1877-1884. (c) Sommer, J. R.; Shelton, A. H.; Parthasarathy, A.; Ghiviriga, I.; Reynolds, J. R.; Schanze, K. S. Chem. Mater. **2011**, 23, 5296-5304. (d) Zakavi, S.; Gharab, N. G. *Polyhedron* **2007**, *26*, 2425-2432. (e) Minaev, B.; Lindgren, M. *Sensors* **2009**, *9*, 1937-1966. (f) Su, W.; Cooper, T. M.; Brant, M. C. *Chem. Mater.* **1998**, *10*, 1212-1213. (g) Chen, P.; Tomov, I. V.; Dvornikov, A. S.; Nakashima, M.; Roach, J. F.; Alabran, D. M.; Rentzepis, P. M. *J. Phys. Chem.* **1996**, *100*, 17507-17512.

60. (a) Lebedev, A. Y.; Cheprakov, A. V.; Sakadzic, S.; Boas, D. A.; Wilson, D. F.; Vinogradov, S. A. *ACS Appl. Mater. Interfaces* **2009**, *1*, 1292-1304. (b) Sasaki, T.; Morin, J.-F.; Lu, M.; Tour, J. M. *Tetrahedron Lett.* **2007**, *48*, 5817-5820. (c) Rao, P. D.; Dhanalekshmi, S.; Littler, B. J.; Lindsey, J. S. *J. Org. Chem.* **2000**, *65*, 7323-7344. (d) Rao, P. D.; Littler, B. J.; Geier, G. R.; Lindsey, J. S. *J. Org. Chem.* **2000**, *65*, 1084-1092. (e) Feng, X.; Chen, L.; Dong, Y.; Jiang, D. *Chem. Commun.* **2011**, *47*, 1979-1981. (f) Yeung, M.; Ng, A. C. H.; Drew, M. G. B.; Vorpagel, E.; Breitung, E. M.; McMahon, R. J.; Ng, D. K. P. *J. Org. Chem.* **1998**, *63*, 7143-7150.

61. (a) Fang, Z.; Liu, B. *Tetrahedron Lett.* **2008**, *49*, 2311-2315. (b) Richardson, C.; Reed, C. A. *J. Org. Chem.* **2007**, *72*, 4750-4755.

62. (a) Hon, Y.-S.; Lee, C.-F.; Chen, R.-J.; Szu, P.-H. *Tetrahedron* **2001**, *57*, 5991-6001. (b) Zhuang, Y.; Hartmann, R. W. *Arch. Pharm.* **1999**, *332*, 25-30.

63. (a) Borst, M. L. G.; Bulo, R. E.; Gibney, D. J.; Alem, Y.; de Kanter, F. J. J.; Ehlers, A. W.; Schakel, M.; Lutz, M.; Spek, A. L.; Lammertsma, K. *J. Am. Chem. Soc.* **2005**, *127*, 16985-16999. (b) Sahu, B.; Muruganantham, R.; Namboothiri, I. N. N. *Eur. J. Org. Chem.* **2007**, 2477-2489. (c) Polyansky, D. E.; Danilov, E. O.; Voskresensky, S. V.; Rodgers, M. A. J.; Neckers, D. C. *J. Am. Chem. Soc.* **2005**, *127*, 13452-13453.

64. Lindsey, J. S.; Schreiman, I. C.; Hsu, H. C.; Kearney, P. C.; Marguerettaz, A. M. *J. Org. Chem.* **1987**, *52*, 827-836.

65. (a) Seybold, P. G.; Gouterman, M. *J. Mol. Spectroscopy* **1969**, *31*, 1-13. (b) Quimby, D. J.; Longo, F. R. *J. Am. Chem. Soc.* **1975**, *97*, 5111-5117.

66. Barker, C. A.; Zeng, X.; Bettington, S.; Batsanov, A. S.; Bryce, M. R.; Beeby, A. *Chem. Eur. J.* **2007**, *13*, 6710-6717.

67. Ayabe, M.; Yamashita, K.; Sada, K.; Shinkai, S.; Ikeda, A.; Sakamoto, S.; Yamaguchi, K. *J. Org. Chem.* **2003**, *68*, 1059-1066.

68. (a) Rigamonti, L.; Babgi, B.; Cifuentes, M. P.; Roberts, R. L.; Petrie, S.; Stranger, R.; Righetto, S.; Teshome, A.; Asselberghs, I.; Clays, K.; Humphrey, M. G. *Inorg. Chem.* **2009**, *48*, 3562-3572. (b) Yao, S.; Ahn, H.-Y.; Wang, X.; Fu, J.; Van Stryland, E. W.; Hagan, D. J.; Belfield, K. D. *J. Org. Chem.* **2010**, *75*, 3965-3974. (c) Mehta, G.; Sarma, P. *Tetrahedron Lett.* **2002**, *43*, 9343-9346.

69. Hassan Omar, O.; Babudri, F.; Farinola, G. M.; Naso, F.; Operamolla, A. *Eur. J. Org. Chem*. **2011**, 529-537.

70. (a) Screen, T. E. O.; Thorne, J. R. G.; Denning, R. G.; Bucknall, D. G.; Anderson, H. L. *J. Am. Chem. Soc.* **2002**, *124*, 9712-9713. (b) Kuebler, S. M.; Denning, R. G.; Anderson, H. L. *J. Am. Chem. Soc.* **1999**, *122*, 339-347.

71. (a) Tomizaki, K.-y.; Yu, L.; Wei, L.; Bocian, D. F.; Lindsey, J. S. *J. Org. Chem.* **2003**, *68*, 8199-8207. (b) Matsuzaki, Y.; Nogami, A.; Tsuda, A.; Osuka, A.; Tanaka, K. *J. Phys. Chem. A* **2006**, *110*, 4888-4899.

72. (a) Tong, S. L.; Zhang, J.; Yan, Y.; Hu, S.; Yu, J.; Yu, L. *Solid State Sci.* **2011**, *13*, 1320-1327. (b) Schmittel, M.; Samanta, S. K. *J. Org. Chem.* **2010**, *75*, 5911-5919. (c) Gao, Y.; Zhang, X.; Ma, C.; Li, X.; Jiang, J. *J. Am. Chem. Soc.* **2008**, *130*, 17044-17052. (d) Ogawa, K.; Ohashi, A.; Kobuke, Y.; Kamada, K.; Ohta, K. *J. Am. Chem. Soc.* **2003**, *125*, 13356-13357. (e) Lee, C. Y.; Farha, O. K.; Hong, B. J.; Sarjeant, A. A.; Nguyen, S. T.; Hupp, J. T. *J. Am. Chem. Soc.* **2011**, *133*, 15858-15861.

Résumé étendu

Les porphyrines sont des **macrocycles aromatiques à 18 électrons π** conjugués, constitués de quatre unités pyrroliques liées entre elles par des ponts méthines. Cette forte conjugaison implique une bonne stabilité et une forte absorption dans le domaine du visible de ces composés.

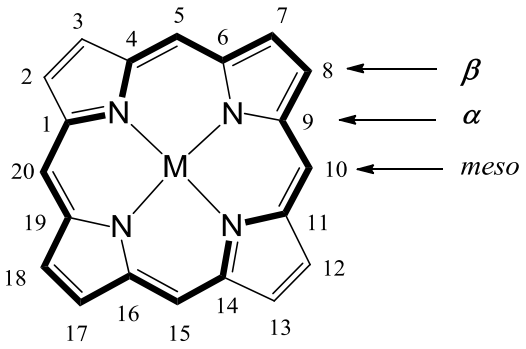

*Structure de la **porphine** proposée par Kuster et numérotation IUPAC*

Les porphyrines peuvent aussi se comporter comme des diacides ou des dibases et elles peuvent par conséquent, être métallées par presque tous les métaux de la classification périodique. Dans le premier cas, la porphyrine est dite “base libre”, dans le second cas, elle est dite “métallée”.

Le but de ce travail est d’utiliser la porphyrine comme brique moléculaire pour l’élaboration de composés ayant des activités optiques linéaires et non linéaires intéressantes.

Le premier chapitre porte dans un premier temps à détailler les méthodes de synthèse et de caractérisation de **porphyrines** décrites dans la littérature.

Nous allons également introduire l’unité **fluorène** qui possède des propriétés photophysiques très intéressantes comme antenne collectrice de lumière. Cette unité fluorène permet l’élaboration de modèles artificiels du système photosynthétique de type dendrimère.

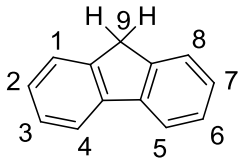

Structure de fluorène

Récemment au laboratoire, une nouvelle famille de composés porphyriniques a été synthétisée. Une porphyrine tétrasubstituée en position *meso* par des groupements fluorènyles, la tétrafluorénylporphyrine (**TFP**), a été obtenue. Des études ont montré qu'après une excitation sélective des antennes fluorènyles par lumière UV ou de la bande de Soret, le cœur de la porphyrine émettait une forte lumière rouge.

De plus, le rendement quantique de luminescence était considérablement amélioré pour ce composé **TFP** comparé à la tétraphénylporphyrine (**TPP**). En effet, le rendement quantique passe de 13% à 22%.

D'où le fort intérêt pour les **dendrimères et les oligomères**, possédant un nombre plus élevé d'antenne fluorène, puis d'étudier les propriétés photophysiques pour tester cet effet d'augmentation du nombre des bras fluorènyles et comparer leurs rendement quantique avec la référence du laboratoire : **TFP.**

Les **dendrimères** forment une famille de molécules possédant une structure arborescente. Ils présentent des propriétés variables qui peuvent être adaptées et contrôlées telles que la taille, la forme de la molécule et la position des groupements fonctionnels.

Ces macromolécules sont constituées d'unité de base, qui s'associent selon un processus arborescent autour d'un cœur polyfonctionnel. Leur architecture rappelle celle des complexes collecteurs de lumière dans les photosystèmes.

Leur construction arborescente s'effectue par la répétition d'une même séquence de réactions qui permet l'obtention à la fin du cycle réactionnel, d'une nouvelle génération appelée **G** et d'un nombre croissant de branches identiques. Ce sont des molécules tridimensionnelles, de taille et de structure bien définies, hautement symétriques, généralement de hauts poids moléculaire, possédant un grand nombre de chaînes terminales afin d'assurer leur solubilité.

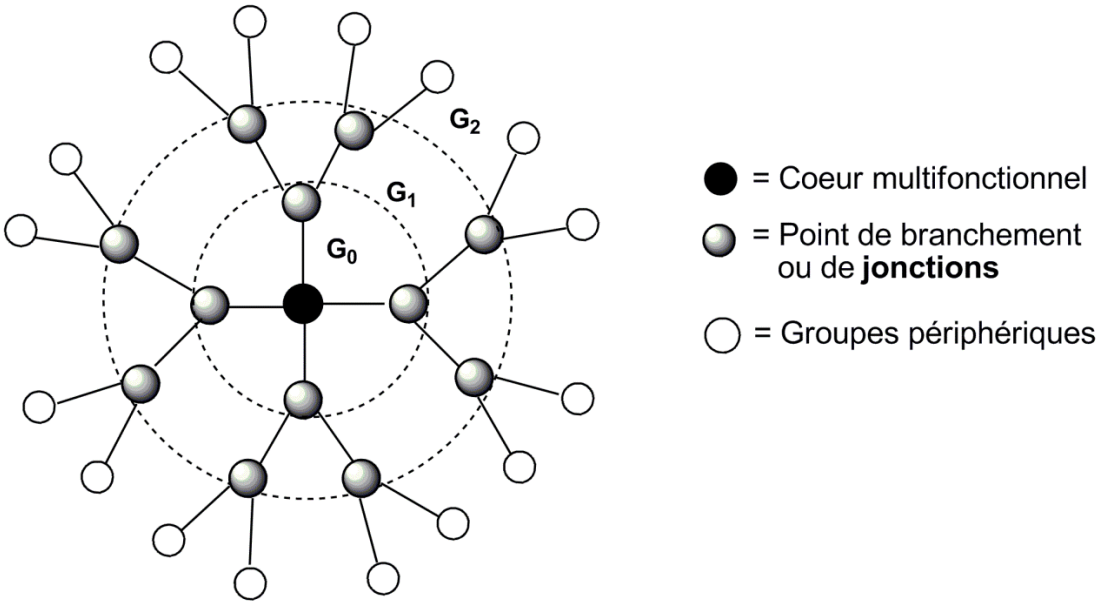

Représentation schématique d'un dendrimère

Il existe deux voix de synthèse principales pour la préparation des dendrimères. La première utilisée fut la synthèse dite **divergente** utilisée par les groupes de Vögtle, Newkome et Tomalia.

Ce n'est que plus tard que la synthèse **convergente** fut introduite par Fréchet et Miller au début des années 90. Elle permet un meilleur contrôle de l'architecture et du placement des groupes fonctionnels.

Nous présentons également les différentes dendrimères reportés dans la littérature, notamment les différentes positions de fixations des porphyrines (boule rouge) dans ces structures :

- Centrale
- Pontée
- Terminale

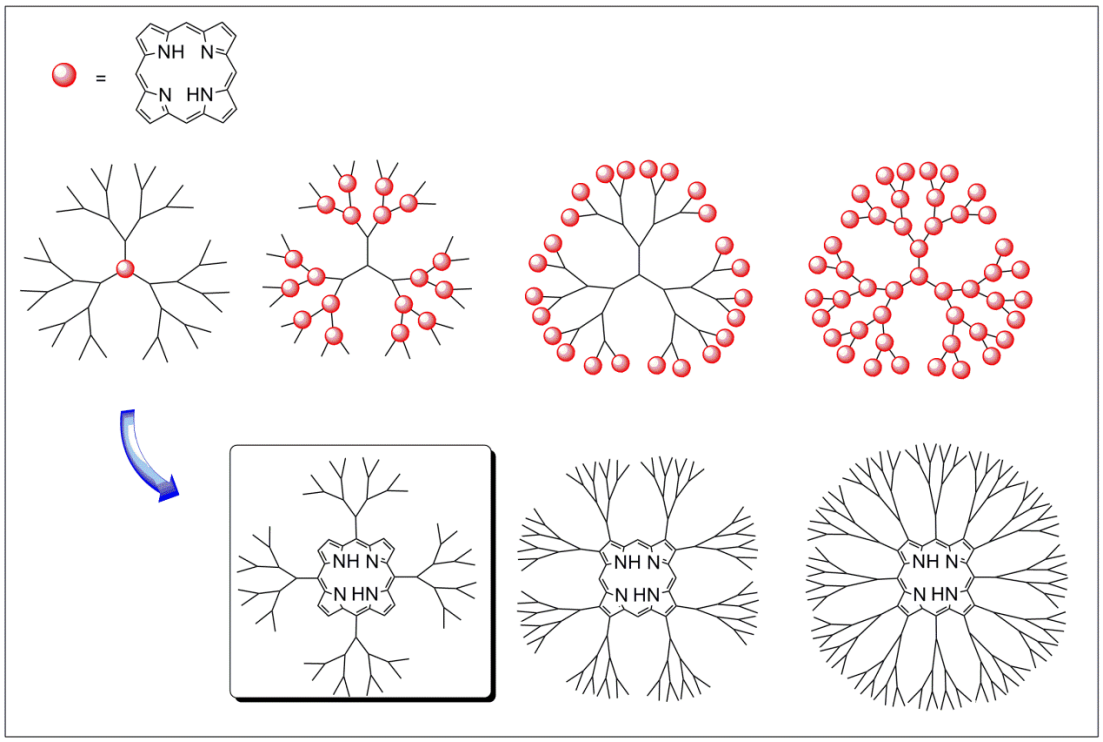

Porphyrin dendrimers with different structures

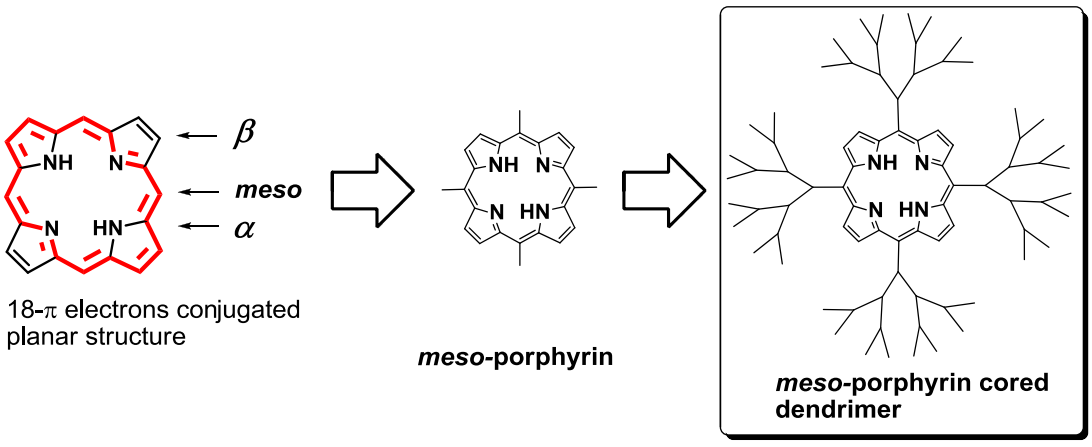

La structure de la porphyrine dendrimère étudiée

Ensuite, nous présenterons les caractérisations classiques de la porphyrine comme la spectroscopie UV-visible, et la luminescence.

Dans un deuxième temps, le **transfert d'énergie** est détaillé:

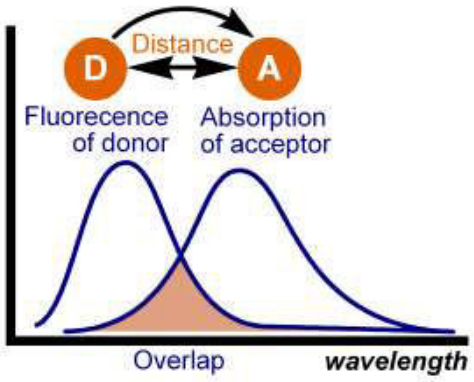

Spectral overlap between donor emission and acceptor absorption

Il existe deux types de transfert d'énergie : le transfert d'énergie de **type Dexter** privilégié dans le cas d'interactions à courte distance et le transfert d'énergie de **type Förster** dans les autres cas. Le transfert d'énergie singulet-singulet, entre deux chromophores maintenus à une certaine distance, peut se représenter de la manière suivante :

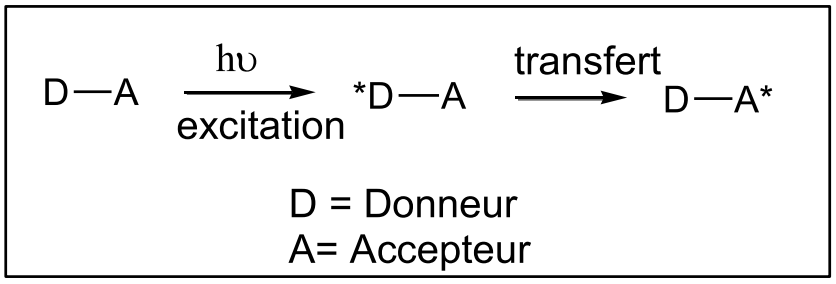

*Transfert d'énergie entre deux chromophores **D** et **A***

Comme exemple, Ci-dessous sont reportés les Spectres d'absorption et d'émission d'un dendrimère de porphyrine méso-base libre et de son diagramme de niveau d'énergie:

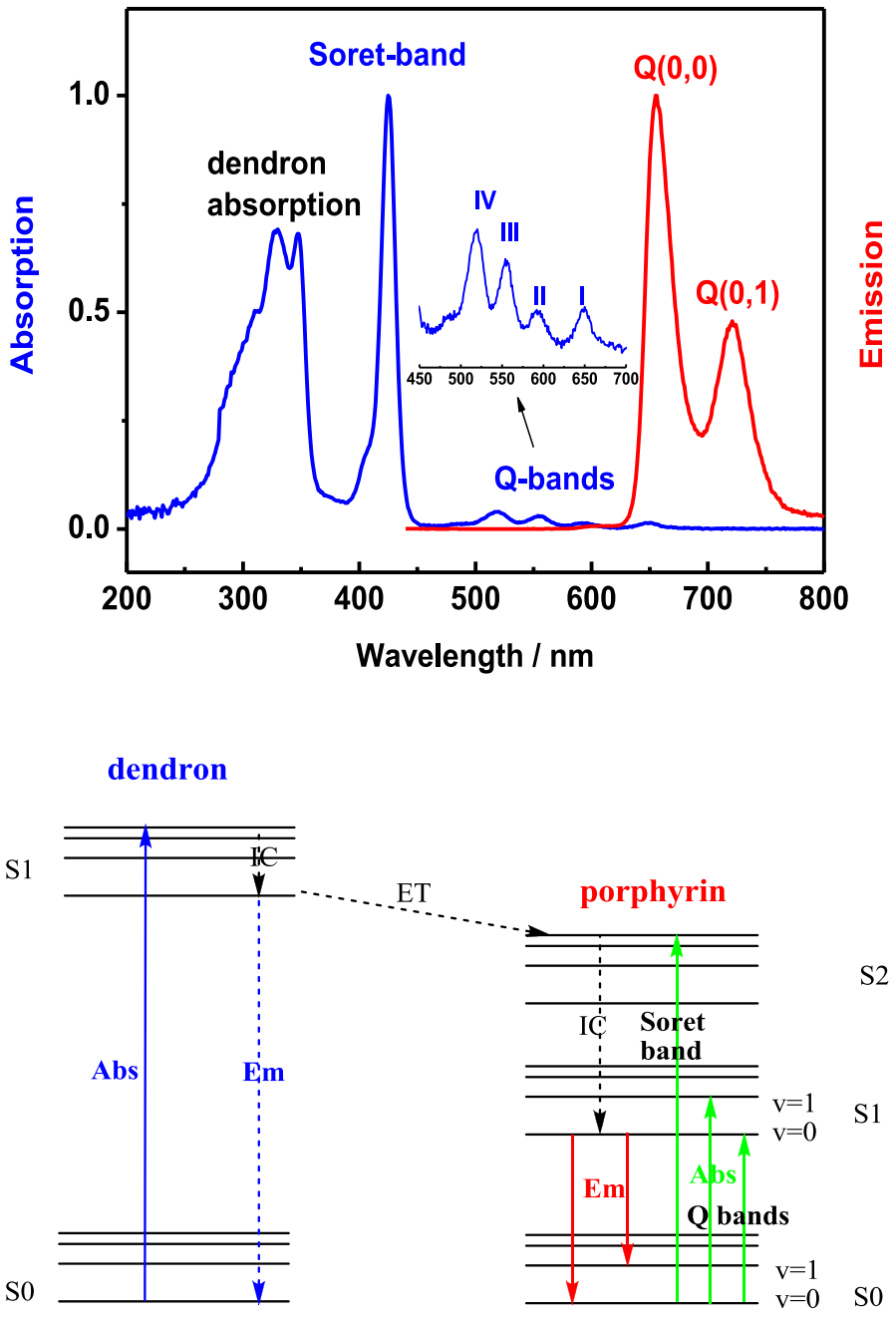

Spectres d'absorption et d'émission d'un dendrimère de porphyrine méso-base libre et de son diagramme de niveau d'énergie

Au cours de cette thèse, nous avons synthétisé et caractérisé trois groupes de dendrimères fluorényle-porphyrine et deux oligomères avec des structures conjuguées :

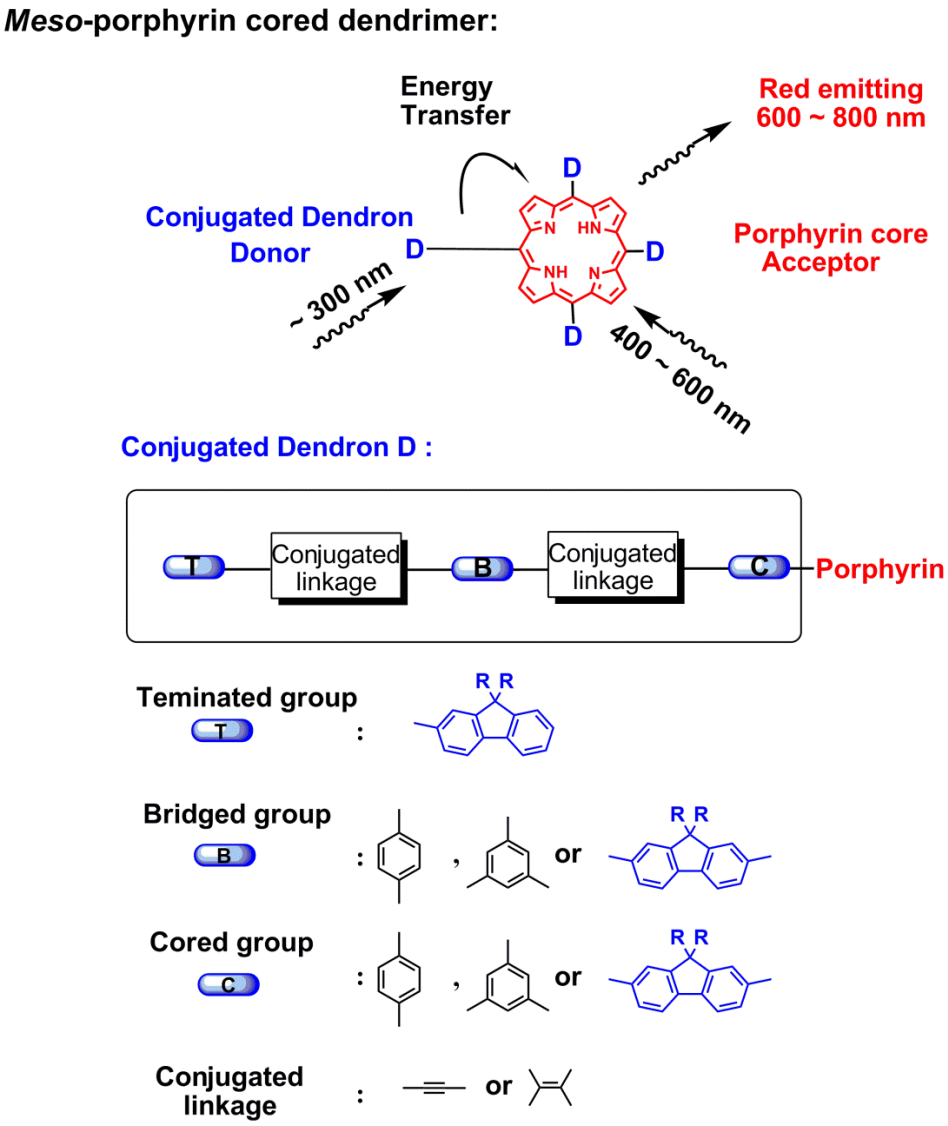

Structures de méso-porphyrine dendrimères

Puis leurs propriétés optiques liées à la structure ont été discuté en détail, ainsi que les comportements de transfert d'énergie à partir du dendron donneur conjugué vers le groupement porphyrine accepteur.

Suite à ces études relatives à une porphyrine dendrimère MONOMERE, il s'avère que ces porphyrines dendrimères sont des briques moléculaires intéressantes pour le transfert d'énergie et donc pour la collecte de lumière. On peut espérer, en

rapprochant ces briques moléculaires dans l'espace, observer un effet encore plus efficace pour la collecte de lumière par effet synergique, en synthétisant des porphyrines dendrimère DIMERE et TRIMERE:

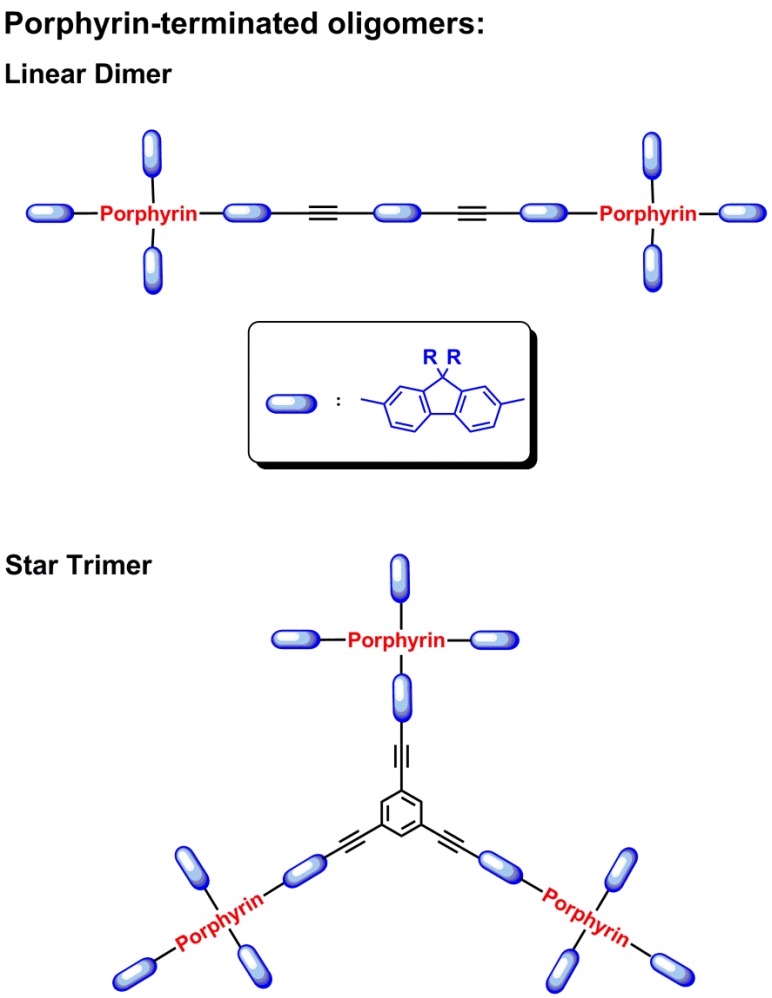

Structures d'oligomères de porphyrine dendrimère Dimere et Trimere

Dans ce chapitre d'introduction, nous avons présenté le contexte général de la chimie de porphyrine en considérant trois aspects: la structure, les propriétés optiques et la méthode synthétique.

Nous avons également présenté les porphyrines étudiées préalablement dans notre groupe de recherche et proposé des nouveaux modèles dans cette thèse. Pour étudier la corrélation sur la propriété optique structure pour ces nouveaux dendrimères porphyrine, nous avons considéré leur structure de deux parties: porphyrine comme base et dendron conjugué.

Nous avons donc décidé d'utiliser le dendron de quatre façons:

-groupe Centrale

-groupe Ponté,

-groupe Terminale

-assemblage Conjugué

Pour la conception des nouveaux **oligomères** de porphyrine, nous avons considéré le groupe fluorényle-porphyrine terminal pour former le dimère linéaire et le trimère en forme d'étoile.

Dans le deuxième chapitre, nous avons étudié l'influence de la position de substitution du phényle du le cœur central, qui est la porphyrine TPP. Deux groupes de nouveaux dendrimères ont été synthétisés avec différentes positions de substitution du phényle de la TPP: série para-substituée **TPP1**, **TPP2** et **TPP3**, et série méta-substituée **TPP4**, **TPP5** et **TPP6**. Ces dendrimères ont tous des dendrons conjugués avec des ponts phényl-alcynes et des groupements fluorènyles terminaux:

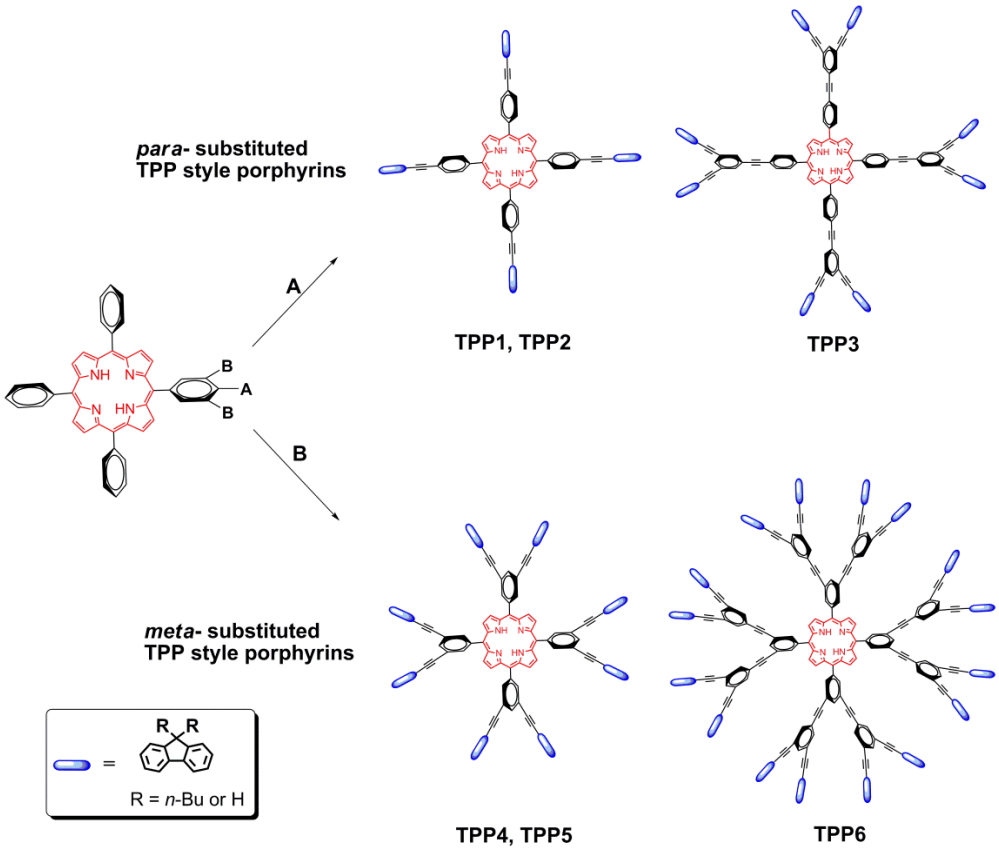

Structures moléculaires de dendrimères de porphyrine avec TPP-central : ***TPP1-TPP6***

Trois stratégies synthétiques différentes ont été considérées, et les dendrimères souhaités ont été obtenus avec succès par condensation du dendron aldéhyde modifié et de pyrrole dans les conditions d'Adler-Longo :

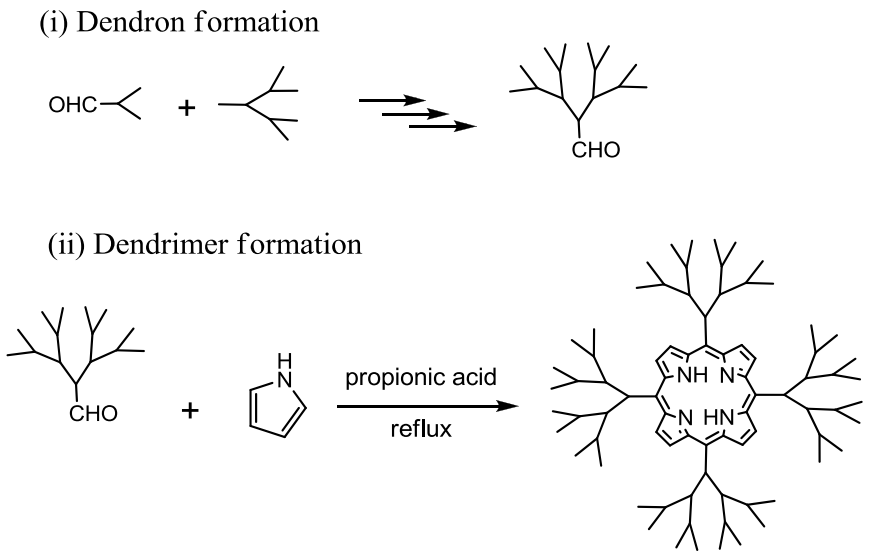

Stratégie de synthèse utilisée pour l'obtention de méso-porphyrine dendrimères

Dans le troisième chapitre, pour étudier l'influence des antennes périphériques, une série de dendrimères de porphyrine à base de TFP avec différentes positions de fluorènyles dans les dendrons conjugués (fluorényle central, fluorényle pontant et fluorényle terminal): **TFP1**, **TFP2** et **TFP3** a été synthétisée.

Le fluorényle central influence principalement l'émission et le rendement quantique, alors que le fluorényle ponté et le fluorényle terminal ont un plutôt un effet sur l'absorption et l'émission du dendron en raison du transfert d'énergie prenant effet. Pour le plus gros dendrimère **TFP3**, lors de l'excitation du dendron, une émission résiduelle lors du processus de transfert est observée due à une trop grande distance entre ce chromophore et le cœur de la porphyrine.

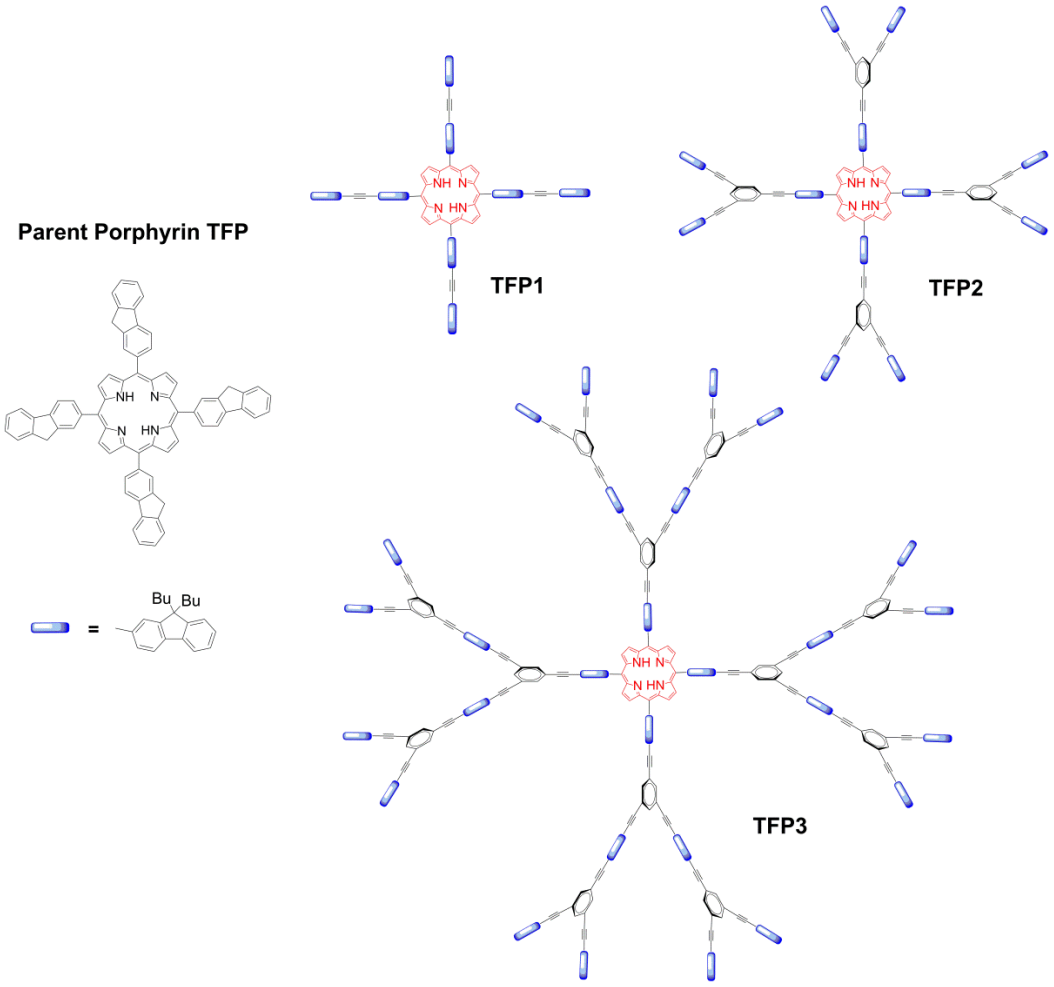

*Dendrimères de porphyrine à base de TFP : **TFP1**, **TFP2** et **TFP3***

Dans le quatrième chapitre, afin d'étudier l'influence des connexions dans le dendron, deux nouveaux dendrimères de porphyrine incorporant des ponts vinyles et alcynyles, **TPP-D** et **TFP-D**, ont été synthétisés et comparés aux analogues avec des ponts alcynes **TPP-T** et **TFP-T**. Ces ponts avec des doubles liaisons influencent dans une certaine mesure les propriétés optiques des dendrimères de porphyrine en fonction des positions occupées. Quand les différents liens conjugués D ou T, **soit TPP-D** et **TPP-T**, respectivement sont connecté à la porphyrine centrale, il y a des changements évidents en spectroscopie. Par exemple pour la bande de Soret en absorption et pour l'émission dans le rapport entre Q(0,0) et Q(0,1), et aussi quelques changements dans les rendements quantiques. Les différentes liaisons conjuguées D ou T dans le

dendron périphérique, par **TFP-D** et **TFP-T**, n'induisent pas de changement dans l'absorption de la porphyrine et les spectres d'émission. Par contre il y a des différences dans le rendement quantique de par l'influence sur les transitions non radiative.

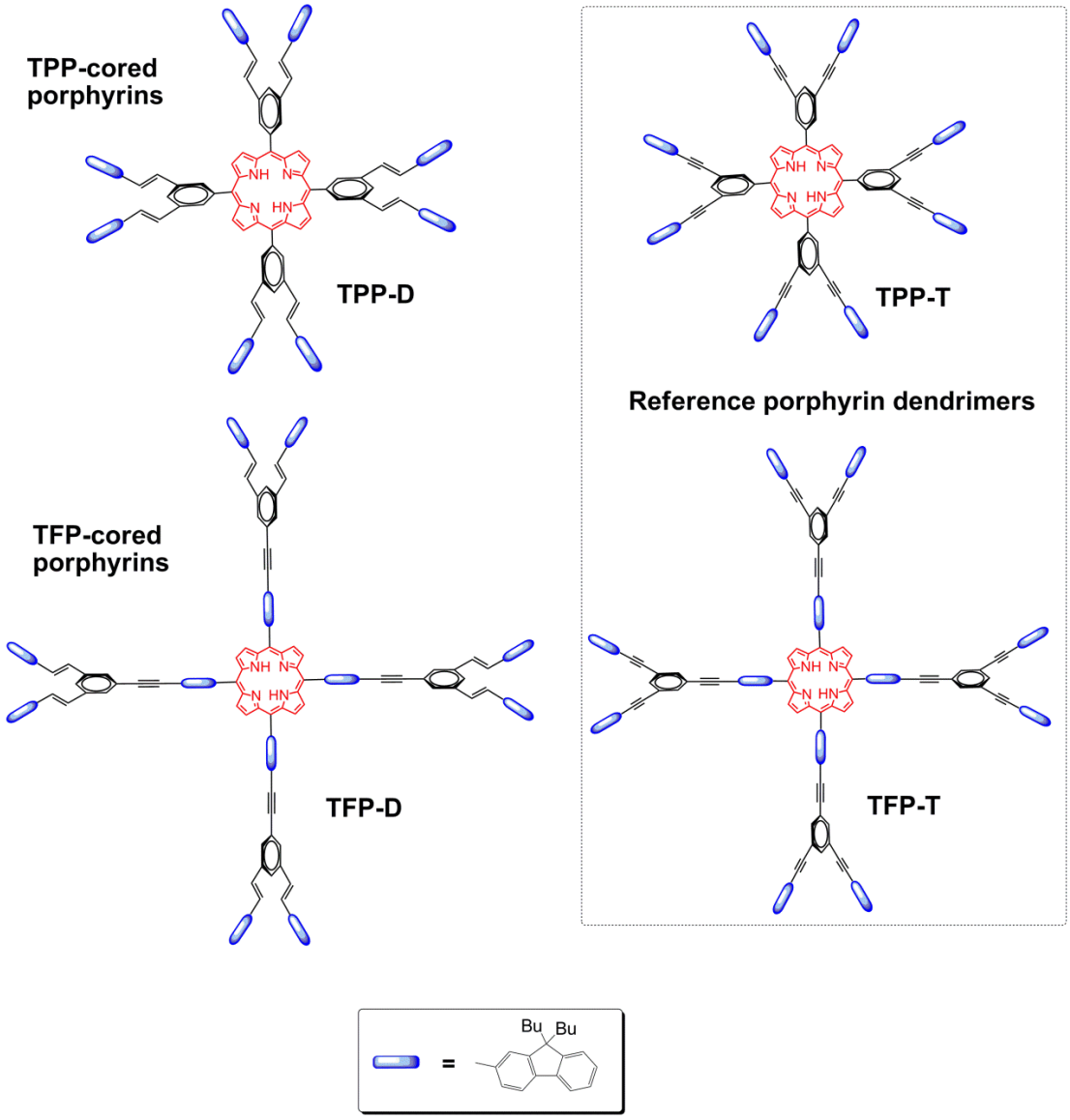

Structures moléculaires de dendrimères de porphyrine avec vinyle ponté (D) et leurs références avec alcynes pontés (T)

Dans le dernier chapitre, deux oligomères (un dimère linéaire et en un trimère en étoile), ont été synthétisés à partir du même monomère de porphyrine avec TFP comme groupement terminaux. Ils ont été synthétisés à partir de la même porphyrine

Monomère, utilisant successivement les conditions de Lindsey, la déprotection des TMS, la réaction de métallisation, couplage catalytique de Sonogashira et réaction de dé-métallisation.

En absorption, les **Dimère** et **Trimère** ont le même déplacement de la bande de Soret que le **Monomère**, mais les intensités des bandes Q montrent plus de différences, en particulier pour Qx(0,0).

En émission, les rapports d'émission Q(0,0) et Q(0,1) améliorent évidemment avec les nombres croissants de porphyrine terminaison, et pour **Trimère**, il montre Q(0,0) comme prédominait émission rouge.

Pour les rendements quantiques, le **Dimère** garde un rendement similaire en tant que **Monomère**, tandis que **Trimère** à la construction en forme d'étoile a le plus haut rendement de 33%.

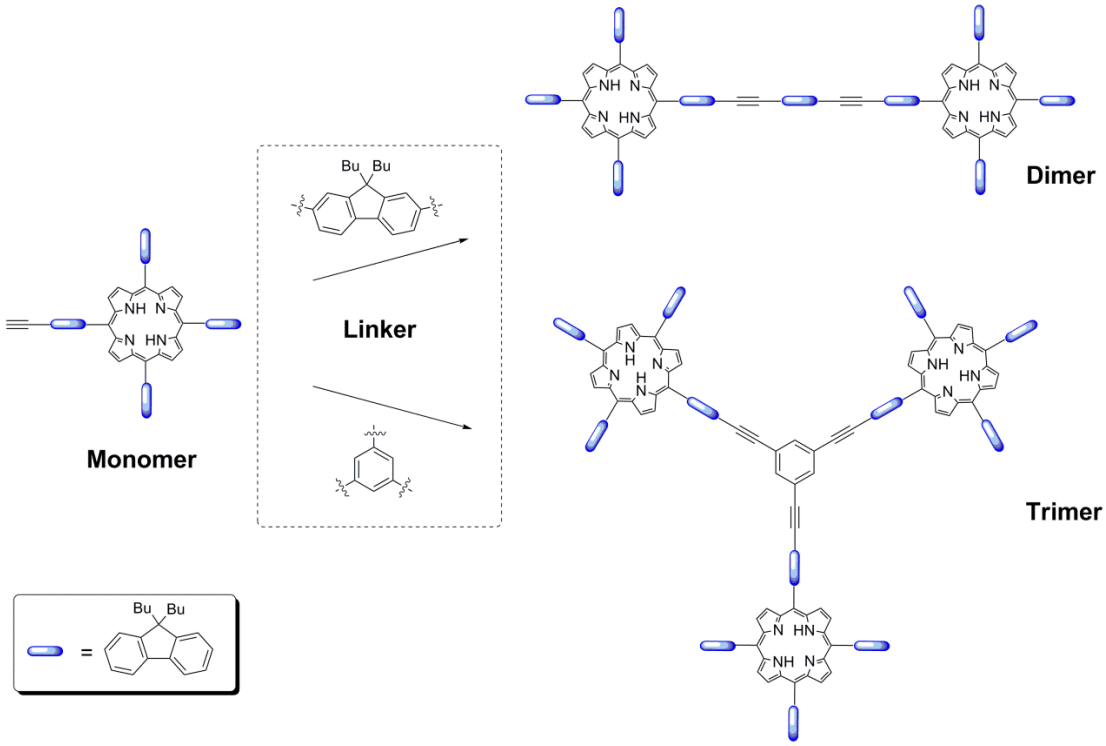

Structures moléculaires des oligomères de porphyrine

Les caractérisations de toutes ces nouvelles molécules synthétiques : dendrimères et oligomères cibles, ont été faites par les mesures RMN ^{1}H et ^{13}C, masse à haute résolution et microanalyse.

Appendix

Compounds in Chapter 2:

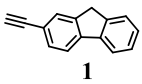

1

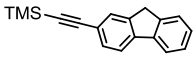

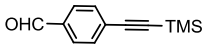

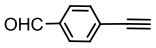

5

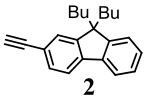

2

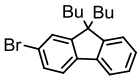

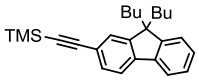

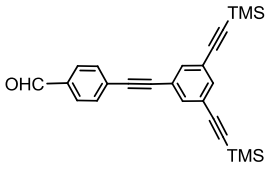

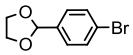

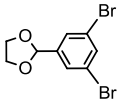

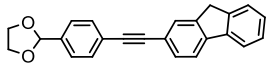

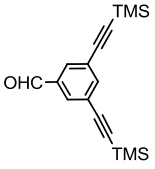

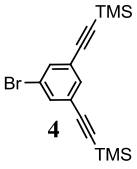

4

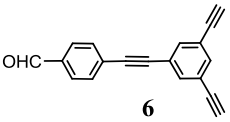

6

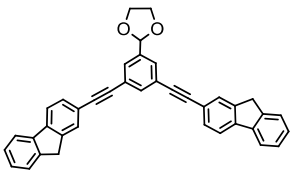

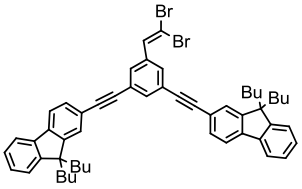

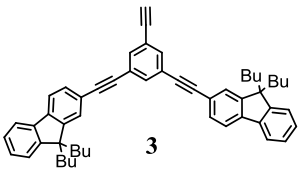

3

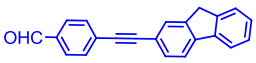

Dendron1

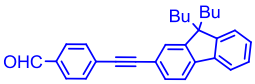

Dendron 2

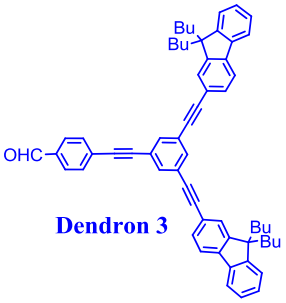

Dendron 3

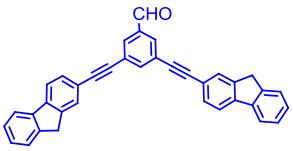

Dendron 4

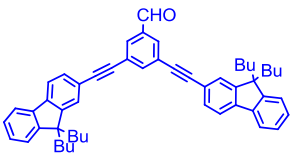

Dendron 5

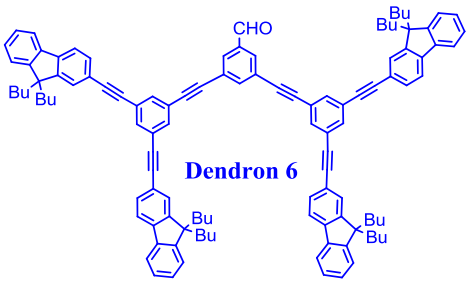

Dendron 6

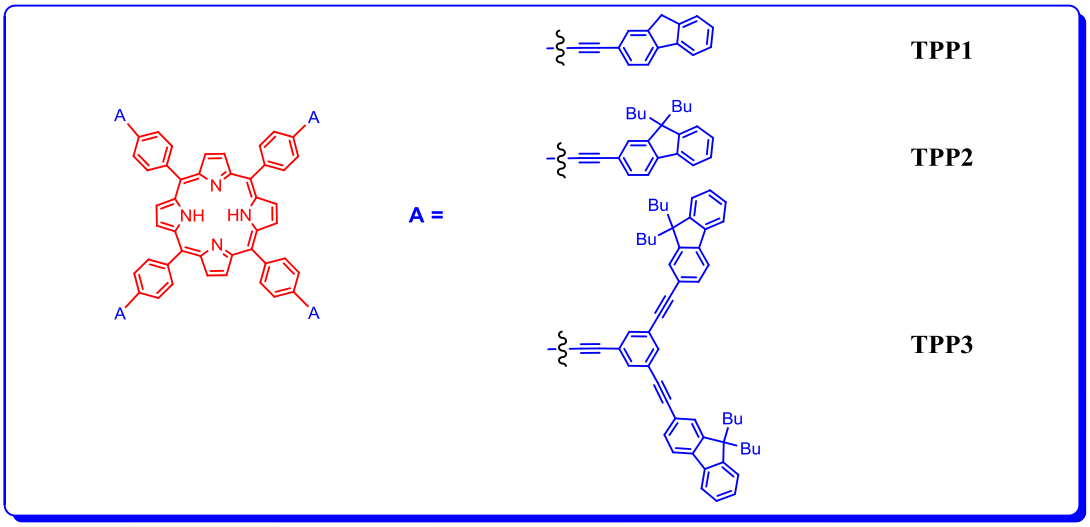

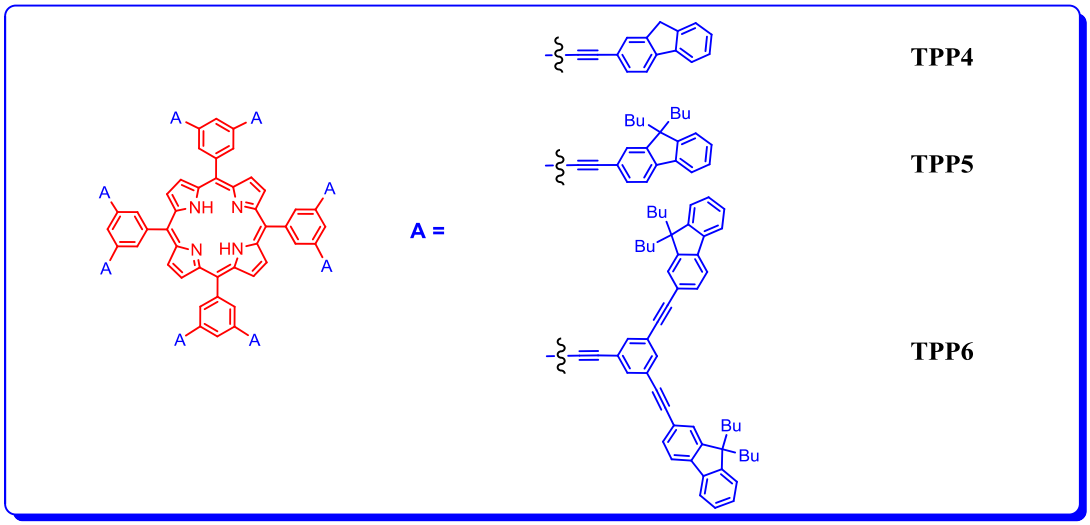

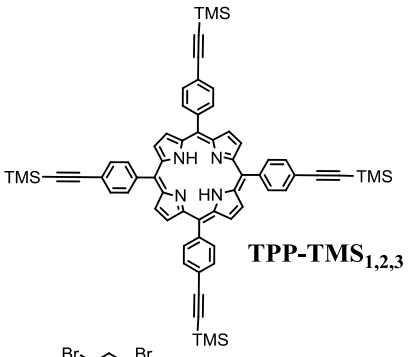

TPP-TMS$_{1,2,3}$

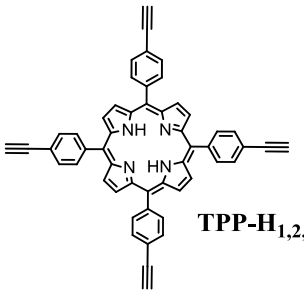

TPP-H$_{1,2,3}$

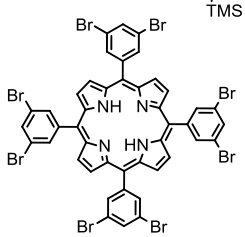

8BrTPP

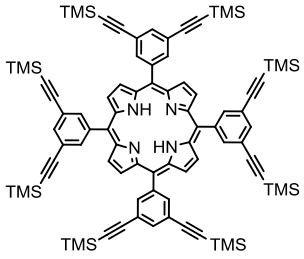

TPP-TMS$_{4,5,6}$

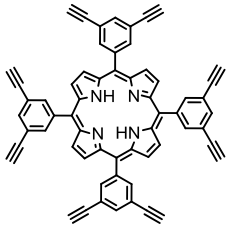

TPP-H$_{4,5,6}$

Compounds in Chapter 3:

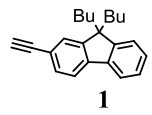

1

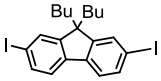

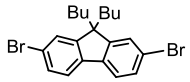

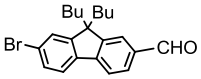

2

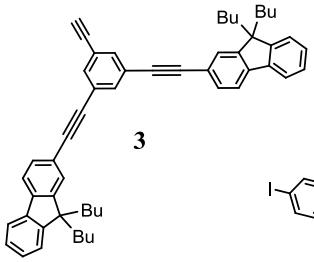

3

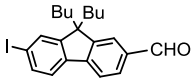

4

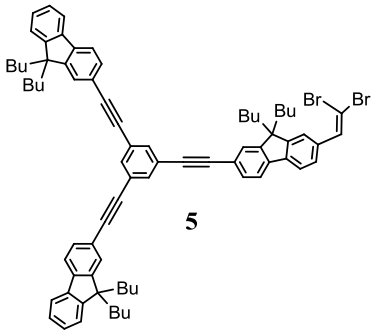

5

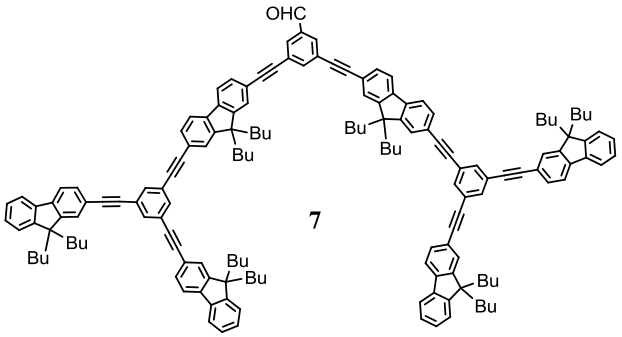

7

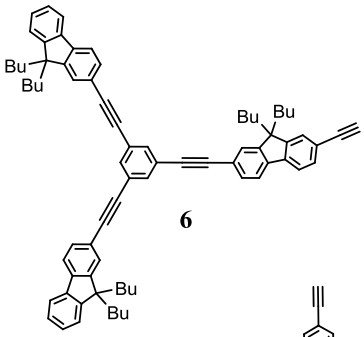

6

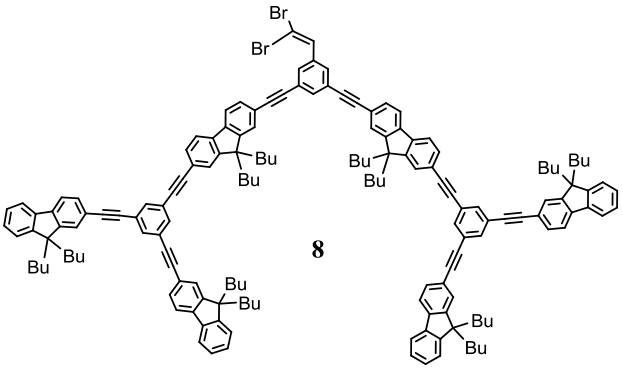

8

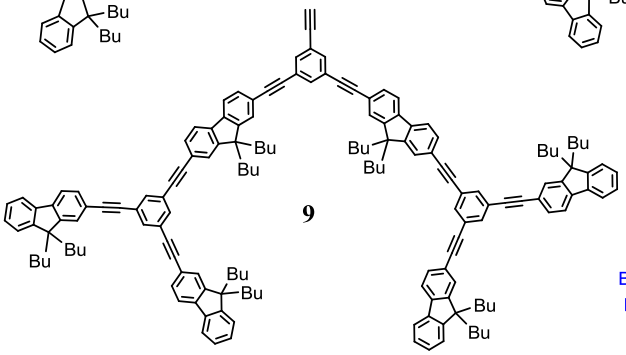

9

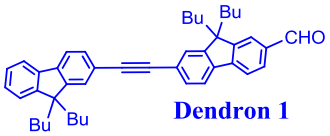

Dendron 1

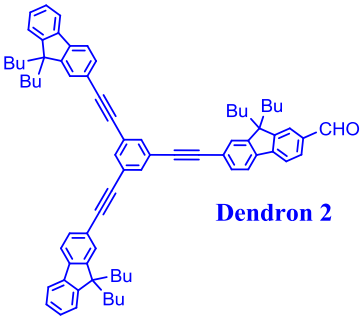

Dendron 2

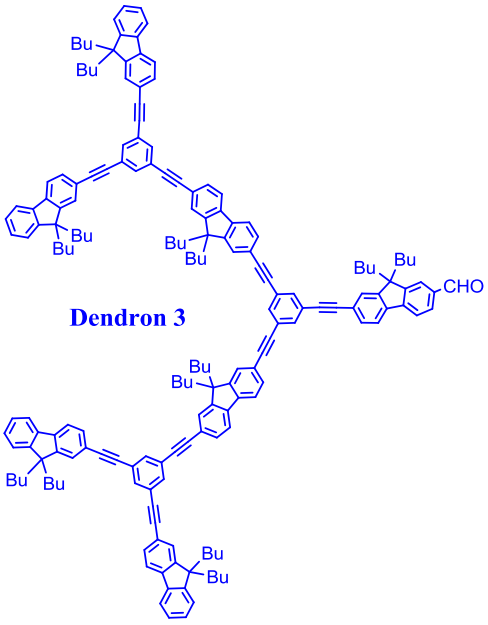

Dendron 3

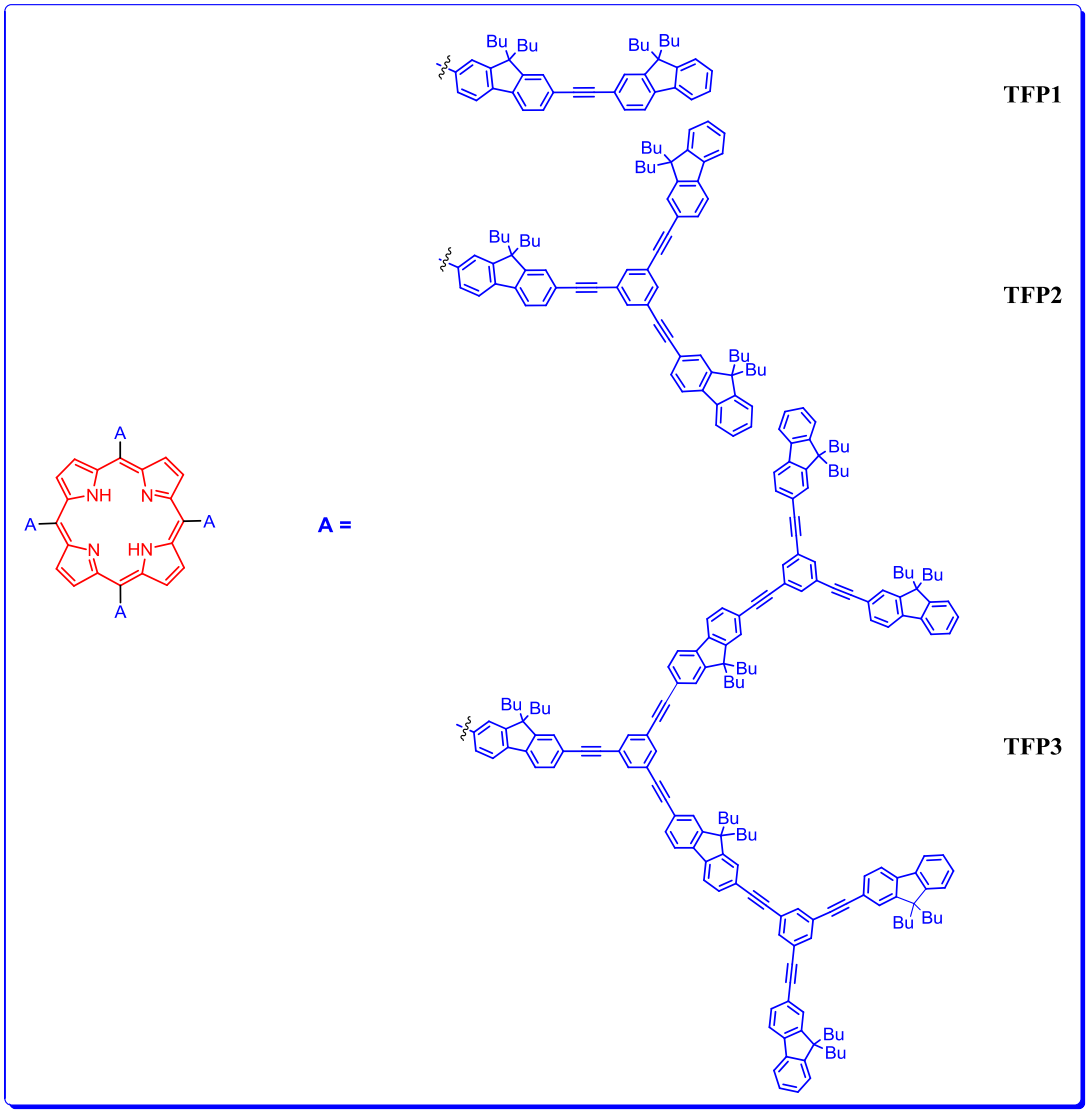
TFP1
TFP2
TFP3
A =
A
NH
N
HN
Bu
Bu

Compounds in Chapter 4:

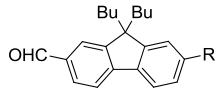

1: R = H
2: R = Br

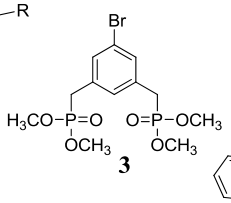

3

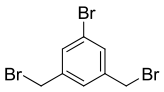

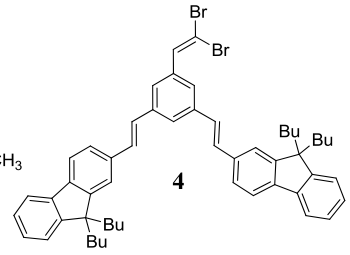

4

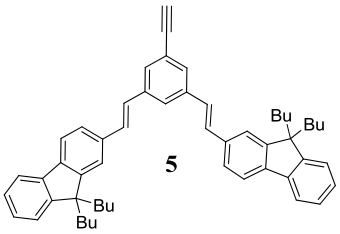

5

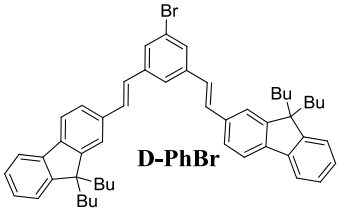

D-PhBr

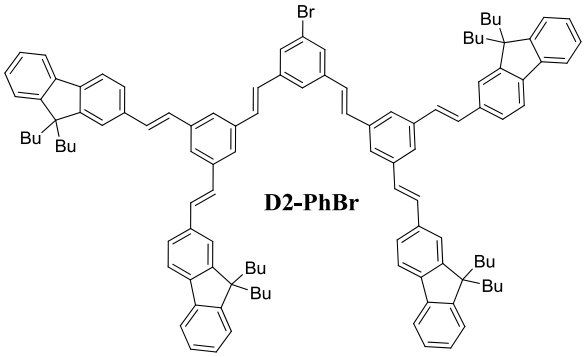

D2-PhBr

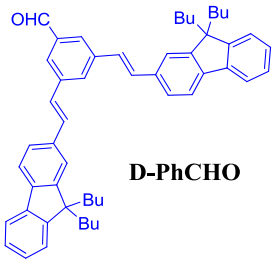

D-PhCHO

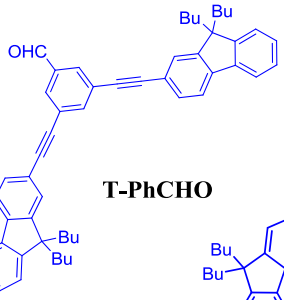

T-PhCHO

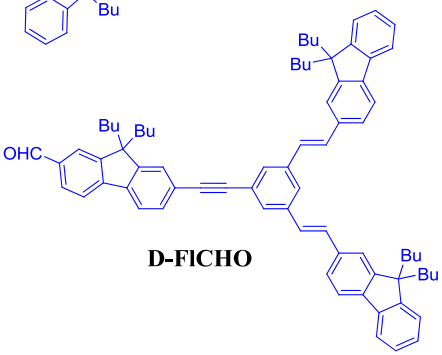

D-FlCHO

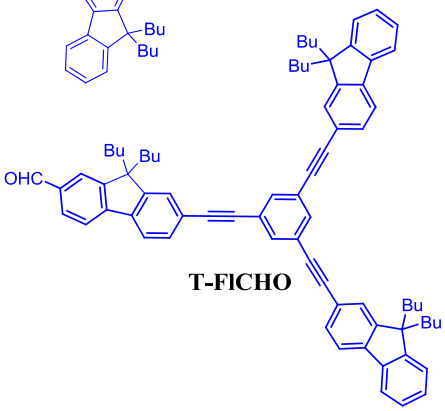

T-FlCHO

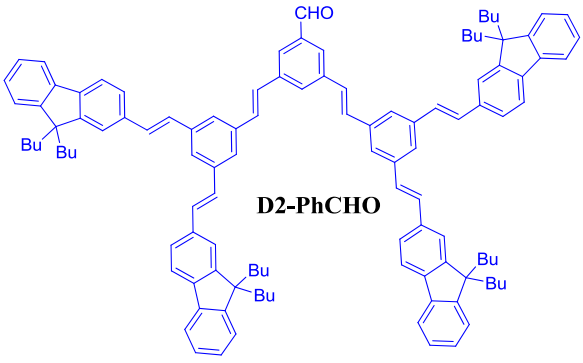

D2-PhCHO

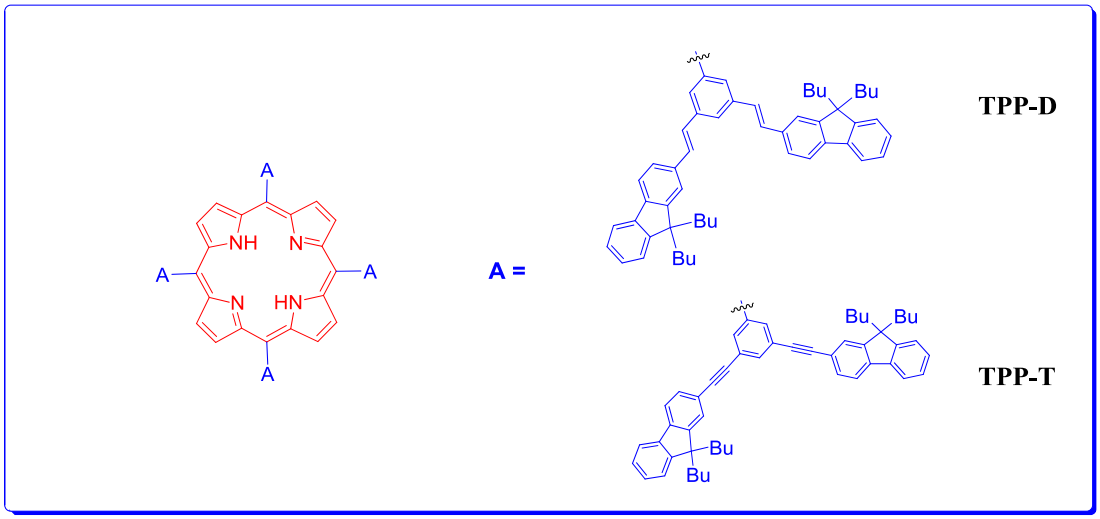
A
NH
N
HN
A =
Bu
TPP-D
TPP-T

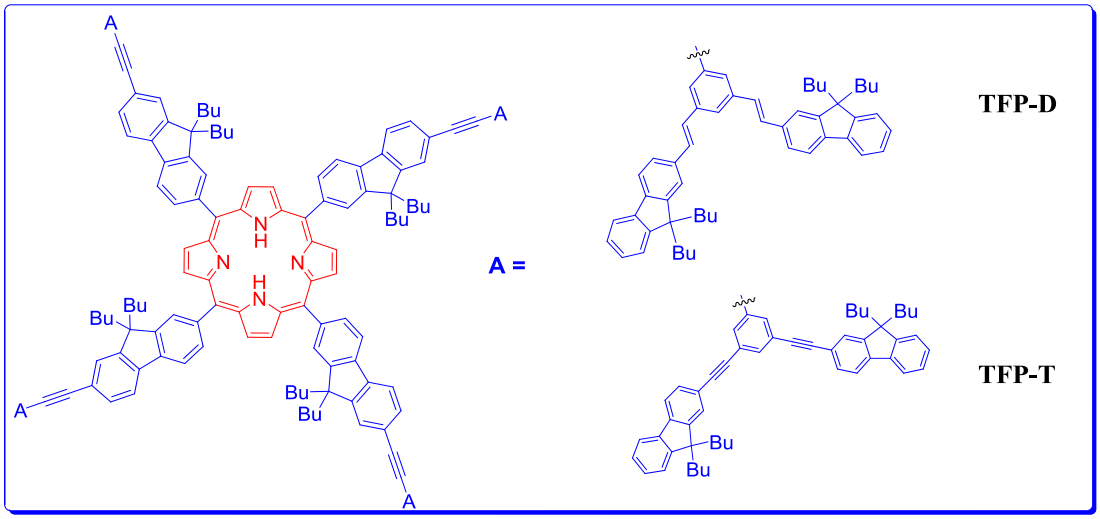
A
Bu
N
H
A =
TFP-D
TFP-T

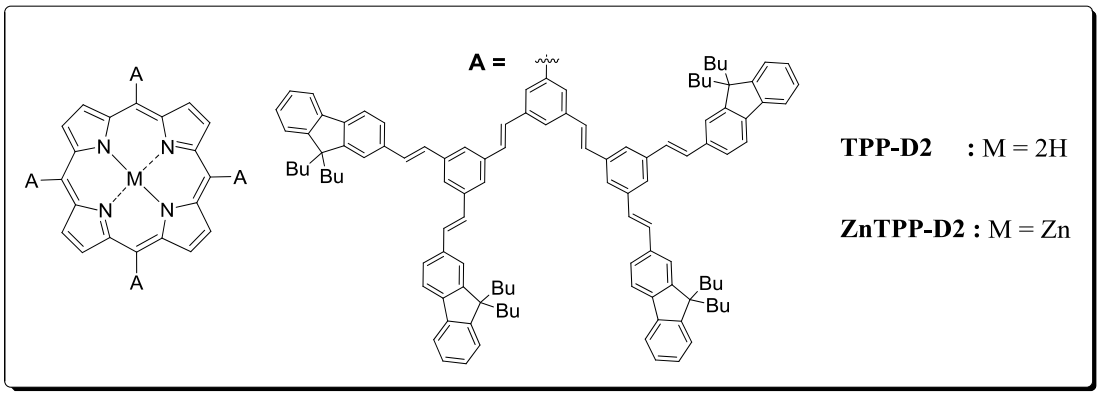
A
N
M
A =
Bu
TPP-D2 : M = 2H
ZnTPP-D2 : M = Zn

Compounds in Chapter 5:

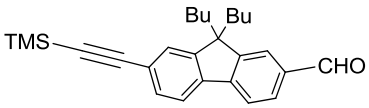

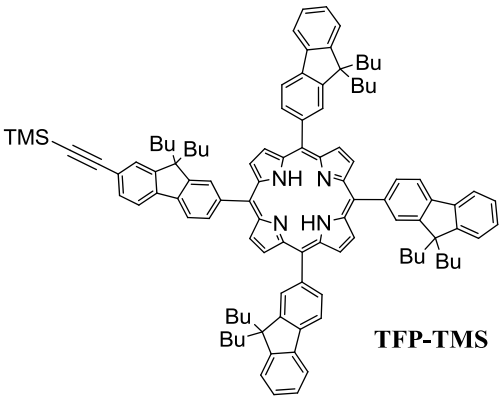

TFP-TMS

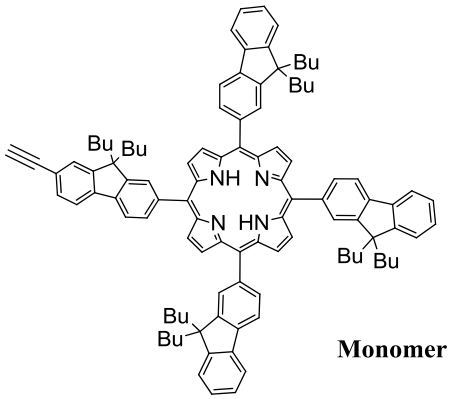

Monomer

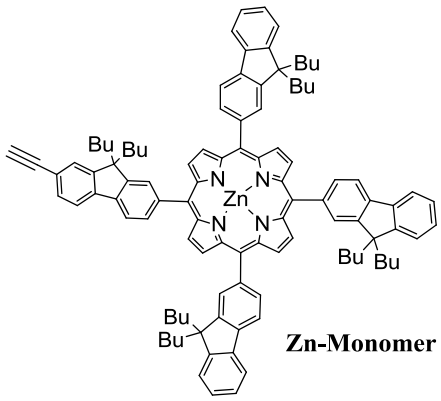

Zn-Monomer

A =

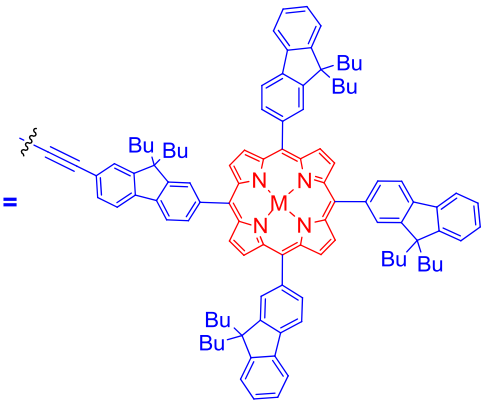

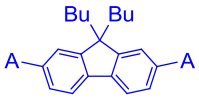

Dimer : M = 2H

Zn-Dimer : M = Zn

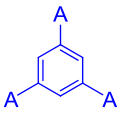

Trimer : M = 2H

Zn-Trimer : M = Zn

INSA de RENNES
Service des Formations

AVIS DU JURY SUR LA REPRODUCTION DE LA THESE SOUTENUE

Titre de la thèse:
Synthesis of new conjugated meso-porphyrin dendrimers and oligomers and study of their optical properties

Nom Prénom de l'auteur : YAO DANDAN

Membres du jury :
- Monsieur MANDON Dominique
- Monsieur BLANCHARD Philippe
- Monsieur MONGIN Olivier
- Madame PAUL-ROTH Christine
- Monsieur HASENKNOPF Bernold
- Monsieur PAUL Frédéric

Président du jury : Dominique MANDON

Date de la soutenance : 16 Mars 2015

Reproduction de la these soutenue

Thèse pouvant être reproduite en l'état
~~Thèse pouvant être reproduite après corrections suggérées~~

Fait à Rennes, le 16 Mars 2015

Signature du président de jury

Le Directeur,

M'hamed DRISSI